Characterization of fronts and zones in the Indian sector of Southern Ocean

Thesis Submitted to Goa University for the Degree of

Doctor Of Philosophy in Marine Sciences

Racheal Chacko

National Centre for Polar & Ocean Research

Headland Sada, Vasco-da-Gama, Goa 403 804, India

December 2018

STATEMENT OF THE CANDIDATE

I hereby state that the present thesis titled "**Characterization of fronts and zones in the Indian sector of Southern Ocean** " is my original contribution, as required under the University Ordinance OB-9.9-(vi) and the same has not been submitted for any other degree on any previous occasion. To the best of my knowledge the present study is the first comprehensive work of its kind in the area mentioned.

Due acknowledgments have been made wherever facilities and suggestions have been availed.

Racheal Chacko

CERTIFICATE

As required under the University Ordinance OB-9.9-(viii), this is to certify that the thesis titled "**Characterization of fronts and zones in the Indian sector of Southern Ocean**", submitted by **RACHEAL CHACKO** for the award of the degree of Doctor of Philosophy in Marine Science, is based on original studies carried out by her under my supervision. The thesis or any part of thesis has not been previously submitted for any other degree or diploma in any university or institution.

Dr. N. Anilkumar
Research Guide
Scientist F
National Centre for Polar & Ocean Research
Vasco-da-gama, Goa 403 804, Goa

For my Appachan and Amma

Contents

Acknowledgements

I wish to express my sincere appreciation to those who have contributed to this thesis and supported me in one way or the other during the journey of my PhD.

Foremost, I would like to express my sincere gratitude to my guide Dr. N. Anilkumar for his patience, motivation and enthusiasm. I have learned so much from him. I am grateful for his unrelenting belief in me and continuous support of my Ph.D study and research. I would like to acknowledge and thank my Department Research Committee members Prof. H.B. Menon and Dr. Aparna for their effort and timely help; without which the submission of this thesis would not have been possible. I would also like to acknowledge the encouragement and motivation provided by past directors of NCAOR Dr. Rasik Ravindra , Dr. Rajan and the present director Dr. M. Ravichandran. I thank my teachers in the Dept. of Marine Science who introduced me to the world of oceanography and let me discover my love for the sea and observational oceanography.

I am indebted to Dr.Sabu who has offered generous comments, advice, and criticism, which helped me improve my work. His insightful advice along the way is hugely appreciated. I have benefitted significantly from my interactions with Dr.Nuncio and am lucky to have had his ideas and guidance. I would like to acknowledge the help provided in data collection by the participants and ships' crew during SOE-2010 and 2011.

I have an amazing group of friends who've been there for me through it all. They've all been great, but I'll name a few specifically here. I can never forget Jenson from whom I have learnt a lot and missed a lot during the writing of this thesis. The adventures that we both had in collecting datasets in difficult conditions will always remain memorable. I am grateful to Melena who has been an amazing friend and my sounding board. Thank you Nisha for all the support and being the tolerant and ever forgiving roommate; Paru and Maha for always being there for me; Tanvi and Nutan were always there for moral support. Venkat, Ravi, Mahesh and Anish, are some of people who've helped me along the way and made life so much more bearable. Manoj, Dipti, Drishya, Celsa, Lathika, Runa, Prerna, Ashish, Gautami, Aritri,

Abhilash, Ajith, Lavkush, Shramik, Swati, Neelu, Roseline are some of my friends and colleagues whom I would like to acknowledge for making my journey in NCAOR quite pleasant and memorable. I would also like to thank Prafila for all her help and support.

My heart felt regard to my father in law, mother in law for their love. A special thanks to Anu and Jaicilettan for their moral support. I can never express in words the belief and support of my husband Manu who has been a strong pillar of strength and joy in my life. Your tireless belief in me has kept me going at my lowest point for which and I am eternally grateful. Last but not the least my parents and my brother Varghese who have supported me continuously throughout my education. Their patience and sacrifice will remain my inspiration throughout my life. Their interest in my work has given me strength and courage without which I would not be able to make it this far and it is to them that I dedicate this thesis.

List of figures

List of Tables

Abbreviations

Θ	Potential Temperature
AABW	Antarctic Bottom Water
AAIW	Antarctic Intermediate Water
AASW	Antarctic Surface Water
AC	Agulhas Current
ACC	Antarctic Circumpolar Current
ACE	Anticyclonic Eddy
AF	Agulhas Front
AMSR-E	Advanced Microwave Scanning Radiometer for EOS
ARC	Agulhas Return Current
ASCAT	Advanced Scatterometer
AVISO	Archiving, Validation and Interpretation of Satellite Oceanographic
AZ	Antarctic Zone
CDW	Circumpolar Deep Water
CDP	Cape Darnley Polynya
CE	Cold Core Eddy
Chl a	chlorophyll
CTD	Conductivity Temperature Depth
DO	Dissolved Oxygen
ECMWF	European Centre for Medium-Range Weather Forecasts
EKE	Eddy Kinetic Energy
ENSO	El-Nino Southern Oscillation
GCM	General Circulation MOdel
GHRSST	Group for High Resolution Sea Surface Temperature
HadISST	Hadley Centre Global Sea Ice and Sea Surface Temperature
HN-LC	High Nutrient Low Chlorophyll
ICOADS	International Comprehensive Ocean-Atmosphere Data Set
IOSSO	Indian Ocean Sector Of Southern Ocean
MADT	Maps Of Absolute Dynamic Topography
MEI	Multivariate Enso Index
MetOp	Meteorological Operational
MIZ	Marginal Ice Zone
MOC	Meridional Overturning Circulation
NSTF	Northern Subtropical Front
ORA	Ocean Reanalysis System
OSCAR	Ocean Surface Current Analysis–Realtime
PET	Princess Elizabeth Trough
PF	Polar Front
PF1	northern branch of Polar Front
PF2	southern branch of Polar Front
PFZ	Polar Frontal Zone
SACCF	Southern Antarctic Circumpolar Current Front
SAF	Subantarctic Front
SAF1	northern branch of Subantarctic front
SAF2	southern branch of Subantarctic front
SAM	Southern Annular Mode
SAMW	Subantarctic Mode Water

SASW	Subantarctic Surface Water
SAZ	Subantarctic Zone
SB	Southern Boundary
SCZ	Subtropical Convergence Zone
SLA	Sea Level Anomaly
SML	Summer Mixed Layer
SO	Southern Ocean
SSS	Sea Surface Salinity
SST	Sea Surface Temperature
SSTF	Southern Subtropical Front
STF	Subtropical Front
STMW	Subtropical Mode Water
STSW	Subtropical Surface Water
Tmin	Temperature minimum
TS	Temperature Salinity
WDW	Warm Deep Water
WG	Weddell Gyre
WML	Winter Mixed Layer
WOCE	World Ocean Circulation Experiment
WS	Weddell Sea
WW	Winter Water
XCTD	Expendable Conductivity Temperature and Depth

1. Introduction

The Southern Ocean (SO) is often referred to the ring of ocean that circles Antarctica. It is bordered by the Antarctic continent on the south but the northern limit of the SO is not so clearly defined. The SO connects the three main ocean basins (Séférian et al., 2012) and the Subtropical Front (STF) - a transition zone between cool, fresh, nutrient-rich sub-antarctic waters and warm, salty, nutrient-poor subtropical waters is usually considered as the northern extent of the SO. Although the position of the STF varies with longitude, it lies roughly along 40°S for much of the SO. The SO occupies about 20% of the surface area of the global ocean and it is the home to strongest winds and largest waves. The 'Roaring Forties' and the 'Furious Fifties' and 'Screaming Sixties' are terms often applied to the strong westerly winds present over this region. These westerlies drive the largest current system on the earth the Antarctic Circumpolar Current (ACC).

1.1The ACC

The ACC is the largest current system in the world, and flows continuously around Antarctica and is the major conduit for inter-basin exchange of heat and fresh water fluxes (Rintoul et al., 2001) (Fig 1.1). The ACC effectively isolates the SO from lower latitudes, giving rise to the coldest temperatures in the world's ocean, deep surface mixed layers, and a large area of seasonal sea ice. It is characterized by strongly tilting isopycnals due to the mixing of water

preferentially along constant density surfaces which bring mid-depth water into contact with the ocean surface and serve as a barrier to southward transport, possibly helping to isolate the Antarctic continent from mid-latitude climate variability (Rintoul, et al., 2001). The ACC connects the Atlantic, Pacific and Indian Oceans to form a global network of ocean currents that redistributes heat around the Earth and so influences climate.

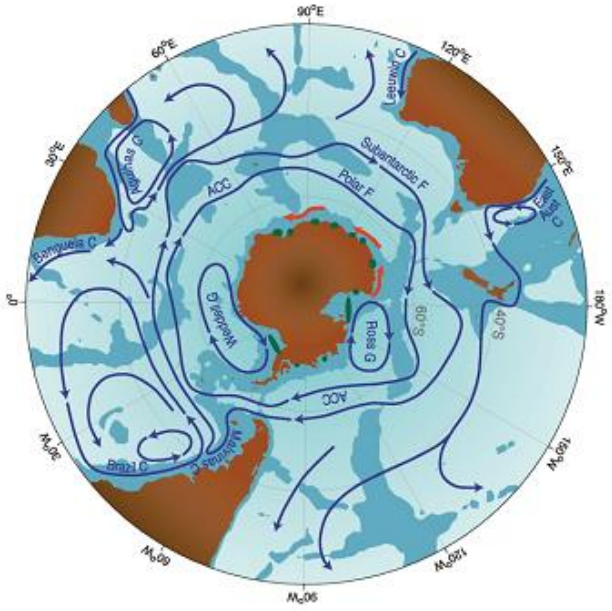

Figure 1.1.Schematic depiction of the major currents in the SO south of 20 °S. (ACC= Antarctic Circumpolar Current; F = Front; C = Current; G =Gyre). Adapted from Rintoul, 2011b.

A series of ocean fronts; narrow, variable bands defined by abrupt changes in water properties, in particular, temperature and salinity divide the surface waters of the SO into several zones (Gordon, 1975; Deacon, 1982; Whitworth, 1988). From north to south, the fronts and zones of the SO are: the Sub Tropical Front

(STF), Subantarctic Zone (SAZ), Subantarctic Front (SAF), Polar Frontal Zone (PFZ), Polar Front (PF) and Antarctic Zone (AZ) (Whiteworth, 1980; Orsi, 1995). The ACC, is steered by topography, such that the position and structure of its jets and fronts deviate from the zonal direction, both spatially (Sokolov and Rintoul, 2009) and temporally (Chapman and Morrow, 2014). These fronts can influence the upwelling and ultimate ventilation of deep waters, which can in turn affect the formation of water masses at the surface (Böning et al., 2008; Meijers et al., 2012; Meijers, 2014) and can act to suppressed meridional exchange of tracers (Ferrari and Nikurashin, 2010; Thompson and Sallée, 2012). Frontal anomalies could also result in anomalous water mass properties being redistributed throughout the ocean by the strong zonal currents that compose the ACC (Sallée et al., 2008).

1.2 Water masses

The SO has a vital role in the global thermohaline circulation, hosting major regions of mixing and upwelling, and being responsible for the production and export of water masses that regulate the planetary - scale climate (Sverdrup et al. 1942; Schmitz 1996; Doney et al. 1998; Rintoul and Naveira-Garabato, 2013; Talley, 2013) (Fig 1.2). The strong north-south tilt of density surfaces associated with the eastward flow of the ACC exposes the deep layers of the ocean to the atmosphere at high southern latitudes. As a result waters that are several hundred years of old often comes into contact with the atmosphere, with which they can exchange heat and carbon (Lumpkin and Speer, 2007). Also new water masses including the comparatively light mode and intermediate waters that sink to a few

hundred meters depth and the dense bottom waters that flood the deepest layers of the global abyss are formed in this region (Johnson, 2008; McCartney, 1977). In this way, SO controls the connection between the deep and upper layers of the global overturning circulation and thereby regulates the capacity of the ocean to store and transport heat, carbon and other properties that influence climate.

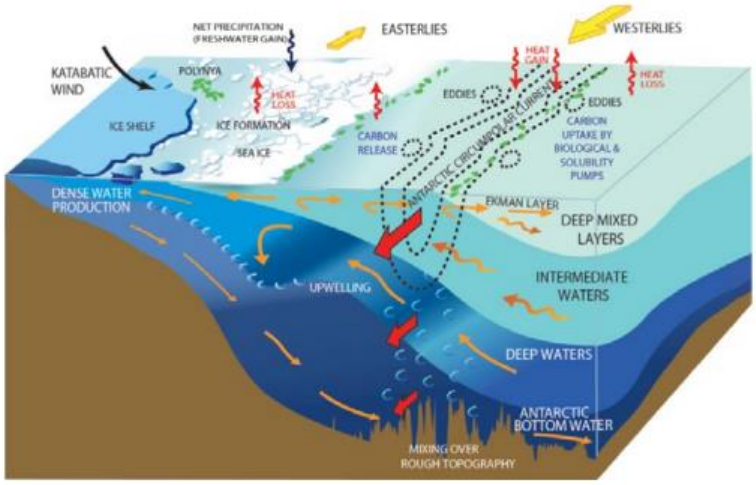

Figure 1.2. Cartoon of SO circulation, sea ice, and mixing, with Antarctica on the left. The entire water column interacts with the surface ocean and atmosphere by advection (straight arrows) and mixing (curly arrows) (after **(**CFSOA;Olbers, D;Speer, K. **)**)

The SO is the source of several intermediate and deep water masses of the world oceans that is one of the dominant driving forces for the global overturning circulation (Tomczack and Liefrient, 2005). The overturning circulation is the major mechanism for ocean heat transport and therefore has a strong influence on the global and regional climate patterns. One of the most important densest water masses of the global ocean, the Antarctic Bottom Water (AABW) is formed in the SO and is an important component of the lower limb of the global overturning

circulation. Another water mass, Circumpolar Deep Water (CDW) is found within the ACC and it is considered the most voluminous water mass of the world oceans (Worthington, 1981). A mixture of North Atlantic Deep Water, AABW and Antarctic Intermediate Water (AAIW), as well as recirculated deep water from the Indian and Pacific constitutes the CDW (Yu and Rienecker 2000). In winter, deep convection on the equator side of the ACC forms a vertically mixed layer known as Sub-Antarctic Mode Water (SAMW; McCartney, 1977). AAIW is located beneath the SAMW and both participate in ventilating the thermocline of the surroundings and of other oceanic regions as they spread northwards together with the deep waters generated within the SO (Rintoul and Bullister, 1999; Talley, et al., 2003). SAMW and AAIW are large volume, lower thermocline, and intermediate water masses that ventilate the intermediate depths of the ocean. It is through these two water masses that atmospheric gases enter the subtropical gyres and climatically and biologically important properties such as heat, freshwater, nutrients, and oxygen gets transferred into the interior ocean (Sallee et al., 2006; Talley et al., 2003; Talley 2008; Toggweiler et al., 1991). A significant fraction of anthropogenic CO_2 is also drawn down by SAMW and AAIW into the world's oceans (Mikaloff-Fletcher et al., 2006; Sabine et al., 2004). Thus, variations in SAMW and AAIW formation have an important role in climate variability and change

The water masses formed in the SO spread throughout the world ocean and the characteristics of more than 50% of the ocean volume reflect the ocean-atmosphere-ice interactions taking place in the SO. These water masses carry oxygen and CO_2 from the sea surface into the deep sea, to renew/ventilate the sub-

surface ocean. About one third of the CO_2 produced by human activities is accumulating in the ocean, slowing the rate of climate change due to the enhanced greenhouse effect. Of this, 40% is being sequestered in the SO by water masses sinking from the sea surface as part of the overturning circulation. In addition to gases the SO also absorbs heat from the atmosphere. The overturning circulation carries the excess heat from the surface down into the interior of the ocean, causing sea-level rise through thermal expansion. The formation, sinking and circulation of SO water masses will contribute to the regional distribution and rate of sea-level rise in the southern hemisphere as the Earth warms in response to the enhanced greenhouse effect.

1.3 Eddies

Satellite and in situ observations show that the SO is a very turbulent region (Sokolov and Rintoul, 2007a,b; Sallée et al., 2008). Satellite observations (Colton and Chase, 1983), buoy trajectories (Hofmann,1985), inertial jet models (Craneguy and Park, 1999) and hydrographic data (Lutjeharms and Baker, 1980; Park et al., 1993; Trathan et al., 1997) have revealed that high mesoscale variability in the SO is closely correlated with regions of prominent bottom relief. This variability also correlates closely with either the terminal region of a major western boundary current such as the Agulhas Current, or where the ACC interacts with prominent bottom topography such as in the Drake Passage or at the Crozet and Kerguelen Plateau (Lutjeharms and Baker, 1980). High eddy kinetic energy (EKE) bands are located in the western part of the global ocean basins and along the ACC and along the main oceanic frontal zones associated with major

currents (Jia et al., 2011; Richardson, 1983; Krauss and Kase, 1984). Most energetic regions coincide with the axis of the ACC (in particular over the Southeast Indian Ridge), the Agulhas Current, the East Australian Current separation, and the Brazil-Malvinas Current confluence (Wilkin and Morrow, 1994). These eddies play an important role in momentum and buoyance fluxes that can potentially influence the global thermohaline circulation (Hughes and Ash, 2001). Enhanced kinetic energy is known to increase the poleward heat flux (Hogg et al., 2008) that can inhibit meridional overturning circulation which is responsible for a large meridional transport of heat and vertical transfer of carbon dioxide between the surface layers and the deep ocean (Rintoul et al., 2001) by strengthening the vertical stratification. Eddies are responsible for a poleward heat flux and play a role in the time-varying heat budget of the SO (de Szoeke and Levine, 1981; Lee et al. 2007).

1.4 Sea Ice

The existence of sea-ice is another important factor contributing to the SO's influence on climate. Each winter, enough sea ice forms around the continent to double the area of Antarctica. Hypotheses, models and observations suggest that the Antarctic sea ice plays an important role in the state and variability of regional and global climate through the ice albedo feedback, insulating effect, deep water formation and fresh water budget (Fletcher, 1969; Walsh, 1983; Curry et al., 1995; Rind et al., 1995). Sea-ice is mostly made up of freshwater, so the salt in the seawater is left behind as the ice freezes, increasing the salinity of the water beneath the ice. Sea water gets denser as its salinity increases and as its temperature falls. In some locations, the cooling by the atmosphere and the salt

released from sea ice together make the water near Antarctica dense enough to sink from the sea surface to the deep ocean. The sinking near Antarctica forms one branch of the global overturning circulation. Changes in sea ice extent and the timing of ice-edge advance/retreat are thought to affect krill biomass (Ross et al., 2008; Steinberg et al., 2015), with potential impacts for krill-dependent fauna at higher trophic levels (whales, seals and penguins) (Massom and Stammerjohn, 2010; Ducklow et al., 2012; Constable et al., 2014; Saba et al., 2014). Sea ice covers vast regions of the SO, spreading over 18 x 106 km^2 in winter, although reducing to only 3 x 10^6 km^2 at its summer minimum (Parkinson, 2004). Sea ice also releases algae to the water as it melts in spring and summer, and this release can lead to major algal blooms near the ice edge (Arrigo et al., 2002), although, at the same time, the presence of sea-ice restricts sunlight to the underlying ocean and restricts the total level of SO primary production (Arrigo & Thomas, 2004).

The seasonal formation and melt of a vast area of Antarctic sea ice strongly influences the sea surface salinity, which in turn affects the density and stratification of SO, thus influencing the global climate and SO ecosystems (Massom & Stammerjohn, 2010). Growing evidence suggest that the SO and its sea ice cover have changed in recent decades. The ocean has warmed, freshened and acidified, and fronts have migrated, altering habitats (Böning et al. 2008; Gille 2008; Sokolov & Rintoul 2009). Sea ice has contracted in some areas while expanding in others, resulting in a net increase in overall extent (Stammerjohn et al., 2012; Holland, 2014). The SO is characterised by a temperature minimum subsurface layer (or Winter Water; WW) in the upper 300 m (Park et al., 1998), a peculiar feature of cold water acts as a physical vertical barrier in the upper layers

of the SO during summer. During the ice-free period, the ocean surface is exposed to winds, which enhances mixing, resulting in this temperature minimum layer becoming mixed with the surface and subsurface layers, thereby altering the heat budget of the region (Yuan et al., 2004). Since the WW has a close relationship with the heat budget, ice melt and freshening in the SO is believed to be a major source of micronutrients (Boyd & Ellwood, 2010), and may regulate the chlorophyll (Chl a) blooms in the region.

1.5 Changes in the SO

Changes in the physical and biogeochemical state of the SO are already underway. Many of the large-scale and regional changes in the physical and chemical components of the SO have been linked to changes in wind forcing, in particular the intensification and southward contraction of the circumpolar westerly winds associated with a positive trend of the Southern Annular Mode (SAM) (Thompson et al., 2000). Coarse-resolution models have suggested that the ACC transport is more sensitive to changes in wind forcing (Fyfe, 2006; Fyfe et al., 2007). The circumpolar SO is warming more rapidly, and to greater depth, than the rest of the global ocean (Gille, 2002; 2008). Warmer ocean temperatures have been linked to an increase in the basal melt rate and the retreat of grounding lines in Antarctica (Rignot et al., 2008). The upper layers of the SO have freshened as the result of increases in precipitation and the melting of floating glacial ice (Curry et al. 2003; Boyer et al., 2005; Böning et al., 2008). Freshening of AABW in the Indian and Pacific regions of the SO may also reflect an increase in basal melting of floating glacial ice (Jacobs, 2004; 2006; Aoki et al., 2005; Rintoul, 2007), with increased melt linked to increased heat flux from the ocean

(Shepherd et al., 2004; Rignot et al., 2008). There have been studies that have shown the warming, freshening, and slowdown of AABW formation (Purkey and Johnson, 2012). Salinity has decreased in the water masses exported from the SO in the upper limb of the overturning circulation (Aoki et al., 2005; Durack and Wijffels, 2010). Since SO processes influence the deep and intermediate water mass formation, biogeochemical cycles, sea-level rise, ocean acidification and marine productivity, hence the changes in the SO would have significant implications on global climate.

1.6 Objectives and Scope of the study

It can be said that the SO has received even less attention than the high northern latitude and the oceanic records are few and sparse (Nielson et. al, 2004). This situation is true in the Indian context as well. Even though oceanographic research in India has been in existence for more than four decades, most of the studies were concentrated on the Arabian Sea, Bay of Bengal or Indian Ocean basin and meagre attention was paid to the southern hemisphere. The contribution to global climate could be better understood by studying more about the circulation, air- sea exchange and sea-air- ice dynamics of this region. Also in a changing climate scenario, a systematic study is needs to be conducted in the SO to understand the frontal dynamics and water mass variability more precisely. The Indian Ocean sector of the SO (IOSSO) has an intricate frontal system of quasi-zonal fronts that merge, split, and steer over the variable bottom topography in the Crozet region and Kerguelen region. The identification of fronts and quantification of their meandering properties are essential elements in tracing upper-level ocean circulation. Also towards the southern part this region is the

site of an important confluence in the polar circulation between eastward extension of the Weddell Gyre in the west and the Prydz Bay gyre in the east. In this region the ACC and its southern fronts, i.e. the southern ACC front (SACCF) and Southern Boundary (SB), are forced southward closer to the Antarctic continent by the Kerguelen Plateau. The other major physical feature of this system is the annual advance and retreat of sea ice and its influence on SO. Considering the complex pattern of fronts, zones, water masses and sea-ice influence on the upper thermohaline structure in the IOSSO, the following objectives were formulated for this doctoral research.

Considering the complex pattern of the fronts and zones in the IOSSO, the following objectives were formulated for this doctoral research.

- To characterise the southern high latitude ocean based on various physico-chemical and biological parameters using in-situ, satellite and model data.
- To understand the effect of seasonal ice cover on the thermohaline structure.
- To study the frontal dynamics and water mass variability in the IOSSO

The thesis summarizes the doctoral research and is organized as follows.

Chapter 2 describes the various data sets that have been used in this thesis and Methodology followed to have a better understanding of the objectives proposed

Chapter 3 characterises the southern high latitude ocean based on various physico-chemical and biological parameters using in-situ, satellite and model outputs. The water masses have been further studied with respect to Dissolved Oxygen (DO), prevailing nutrients and Chl in the study area.

Chapter 4 explains the effect of seasonal ice cover on the thermohaline structure of the study area.

Chapter 5 describes the frontal dynamics and water mass variability in the IOSSO. Under this chapter three significant aspects of the study area has been addressed i.e. frontal variability, role of eddies and sea ice in modifying the thermohaline structure in the study area.

Chapter 6 summarizes the salient findings of this doctoral research

2. Materials and Methods

2.1 Study Area

The southwest Indian Ocean (Fig. 2.1) region needs to be investigated systematically since the data available from this region are sparse, hampering the knowledge regarding the influence of SO in the climatic changes. This region is characterized by the confluence of warm Agulhas Return Current (ARC) and Subtropical Convergence. The areas west of the Crozet Plateau and the east of Kerguelen-Amsterdam Passage are the key regions which have an intricate frontal system of quasi-zonal fronts that merge, split, and steer over the variable bottom topography.

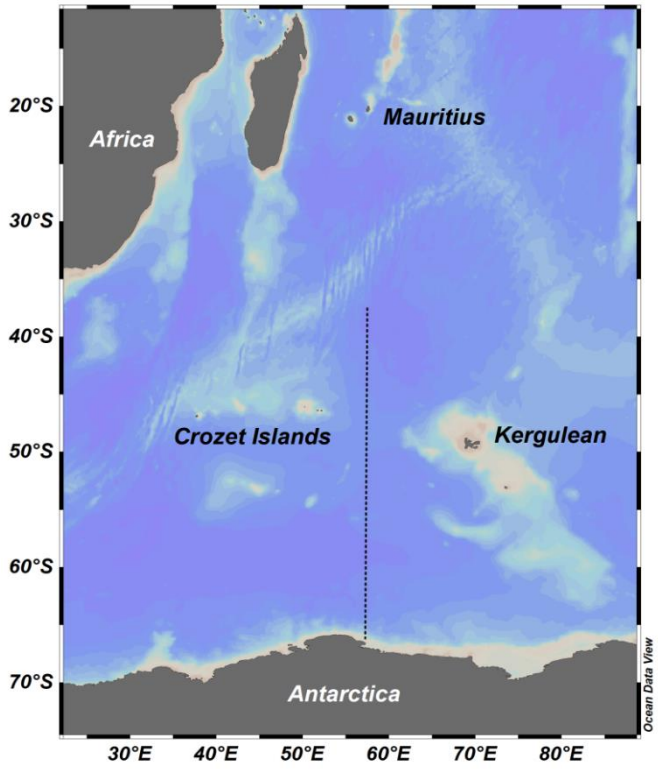

Fig 2.1 Map of study area showing the cruise track

2.2 Materials

2.2.1 In-situ data

Ship-based observation is the only method for obtaining high-quality measurements with high spatial and vertical resolution of a suite of physical, chemical, and biological parameters over the full ocean water column, and in areas of the ocean inaccessible to other platforms. As part of the Indian SO programme, expeditions have been conducted over the Indian Ocean Sector of Southern Ocean (IOSSO) during the austral summer for two years 2010 and 2011 (Table 2.1). During 2010, observations were made from 40°S 57° 30′E to the coastal waters of Antarctica (65°27′S 53°28′E) and during 2011, observations were made from 40°S to 60°S along the meridional section 57°30′E (Fig 2.2).

High resolution hydrographic data was collected across various fronts using both Conductivity Temperature Depth (CTD) and Expendable Conductivity Temperature Depth (XCTD) probes. A CTD (make: Sea-Bird Electronics, USA; temperature precision: $\pm$0.001°C, conductivity: $\pm$0.0001 S/m and depth $\pm$0.005% of the full scale) and XCTDs (Make: Tsurumi-Seiki Co. TSK Ltd., Yokohama, Japan. type: XCTD-3; precision $\pm$ 2% of depth, $\pm$ 0.03 mS/cm for conductivity, and $\pm$ 0.02°C for temperature) were deployed to collect the temperature and salinity profiles. The salinity data from CTD were calibrated against water samples analyzed using a high-precision salinometer (Guildline AUTOSAL).

Cruise	Vessel	Duration	Instrument Used
SOE-2010	ORV Sagar Nidhi	February 2010	CTD, XCTD,
SOE-2011	ORV Sagar Nidhi	February 2011	CTD, XCTD

Table 2.1 Details of expedition and instrument used

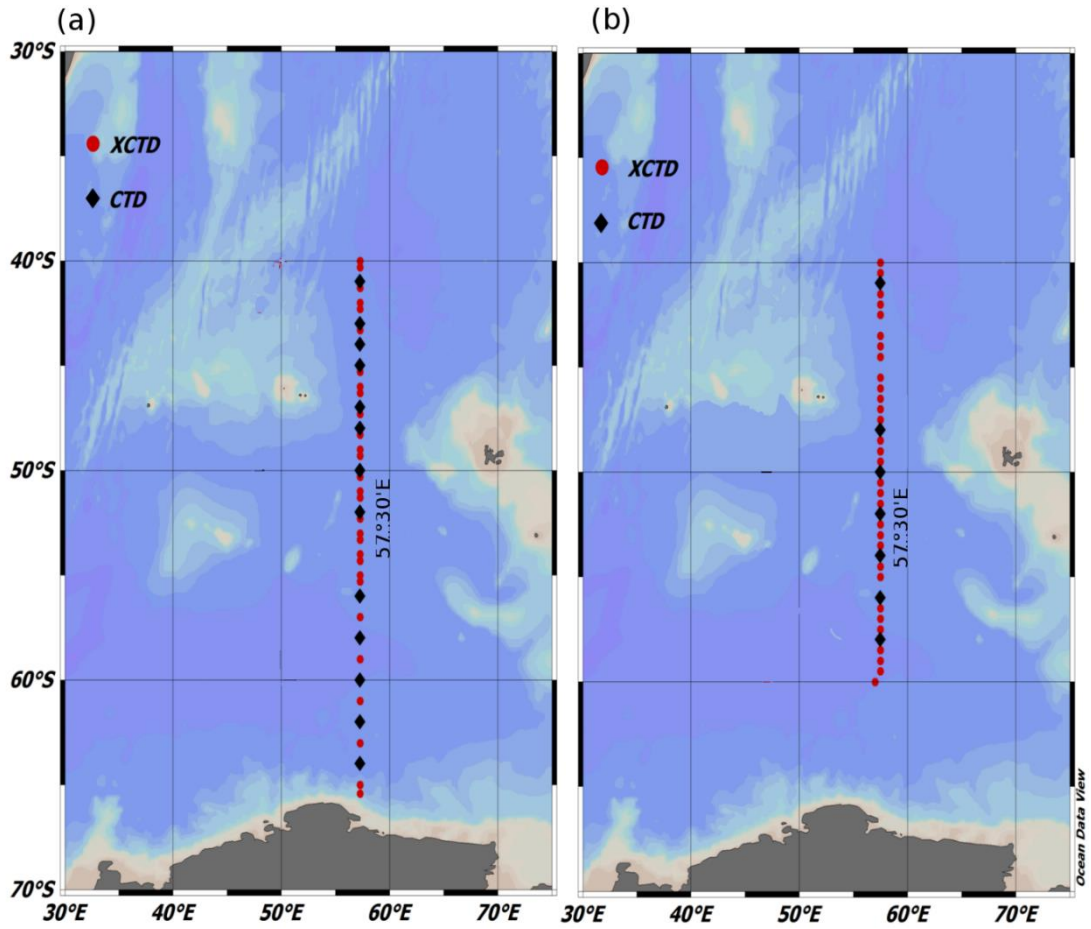

Fig 2.2 CTD and XCTD locations in (a) February 2010 and (b) February 2011

2.3 Other Data sets used

2.3.1 SST

Monthly SSTs from the Group for High Resolution Sea Surface Temperature (GHRSST) on 1/4° grids (http://podaac.jpl.nasa.gov/dataset/NCDC-L4LRblend-GLOB-AVHRR_ AMSR_OI) was used to identify the fronts in the study region.

2.3.2 Winds

The Advanced Scatterometer (ASCAT) on the Meteorological Operational (MetOp) satellite of the European Organization for the Exploitation of Meteorological Satellites (EUMETSAT) is a C band radar, whose primary objective is to determine the wind field at the ocean surface (Figa-Salda˜na et al. 2002). Monthly ASCAT wind stress, Ekman current data from ERDDAP were used.

2.3.3 Sea-Level Anomaly (SLA)

In addition to in-situ data the fronts were identified using Maps of Absolute Dynamic Topography (MADT) from CLS/Archiving, Validation and Interpretation of Satellite Oceanographic (AVISO). The MADT is the sum of the sea level anomaly data and a mean dynamic topography (Rio05-Combined Mean Dynamic Topography (CMDT) (Rio and Hernandez, 2004)). Satellite-derived SLA maps overlaid by the geostrophic velocities were utilized to show the presence of eddies in the study area. Geostrophic velocities were downloaded from AVISO (http://www.aviso.oceanobs.com/duacs/). Satellite altimeter SLA

data were obtained from AVISO on a 1/3 Mercator grid at 7 day intervals 24. Contour maps of dynamic height were prepared using the SLA data.

2.3.4 Surface Currents

Ocean Surface Current Analysis–Realtime (OSCAR; http:// www.oscar.noaa.gov) data were used to plot surface ocean currents (Bonjean & Lagerloef, 2002)

2.3.5 Sea Ice

The ice coverage data has been obtained from the Advanced Microwave Scanning Radiometer for EOS (AMSR-E) which is a passive microwave radiometer on the Aqua satellite that measures the radiance of microwave radiation from the Earth's surface. The Hadley Centre Global Sea Ice and Sea Surface Temperature (HadISST) (1 x 1°) has also been used and it is a combination of monthly globally complete fields of SST and sea ice concentration for 1871-present.

2.3.6 Chlorophyll (Chl a)

Mean monthly Moderate Resolution Imaging Spectroradiometer (MODIS)- chl-a at 9-km spatial resolution has been used to study the chl a distribution in the study area

2.3.7 Climatology data

In addition, the World Ocean Atlas 2013 version 2 (WOA13 V2) ; a set of objectively analyzed (1° grid) climatological fields of temperature, salinity, dissolved oxygen, Apparent Oxygen Utilization (AOU), percent oxygen saturation, phosphate, silicate, and nitrate at standard depth levels for annual,

seasonal, and monthly compositing periods for the World Ocean has been used to understand the variability of nutrients with various water masses. This dataset also includes associated statistical fields of observed oceanographic profile data interpolated to standard depth levels on 5°, 1°, and 0.25° grids. In this study the 1° resolution data has been used.

2.3.8 International Comprehensive Ocean-Atmosphere Data Set (ICOADS)

The ICOADS Data Set offers surface marine data spanning the past three centuries, and simple gridded monthly summary products for 2° latitude x 2° longitude boxes back to 1800 and 1°x1° boxes since 1960. To understand the long term changes in the sea surface temperature (SST), air temperature, wind and sea ice concentration were studied using ICOADS data sets (1°x1°)

2.3.9 Climatic Indices

The Southern Annular Mode (SAM) and Multivariate Enso Index (MEI) from the NOAA Climate Prediction Center website (http:// www.esrl.noaa.gov/psd /data/climateindices/list) were used to understand the long term variability of SAM and ENSO.

2.3.10 Model data

The ECMWF (ORAS4) model data output was also used in the study. The model uses the NEMO V 3.0(Madec, 2008), in the ORCA1 configuration (approximately 1 x 1° with equatorial refinement) and gives data from 42 levels in the vertical, 18 of which are in the first 200 m (http://apdrc.soest.hawaii.edu/). Atmospheric derived daily surface fluxes are used to force this ocean model. Daily fluxes of

solar radiation, total heat flux, evaporation-minus-precipitation and surface wind stress are taken from the ERA-40 reanalysis (Uppala et al., 2005) from September 1957 to December 1989, ERA Interim reanalysis (Dee et al., 2011) from January 1989 to December 2009, and the ECMWF operational archive from January 2010 onwards. ORAS4 has been produced by combining the output of an ocean model forced by atmospheric reanalysis fluxes and quality controlled ocean observations every10 days. These consist of temperature and salinity (T/S) profiles from the Hadley Centre's EN3 data collection (Ingleby and Huddleston, 2007), which include expendable bathythermographs (T only, with depth corrections from Table 1 of Wijffels et al. [2008]), conductivity-temperature-depth sensors (T/S),TAO/TRITON/PIRATA/RAMA moorings (T/S), Argo profilers (T/S), and autonomous pinniped bathythermograph(or elephant seals, T/S). Altimeter-derived along track seaORAS4 has been produced by combining the10 days output of an ocean model forced by atmospheric reanalysis fluxes and quality controlled ocean observations. Gridded maps of SST from NOAA are used to adjust the heat fluxes via strong relaxation, and altimeter global mean sea-levels are used to constrain the global average of the fresh-water flux. The ocean model horizontal resolution is approximately 1, refined meridionally down to 1/3 at the equator. There are 42 vertical levels with separations varying smoothly from 10 m at the surface to 300 m at the bottom, with partial cell topography.

2.4 Methods

2.4.1 Frontal Identification

Oceanic fronts were identified using the characteristic property indicators following the criteria listed by Peterson and Whitworth (1989); Park et al. (1993); Belkin & Gordon (1996), Sparrow et al. (1996), Holliday & Read (1998), Kostianoy et al.(2004), and Billany et al. (2010) [Table 2.2].

Front	**Temperature**	**Salinity**
Northern Subtropical Front (NSTF)	21–21–221–22 ℃ at surface	surface salinity ~35.5
Agulhas Return Front (AF)	19–17 ℃ at surface; 10 ℃ isotherm from 300 to 800 m	35.54–35.39 at surface; 35.57–34.90 at 200 m
Southern Subtropical Front (SSTF)	17–11 ℃ at surface; 12–10 ℃ at 100 m	35.35–34.05 at surface; 35–34.6 at 100 m; 34.92–34.42 at 200 m
Subantarctic Front (SAF1)	11–9 ℃ at surface; 8–5 ℃ at 200 m (along 45°E) 11–10 ℃ at surface; 8–5°Cat 200 m (along 57°30′E)	34.0–33.85 at surface; 34.40–34.11 at 200 m

Subantarctic Front (SAF2)	7–6 °C at surface 4° C isotherm at 200 m depth (along 45°E) 9–8°C at surface 4° C isotherm at 200 m depth (along 57°30′E)	surface salinity ~33.85 south of SAF
Polar Front 1 (PF1)	5–4 °C at surface northern limit of the 2 °C isotherm below 200 m	33.8–33.9 at surface
Polar Front 2 (PF2)	3–2 °C at surface	33.8–33.9 at surface
Southern Antarctic Circumpolar Current Front (SACCF)	Temperature maximum T_{max}>1.8°C	Salinity maximum S_{max}>34:73
Southern Boundary of ACC (SB)	1.5 °C isotherm	

Table 2.2 Properties used for frontal identification

2.4.2 Water mass Properties

The different water masses found in the study area was demarcated using the criteria followed by authors such as Anilkumar et al., 2006 (Table 2.3).

Water mass	**Characteristics**			**Depth (m)**
	Temperature (°C)	**Salinity**	**Density (kg m^{-3})**	
Subtropical Surface Water (STSW)	> 12	> 35.1		0-200
Subantarctic Surface Water (SASW)	9	<34		0-200
Antarctic Surface Water (AASW)	<5	<34		0-200
Sub Tropical Mode Water(STMW)	11 to 14	35 to 35.4	26.5 to 26.8	400-700
Antarctic Intermediate Water (AAIW)	~4.4	~34.42	~27.24	700-1200m
Circumpolar Deep Water (CDW)	~2	~34.77	~27.8	2000-3800m
Antarctic Bottom Water (AABW)	~− 0.165 to − 0.62	~34.67 to 34.652	~27.85 to 27.85	>3000m

Table 2.3 Properties used for water mass identification

2.4.3 Freshwater thickness

The thickness of fresh water input in the surface layer relative to WW in the study region was estimated using the formula of Park et al. (1998):

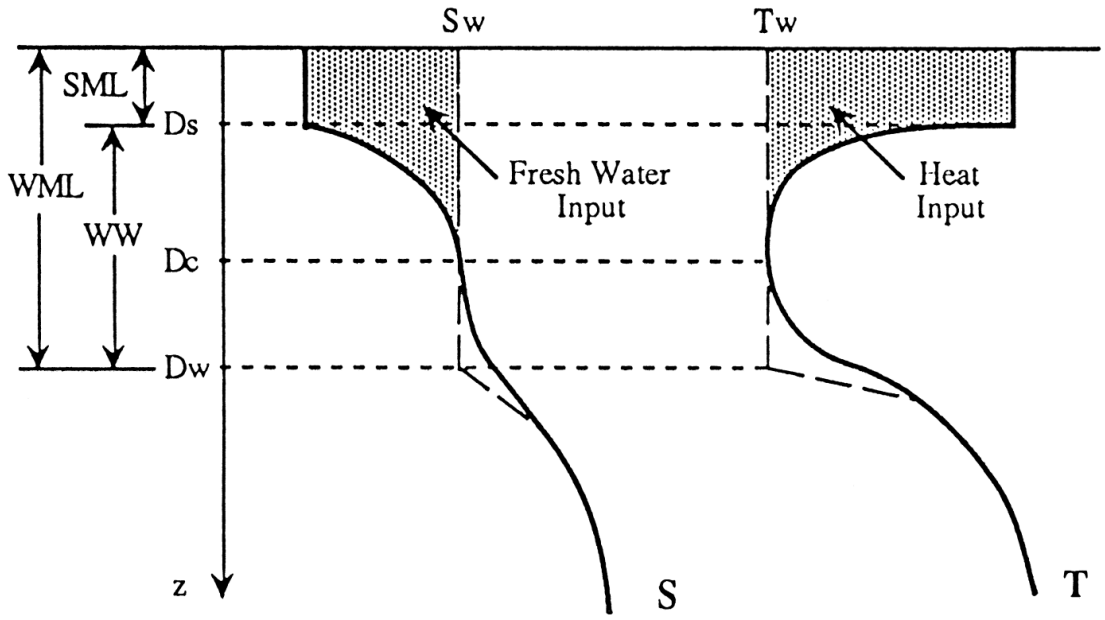

Fig. 2.3 Schematic of typical vertical profiles of temperature *T* and salinity *S*. in summer (Taken from Park et.al., 1998). Dashed vertical lines indicate the hypothetical profiles of the winter mixed layer (WML) temperature (*T*w) and salinity (*S*w), which are homogeneous down to the depth *D*w. *D*s and *D*c denote the surface mixed layer (SML) depth and Winter Water (WW) core depth, respectively.

$$h=\frac{D_C(S_W-S^{bar})}{S_W},S^{bar}=\frac{1}{D_C}\left[\int_{-D_C}^{0} Sdz\right],$$

Where h is the thickness of the freshwater input per unit surface area, D_c is the WW depth, S_w is the WW salinity, and S^{bar} is the depth-averaged salinity between the surface and WW depth.

2.4.4 Eddy Kinetic Energy (EKE)

EKE was calculated by using the following formula

$$EKE = \frac{1}{2}\left(u^2 + v^2\right)$$

where u and v are zonal and meridional geostrophic current components

2.4.5 Geostrophic Velocity

Geostrophic velocity was calculated using the SLA data following the below mentioned formulae by Pond and Pickard (1978)

$$U = {}^{-g}\!\!\diagup_{f}\left(\frac{\partial SLA}{\partial y}\right)$$

$$V = {}^{-g}\!\!\diagup_{f}\left(\frac{\partial SLA}{\partial x}\right)$$

Where g is the acceleration due to gravity and f is the Coriolis force and u and v are the geostropic velocity components

2.4.6 Eddy tracking

From the maps, dynamic heights > 20 cm were considered as anticyclonic eddies and those < –20 cm corresponded with cyclonic eddies. The eddies observed in the study area were visually tracked in order to have an understanding of their time and location of evolution. They were tracked for a period of eight months in the time span ranging from October 2010 to May 2011. The position of the eddy cores was identified from the weekly maps and then the track followed by them was plotted.

3. Characterization of the southern high latitude ocean based on various physico-chemical and biological parameters using in-situ, satellite and model data

3.1 Introduction

Satellite and *in situ* observations showed that the SO is a very turbulent region (Sokolov and Rintoul 2007; Sokolov and Rintoul 2007; Sallée et al., 2008). This is particularly true for the ACC which flows eastward not as a homogeneous wide flow but in the form of a number of quasi-permanent circumpolar jets which are characterised by enhanced meridional gradients of water properties(Deacon 1937; Nowlin and Clifford 1982; Orsi et al. 1995; Belkin and Gordon 1996). These jets are limited by fronts that dynamically separate water masses. Their positions are determined by topographic steering (Gordon et al., 1978; Rintoul and Sokolov 2001) and wind stress curl (Nowlin and Klinck, 1986). (Belkin and Gordon, 1996) have shown that Southern Indian Ocean has a complicated frontal system of quasi-zonal fronts with remarkable regional differences which is determined by peculiarities of bottom topography. The ACC is characterized by multiple narrow frontal jets. From north to south, the fronts and zones of the SO are: the Sub Tropical Front (STF), Subantarctic Front (SAF), Polar Front (PF) and Antarctic Zone (AZ) (Whiteworth, 1980, Orsi, 1995). The ACC, is steered by topography, such that

the position and structure of its jets and fronts deviate from the zonal direction, both spatially (Sokolov and Rintoul, 2009) and temporally (Chapman and Morrow, 2014). These fronts can influence the upwelling and ultimate ventilation of deep waters, which can in turn affect the formation of watermasses at the surface (Böning et al., 2008; Meijers et al., 2012; Meijers, 2014) and can act to suppressed meridional exchange of tracers (Ferrari and Nikurashin, 2010; Thompson and Sallée, 2012). Frontal anomalies could also result in anomalous water mass properties being redistributed throughout the ocean by the strong zonal currents that compose the ACC (Sallée et al., 2008). Also, approximately 80% of the net heat content increase in the Southern Hemisphere oceans appears to have occurred south of 30° S, largely within the ACC (Gille, 2008). A number of studies have noted that the warming trend identified in the ACC region has been characterized as being consistent with displacing the ACC poleward by about 1° latitude every 35 years (Gille, 2008; Sprintall, 2008; Morrow, et. al., 2008). This complex frontal system also plays a key role in the global carbon cycle. The upwelling deep water south of the PF brings to the surface dissolved nutrients and carbon dioxide (CO_2), and releases this gas to the atmosphere. In contrast, the Intermediate Water and Mode Water masses sinking north of the PF transport heat, carbon and other properties into the ocean interior. The balance between upwelling and outgassing versus subduction of carbon into the ocean interior determines the strength of the SO sink of CO_2. This balance depends on wind forcing and eddy dynamics of the ACC. The location and intensity of ACC fronts have a significant influence on the heat, salt, and nutrient exchange in the world ocean (Rintoul and Sokolov,

2001) as part of the global meridional overturning circulation (MOC). Hence understanding the structure and location of the major fronts of the SO is of considerable importance. In this chapter the physical parameters are utilised to demarcate the fronts and watermasses and in addition chemical and biological parameters are further analysed to see if they follow the same zonation.

3.2 Results and Discussion

An attempt has been made to study the different fronts and water masses in the study area using physical, chemical and biological parameters. Temperature, salinity, SST gradient and Maps of Absolute Dynamic Topography (MADT) are the factors that have been considered under the physical parameter. Under chemical parameters, Dissolved Oxygen (DO) and nutrients have been selected and Chl a has been associated with biological parameter.

3.2.1 Temperature and Salinity

The Indian sector of SO has a complicated frontal system of quasi-zonal fronts with remarkable regional differences, determined by peculiarities of bottom topography (Park et al., 1993; Belkin and Gordon 1996; Kostianoy et al., 2004). Recognition of the multiple branches of the SO fronts helps in reconciling the differences between front locations determined during the earlier observations. The intensity of the fronts (as measured by the cross-front gradients of sea surface height) varies along the fronts and the individual

branches merge and diverge, often in response to interactions with bathymetry (Sokolov and Rintoul 2007, 2009). The frontal structures are more complex in the western region of the Indian sector of the SO due to the influence of the Agulhas Retroflection and bottom topography (Belkin and Gordon, 1996). The SO features several frontal systems that together form the eastward flowing ACC. Various fronts of the ACC in their circumpolar path accord with precise contours of sea surface height and the earlier reports that portrayed the concurrence of frontal positions located from both MADT and *in-situ* hydrographic data (Sokolov and Rintoul, 2007; Swart et al., 2008; Sokolov and Rintoul, 2009; Swart et al., 2010). As the ACC plays a major role in the climate system (Gordon 1986; Rintoul, 1991; Speich et al., 2001) it is imperative to study the ACC fronts in detail.

The Subtropical Front (STF) in the southern hemisphere is a major zonal oceanic feature in the Indian, Pacific, and Atlantic Oceans between 30°S and 40°S (Belkin and Gordon 1996, Fig.5) and is a boundary between subtropical waters and subantarctic waters (Deacon, 1937; Hamilton, 2006). Lutjeharms and Valentine (1984) described a broad frontal zone in the subtropical region and named it as subtropical frontal zone. The STF is differentiated by a zonal band of enhanced meridional sea surface temperature (SST) and sea surface salinity (SSS) gradients and it lies towards the pole ward side of the Subtropical Convergence Zone (SCZ) (James et al., 2002). Studies have shown that this front is extending from the coast of Argentina around 30°S, then gradually shifting southward to 40°S south of Africa and along the same position in the

Indian and central Pacific Ocean and again shifts northwards to the coast of Chile around 25°S (Tomczak and Godfrey,1994). The STF separates the subtropical gyres form the eastward flowing ACC (Stramma and Peterson, 1990; Stramma, 1992; Stramma et al.,1995). Jasmine et al. (2009) reported that frontal zones and frontal regions exhibited wide differences in hydrography as well as biological characteristics. The STF defines the southern limit of the subtropical gyres, separating them from the broad westward flow of the Circumpolar Current which lies further south (Stramma and Peterson, 1990; Stramma, 1992; Stramma et al., 1995). Another peculiarity of this front is that it is located in a region of short term and seasonal variability with a high incidence of eddy formation and eddy shedding (Hamilton, 2006) and is also known to be a region of enhanced primary productivity and water mass formation.

The Antarctic Polar Front (PF), or Antarctic Convergence, is circumpolar in nature and marks the location where Antarctic surface waters moving northward sink below Subantarctic waters (Deacon, 1933). Previous studies (Botnikov, 1963; Lutjeharms and Valtentine, 1984; Moore et al., 1997, 1999a) suggested that the Antarctic PF has both surface and subsurface expressions. It is commonly defined by the northernmost extent of the subsurface temperature minimum (Tmin) cooler than 2°C, where the Tmin ends or dips abruptly below 200 m (Belkin and Gordon, 1996).The southern ACC front (SACCF) and southern boundary of ACC (SB) shall be identified from the most southerly position of the sub-surface 1.8 and 1.5 °C isotherms, respectively.

Temperature and salinity section along 57°30'E during 2010 are presented in Fig. 3.1a and b. Along this transect, the SSTF was noted between 41°S and 45°S; SAF1 between 45°S and 47°S; SAF2 between 47°S and 48°S; PF1 between 50°S and 52°30'S and PF2 as a wide front between 55°S and 59°30'S. SACCF was demarcated between 60°S and 61°S and the SB, between 64°S and 64°30'S. Holliday and Read (1998) reported the occurrence of STF between 40°S and 42°S along 55°E. During 2004, along 57°30'E, the merged Agulhas Front (AF) and Subtropical Front were identified between 43°30'S and 45°S, SAF1 and SAF2 between 45°30'S and 46°30'S and south of 47°S, respectively (see Figs. 5 and 6 in Anilkumar et al. 2006).

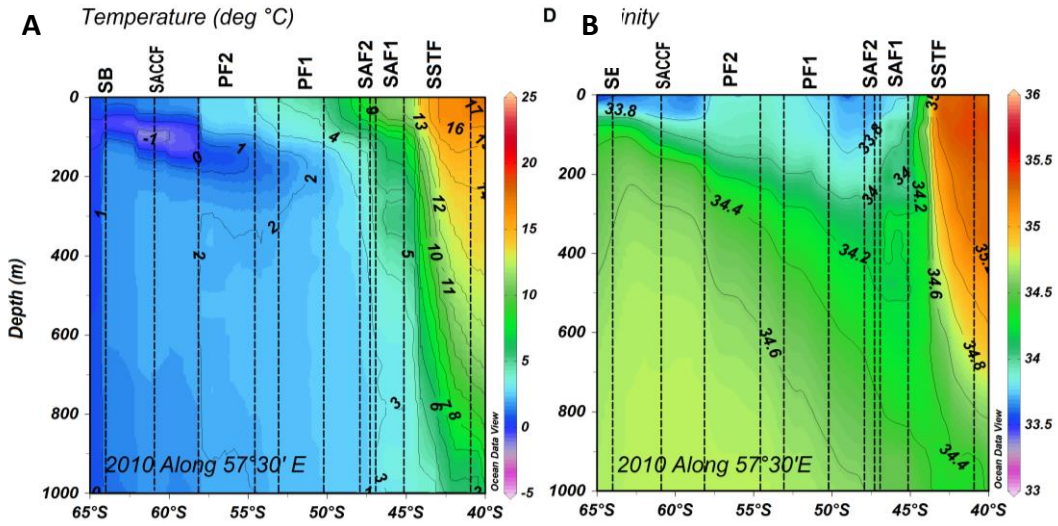

Figure 3.1 Vertical structure of (a), temperature (°C) and (b) salinity along 57 °30'E in 2010

During 2011 AF+SSTF+SAF1 was identified as a merged wide frontal system between 40°30'S and 46°30'S (Fig. 3.2 a and b). East of 54°E, this merged frontal system has been reported as the Crozet Front by Belkin and Gordon

(1996). Park et al., (1993) Sparrow et al., (1996) and Kostianoy et al., (2004) have reported this merged frontal system with more spatial variation compared to the present findings. The SAF2 was identified between 46°30'S and 47°30'S. PF1 was identified between 50°30'S and 52°S. PF2 was observed as a relatively wider front between 53°30'S and 56°30'S along 57°30'E. Moore et al., (1997, 1999) used satellite SST maps to study the dynamics of the PF, which showed its position between 49°30'S and 52°S, but this is not compatible with the position of PF1 and PF2 identified in this study. During 2011 the AF was identified as a separate front, thereby confirming the earlier finding of Belkin and Gordon (1996). Kostianoy et al., (2004) opined that the AF's cyclonic meander can increase the distance between the AF and STF/SAF up to 3° of latitude.

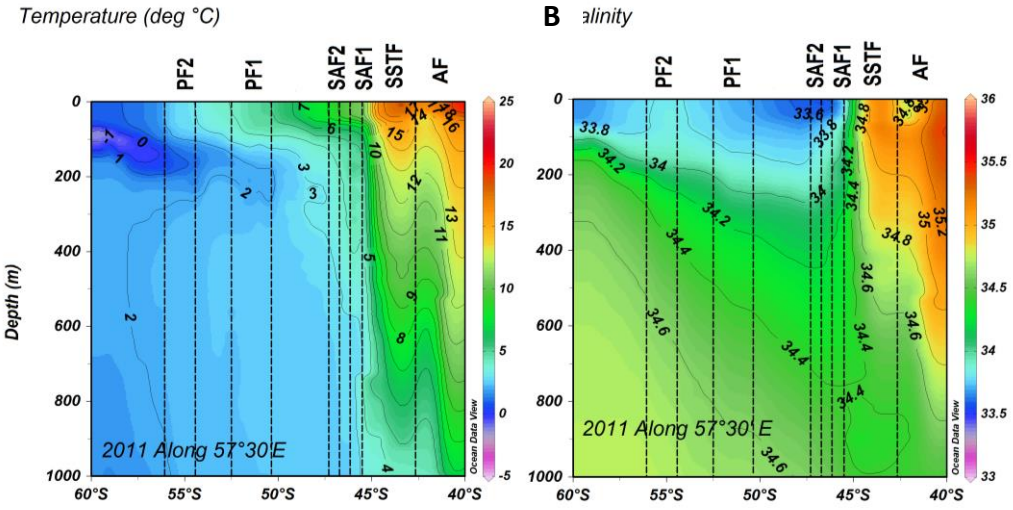

Figure 3.2 Vertical structure of (a), temperature (°C) and (b) salinity along 57 °30'E in 2011

Gladyshev et al., (2008) reported that the locations of the SAF, PF and SACCF are controlled by the neighbouring ridges. Compared to the previous studies

(Park et al., 1993; Belkin and Gordon 1996; Sparrow et al., 1996), some differences were noted in the position of the SAF in the present study. SAF was distinguished as SAF1 and SAF2 along all the tracks. In earlier reports it was observed as surrounding the Crozet Plateau (Moore et al., 1999). Holliday and Read (1998) reported a width of ~1.5° latitude along 45°E for SAF. Lutjeharms and Valentine (1984) reported the width of SAF as ~2.5° latitude. These results attest to the significant inter-annual variability in the frontal systems of the SO.

3.2.2 MADT and SST Gradient

Following the method of Swart & Speich (2010), the mean MADT calculated from 1992 to 2010 was used to compute the meridional gradients per 100 km of mean MADT. These gradients were then used to identify the core locations of various fronts 57°30 ′E (Fig. 3.3). Swart & Speich (2010) suggested that isolines of MADT coincide with constant water mass.

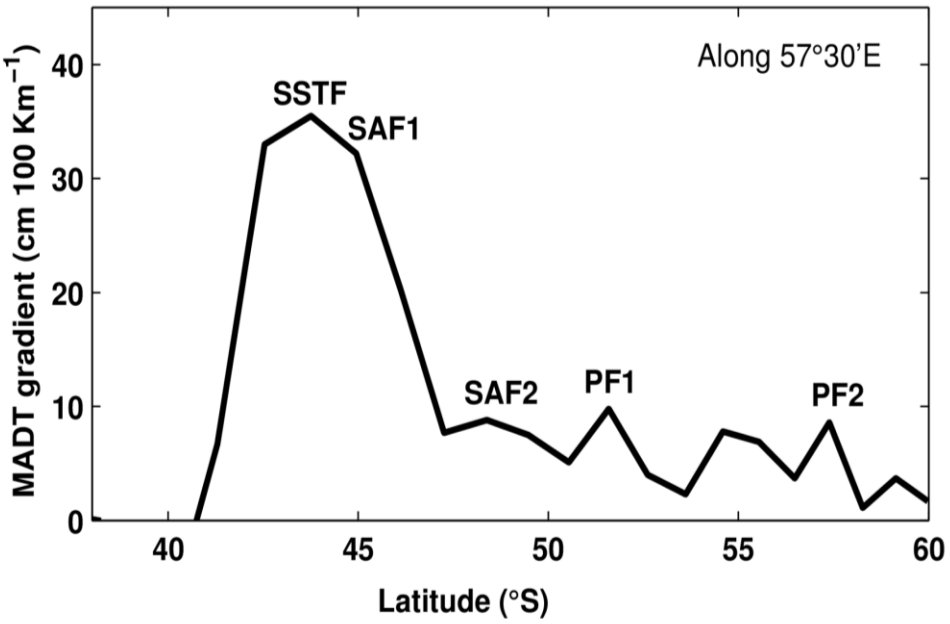

Figure 3.3 Mean MADT gradient (cm 100 km− 1) (computed from weekly MADT data from 1992 to 2010

Along 57°30 ′ E, the SSTF, SAF1 and SAF2 were identified at 43°30 ′ S, 45°S and 48°30 ′ S, respectively. Further, the PF1 and PF2 were observed at 51°30 ′ S and 57°30 ′ S, respectively. The locations of the gradient maxima and the associated lines of MADT were almost identical to the frontal positions identified using the hydrographic data. Also the core locations of fronts derived from the satellite SST were consistent with those of the hydrographic data (Fig 3.4).

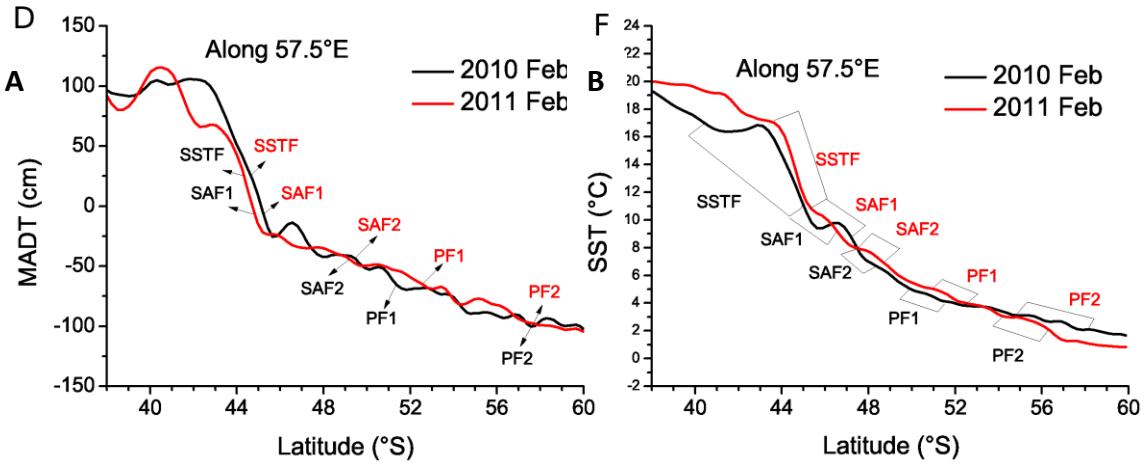

Figure 3.4 Core frontal locations determined using MADT and frontal location and its width using satellite SST (GHRSST) along 57°30 ′ E.

3.2.3 Water mass

The water masses were identified based on the scatter plots of Potential temperature (θ °C)–Salinity (S) criteria put across by various studies and the nature of the individual water masses is discussed below.

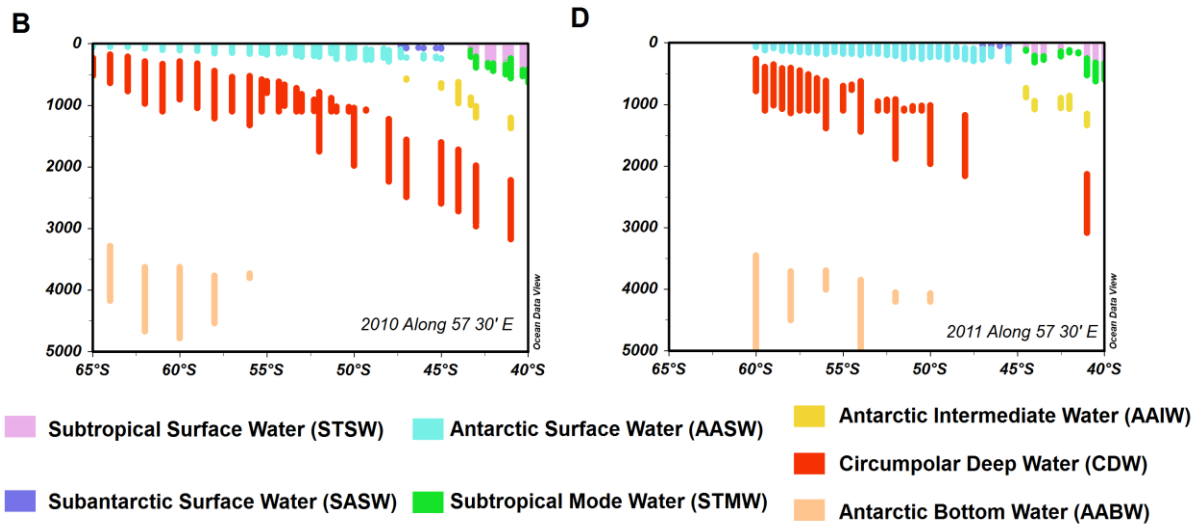

Figure 3.5 Water masses along 57°30'E A, 2010 and B, 2011

The subtropical surface water (STSW) is characterized by high salinity water (S>35.1) with temperature θ >12°C above 200m depth. The STSW is observed north of the subtropical front (STF). Subantarctic Surface Water (SASW) is found between the STF and the SAF (Deacon, 1937; Read and Pollard, 1993). It is characterized by low temperature and salinity (θ=9 °C, S<34.0) (Park et al., 1993). Antarctic Surface Water (AASW) can be identified by the characteristic (θ <5 °C, S<34.0). The AASW is typically encountered at the PF (Anilkumar et al., 2006, Luis and Sudhakar, 2009). The Subtropical Mode Water (STMW) is formed by wintertime convection in the area immediately north of the ACC and appears as a pycnostad or thermostad below the seasonal pycnocline (Park et al., 1993, Stramma and Lutjeharms, 1997). This water mass is characterized by a wide range of property (11 < θ < 14 °C; 35.0<S<35; 26.5<σ_θ<26.8 kg/m^3). The features of AAIW characterized by its properties (θ~4.4 °C; salinity minimum (S_{min}) ~34.42 and σ_θ~27.24 kg/ m^3) (Anilkumar et al., 2006). AAIW is formed continuously near the PF spanning 50° to 55°S, where water with θ~2.2 °C and S~33.87 sinks and spreads northward (Sverdrup et al., 1942). Fine (1993), Toole and Warren (1993) reported that the region near the Kerguelen Plateau is a source of AAIW entering Indian Ocean and confined its presence in the Crozet Basin. AAIW is generally found between the depths of 800 to1200 m in the southwest Indian Ocean (Wyrtki, 1971). The Circumpolar Deep Waters CDW, which occurs below the AAIW, is the voluminous water mass in the SO with its remarkable features (θ~2 °C; S~34.77; and σ_θ~27.8 kg/m^3). It occupies the depth range 2000–3800 m north of 45°S and it rises sharply to shallower depths towards the south. The

Antarctic Bottom Water (AABW) has a range of characteristic properties, $\theta \sim -0.165$ to -0.62 °C, S~34.671 to 34.652 psu and $\sigma_\theta \sim 27.848$ to 27.856 kg/m^3 at 4100 to 4700 m depth (Anilkumar et al., 2006).

Signatures of the STSW was observed up to 44°S in 2010 and 45°S in 2011 along 57°30 ′E. The signatures of the STMW that were observed in the present investigation were similar to those reported previously by McCartney (1977) and Park et al., (1991), whereas Tsubouchi et al. (2010) observed its signatures in the regions 28°E –45°E and 60°E –80°E. The STMW can be identified in the depth range of 400 to 700 m, with a potential density anomaly range of 26.5 to 26.8 kg/m^3, where the potential density pycnostad develops (Park et al., 1993). It has been reported that the STMW is formed in the Crozet Basin (Fig. 4 of Belkin & Gordon 1996). Along 57° 30 ′E, the STMW was identified up to 44°S and 45°S in 2010 and 2011, respectively. The Antarctic Intermediate Water (AAIW) from the southwest IOSSO is the dominant AAIW type east of the Agulhas Current retroflection (Roman & Lutjeharms, 2010). The AAIW identified in the Crozet Basin mainly originates from the region near the Kerguelen Plateau (Molinelli,1981; Fine, 1993; Toole & Warren, 1993). The depth of this water mass has been reported to be between 1000 and 1300 m (Park et al., 1993; Bindoff & McDougall, 2000). In the present study, the features of the AAIW were observed between 1000 and 1500 m. The southward extent of the AAIW was observed up to 45°S in 2010 and 2011 along 57°30 ′E. Signatures of the Subantarctic Surface Water (SASW) were observed between 45°S and 47°S along 57°30 ′E. The Antarctic Surface Water

(AASW) was identified up to 45°S along 57°30 ′E in 2010 and 2011. The CDW was identified up to 58°S –60°S along 57°30 ′E. However, the CDW was observed deeper than 2000 m north of 45°S, and its northward intrusion was seen beyond 42°S during 2010 and 2011. According to Toole & Warren (1993), the CDW occupies a depth range of 2000 –3800 m north of 45°S and rises sharply to shallower depths south of this latitude. A northward intrusion of AABW was observed up to 56°S. The temperature minimum layer (1.4 ℃ lower than the surface temperature) was located at 50–200 m, south of 50°S in the study region in both 2010 and 2011. This temperature minimum layer corresponds with the AASW and is capped above the CDW (Yuan et al., 2004), and can be attributed to the WW. Below this layer, the temperature gradually increased by 2 ℃ up to 350 m and then exhibited isothermal characteristics further down.

Water masses are often characterised by their conservative thermohaline properties. However, it is possible to infer water sources and movement in relation to chemical concentrations in the ocean (Keeling & Bolin, 1967). Biogeochemical and physical processes determine the nutrient and oxygen distribution in the world's oceans. Despite their non-conservative properties, chemical tracers like nutrients and oxygen can help us to more accurately define water masses and can indicate processes that have occurred along their path. Oxygen content in seawater is controlled by direct fluxes from the atmosphere when the water mass is formed, and by respiration and photosynthesis. The flux of atmospheric oxygen into seawater is temperature

dependent, with colder water absorbing more oxygen than warm water. (McGrath et. al., 2012). Natural sources of nutrients to the open ocean are from atmospheric deposition, nitrogen fixation, land erosion and volcanic activity, while anthropogenic inputs from agriculture, industry and fossil fuel consumption may also reach the open ocean via rivers, rainfall and the atmosphere. Biological drawdown of nutrients through photosynthesis, remineralisation of organic material and physical mixing, largely determine the vertical profile of nutrients in the ocean (Williams and Follows, 2003).

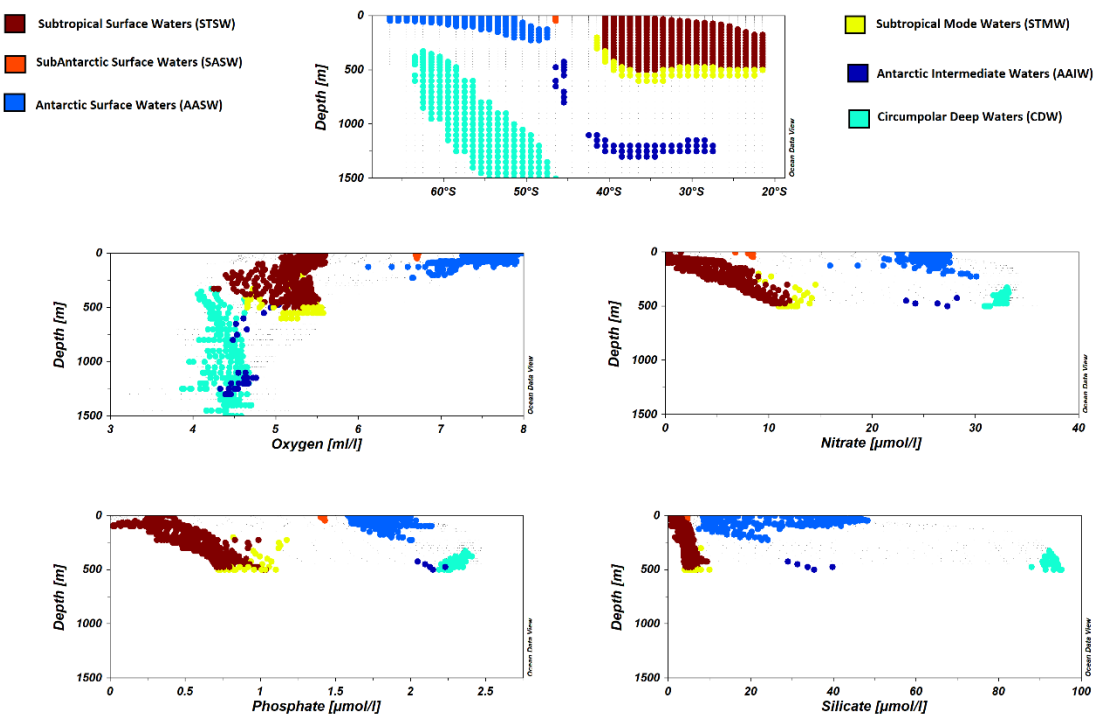

Figure 3.6 Dissolved oxygen and Nutrient variability along 57°30'E

Persistently high nutrient concentrations especially nitrate (NO_3), phosphate (PO,), and silicic acid ($H4Si0_4$), in Antarctic surface waters are distinctive

characteristics of the Southern Ocean (Harrison and Cota, 1991). Nutrient concentrations south of the Polar Front (50°S) are among the highest in any surface waters in the world; NO3, H4Si04, and PO, levels in summer can exceed 20 mmol/m^3, 50 mmol/m^3, and 2 mmol/m^3, respectively (Priddle et al., 1986; Jones et al., 1990). Though nutrient concentrations decrease in response to the phytoplankton growth cycle, they are rarely consumed to depletion, even during massive blooms (El-Sayed, 1984).

The distribution of DO and Nutrients is described by Fig. 3.6. The STSW is observed to have oxygen concentration in the range of 4-5.5 ml/l. The nutrient concentration in this water mass is relatively low with nitrate showing values ranging from 0-12 µmol/l phosphate values from 0-1 µmol/l and silicate from 0-15 µmol/l. The SASW is has oxygen concentration in the range of 6.5-7 ml/l. The nutrient concentration in this water mass is as follows with nitrate showing values ranging from 5-10 µmol/l phosphate values from 1-1.5 µmol/l and silicate from 0-10 µmol/l. The AASW exhibits the highest oxygen concentration in the range of 6-8 ml/l. Nitrate values fall in the range from 20-30 µmol/l phosphate values are between 1.5-2.5 µmol/l and silicate from 15-45 µmol/l

The STMW has oxygen values in the range from 4.5-5.5ml/l. The nitrate values in the watermass is from 10-15 µmol/l. Phospate and silicate values are 0.75-

1.25 µmol/l and 0-15 µmol/l. The AAIW shows values ranging from 4-5ml/l. This water mass has nitrate concentration in the range 20-30 µmol/l, phosphate in the range of 2-2.5 µmol/l and silicate in the range 25-40 µmol/l.

The CDW has oxygen values in the range from 4-4.5ml/l. The nutrient values are as follows with nitrate concentration lying between 30-35 µmol/l, phosphate concentration lying between 2-2.5 µmol/l and silicate concentration lying between 80-100 µmol/l.

3.2.4 Chlorophyll

Chl a concentration in the SO are typically quite low despite the high concentrations of the nutrients in the surface waters. Hence, the SO is known as the largest high nutrient-low Chl (HN-LC) regions in the world ocean. Light limitation through deep mixing (Mitchell et al., 1991; Nelson and Smith, 1991), grazing pressure (Dubischar and Bathmann, 1997), non availability of trace metal (Martin and Fitzwater, 1988; Martin et al., 1990), photosynthetic rate limited by low water temperature (Tilzer et al., 1986; Sakshaug and Slagstad, 1991) are some of the reasons attributed for the low productivity in this region. However, these limitations are ameliorated in the region of the marginal ice zone (MIZ). Input of low saline water through sea-ice melting and through elevated levels of micronutrients in coastal waters perhaps stimulate the significant phytoplankton blooms in the SO (Smith and Nelson, 1985, 1986; Park et al., 1999).Previous studies (Jasmine et al., 2009; Gandhi et al., 2012) have reported that the SSTF is one of the most productive regions in the SO.

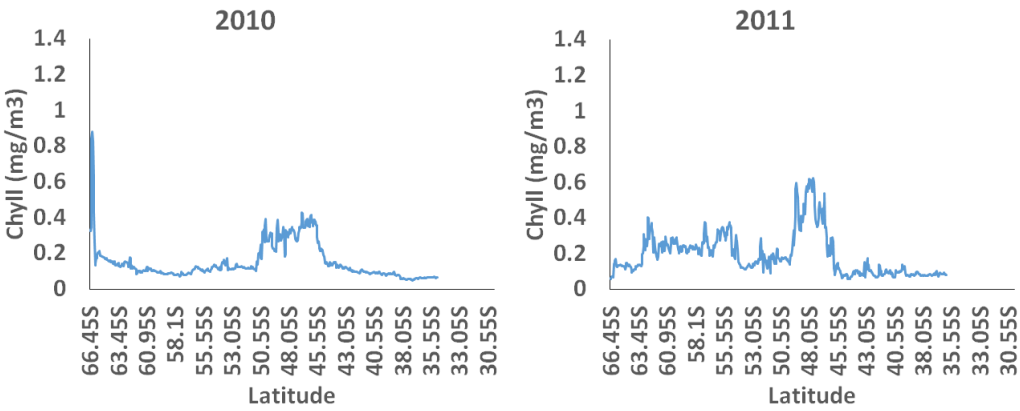

Figure 3.7 Monthly Chl a (mg m−3) along 57°30'E (A) 2010 and (B) 2011.

In the present study (Fig 3.7) the SSTF was characterised by high surface concentrations of Chl a (> 0.24 mg/m^3) along both transects during 2010 and 2011. However, a higher concentration of Chl a was observed during 2010 (0.5 mg/m^3) than 2011 (0.24 mg/m^3). Higher values of Chl a (~0.8 mg/m^3) was observed in the coastal waters of Antarctica as compared to the subtropical waters (~0.5 mg/m^3) in 2010. In 2011 other than in the STF no high values of Chl a were observed elsewhere. The influence of low saline waters due to melting of ice and snow from the Antarctic continent could be the major cause for the high concentration of Chl a observed near the coastal waters of Antarctica

3.3 Conclusion

In this chapter an attempt has been made to characterise the southern high latitude ocean based on various physico-chemical and biological parameters using in-situ and satellite and model outputs. The fronts and water masses in the study region is well identified using in-situ data. MADT and satellite

derived SST gradients can be used as an additional tool for the identification of various fronts in the study area. The watermasses has been further studied with respect to DO, prevailing nutrients and Chl a in the study area. It is noticed that the surface watermasses in the polar region are rich in oxygen concentration whereas the Intermediate waters and Subtropical watermasses are relatively poor in oxygen concentration. With respect to nutrients concentration, the watermasses in the polar region again show higher nutrient concentration in comparison to the watermasses in the tropical region. The CDW shows the highest concentration of nutrients as compared to the watermasses identified in the study area. The Chl a distribution shows higher values in the Subtropical frontal region but for the other fronts the concentration is lower except for the Antarctic coast which shows high value for one year. Even though DO, nutrients and Chl a in the study area showed clear discrimination between polar and subtropical waters, these chemical and biological indicators may not be useful tool for the identification of watermasses in the study area since its distribution mainly depends on the different scale physical and biological processes occurring in that region.

4. Effect of seasonal ice cover on the thermohaline structure.

4.1 Introduction

The upper ocean structure south of the PF (in the AZ) in austral summer shows a relatively warm, fresh and well mixed surface layer which lies above a subsurface temperature minimum layer (T_{min}) or winter water (WW) (Chaigneau et al., 2004). The WW is formed by winter cooling and is the remnant of the previous winter mixed layer capped by seasonal warming and freshening (Deacon, 1937). This WW is characterized by a temperature minimum subsurface layer in the upper 300 m (Park et al., 1998). The boundary between the surface mixed layer (SML) and the WW is marked by the strong seasonal thermocline, halocline, and pycnocline. The SML and WW constitute the AASW in summer sections. The lower boundary of WW is also demarcated by relatively strong vertical gradients of temperature and salinity, but it is not so evident in the vertical density structure. Due to the stable stratification, the lower part of the winter surface layer cannot be reached by the heating from the surface and so it keeps its near-freezing temperature. During the ice free period, the exposure of ocean to the wind enhances mixing and this WW gets mixed with surface and sub surface layers and alters the heat budget (Yuan et al., 2004). The salinity of the WW plays a significant role in the stability of the upper water column, as a higher WW salinity

will ease convective overturning (Behrendt et. al., 2013). Water mass properties in the WW core therefore reflect the integrated variability of air-sea-ice interactions, and so it is one of the key layers in tracing the effects of climate variability (Aoki et al., 2013).

The AASW acquires its low salinity during its flow around Antarctica (Gordon and Molinelli, 1982; Sievers and Nowlin, 1984) as freshwater is supplied by melting of glacial ice and sea ice, and from the excess of precipitation over evaporation. This continuously modified water mass is advected northward by Ekman transport and eastward by the geostrophic flow. Crossing the PFs to the north, it can modify the properties of the mode and intermediate water masses, which are formed and subduct north of these fronts (Rintoul and England, 2002). Observations in the Drake Passage has shown that changes in two important water masses namely the SAMW and AAIW are dependent on variations in WW properties resulting from fluctuations in wintertime air-sea turbulent heat fluxes and spring sea ice melting, both of which depend strongly on the intensity of (partially ENSO and SAM-forced) meridional winds to the west of the Antarctic Peninsula (Meredith et. al.,2008).

Sea ice forms mostly in open leads near the coast and is transported by wind and currents farther north, exporting very large amounts of fresh water from the SO's shelf seas (Silva et. al., 2006). The effect of the melting of icebergs (and ice shelves) differs from precipitation or sea ice melting in that the fresh water can be released below the very cool surface WW, and by mixing with the warmer CDW

it may increase its buoyancy and cause warm water intrusions at the surface (Jenkins, 1999). This has the effect of warming the surface, potentially reducing sea ice formation and increasing the water column stability. Winter sea ice reduces the heat and momentum fluxes between the atmosphere and ocean. After the ice melts, the upper ocean is exposed to the atmosphere and the surface forcing directly influences its structure. Therefore, the length of the ice-free period since the previous winter and the strength of surface wind stirring during this period are two major factors determining the temperature structure in the upper ocean (Yuan, 2004).

The SO plays pivotal roles in the meridional overturning circulations of the global oceans. Salinity and freshwater flux, which is defined as precipitation plus glacial and sea-ice meltwater minus evaporation, are key factors that affect the overturning circulations. The freshwater flux provides positive buoyancy forcing, which transforms upwelled deep water into lighter surface water (Warren et al., 1996). Precipitation dominates evaporation in the SO and glacial melt supplies freshwater to the ocean. Sea ice also contributes to the freshwater redistribution: melting of sea ice adds freshwater, while sea-ice formation increases salinity of the underling seawater there. Studies in the Weddle Sea (WS) has shown that three processes are potentially responsible for water mass properties variations of the WW in the Weddell gyre namely variation of the interactions with the underlying waters, variations of sea-ice formation and variations of external freshwater sources (Behrendt et al.,2013).

Due to the close relationship of WW with ice melt and freshening in the polar ocean; the study of WW has climatic importance. Further this WW is believed to be a major source of micro nutrients in the region (Boyd and Ellwood, 2010) and eventually regulating the Chl a blooms in the region. The region between 30 and 80°E is relatively poorly sampled in comparison with other regions around Antarctica. This region is the site of an important confluence in the polar circulation between the region west of Weddell-Enderby Land, Kerguelen Plateau to the north and the Australian-Antarctic Basin to the east. The survey region is contained inside the Weddell-Enderby basin, with the Kerguelen Plateau immediately to the north-east and the shallowest point of the Princess Elizabeth Trough (PET) to the east. Also it is here that the ACC and its southern fronts, i.e. the southern ACC front (sACCF) and Southern Boundary (SB) (Orsi et al., 1995), intrude into the domain from the north, are forced southward by the Kerguelen Plateau, and flow eastward through the PET, thus, making it an interesting region to study.

4.2 Results and Discussion

The WW depth *Dc*. is defined as the WW core depth where the absolute minimum of subsurface temperature is observed. This depth is different from the total winter mixed-layer depth (Dw), which is difficult to determine from summer sections, because the boundary with the underlying CDW is not sharp but appears more rounded, due probably to turbulent diffusion and mixing processes across the boundary. The same is true at the upper boundary of the WW with the summer

mixed layer (SML). The WW properties are thus represented best by property values at *D*c.

The temperature minimum layer (reduction from surface values by ~ 1.4°C) was located between 50 and 200 m south of 50°S in the study region in 2010 and 2011 (Fig.2). This temperature minimum layer corresponds to AASW and capped above the CDW (Yuan et al., 2004). This subsurface minimum layer can be attributed to the WW. Below this layer the temperature increased gradually by ~2°C up to 350 m and further down the temperature exhibited isothermal characteristics. Following Park et al. (1998) WW depth (D_c) is defined as the WW core depth where absolute minimum in subsurface temperature is observed. In both sections during 2010 and 2011 the WW was noted up to PF1 from south. The temperature and core depth of WW from south to north increased in all sections. The shallowest WW depth is noted in the Antarctic divergence region (~63°S to 60°S). In general cooler WW was noted during 2011 compared to that of 2010. Further fresh water thickness computed following Park et al. (1998), showed higher values during 2011 (~53.47m) than that of during 2010 (~ 51.69) (Fig. 4.1).

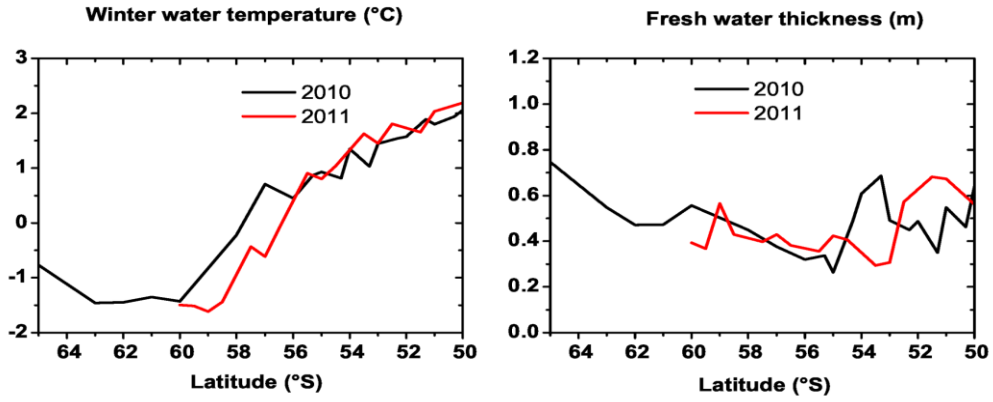

Fig 4.1 WW temperature and Freshwater thickness (m) along 57°30'E in 2010 and 2011.

This layer of low temperature, the WW, is the result of surface freshening during austral summer, mainly because of ice melting and subsequent warming of surface layer (Park 1993). The other mechanism involved in the surface freshening may be the precipitation and advection of melt water. A low value of precipitation (30 cm/yr) at 50°S has been reported by Bromwich et al., (1995), based on the analysis of zonal averaged net precipitation derived from the ECMRWF.

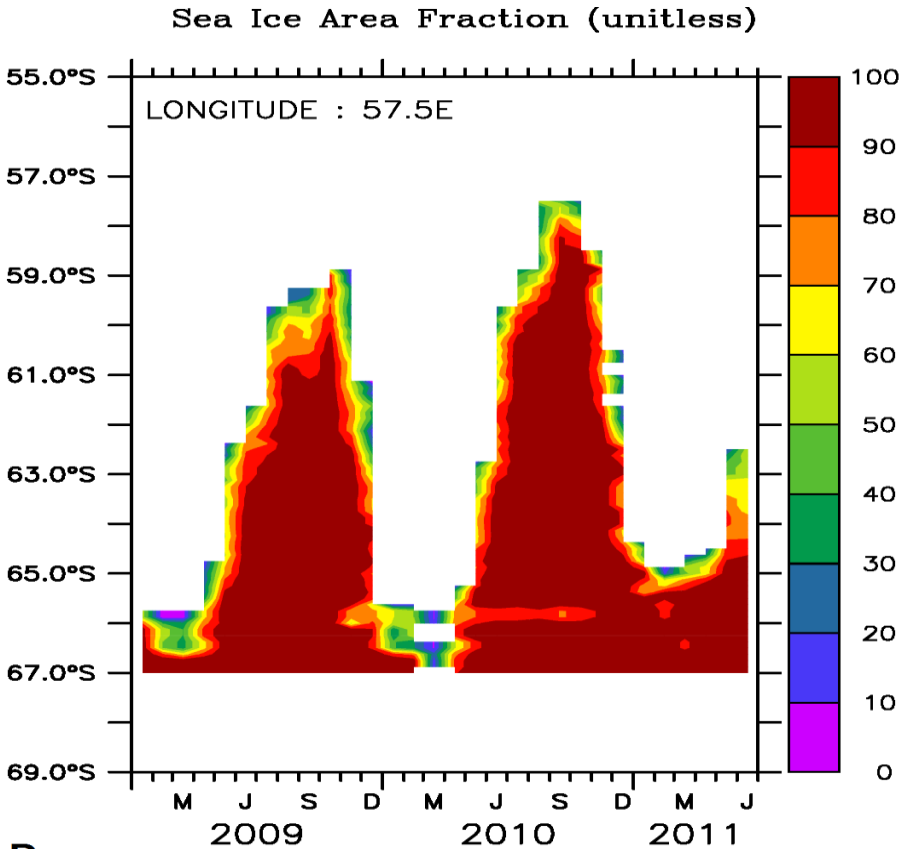

Fig 4.2 Sea ice fraction derived from AMSRE along 57°30' E

In the present study, the freshwater input received south of 50°S is not attributed to net precipitation. The source of fresh water could be the locally produced melt water or/and advection from *insitu* melting of sea ice originating from the south and west. It can be seen that the maximum sea ice limit was up to ~59°S during 2009 winter and up to ~57°S during 2010 winter (Fig 4.2).

The peak extent of sea ice was in September and then it started to melt till March. This increase of sea ice and its northern extent during 2010 winter compared to that of 2009 winter can be a reason for the increased fresh water thickness and cold WW temperature observed in the summer of 2011. The Ekman currents overlaid on the averaged wind stress suggest northward Ekman transport of melt water from south (Fig. 4.3). It could also be noted that the high stress patch (~0.3 Pa) of westerlies centred at 50°S during February 2010 was shifted further south to 56°S during February 2011. The increase in the northward Ekman transport from south (~60°S) during February 2011 could be due to the southward shift of the westerlies. This shifting of westerlies can be a manifestation of positive SAM (SAM index 0.86) during 2011 February and negative SAM (SAM index -2.12) during 2010 February (Marshall, 2003). Thus the increased northward Ekman transport of melt water from south also can be a reason for the comparative increase in freshwater thickness during February 2011. Recent studies suggest an increased rate of melting in the Bellingshausen - Amundsen Sea, west of the Antarctic Peninsula (Pritchard et al., 2012; Rignot et al., 2013) and this low saline melt water perhaps carried by the ACC enters the Indian Ocean sector. Hence, the melt water transported

from west of the Antarctic Peninsula may also contribute to low saline waters observed in the Indian Ocean sector of SO. Previous studies suggested that generally Ekman currents are weak compared to the background geostrophic currents (Lenn and Chereskin, 2009). It is also expected that melting in the Weddell Sea would have contributed to the observed freshwater thickness; however the northward flow in the Weddell sea was found to be weak during 2010 summer (Fig. 4.3). The Weddell Gyre is a cyclonic circulation regime centred at ~30°W and it has a major role in transferring heat and salt from the ACC to the Antarctic continental shelves (Orsi et al.,1993) which eventually helps in the sea ice melting in the region.

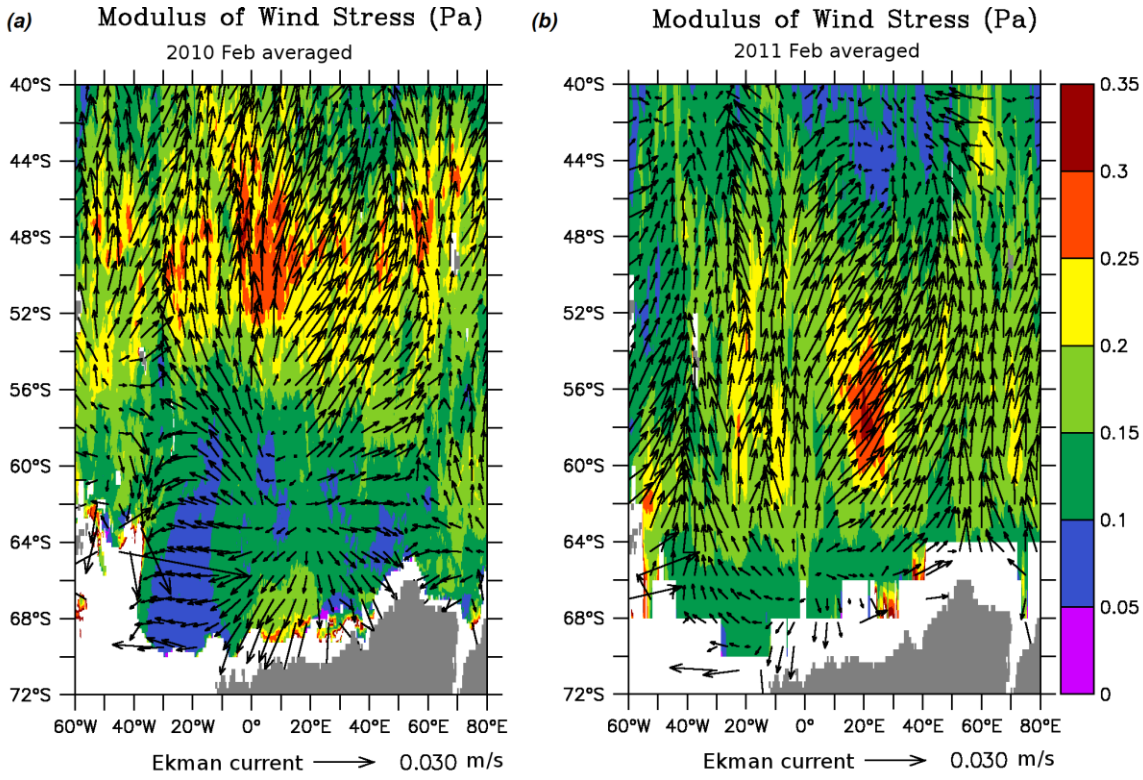

Fig 4.3 Wind stress (Pa) overlaid by Ekman currents (m/s) derived from ASCAT during 2010 February and 2011 February.

One of the major constraints for the Chl a production in the SO is the low availability of micronutrients, especially iron (Holm-Hansen et al., 2005). In general, PF2 region between 40°E and 60°E which is deeper than 2000 m is less Chl productive. It was reported earlier that in oceans associated with deep bottom topography, the supply of iron from bottom to surface through upwelling associated with deep currents of ACC is very less (Sokolov and Rintoul 2007b, Holm-Hansen et al. 2005).

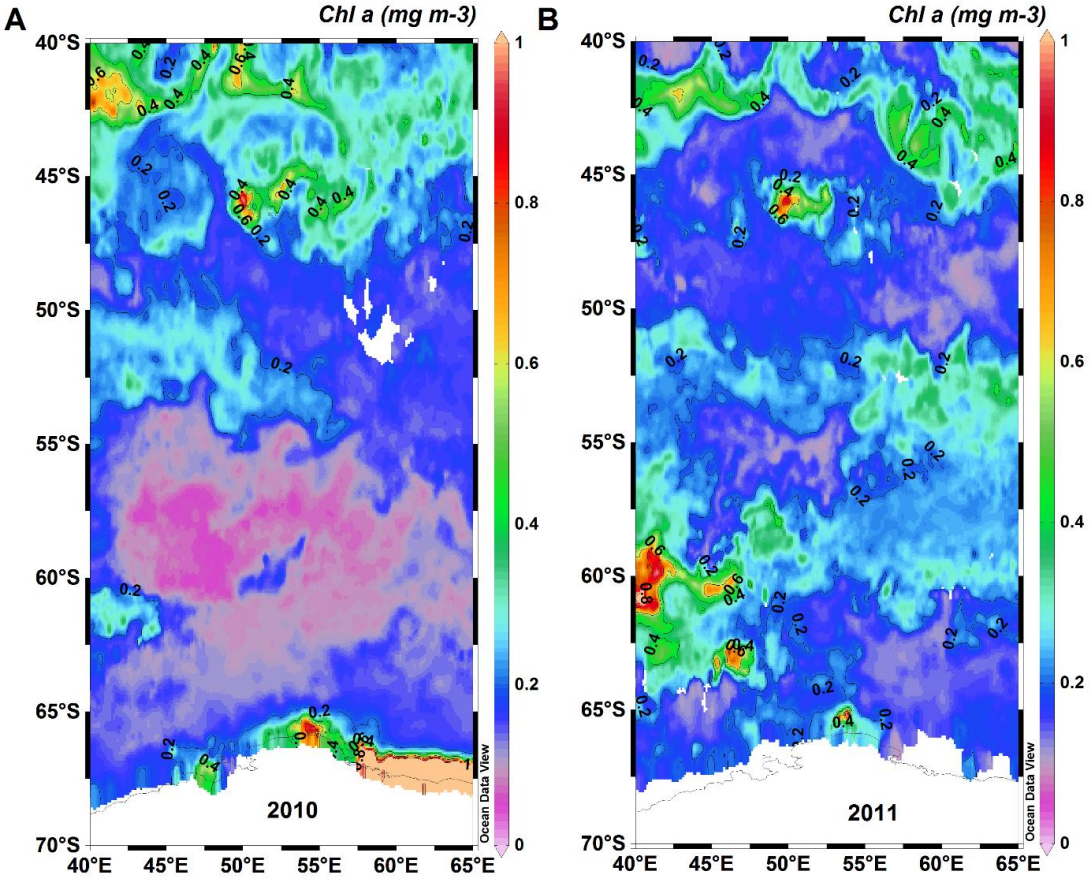

Fig 4.4 Monthly Chl a (mg/m^3) images over the study area during 2010 and 2011.

The relatively high value of Chl a observed at PF2 in 2011 compared to that in 2010 can be attributed to the increased sea ice amount and northward sea ice extent (Fig 4.4) during the 2010 winter compared to 2009 winter. Melting sea ice is known as one of the major sources of iron because of the accumulation of aeolian deposition (Gao et al., 2003) and subsequent release during the ice melting period. The supply of micronutrients resulted from the melting of sea ice perhaps increased the Chl a concentration (Boyd and Ellwood, 2010). Melt water can also enhance stratification resulting in shallow mixed layer leading to increased light availability for phytoplankton growth (Park et al., 2014). Increased fresh water thickness seen in the hydrographic section during 2011 February also supports the observed high Chl a. A high value of the *in situ* Chl a concentration was observed in the coastal waters of Antarctica (~4 mg/m^3) during 2010. The monthly averaged satellite data during 2010 and 2011 also showed high value of Chl a (~0.8 mg/m^3) in the coastal region (Fig. 5). Elevated levels of micronutrients in the coastal waters from glacial melting perhaps stimulate the significant phytoplankton blooms in the SO (Smith and Nelson, 1985; Park et al., 1999). Previous studies reported that the SO is a high nutrient-low Chl (HN-LC) region due to light limitation through deep mixing (Mitchell et al., 1991; Nelson and Smith, 1991), grazing pressure (Dubischar and Bathmann, 1997), non availability of trace metal (Martin et al., 1990), photosynthetic rate limited by low water temperature (Tilzer et al., 1986; Sakshaug and Slagstad, 1991). However, the high concentrations of Chl a observed south of PF1 during 2011 in the present investigation can be

attributed to the local melting of sea ice and advected melt water from south and west.

4.3 Conclusion

In this study it was noticed that the temperature and core depth of Winter Water (WW) increased from south to north. The shallowest WW depth is noted in the Antarctic divergence region (~63°S to 60°S). Cooler WW was noted during 2011 compared to that of 2010. Fresh water thickness computed showed higher values during 2011(~53.47m) than that of during 2010 (~ 51.67m). The source of fresh water could be the locally produced melt water or/and advection from in-situ melting of sea ice originating from the south and west. During 2009 winter the maximum sea ice limit was up to ~59°S whereas in 2010 winter it was upto ~57°S. This increase of sea ice and its northern extent during 2010 winter compared to that of 2009 winter can be a reason for the increased fresh water thickness and cold WW temperature observed in the summer of 2011. The high value of Chl a observed at PF2 in 2011 compared to that in 2010 can be attributed to the increased sea ice amount and northward sea ice extent during the 2010 winter compared to 2009 winter.

5. The frontal dynamics and water mass variability in the Indian Ocean sector of Southern Ocean

5.1 Overview

The standout feature of the SO circulation is the presence of the strong circumpolar eastward flowing current; the ACC. The past five to six decades have shown that there is a distinct pattern of change over the SO, the winds that force it and the cryosphere to the south (Gille, 2014). Hydrographic data indicate that the SO has undergone significant warming in the past five to six decades (Böning et al., 2008; Gille, 2008) and suggest that 80% of the observed SO warming has occurred south of 30°S. This warming could be assumed to be a potential source of heat that might contribute to destabilization of the ice shelves around Antarctica and eventually to accelerate sea level rise (Jacobs et al., 2011). The warming trend identified in the ACC region has been characterized as being consistent with displacing the ACC poleward by about 1° latitude every 35 years as noted by earlier studies (Gille, 2008 ; Sprintall,2008; Morrow et. al., 2008). As the ACC is topographically constrained in some locations and more free to migrate in other areas (Gille, 1994; Dong, 2006), its poleward displacement would not be expected to be uniform. Glaciers around the Antarctic Continent have

experienced rapid melting, particular for glaciers with outlets in the Amundsen Sea Embayment, though also near 80°E and 120°E (Rignot, 2008). These regions are located where the ACC flows near the Antarctic continent leading to speculations that changes in the ACC could be responsible for delivering supplemental warm CDW to the Antarctic marginal seas, thus contributing to basal melting of the Antarctic ice shelves, and reducing the efficacy of the ice shelves in buttressing the continental glaciers (Jacobs et. al., 2001; Pritchard et. al., 2012). The recent circulation changes have been confirmed by measurements of dissolved passive tracers (Waugh et al., 2013; Waugh, 2014). The dense waters originating around the Antarctic continent via intense air–sea–ice interaction over the continental shelf regions, including exchanges with the Antarctic ice sheet (Gill, 1973; Foster, 1976) are key components of the global ocean circulation (Lumpkin, 2007). These waters which get exported northward cool and ventilate much of the global ocean abyss (Johnson, 2008; Orsi et. al., 2001). The SAM is an index for winds that drive the ACC and it has shown to have increased over the past several decades (Marshall, 2003; Fyfe, 2006). The SAM is a measure of the pressure difference between Antarctic and mid-latitudes, and increase in the SAM index translates into winds that are both stronger and further poleward. Climate models simulated pronounced internal decadal to multi-decadal SAM variability with most of the studies attributing it to the combined anthropogenic effects of increasing greenhouse gases and decreasing stratospheric ozone (Thompson et.al., 2011). Observations suggest a hypothesis that the long-term strengthening of the SAM has resulted in a poleward shift in the ACC, which, in turn, has perhaps brought more warm circumpolar deep water

south to the periphery of the Antarctic continent (Gille, 2014). All these studies have shown that the changes in the physical and biogeochemical state of the SO are already underway. Also in a changing climate scenario, a systematic study needs to be conducted in the SO to understand the changes in the properties of bottom water masses occurring in the oceans below 2000 m. Recent several (Sokolov et al., 2004; Jacobs, 2006; Gille, 2008, Iudicone et al., 2008) studies have reported the notable freshening of deep water masses mainly in the SO. One of the important water masses participating in the overturning circulation is the cold, dense AABW. In this chapter, an attempt has been made to understand the changes in the salinity, potential temperature and neutral density of the AABW at two locations in the IOOSO using hydrographic data collected in the Indian expeditions to SO in comparison with WOCE data and described in the section 5.1

The SO is comprised several quasi-zonal frontal systems such as AF, STF, SAF and PF (Orsi et al., 1995; Belkin and Gordon, 1996) and these fronts are integral part of ACC, Therefore to understand the variability of ACC, it's essential to understand the variability of these fronts and also the different processes occurring across these fronts. The location of fronts and its variability in the SO is important for climate. Several previous studies have reported that the STF is a region of mesoscale eddies and these eddies may play a major role in the southward shift of STF. Similarly, several studies have reported the close relationship between PF and westerly winds in the SO. Modeling studies have showed the shift of westerlies towards south in the recent decades which may have significant influence in the northward shift of PF. In this chapter, an attempt

has also been made to understand the prominent shifts of these fronts associated with the various oceanographic and atmospheric processes and explained as sections 5.2 and 5.3.

5.2 Freshening of Antarctic Bottom Water in the Indian Ocean Sector of Southern Ocean

5.2.1 Introduction

The transport of heat, carbon, and other climatically important tracers around the planet is mainly controlled by the meridional overturning circulation (Ganachaud and Wunsch, 2000). Hence overturning circulation is one of the key mechanisms that determine Earth's climate. It is driven by the global network of deep western boundary currents, which exports the cold, dense water formed in the high-latitude North Atlantic Ocean and the SO and is supplied as the deep branch of overturning circulation (Stommel and Arons, 1959). Orsi et al., (2002) have reported that the SO limb of the overturning ventilates the deep ocean at about the same rate as the North Atlantic and is dynamically coupled to the Atlantic overturning (Weaver et al., 2003) and this is also potentially sensitive to future climate change (Meehl et al.,2007). During the past four decades a significant decrease in salinity of the North Atlantic Deep Water has been observed (Dickson et al., 2002). In the abyssal layer, around 30-40% of the global ocean mass is accounted by the cold, dense AABW (Johnson, 2008). For global overturning circulation, AABW production is a key contributor (Johnson, 2008; Marshall, and Speer, 2012) and is also an important sink for heat and CO_2 (Sigman and Boyle, 2000). The AABW is generally produced at a few specific high-latitude regions of the SO (Couldrey et al.,2013). The largest source of AABW is the Weddell Sea which supplies 60% of the total volume (Orsi et al.,2002). The remaining is

supplied by the Ross Sea and the Mertz Polynya region of the Ade´lie Land coast near 145°E (Orsi et al., 2002; Rintoul, 1998). A recent study by Ohshima et al, (2013) also reported Cape Darnley polynya (CDP) region (65°- 69°E) as a significant source of AABW.

The air-sea-ice interactions near the Antarctic margins play a key role in the formation of AABW and are sensitive to climatic forcing (Orsi et al., 1999). In many regions AABW has warmed significantly, most strongly in the Atlantic (Meredith et al., 2008; Zenk and Morozov, 2007). In the North Atlantic, this warming has slowed down the meridional overturning of Antarctic-derived waters (Johnson et al., 2008) and is significantly influencing the global heat budget and calculations of sea level rise (Purkey and Johnson, 2010). Further, Whitworth, (2002) reported a shift from salty mode to fresh mode of bottom water in the Australian Antarctic basin. Also, in the region between 140°E and 150°E and southwards of 65°S, Jacobs (2004, 2006) has reported that the bottom water properties vary strongly with season and location, reflecting the narrow bottom currents and rough bathymetry over the continental rise and slope (Chase et al., 1987). From repeated hydrographic sections Rintoul (2007) has reported that the freshening of AABW has been increased from 1995 to 2005. Even though the observations are limited in the present study, an attempt has been made to compare the rate of freshening of AABW in the IOSSO with the previously published results.

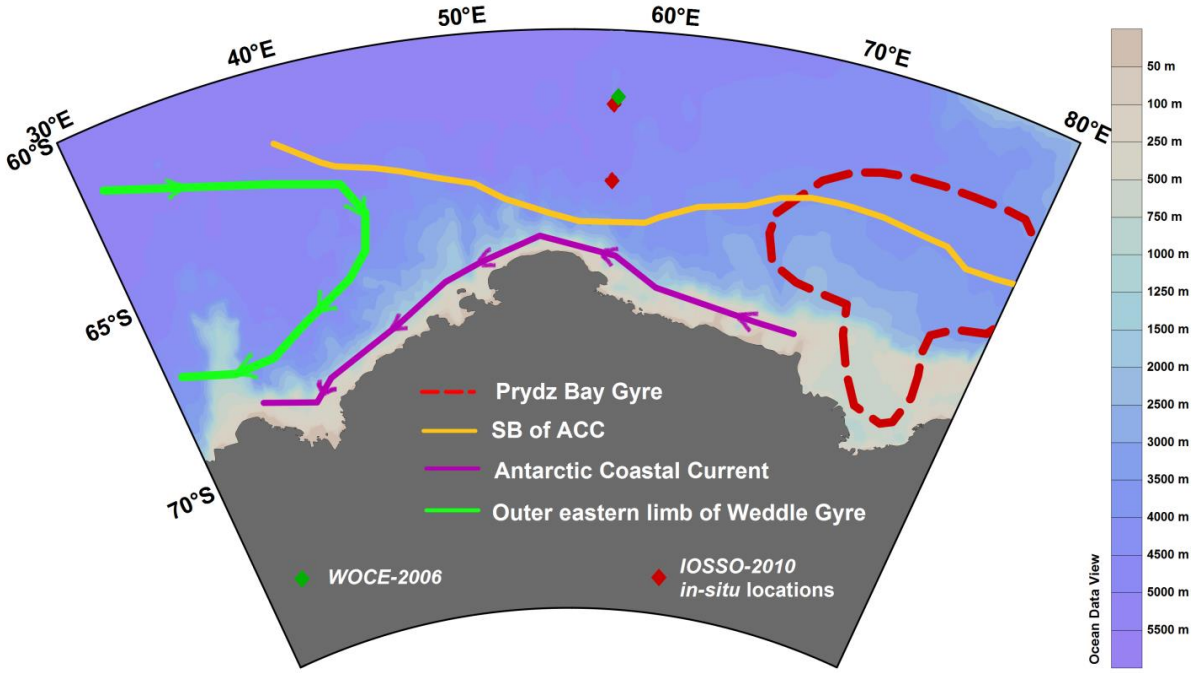

Fig. 5.1. Schematic representation of the general circulation (Williams et al., 2010) of the study area. Red and green dots represent Southern Ocean Expedition 2010 and WOCE 2006 location, respectively

5.2.2 Results and discussion

Analysis of the ORAS4 (Fig. 5.2) showed that from 1995 to 2009, the potential temperature changed from -0.573 to -0.589 °C while the salinity varied from 34.658 to 34.657. Potential temperature, overall showed an increasing (warming) trend and salinity showed a decreasing trend (freshening). As compared to 1995, the temperature increased by 0.003 °C in 2006 but from 2006 to 2009 the change in temperature was by 0.017°C. Similarly decrease in salinity was negligible from 1995 to 2006 but from 2006 to 2009, salinity decreased by 0.001.

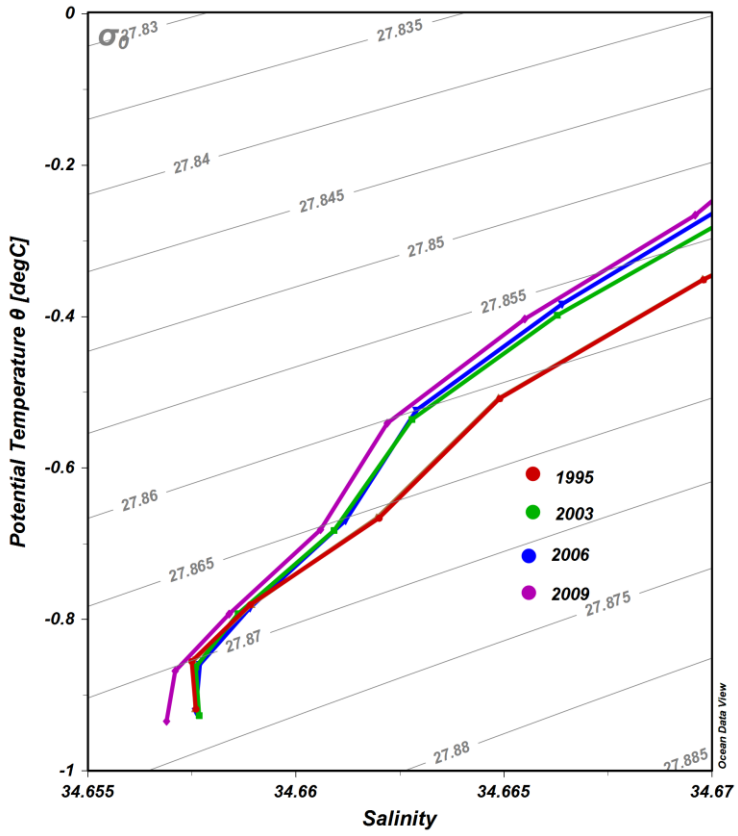

Fig 5.2. θ-S plot showing the freshening of AABW from 1995 to 2009 using model data (ECMWF (ORAS4))

In-situ data from a point location (62°S 57°30'E) were taken and the T-S distribution has been plotted to observe the variability in AABW for two years 2006 and 2010. AABW was identified at depths > 3026m at 62°S 57° 30'E and > 2748 m at 64°S 57° 30'E (Fig. 5.2). AABW exhibited a freshening of ~0.01 below 3500m at 62°S in 2010 compared to that in 2006 and the AABW became lighter by 0.01 kg/m^3 from 2006 to 2010 (Fig. 5.3 a &b). The temperature profiles showed warming of ~0.04°C below 4500m depth during the same period (Fig. 3c).

During 2010 observation, the near bottom salinity at 62°S and 64°S along 57°30'E were ~ 34.647 and ~ 34.636 (Fig. 5.3 d). AABW was observed to be nearly isohaline with salinity between ~34.675 and ~34.670 during 1990 which was warmer than that observed in 1971, and further in 2005, it was warmer, fresher and less dense than that observed in the mid-1990s (Rintoul, 2007). These studies indicate that the decadal decrease of salinity was negligible from 1970's to 1990's, however from 1990's to 2005, it decreased by ~0.01. In the present investigation, a higher degree of decrease in salinity (~0.01) from 2006 to 2010 was exhibited by the in-situ data collected from the IOSSO (Fig. 5.3 d). As mentioned earlier, the previous studies using *in-situ* data have reported that the rate of freshening between 1995 and 2005 (~ 0.01) was greater than that observed between 1970 and 1995 (~0.005). In the present investigation, the observations made during the period between 2006 and 2010 exhibited that the AABW became warmer (~0.05°C), fresher (~0.01) and lighter (~0.01 kg/m^3) with a higher rate of freshening compared to the earlier observations. In the present study both the model and in-situ data portrayed the freshening of AABW however the model data underestimated the degree of freshening compared to *in-situ* data.

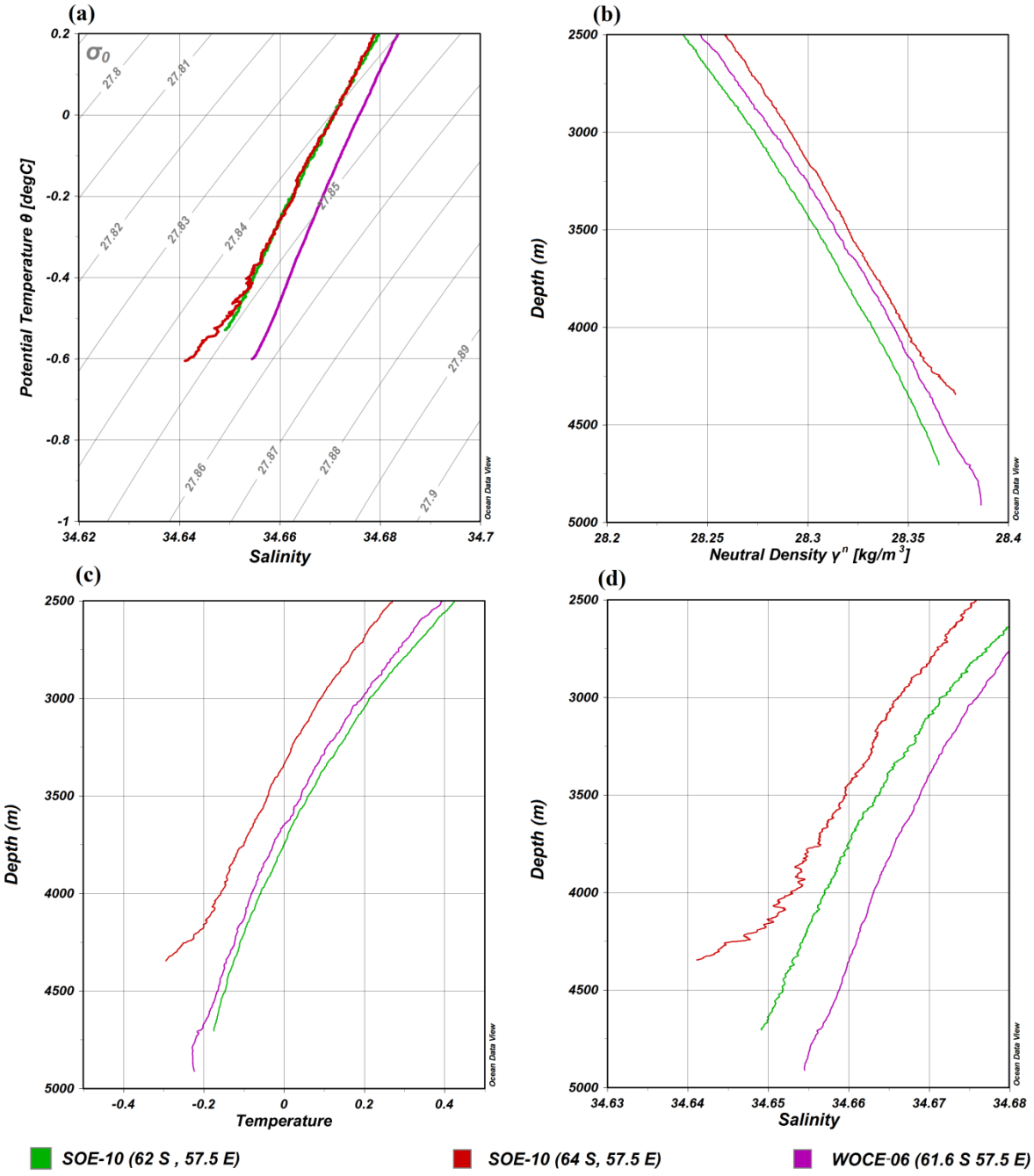

Fig. 5.3. Comparison between Southern Ocean Expedition 2010 (SOE-10) and WOCE 2006 (WOSE-06) (a) θ-S plot showing the presence of AABW (b) vertical structure of neutral density (c) vertical structure of temperature (d) vertical structure of salinity.

Jacobs et al., (2002) and Shepherd et al., (2004) reported the freshening of Ross Sea shelf waters of 46 Giga ton /annum (Gt/ a^1) because of inflow of melt from glaciers to the east. In the Australian Antarctic Basin (80°E to 140°E), freshening observed between 1995 and 2005 was 13 ± 5 Gt/a^1 (Rintoul, 2007). In the present study, the height of fresh water added per unit area computed at 62°S for 500m thickness (4000-4500m) between 2006 and 2010 was 2.2 cm/annum [cm/a^1]. This value reflects the influence of additional freshwater supply from external sources that may be one of the probable reasons for the freshening of AABW observed in the study region. The characteristics of AABW observed in the present study are comparable with the AABW reported from the Weddell Sea and Cape Darnley (Table. 1).

Region		Temperature [°C]	Salinity	Neutral Density [kg/m^3]
Weddell Sea on *et al.*, 2013)	Lighter AABW	$-0.7 < \theta < 0$	$34.665 < S < 34.67$	$28.26 < \gamma^n < 28.31$
	Denser AABW	$\theta < -0.07$	$S < 34.64$	$\gamma^n > 28.31$
Cape Darnley (Couldrey *et al* 2013)		$-0.7 < \theta < -0.6$	$S < 34.64$	$\gamma^n > 28.27$

Table 5.1 Characteristics of AABW

Hence the signatures of AABW observed in the present investigation could be attributed to the AABW originated from Cape Darnley or Weddell Sea.

The CDP situated between 65°E to 69°E located northwest of the Amery Ice Shelf, has the second highest ice production around Antarctica after the Ross Sea Polynya (Tamura et al., 2008) and more melt water can be expected from this region. Rintoul (2007) has attributed the freshening of dense water formed in both hemispheres to the high latitude freshwater balance and the rapid transmission of these changes in surface climate into the deep ocean. The most likely cause of the freshening is an increase in the influence of melt water from continental ice (Jacobs, 2006). To understand the influence of surface climatic indices into the deep ocean, long term SST, wind, air temperature, SAM and ENSO from 1980 to 2010 were analyzed in the region between 60°- 67°S and 40°- 80°E.

The yearly average of SST and air temperature exhibited a decreasing trend from 1980 to 2010 (Fig. 5.4 a & b) whereas the sea ice concentration and wind (Fig. 5.4 c & d) portrayed an increasing trend for the same period. In previous studies (Marshall et al., 2004; Thompson and Solomon, 2002) they have reported that the westerly winds at high southern latitudes are strengthened with poleward shift over the past thirty years due to the positive trend in the SAM.

This causes a southward shift and strengthening of the ACC, stronger northward Ekman transport and upwelling of relatively warm deep water (Hall and Visbeck, 2002). Jullion et al., (2013); Martinson, (2012) reported that that across a wide sector of the SO there has been a marked freshening of the shelf and bottom waters is attributed to accelerated glacial melt in response to a southward shift and

further greater flux of warm waters from the ACC onto the shelves of West Antarctica.

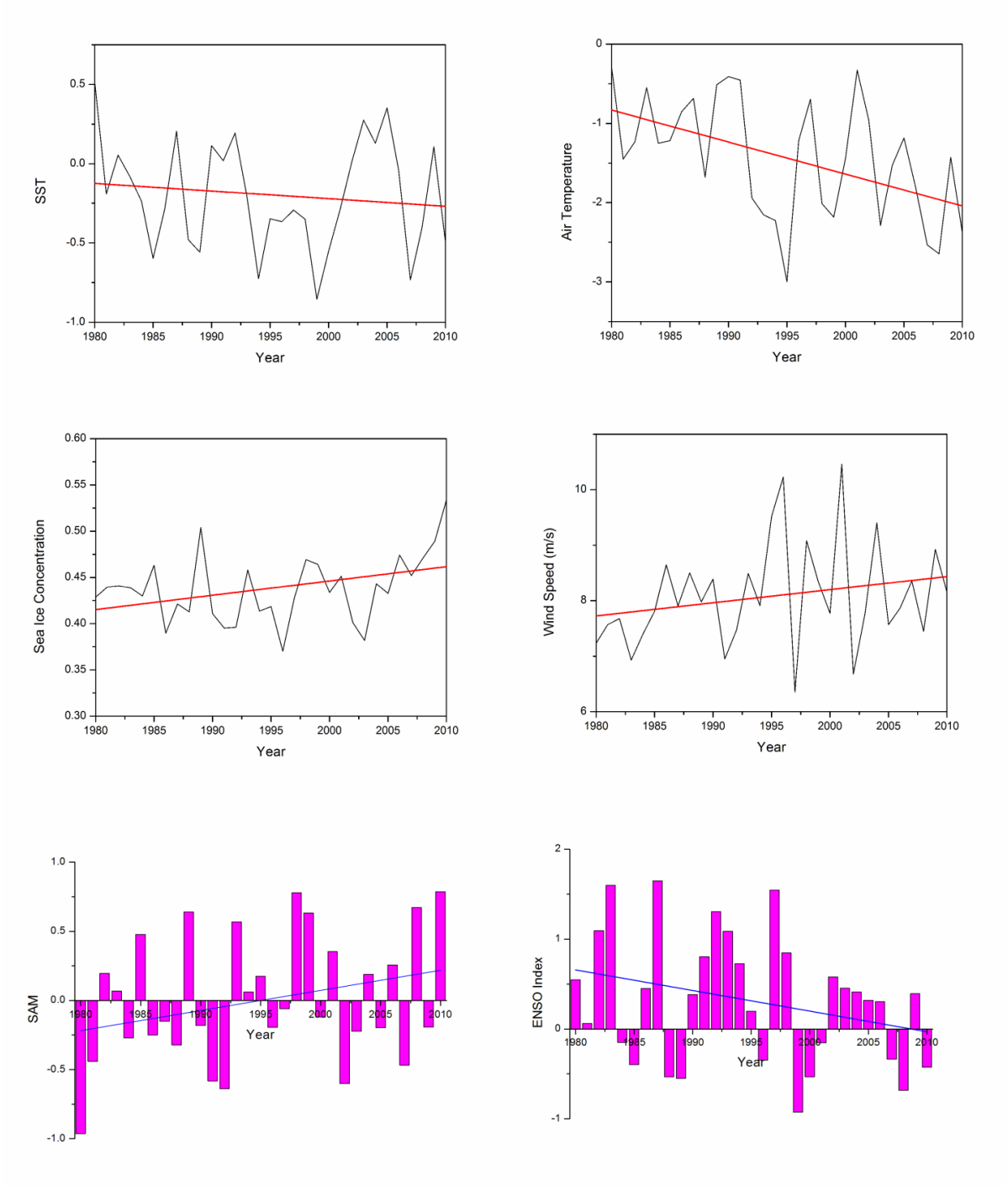

Fig.5.4. Long term annual mean of (a)SST (b) Air temperature (c)sea ice concentration (d) wind speed (e) Sam index and (f) ENSO index

In the present study, the SAM index and the sea ice concentration over the last 30 years exhibited a positive trend (Fig. 5.4 c & e). For the Indian Ocean sector, south of 55°S positive correlations have been found between the SAM index and surface salinity (Lefebvre et al., 2004) and sea ice extent (Rayner et al., 2003). A strong positive correlation was portrayed between annual sea ice concentration anomaly and SAM index (Fig. 5.5). Studies have also shown that ENSO variability can be related to sea-ice extent in the Southern Indian Ocean, as well as the speed and variability of the ACC (Carleton, 2003).

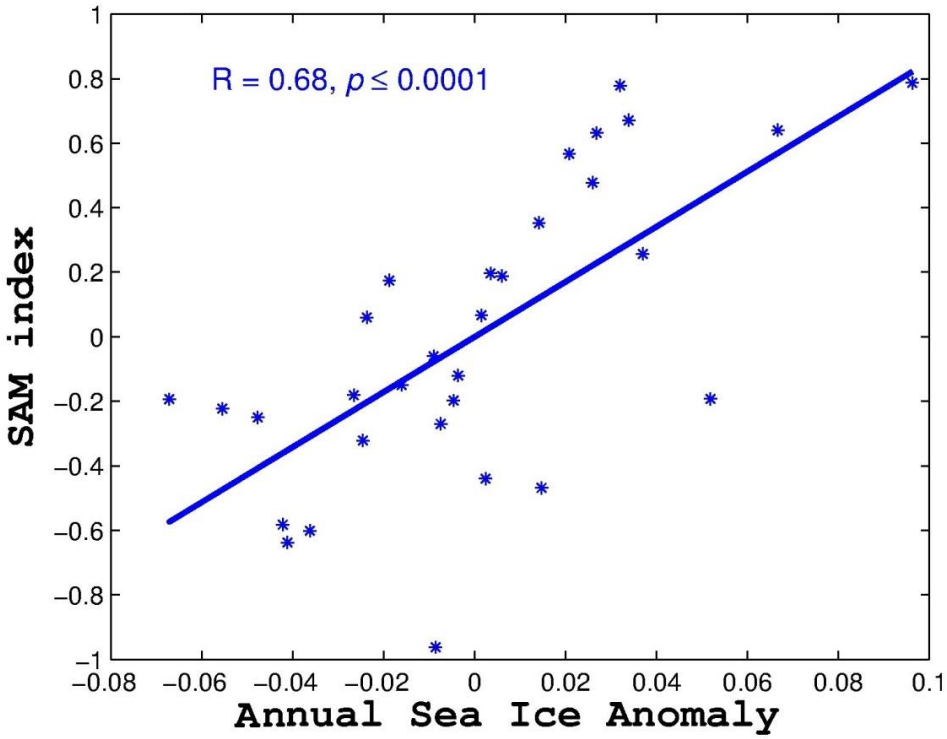

Fig. 5.5 Correlation between SAM index and annual sea ice anomaly

Stammerjohn et al., *(*2008) have reported the positive relation between the La Nina and sea ice concentration around Antarctica. Long term MEI index showed

an increasing occurrence of strong La Nina events on a global scale since 1995 (Fig. 5.4 f), which may be another possible reason for the increase in sea-ice concentration around Antarctica. Accelerated basal melting of Antarctic ice shelves is likely to have contributed significantly to sea-ice expansion (Bintanja et.al., 2013) and the further melting of this sea ice may cause the freshening of AABW.

Widespread warming of AABW since 1980 across much of the global ocean abyss has been reported by Purkey and Johnson (2010, 2012). In the earlier studies (Jacobs et al., 2002; Rintoul, 2007; Jacobs and Giulivi, 2010) it has been reported that in the Ross Sea and off Adélie Land the AABW formed had freshened by ~0.01 between the late 1960s and 1990s, but between the mid-1990s and the mid-2000s the freshening was ~0.03 (Aoki et al., 2005; Rintoul, 2007). The degree of freshening indicated by the in-situ data in IOSSO during this study was higher (~0.01 in four years) compared to the freshening observed from 1990 to 2005 (~0.01 in 15 years) by Rintoul (2007). This increase in the rate of freshening has not been reported in the IOSSO so far. Mass loss of ice sheet in Antarctica by enhanced basal melting linked to shelf water freshening could be the reason for the freshening of AABW (Jacobs et al., 2002; Jacobs and Giulivi, 2010; Pritchard et al., 2012). Indeed, the nearby CDP was reported as a significant source of new bottom water, contributing of Atlantic sector AABW production, although the role of the Amery Ice Shelf could not be dismissed (Ohshima et al., 2013). The eastward flow pattern exhibited in this study for 1000m depth (Fig.

5.6a) and 4000m depth (Fig. 5.6b) indicate the influence of AABW of CDP origin to the IOSSO region.

The Weddell Sea (WS) is a deep embayment of the Antarctic coastline that forms the southernmost tip of the Atlantic Ocean. Centering at about 73° S, 45° W, the WS is bounded on the west by the Antarctic Peninsula of West Antarctica, on the east by Coats Land of East Antarctica, and on the extreme south by frontal barriers of the Filchner and Ronne ice shelves. The WS is one of the few places in the world ocean where deep and bottom water masses participating in the global thermohaline circulation are formed. Weddell Gyre (WG), the large-scale horizontal circulation in the WS, is one of the most conspicuous circulation features of the Antarctic Zone of the SO. To the south and to the west, the WG is bounded by the Antarctic continent and the Antarctic Peninsula. The ridge system north of 55°S, which consists of the South Scotia, North Weddell and Southwest Indian Ridge, forms the approximate northern boundary. WG extends as far as about 30°E into the Enderby Basin (Deacon, 1979; Gouretski and Danilov, 1993), where the water mass transition between the WG and the ACC bends southwards and approaches the Antarctic continent as close as a few hundred kilometers (Orsi et al., 1993).

Previous studies have reported that the seawater density modification through air-sea-ice interactions near the Antarctic margins plays a role in the formation of AABW (Orsi et al., 1999). Interactions between ocean, atmosphere and cryosphere in the margins of Antarctica, often determine the characteristics of

AABW, are very sensitive to the climatic changes occurring in the region (Foster and Carmack, 1976; Gill 1973; Orsi et al., 1999; Jacobs 2004; Nicholls et al., 2009). West of 30°W, Warm Deep Water (WDW) interacts with the dense shelf waters off the Filchner-Ronne Ice Shelf (Whitworth et al., 1998) that are made saline by brine rejection during sea ice formation results in AABW formation (Killworth, 1974; Carmack and Foster, 1975; Foldvik et al., 2004; Wilchinsky and Feltham, 2009; Jullion et al., 2013). Although the Filchner-Ronne Ice Shelf have been traditionally regarded as the principal source region of AABW in the WS, significant AABW production has been reported off the eastern Antarctic Peninsula, particularly near the Larsen Ice Shelf (Fahrbach et al., 1995; Weppernig et al., 1996; Gordon, 1998). Accelerated melting of the ice shelves of West Antarctica may be the origin of freshening trend in the Indo-Pacific sector of the Southern Ocean (Shepherd et al., 2004; Rintoul, 2007; Jacobs et al., 2002; Jacobs and Giulivi, 2010), where the warm water brought by ACC flood the coastal areas of the continent (Thoma et al., 2008; Jacobs et al., 2011). Jullion et al., (2013) suggested that the increased glacial loss from the Larsen ice shelves is likely to be a significant player in the freshening of AABW exported from the WS. Previous studies (Jullian et al., 2013; Thomson and Solomon, 2002; van den Broeke, 2005; Marshall et al., 2006) indicated that the summer time intensification of westerly winds over SO leads to advection of warm maritime air to eastern side of Antarctica peninsula and further increase in air temperature during summer resulting the glacier melting.

The current pattern at 4000m depth levels from the model data showed a cyclonic circulation pattern between 40°W and 60°E indicates the influence of WS waters in the study area. The flow of water from the west (WS region) by the eastwards flowing currents (Fig. 5.6b) also could be one of the causative factors affecting the freshening of AABW observed in the study region.

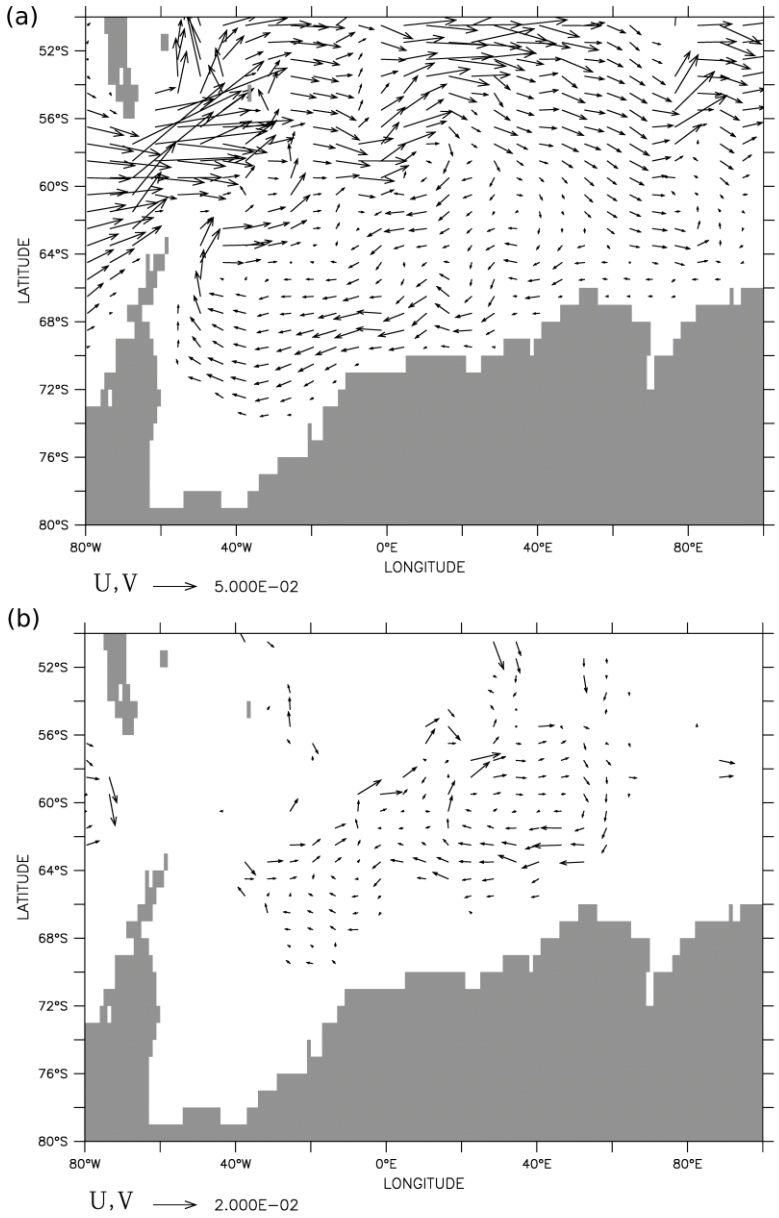

Fig. 5.6 Current pattern (a) 1000m depth and (b) 4000m depth

Hence the signatures of the AABW observed in the present study could be of WS and CDP origin. To substantiate these results more long term observations are required to be carried out in the IOSSO region in future.

5.2.3 Conclusion

Studies of southern hemisphere climate variability have been severely hampered by the lack of sustained observations. The monotonic freshening of AABW reported in earlier studies and the fact that a consistent signal observed in the decline of salinity in the present and previous studies support the argument that the changes described here reflect a sustained freshening of the bottom water. Earlier studies reported that the rate of freshening between 1995 and 2005 (~0.01) is greater than that observed between 1970 and 1995 (~0.005). The results obtained from the *in-situ* data corroborate with the model data, exhibited an increased rate of freshening in the period 2006-2010. Swifter freshening in the same direction from 2006 to 2010 has been portrayed in the present study and in the same period the AABW became warmer (~0.05°C) and lighter (~0.01 kg $m^{-}3$). The height of fresh water added per unit area computed was 2.2 cm a^{-1}. The increased fresh water input may be attributed to melting of ice shelves as well as changes observed in sea-ice formation, sea surface temperature and climatic indices. Earlier reports suggested that the causes for the freshening of dense water could be the freshwater balance and rapidly transmitting signature of changes in surface climate into the deep ocean. The AABW observed in the present investigations shall be attributed to both the WS and CDP origin. The

hydrographic data used here is inadequate to distinguish between a trend and high frequency variability in the freshening of AABW. However an understanding of the global overturning circulation and its response to changes in forcing require an observing system that provides sustained measurements of the main pathways of the overturning circulation in both hemispheres.

5.3. Variability of the polar front in the Indian sector of Southern Ocean

5.3.1 Introduction

The SO plays a critical role in driving, modifying, and regulating global change and the ACC is an important part of the SO plays a very important role in the global ocean circulation. It accounts for ~10% of the global ocean surface area, connects all major ocean basins and is a major region for water mass formation and modification. The major fronts across the ACC are circumpolar in extent are not identical in all sectors of the SO. The frontal structure in the SO varies from region to region. The identification of fronts and quantification of their meandering properties are essential elements in tracing upper-level ocean circulation as well as to understand its role on climate. The Polar Front (PF) is one of the major fronts contained within the ACC and it is the region where the Antarctic surface waters moving northward sink below Sub Antarctic waters (Deacon, 1933).

The PF marks the northern limit of the AZ(Gordon et al., 1977). Previous studies (Botnikov, 1963; Lutjeharms and Valtentine, 1984; Moore et al., 1997, 1999) have suggested that the Antarctic PF has both surface and subsurface expressions. It is commonly defined by the northernmost extent of the subsurface temperature

minimum (Tmin) cooler than 2°C, where the Tmin ends or dips abruptly below 200 m (Belkin and Gordon, 1996). Analysis of historical hydrographic measurements of the PF shows that the along-front variability of the surface temperature is small (Buinitsky, 1973), and the PF is well approximated by the 2°C isotherm in the subsurface (Tmin) layer almost everywhere in the SO (Botnikov, 1963). In the Indian sector of the SO, PF is observed to be splitting into two branches as northern (PF1) and southern (PF2) branch and has been identified with a sea surface temperature (SST) of 4 -5°C and 2-3°C for PF1 and PF2 respectively. Climatologically the PF1 is located between 48-50°S and PF2 between 52-54°S.

5.3.2 Results and Discussion

In 2010 the PF was identified between the latitudes of 50°S and 52°30'S and PF2 as a wide front between 55°S and 59°30'S 50°S whereas in 2011 it was identified between 50°30'S and 52°S and PF2 was observed between 53°30'S and 56°30'S (Fig 5.7 a and b).

The temperature is seen to be decreasing form north to south with surface temperatures ranging from 11 to 1.5°C in 2010 and from 13 to 1°C in 2011. The dicothermal layer is a prominent feature in both the years with a minimum temperature of about 1.5°C.

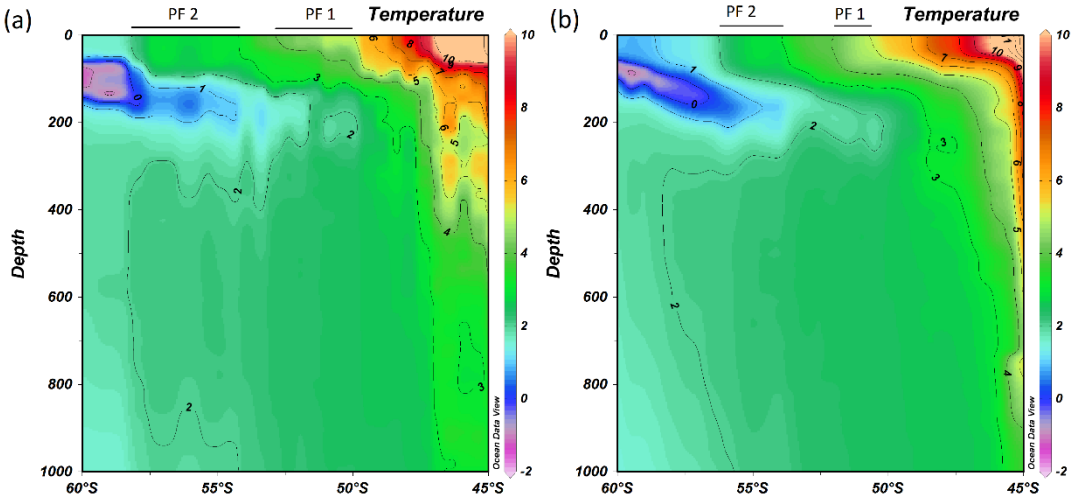

Fig 5.7 Vertical section of temperature in (a) 2010 and (b) 2011

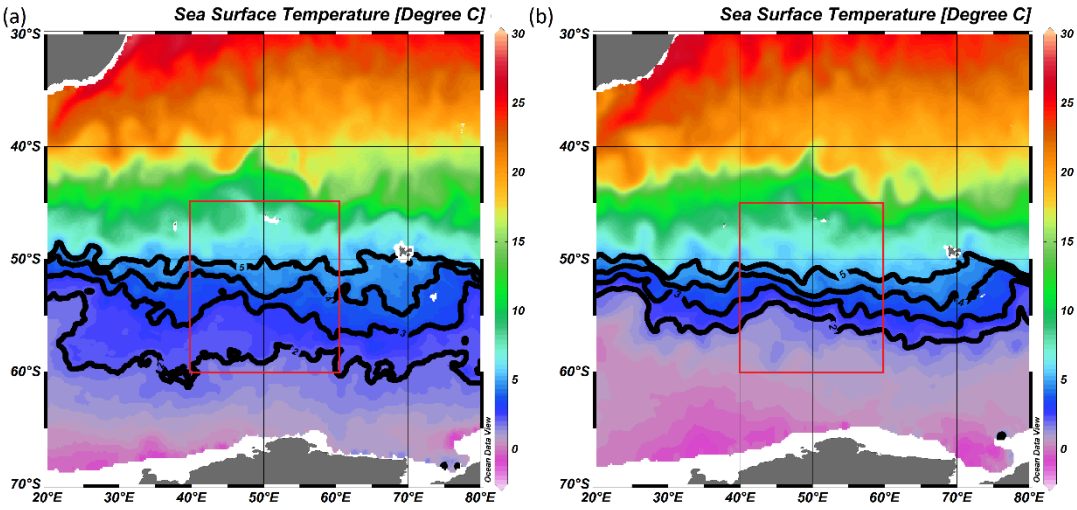

Fig 5.8 Satellite SST in (a) 2010 and (b) 2011

Monthly satellite surface temperature was also well correlated with the insitu frontal positions with the PF showing a north ward movement by almost 2°C (Fig 5.8 a and b).

Analyses of both hydrographic data (Gordon et al., 1978) and satellite altimeter measurements (Chelton et al., 1990; Gille, 1994) indicated that the fronts are steered by bottom topography.

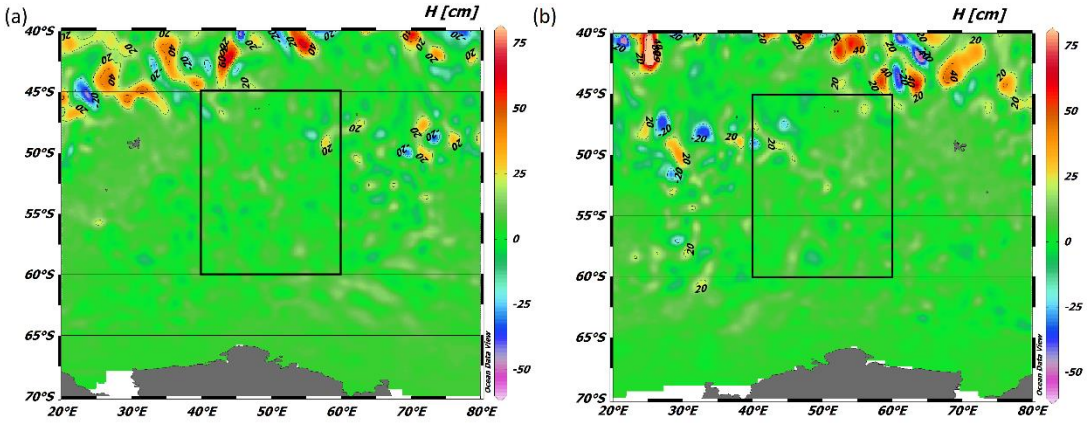

Fig 5.9 Sea level anomalies in (a) 2010 and (b) 2011

Many studies (Deacon, 1937; Gordon et al., 1978; Chelton et al., 1990; Gille, 1994; Moore et al., 1999) have suggested that topography plays an important role in the Antarctic PF path and its variability. It has been reported that the PF intensified (increased width and temperature change across the front) at major bathymetric features, including the Pacific-Antarctic Ridge, Drake Passage, the Kerguelen Plateau, and crossing the Southeast Indian Ridge (Moore et.al, 1999). However, the present study region is far away from these islands the average depths in this area are around 4500 m hence the effect of bottom topography in the PF variability has been ruled out. To rule out the effect of meso scale features analysis of monthly SSHA was carried out. The study area does not show the presence of any major warm core or cold core eddy (Fig 5.9).

Winds over the study region are westerly in nature. In 2010, the core of these winds is seen to be lying around 50°S but in 2011 the core has shown a southward shift and is seen to be around 60°S (Fig 5.10).

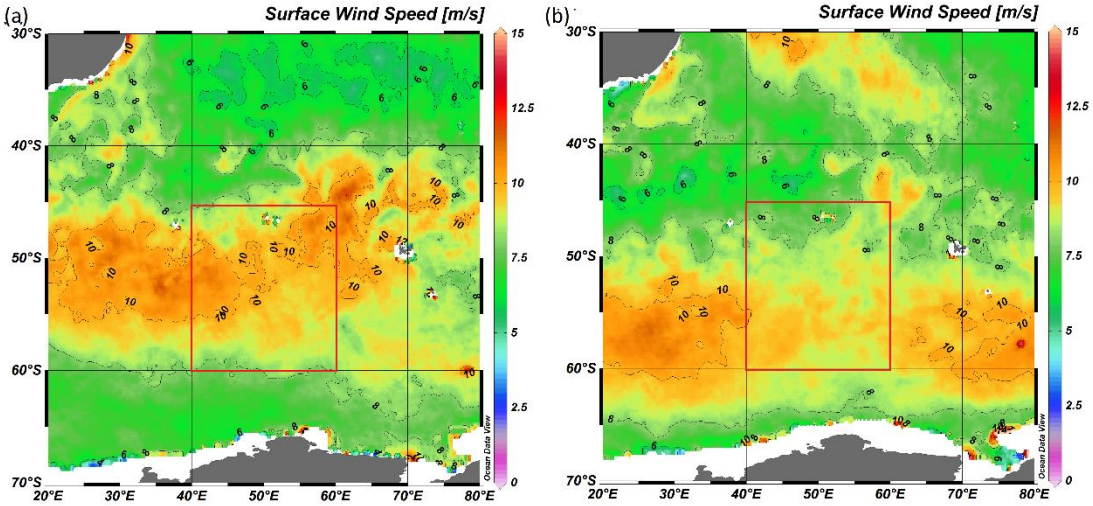

Fig 5.10 Surface winds over the study area in (a) 2010 and (b) 2011

The SAM is the most important mode of climate variability in the Southern Hemisphere middle and high latitudes on intraseasonal and interannual timescales (Lovenduski and Gruber, 2005) and is associated with north–south movements of the westerly winds. The SAM index (Marshall, 2003; Visbeck, 2009) has been moving towards a more positive mode since the 1970s (Thompson and Solomon, 2002), indicating a poleward intensification of the southern hemisphere winds. It is characterized by a large-scale alternation of atmospheric mass between the mid- and high-latitudes, and is associated with a meridional shift in the atmospheric westerly winds (Hartmann and Lo, 1998). These westerly winds are responsible for driving the circulation of the SO, and studies using general circulation models have shown that wind shifts associated with the SAM alter SO circulation patterns substantially (Hall and Visbeck, 2002; Oke and England, 2004; Watterson, 2000).

Since air-sea CO_2 flux is directly influenced by wind speedwind anomalies can alter the circulation and biogeochemistry of the ocean, and hence the oceanic pCO_2, it is likely that wind anomalies associated with the SAM can impact the flux of CO_2 between the atmosphere and the Southern Ocean.

This shift in westerly wind observed over the study area could be due to the influence of SAM. Analysis of the SAM index showed it to be positive in 2011 and negative in 2012 (Fig 5.11). A positive SAM induces anomalous northward Ekman transport in the high latitude region of the Southern Hemisphere (Hall and Visbeck 2002). This gives rise to surface cooling poleward of 50°S. Bitz and Polvani (2012) explain that poleward intensification by itself can lead to a positive SST response via anomalous Ekman upwelling of warmer water in the salinity stratified circumpolar region.

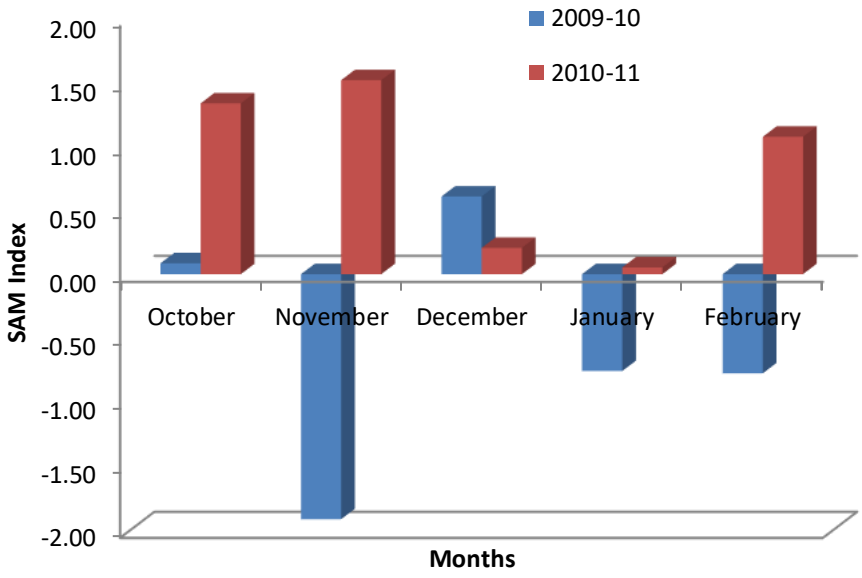

Fig 5.11 SAM index

Ferreira et al. (2015) used two different coupled GCMs to demonstrate the SO response to winds in forced ozone depletion simulations. An atmospheric pattern similar to a positive SAM triggers short-term cooling followed by slow warming around Antarctica. The fast response is dominated by horizontal Ekman drift advecting colder water northward, while the slow response is sustained by Ekman upwelling of warmer water.

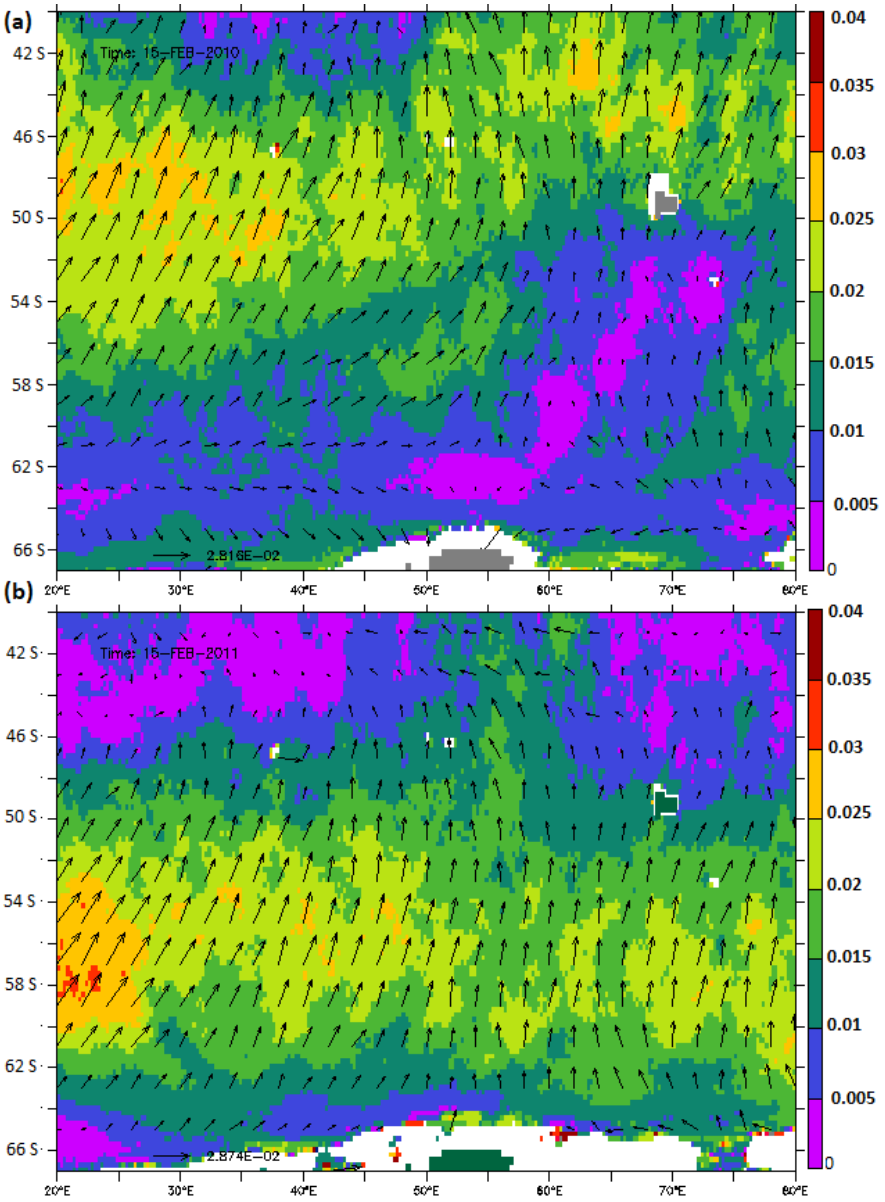

Fig 5.12 Ekman transport over the study area during (a) 2010 and (b) 2011

5.3.3 Conclusion

This study explains the significant spatial and temporal variation of Polar Front2 (PF2) in the IOSO based on satellite and in-situ hydrographic data (2010, 2011) collected during Indian expeditions to SO. A southward shift of approximately about 2 degrees was also observed in the PF2. Bottom topography and mesoscale variability does not play a significant role in this variation. The core of the westerly winds shows a southward shift from 55°S in 2010 to 60°S in 2011. This southward shift in winds may be explained by the positive SAM seen during 2011. This southward shift in winds lead to increased Ekman transport from the coast leading to an increase in cooler waters being transported northwards which subsequently led to the northward movement of the PF2 in 2011.

5.4 Observational evidence of the southward transport of water masses in the Indian sector of Southern Ocean

5.4.1 Introduction

The SO is a key player in the earth's climate for its importance in the global ocean circulation and water mass formation, inter-basin connections, and air–sea exchanges of heat, freshwater, and tracer gases (Farnetti et al., 2010). The SO is characterised by a wide spectrum of variability. The high frequency variability largely arises from the wind-driven ocean variability (Meredith and Hogg, 2006, Hughes, 1999, Gille, 1999). Low frequency variability of inter decadal timescales also occur in the SO and to an extent depend on the mesoscale eddies (Hogg and Blundell, 2006), suggesting the role of intrinsic variability in the decadal variability (Dijkstra and Ghil, 2005). The Eddy Kinetic Energy (EKE) ,which is a measure of mesoscale activity, in topographically constrained areas in SO and within the ACC is often dependent on changes in wind forcing on interannual-to-interdecadal timescales largely associated with major climatic modes such as the SAM and ENSO (Meredith and Hogg, 2006, Sheen et al., 2014, Morrow et. al., 2010). Model studies reveal that different geographic regions within the SO respond differently. The Pacific sector is characterised by intrinsic disturbances that respond to SAM and ENSO, whereas the Atlantic sector is largely wind driven. Satellite observations (Colton and Chase, 1983), buoy trajectories

(Hofmann, 1985), inertial jet models(Craneguy and Park, 1999) and hydrographic data (Lutjeharms and Baker, 1980, Trathan et. al., 1997) have revealed that high mesoscale variability in the SO is closely correlated with regions of prominent bottom relief. This variability also correlates closely with either the terminal region of a major western boundary current such as the Agulhas Current, or where the ACC interacts with prominent bottom topography such as in the Drake Passage or at the Crozet and Kerguelen Plateau (Lutjeharms and Baker, 1980). Eddies are also an important feature in the SO. In SO poleward heat flux that regulates the meridional overturning circulation is influenced by mesoscale eddies (Hogg et. al., 2008; de Szoeke and Levine, 1981; Lee et. al., 2007). Recent literature show that, eddies in the Agulhas retroflection entrap subtropical properties like low oxygen and CFC and transport to the sub Antarctic zone mostly by eddy translation (Arhan et. al., 2011).

5.4.2 Results and Discussion

The southwest Indian sector of the Southern Ocean, is characterised by the confluence of warm Agulhas Return Current (ARC) and the Subtropical Convergence (Park, et. al., 1991, 1993). This region is known for its enhanced primary productivity and water mass formation and high incidence of mesoscale features (Lutjeharms and Valentine, 1988). The present study was carried out in the south western IOSSO during the Indian scientific expedition to the SO in the austral summer of 2010 and 2011. The study has analyzed the thermohaline variations in an area characterised by meso-scale disturbances and attempted to

understand the role of eddies in the southward water mass transport as well as examine the year to year variability in the region using available data sets and to link it with the large scale variability.

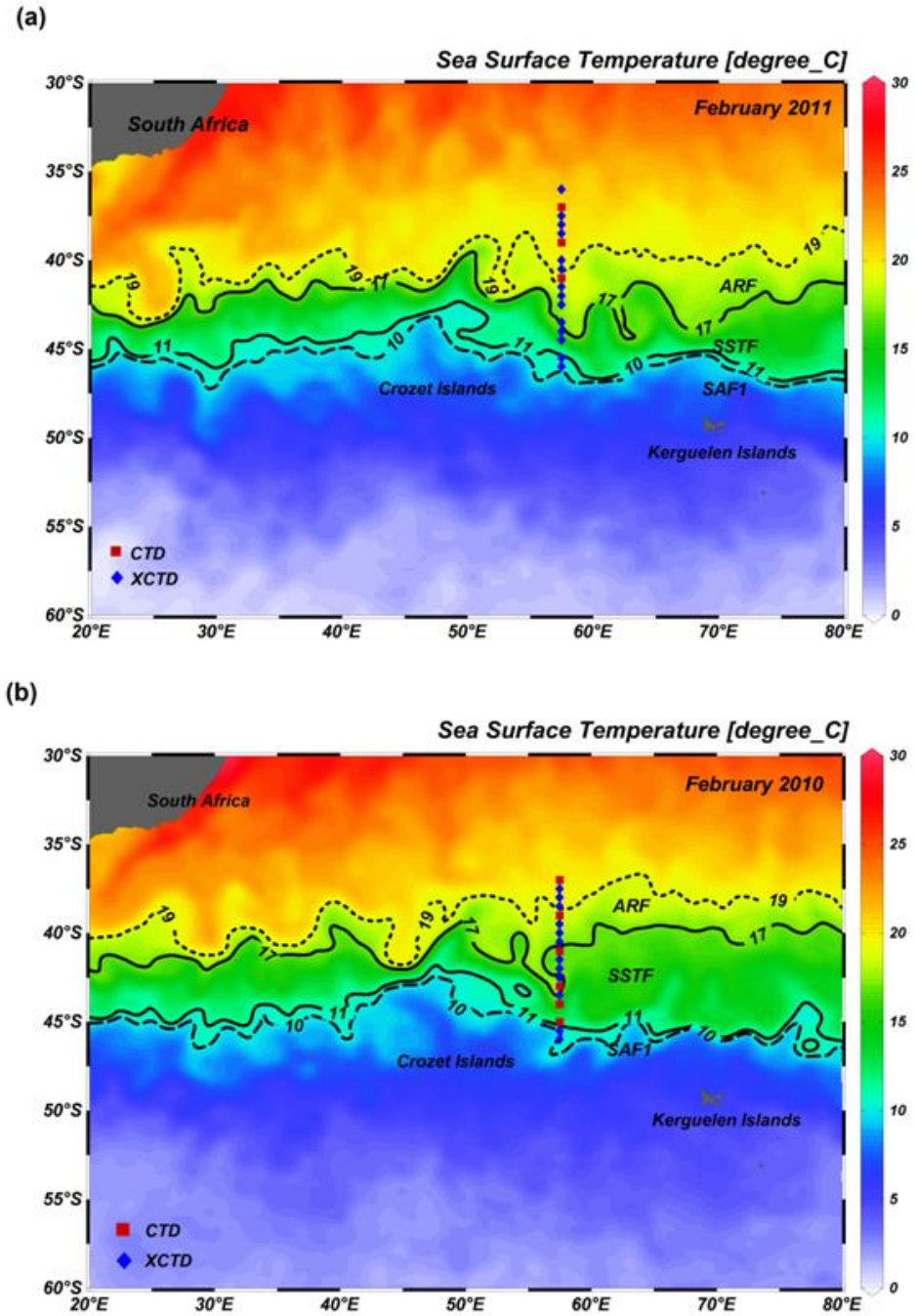

Figure 5.13 Cruise track overlaid on SST maps of February (a)2011 (b)2010. The fronts along the cruise track has been delineated.

Figure 5.13 a and b shows the AMSRE monthly averaged SST during February 2011 and 2010. It is clear from the figure that generally in the SO the temperature gradually decreases southward and at the frontal locations there is a sudden decrease in temperature (Deacon, 1937). The Agulhas Return Front (ARF), Southern Subtropical Front (SSTF), and Subantarctic Front (SAF) are deemed as the regions where SST decreases suddenly from 19°C to17°C, 17°C to 11°C and 11°C to 9°C respectively (Belkin and Gordon, 1996, Holliday and Reed, 1998, Anilkumar, et. al., 2015). These fronts are highlighted in the Figure 5.13 a and b. From the satellite maps of SST it is clear that the SSTF in 2011 is a narrower front as compared to that in 2010. It has been noted in earlier studies that in the western Indian sector of SO the ARF, SSTF and SAF1 are merged as a single front (Anilkumar et. al., 2006, 2015). The thermohaline section showed in the Figure 5.14 suggest that during 2011 the section of temperature (Figure 5.14 a) and salinity (Figure 5.14 b) is characterized by troughs and ridges.

However, during 2010 (Figure 5.14 c and Figure 5.14 d) no such features were observed except for one at 41°S where the isotherm shoaling was noticed, but this was limited to the subsurface levels. It can also be noted that the undulation in isolines of temperature and salinity during 2011 reached up to 1000m. These undulations were clearly evident in the 11°C isotherm that shoaled from 600 – 700 m depth at 40° 30'S to about 300 m at 42°S. During 2010, the surface temperature gradually decreased from 20°C at 36°S to about 11°C at 46°S (Figure 5.14 c). Salinity varied from 35.4 at 37°S to 33.8 at 46° S (Figure 5.14 d). This gradual variation is in contrast with the north south variability during 2011 where

low SST (17°C) is noted at 42°S and again higher SST (18°C) is noted further south at 44°S.

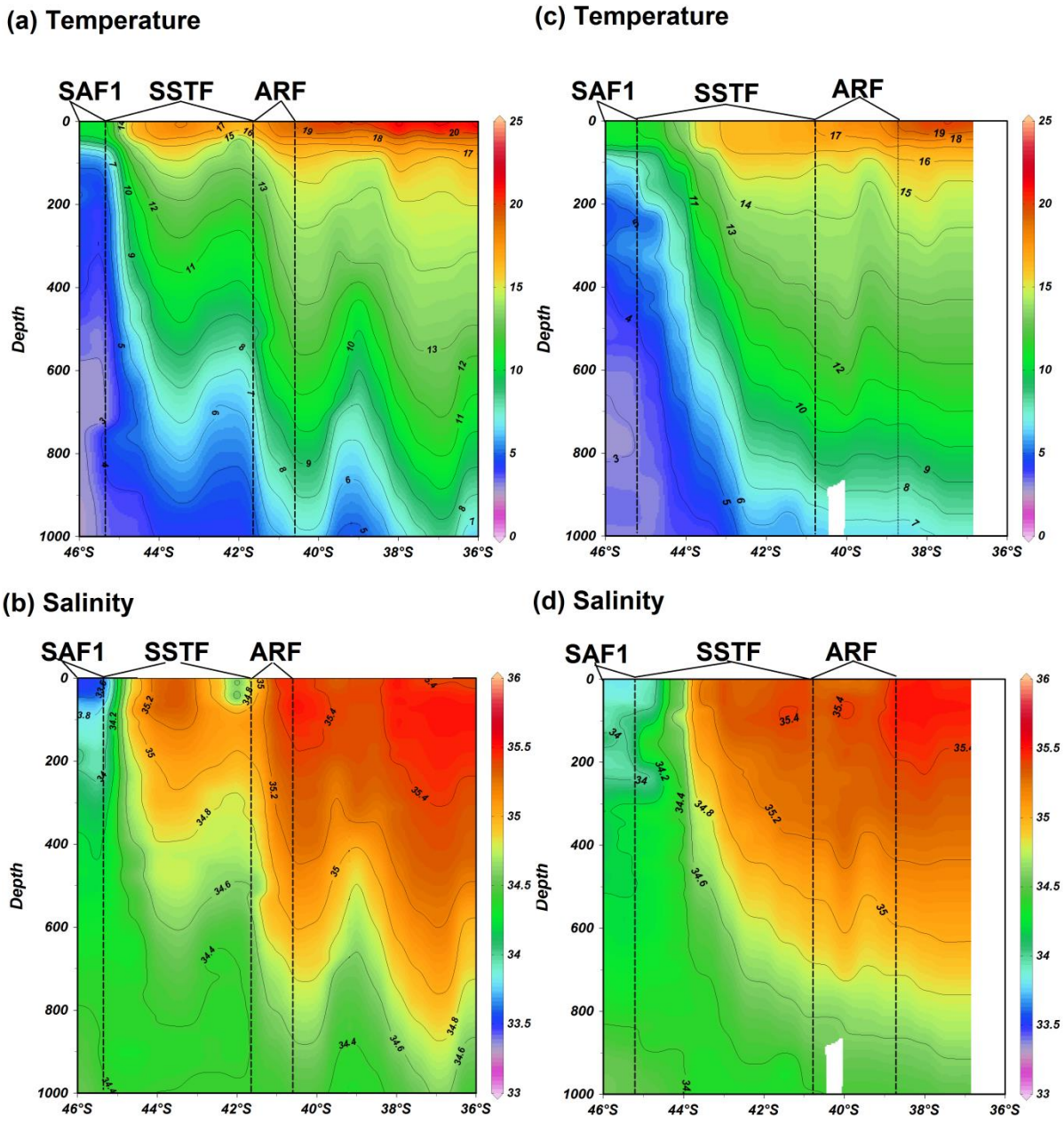

Figure 5.14 Vertical section of temperature and salinity in 2011 (a,b) and 2010 (c,d)

The undulations (troughs and ridges) noted in the thermohaline sections are due to the vertical water column movements. These vertical water column movements can be associated with Ekman pumping or presence of eddies across the cruise track. To understand the role of eddies along the cruise track we will further analysis the SLA plots during February 2011 and 2010.

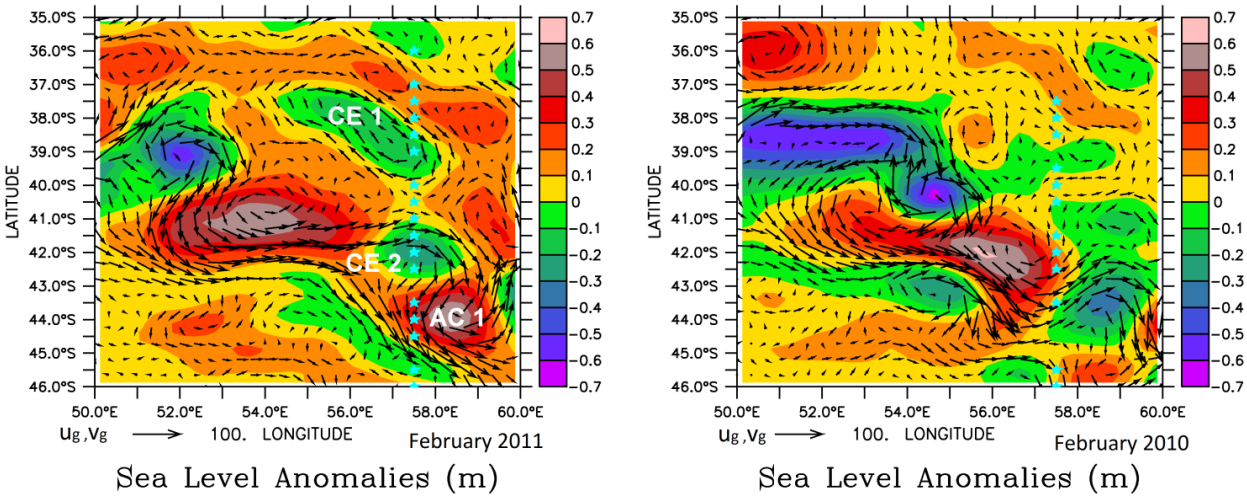

Figure 5.15 SLA overlaid by the geostrophic velocities over the study area during (a) 2011 and (b) 2010.

The Figure 5.15a and 5.15b showed the SLA plots overlaid by the geostrophic velocities during February 2011 and 2010 respectively. The satellite SLA for the observation period of 2011 (Figure 5.15a) was characterized by two cyclonic (Characterized by negative SLA) and one anticyclonic (Characterized by positive SLA) circulation pattern centred at 39°S, 42°S and 44°S, respectively, which

coincides with the locations of the troughs/ridges in the temperature and salinity sections (Figure 5.14 a and b). Hence, it is apparent that the troughs and ridges in the thermohaline structure are the manifestations of cyclonic and anticyclonic eddies. We name these eddies as CE1, CE2 and AC1 located respectively at 39°S, 42°S and 44°S. The hydrographic transect occupied during the survey passes through the centre of CE2 and along edges of CE1 and AC1. The trajectories of the three eddies have been studied for a period of eight months from October 2010 to May 2011 (Figure 5.16). The cold core eddy CE1 has developed in the study area on 17th November 2010. This eddy propagated in a south-westerly direction and was seen at the station location on 2nd February 2011 after which it moved westwards. The second cold core eddy CE2 was located at 43°S 57°E on 6th October 2010. CE2 propagated in a northerly direction until 15th December 2010 after which it turned eastward and persisted at the station location for a period of almost 20 days and eventually moved westwards. After 2nd March 2011, it was observed that CE2 turned eastward. The warm core eddy AC1 observed at station location 44°S moved in a south westerly direction from October 2010.

From the track followed by AC1 it is evident that this eddy was present near the station location for approximately 8 months. Thus except for CE1, CE2 and AC1 persisted at the station location for at least about 8 months. The track of eddies identified by the visual observations were highlighted in the Figure 5.16. One can also notice from the figure 3b that during February 2010 there were no eddies across the cruise track.

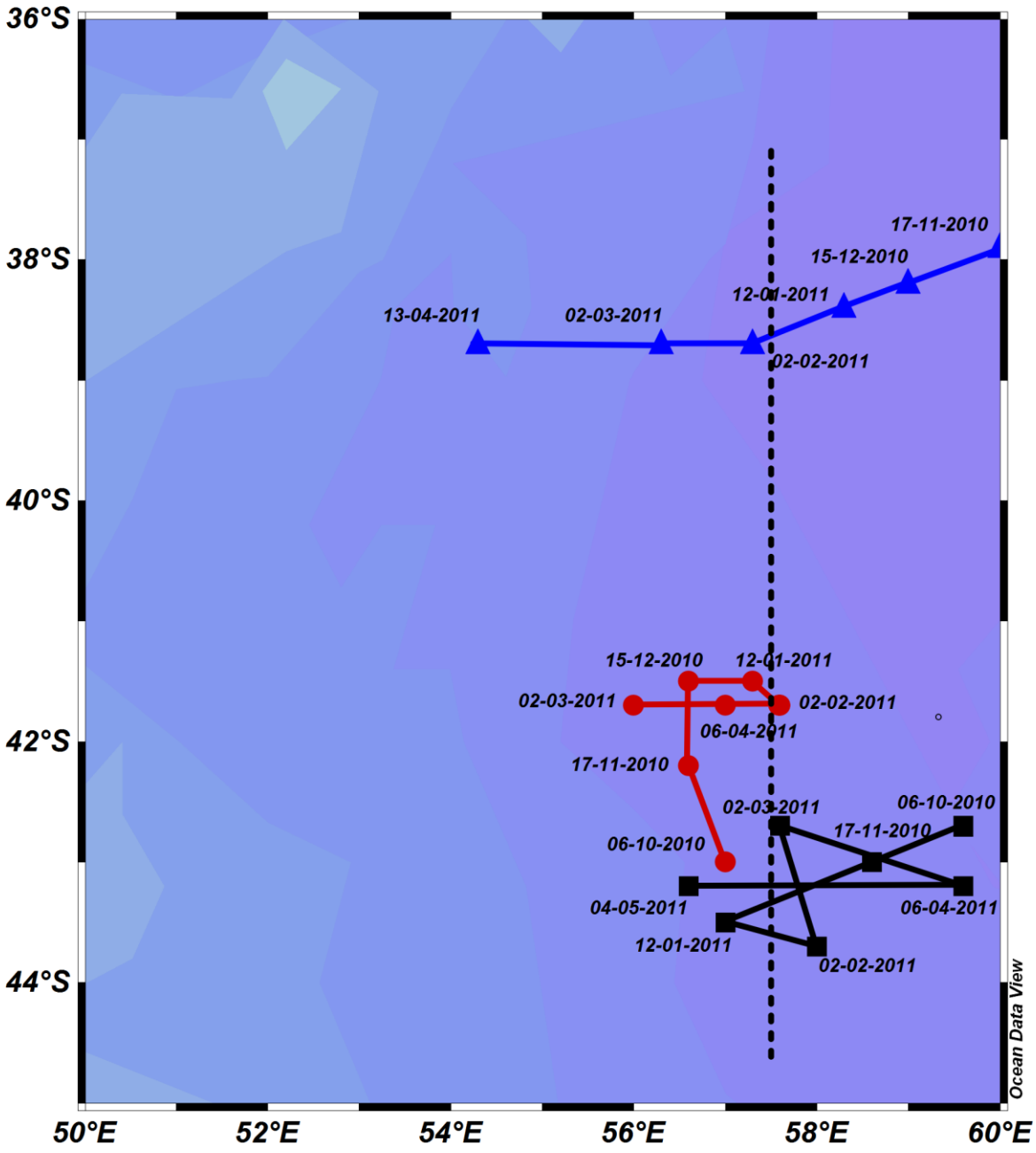

Figure 5.16 Eddy trajectory showing the movement of the 3 eddies identified in the study location CE1 (blue triangle), CE2 (red circle) and ACE1 (black square). The black dotted line shows the cruise track along which observations have been carried out.

To further understand the vertical thermohaline structure of eddies noted during February 2011 the profiles of temperature, salinity and density at the eddy stations were plotted (Figure 5.17 a, b and c respectively). One of the evident features in the profiles is the fresher and colder water column at the cyclonic eddy observed at 42°S. The profile was characterized by well-developed subsurface temperature minimum layer capped in the upper 100 m by a relatively warm and fresh surface layer. On the other hand at the anticyclonic eddies the water column was warmer and saltier than the cyclonic eddies. The eddies appear to be density compensated below 200m.

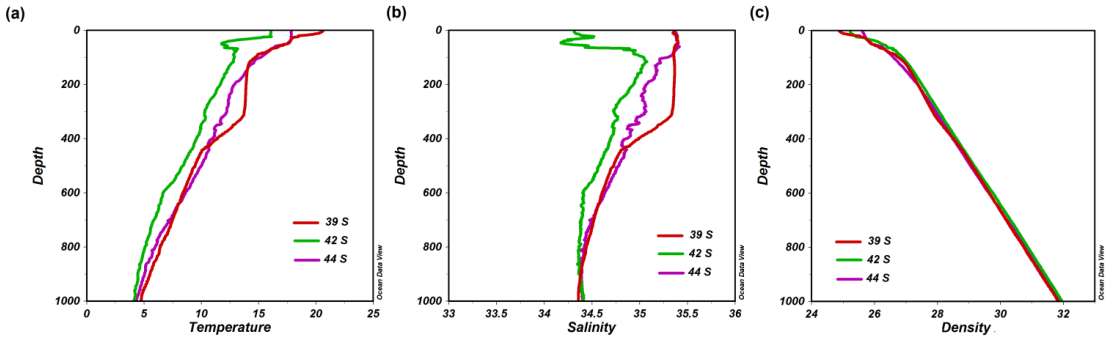

Figure 5.17 Profiles of the temperature (a) salinity (b) and (c) density at the eddy location during 2011 expedition.

The water mass analysis using the TS plots (Figure 5.18a and b) during 2011 and 2010 showed different water masses in the region. The major water mass in the upper 1000m noted in the region is STSW, SASW and STMW. The STSW originates between 29°S and the Subtropical front at about 40°S. The Subtropical front is the boundary between the warmer and higher saline STSW and cooler, fresher SASW. STSW is defined by temperature of 15°C to 24°C and salinities of 35.50 to 34.60 (Darbyshire, 1996), and in the Crozet Basin it is characterized by

relatively high temperature and salinity (T> 12°C, S> 35.1)(Park et. al., 1993). SASW is defined by the characteristics temperatures of around 9°C and salinity < 34. STMW is usually identified in the temperature range of 11-14°C and salinity range of 35-35.4.

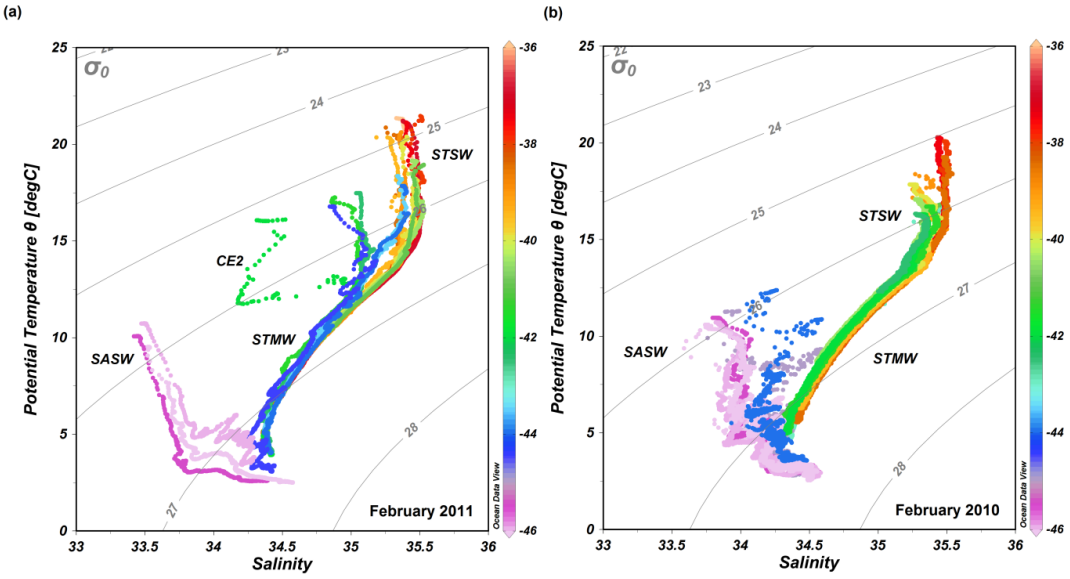

Figure 5.18 Watermasses seen along the cruise track (a) 2011 (b) 2012.

In the present study, the characteristics of STSW provided by Park et. al., 1993 has been considered because the study area is close to the Crozet Basin. T-S plots for station locations during 2011 showed the presence of STSW up to 44°S (Figure 5.18 a), but, the presence of this water mass was not noticed at 42°S where a shoaling of the isolines was noticed in the thermohaline structure. The surface waters at 42°S showed neither T-S characteristic of STSW nor SASW. Studies along the south west Indian ridge has shown that surface waters in eddy regions often get modified either due to air sea interactions at those latitudes or due to the injection of surface waters from different locations (Read et. al.,2000). T-S plots for 2010 revealed characteristics of STSW up to 42°S (Figure 5.18 b).

At 44°S, where signatures of STSW were noticed during 2011, was characterized by temperatures in the range 2.5-12°C and salinities in the range of 34-34.5. Thus, it is apparent that during 2011 the southward extent of the STSW was till 44°S whereas during 2010, STSW was confined only to the source region. The increased southward presence of STSW during February 2011 compared to that of 2010 can be mediated by eddies in the region.

The eddies noted in the study area is associated with highly dynamic Agulhas return current (ARC) flowing from the southern tip of Africa to the east up to 80°E (Read et. al.,2000; Beal et. al., 2011). This is the part of Agulhas current which loop and return eastward off coast of southern Africa. This current flows parallel or juxtaposed to the Subtropical front (Lutjeharms and Ansorge, 2001). Due to the presence of ARC which is dynamically very unstable, STF in the SO is characterized by high mesoscale turbulence (Darbyshire, 1966). Figure 5.19a and 5.19b shows the EKE distribution during the 2011 Feb and 2010 February respectively. The most evident feature in the figure is the high EKE patch and its southward meandering noted east of the 50E. The Figure 5.19c and 5.19d shows the OSCAR currents during 2011 and 2010 respectively. From the figure it is clear that the high EKE patch was associated with the ARC. Previous studies (Holliday and Reed, 1998, Anilkumar et. al., 2015) suggested that according to the meandering of the ARC the fronts shift southward and hence the presence of STSW can be noted further south.

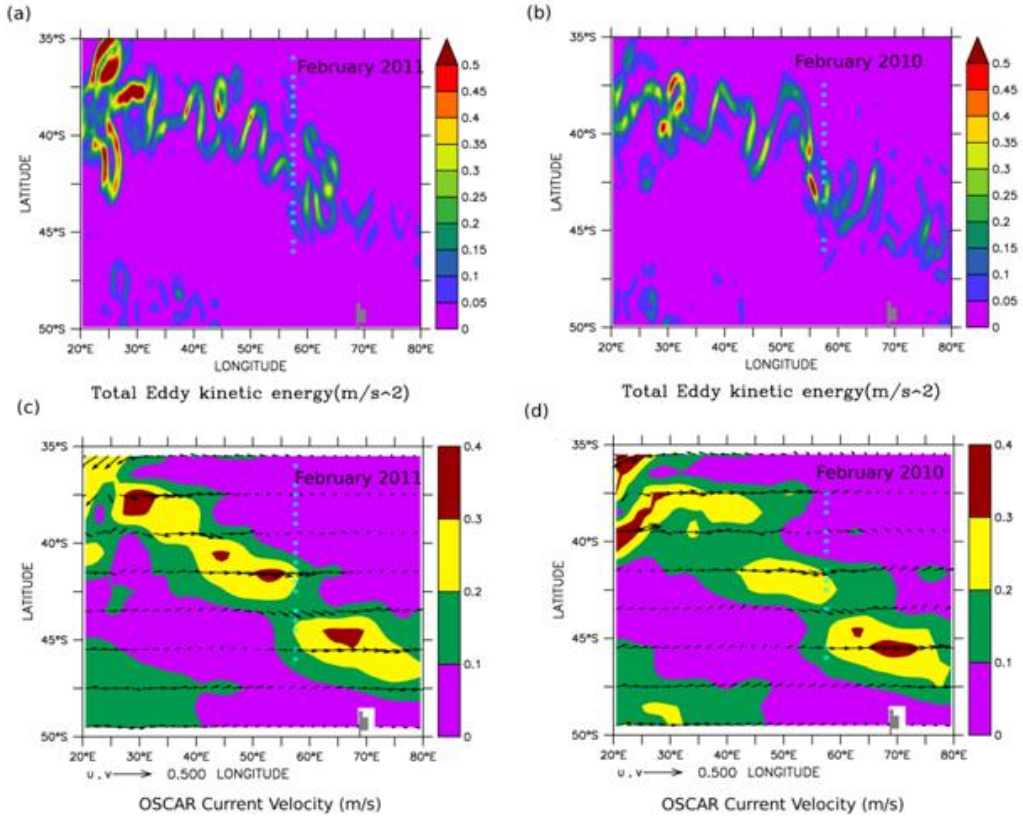

Figure 5.19 EKE maps over the study area during February 2011(a) and (b) 2010. OSCAR currents over the study area during February (c) 2011 and (d) 2010.

The meandering of the ARC is mainly attributed to the presence of bottom topographic features (Nuncio et. al., 2011). The presence of southward extension of Subtropical Surface water during 2011 February can be attributed to the southward meandering of ARC. As the ARC passes from shallow topographic features in the west to deep ocean bottom eastern region to maintain the potential vorticity the current meanders southward. However satellite derived frontal location based on satellite SST averaged over the February 2010 and 2011 along 57.5°E clearly suggested that the SSTF location was slightly different between February 2010 and 2011 (Figure 5.20). These observation invites a detailed interpretation of the presence of STSW further south during 2011.

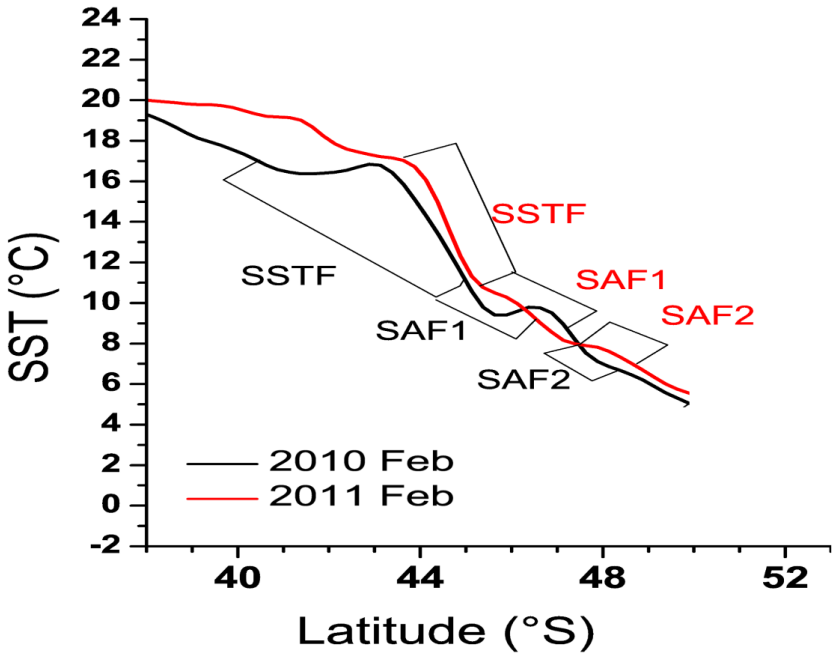

Figure 5.20 MADT profiles showing the frontal extend during 20111 and 2010.

It is clear from the satellite pictures that the large scale circulation pattern and frontal locations were different during February 2011 and 2010. It indicates that meandering of ARC and individual eddies which is pinched of from the core of ARC can transport STSW further southward. The presence of eddies is evident from the undulations of isotherms during the cruises. The station locations were on the eastward edge of CE1, at the centre of CE2 and at the westward edge of the anticyclonic eddy AC1. Eastward and Westward edge of the cyclonic and anticyclonic eddies respectively are characterized by southward flow that transport the warm high saline subtropical surface waters to the south. T-S plots for the station locations (Figure 5.18 a) revealed that along the peripheries of the eddies watermass characteristics were intact, whereas in the interior of the eddy

the watermass characteristics are modified. This shows that peripheries of the eddies promote unaltered southward transport of the STSW and is illustrated schematically in Figure.5.21. At the centre of the cyclonic eddy, water masses were modified as seen in the T-S plots from the stations (Figure 5.18a). STSW could not be traced south of 45°S. 45°S was characterized by sharp gradients in temperature and salinity, marking the SAF. When STSW reached 45°S it might have either subducted or transported eastward by the ACC. During 2010, even though the meandering of the ARC was not significantly different, the absence of eddies (Figure 5.15b) along the hydrographic transect could have reduced the southward transport of the STSW. We do not notice this transport for deeper water masses. Evolution of eddies encountered during 2011 showed they are persistent features of the region at least for 8 months. Persistence of these eddies for about 8 months indicate a large transport of STSW towards SAF. When compared to 2010, 2011 was characterized by more eddies. This, however, could be a chance occurrence, since our survey was one time spot measurements and may not reflect the large scale interannual variability of eddy characteristics in the region.

An estimate of the eddy induced transport is carried out by noting the width of the maximum transport along the southward flowing limb of the AC1 and average velocity along that width. This was then multiplied with the depth of mixed layer in which the STSW can be found. The estimated amount is close to about 0.44 Sv towards the SAF. Persistence of these eddies for about 8 months indicate a large transport of STSW towards SAF during years of increased EKE. The negative

trend of v component of geostrophic velocity (V_{geo}) (Figure 5.22 a) obtained in the present study implies an increase in southward movement of the water masses. A coarse-resolution climate modelling study (Fyfe, 2007) has demonstrated that enhanced mesoscale eddy activity, following an increase in the wind stress, increases the pole ward heat transport. Our analysis also supports these observations by the more southerly presence of STSW in 2011.

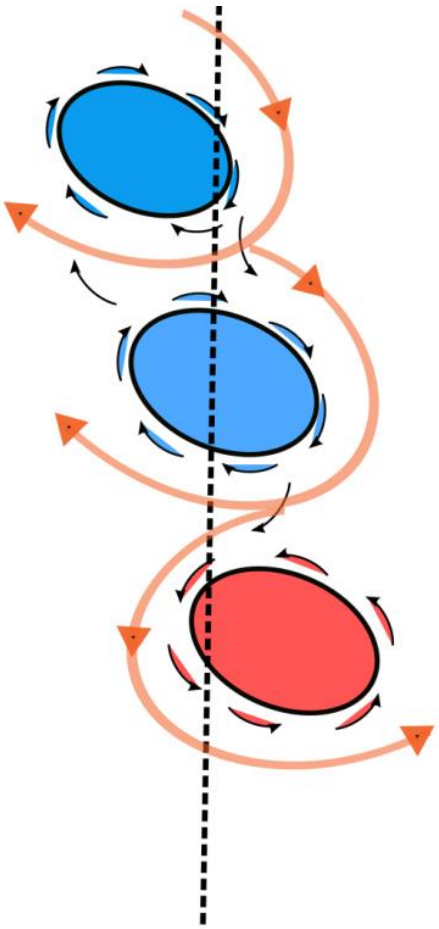

Figure 5.21 Schematic diagram showing the path of STSW (thick orange line) facilitated by the eddies present

In order to gain insight into this interannual variability and to investigate whether one time measurements reflects large scale processes, we computed the EKE averaged over a box(40 to 80°E, 35 to 45°S) in the IOSSO (Figure 5.22b). EKE is characterized by an increasing trend with a biennial variability. It is well evident in the plot that EKE was low during 2010 and reached the maximum during 2011. Thus the difference in the number of eddies we noted during 2010 and 2011 is a basin wide characteristic hence large scale processes may be involved in the realization of observed variability in the thermohaline structure and water masses.

In the SO, interannual variability in EKE may result from the changes in SAM. In an analysis of oceanic EKE and changes in SAM, it was observed that EKE and SAM is characterised by a 2-3 year lag, especially for the Indian Ocean sector. In our case the lag is ~1 year, somewhat faster than expected (Figure 5.22 c). To explore the EKE – SAM relationship further used an eddy-resolving quasi-geostrophic mode (Meredith and Hogg, 2006). The model results varied under different scenarios. For standard perturbation of a wind stress of ~0.21Nm^{-2} the lag in peak kinetic energy was 1.2 to 2 years whereas for a strong perturbation with a wind stress of ~0.25Nm^{-2} the lag was found to be ~1 year. Thus the fast response we observed could be due to a strong perturbation in the wind fields. This increase in EKE was associated with the increase in the circumpolar wind stress and the lag is due to the time taken to influence the circulation in the deep ocean (Meredith and Hogg, 2006). Thus the observed interannual variability in the thermohaline structure and the watermass is a result of large scale variability arising from changes in annular mode.

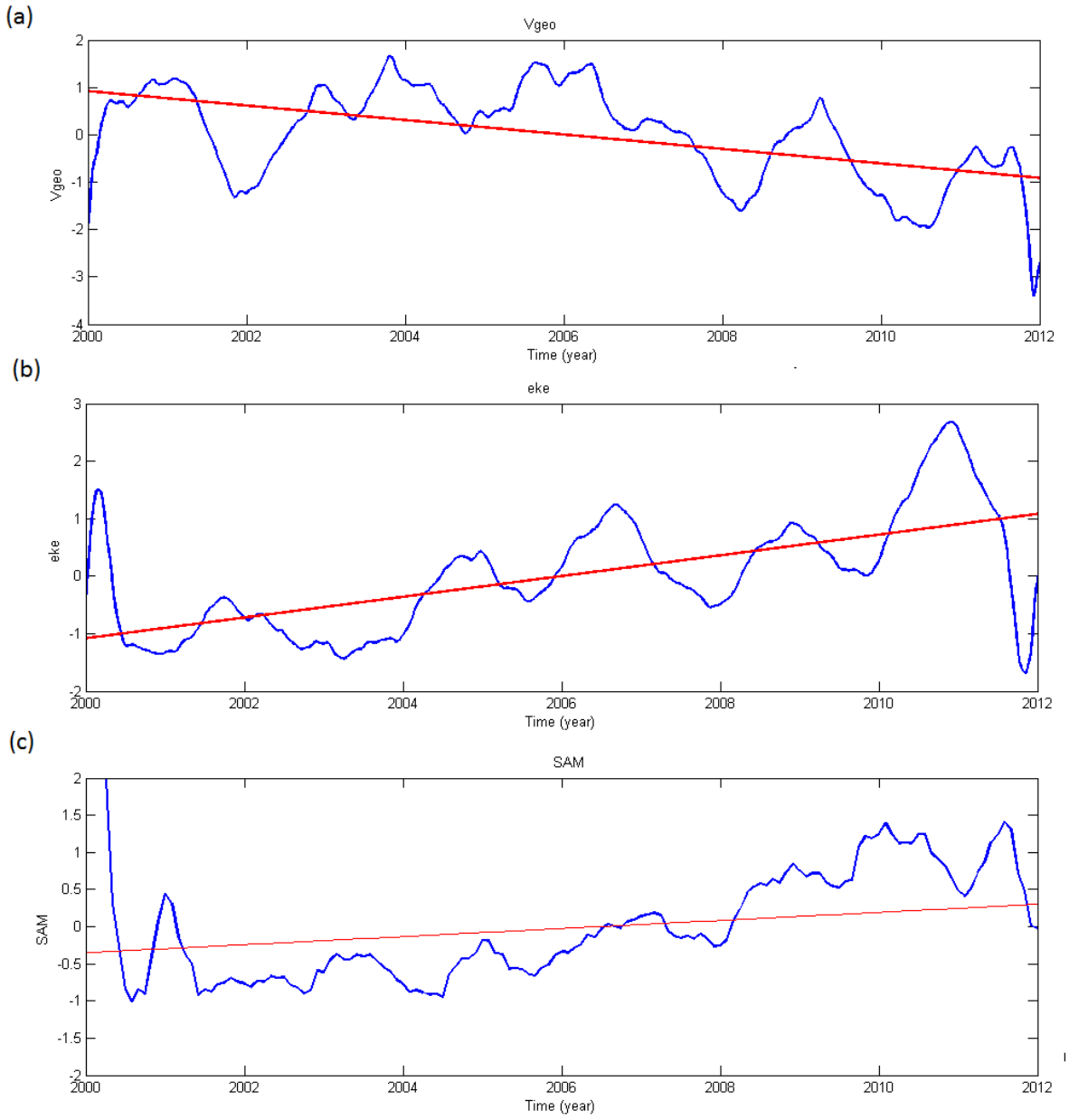

Figure 5.22. The variation of (a) v component of Geostrophic velocity (v_{geo})(b) eddy kinetic energy and (c) SAM index.

5.4.3 Conclusion

Data obtained from expendable probes and CTD during the expedition to SO along $57^{0}30'$E during the austral summer 2010 and 2011 were analyzed. The analysis reveal that the year to year variability in the hydrographic structure was due to the presence of eddies. Troughs and ridges of isotherms and, isohalines were dominant in the vertical section of temperature and salinity during 2011. SSHA data clearly indicated the presence of cyclonic and anti-cyclonic eddies along the cruise track. The eddies present in the study area transported Subtropical surface waters (STSW) southward by means of the enhanced meridional velocities along the peripheries of the eddies. Absence of eddies during 2010 restricted the southward transport of STSW to the region of its origin. Signatures of STSW south of 45°S were not clear. STSW might have either subducted or transported eastward along the SAF. Analysis of EKE shows that it peaks a year after the peak value in the SAM suggesting the role of large scale variability in controlling the EKE. Positive linear trend in the EKE suggests more southward transport of subtropical water masses which will have implications on the SO vertical mixing, air-sea interaction, sea-ice and water mass formation.

6. Summary and Conclusion

The thesis makes use of in-situ data from a region which is known to be sparse in data because of its difficulty in being accessed as well as because of the unpredictable and strong wind regime. As outlined in the introductory chapter, the study discussed about the fronts water mass, WW variability, role of eddies on water mass transport, influence of sea-ice on fronts and Chl a, SAM on PF variability and the possible causes for the freshening of AABW in the IOSO based on the high spatial and temporal resolution hydrographic data collected during the SO expeditions during 2010 and 2011 as well as satellite and model outputs.

An attempt has been made to characterise the IOSO based on various physico-chemical and biological parameters using in-situ, satellite and model outputs. The fronts and water masses in the study region identified well in the in-situ data. MADT and satellite derived SST gradients can be used as an additional tool for the identification of various fronts in the study area. The water masses in the study area have been further studied with respect to DO, nutrients and Chl a. It is noticed that the surface water masses in the polar regions are rich in oxygen concentration whereas the Intermediate waters and Subtropical water masses are relatively poor in oxygen concentration. With respect to nutrients concentration, the water masses in the polar waters again show higher nutrient concentration in comparison to the water masses in the subtropical waters region. The CDW shows the highest concentration of nutrients as compared to the watermasses identified

in the study area. The Chl a distribution shows higher values in the Subtropical frontal region but for the other fronts the concentration is lower except for the Antarctic coast which shows high value for one year. Even though DO, nutrients and Chl a in the study area showed clear discrimination between polar waters and subtropical waters, these chemical and biological indicators may not be useful tool for the identification of watermasses in the study area since its distribution mainly depends on the different scale physical and biological processes occurring in that region.

The study also addressed the effect of seasonal ice cover on the thermohaline structure of the study area. It was noticed that the temperature and core depth of WW increased from southern side of the study area to northern side. The shallowest WW depth is noted in the Antarctic divergence region (~63°S to 60°S) in 2010. Cooler WW was noted during 2011 compared to that of 2010. Fresh water thickness computed showed higher values during 2011 than that of during 2010. The source of fresh water could be the locally produced melt water or/and advection from in-situ melting of sea ice originating from the south and west. During 2009 winter the maximum sea ice limit was up to ~59°S whereas in 2010 winter it was upto ~57°S. This increase of sea ice and its northern extent during 2010 winter compared to that of 2009 winter can be a reason for the increased fresh water thickness and cold WW temperature observed in the summer of 2011. The high value of Chl a observed at PF2 in 2011 compared to that in 2010 can be attributed to the increased sea ice amount and northward sea ice extent during the 2010 winter compared to 2009 winter.

As discussed earlier, several previous studies have reported the recent freshening of the AABW in the SO. The present research also reported the rapid freshening of AABW in the IOSSO during the recent decades. The study shows that the AABW became warmer (0.05 1°C), fresher (0.01) and lighter (0.01 kg m^3) in the study area. The decadal changes indicate an enhanced sea-ice formation, due to increased positive phases of SAM, which may have led to the increase in fresh water input, resulting in freshening of AABW. All these changes imply a global-scale contraction of AABW, suggesting a possibility of a global scale slowdown of the bottom, southern limb of the global overturning circulation. Such a situation can lead to changes in the movement of heat, salt and CO_2 within the ocean basins.

The SAM is related well with the positions of the fronts particularly PF in the SO. The study also attempted to explain the significant spatial and temporal variation of PF1 and PF2 in the IOSSO with SAM. A southward shift of approximately about 2 degrees was also observed in the PF2. Bottom topography and mesoscale variability does not play a significant role in this variation. The core of the westerly winds shows a southward shift from 55°S in 2010 to 60°S in 2011. This southward shift in winds may be explained by the positive SAM seen during 2011. This southward shift in winds lead to increased Ekman transport from the coast leading to an increase in cooler waters being transported northwards which subsequently led to the northward movement of the PF2 in 2011.

The southward transport of watermasses in the STF due to eddies is also discussed. It was observed that the eddies present in the study area transported STSW southward by means of the enhanced meridional velocities along the peripheries of the eddies. Absence of eddies during 2010 restricted the southward transport of STSW to the region of its origin. Signatures of STSW south of 45°S were not clear. Analysis of EKE shows that it peaks a year after the peak value in the SAM, suggesting the role of large-scale variability in controlling the EKE. Positive linear trend in the EKE suggests more southward transport of subtropical watermasses which will have implications on the SO vertical mixing, air–sea interaction, sea-ice and water mass formation.

With the help of insitu and other available data sets, the thesis has attempted to throw light on several processes such as freshening of AABW, eddies on water mass transport, etc. occurring in the IOSO. Future studies could include detailed study on the WW region and its role in the upper ocean dynamics in the polar region. The role of SAM in frontal variability and watermass modification needs to be addressed in detail. The rapid freshening of the AABW in the IOSO reported here based on the in-situ data is still to be investigated with the help of both observational and modeling efforts. Considering the small and large scale variability of these processes in the IOSO, an improved understanding with more high temporal and spatial resolution is of utmost importance as it is imperative in understanding the role of SO on global climate and how natural variability and change in climate play a role on the SO processes.

References

- Anilkumar, N., Luis, A.J., Somayajulu, Y.K., Babu, V.R., Dash, M.K., Pednekar, S.M., Babu, K.N., Sudhakar, M. and Pandey, P.C., 2006. Fronts, water masses and heat content variability in the Western Indian sector of the Southern Ocean during austral summer 2004. *Journal of Marine Systems*, *63*(1-2), pp.20-34.
- Anilkumar, N., George, J.V., Chacko, R., Nuncio, N. and Sabu, P., 2015. Variability of fronts, fresh water input and chlorophyll in the Indian Ocean sector of the Southern Ocean. *New Zealand Journal of Marine and Freshwater Research*, *49*(1), pp.20-40.
- Aoki, S., Rintoul, S.R., Ushio, S., Watanabe, S. and Bindoff, N.L., 2005. Freshening of the Adélie Land Bottom water near 140 E. *Geophysical Research Letters*, *32*(23).
- Aoki, S., Kitade, Y., Shimada, K., Ohshima, K.I., Tamura, T., Bajish, C.C., Moteki, M. and Rintoul, S.R., 2013. Widespread freshening in the Seasonal Ice Zone near 140 E off the Adélie Land Coast, Antarctica, from 1994 to 2012. *Journal of Geophysical Research: Oceans*, *118*(11), pp.6046-6063.
- Arhan, M., Speich, S., Messager, C., Dencausse, G., Fine, R. and Boye, M., 2011. Anticyclonic and cyclonic eddies of subtropical origin in the subantarctic zone south of Africa. *Journal of Geophysical Research: Oceans*, *116*(C11).

- Arrigo, K.R., van Dijken, G.L., Ainley, D.G., Fahnestock, M.A. and Markus, T., 2002. Ecological impact of a large Antarctic iceberg. *Geophysical Research Letters*, *29*(7), pp.8-1.
- Arrigo, K.R. and Thomas, D.N., 2004. Large scale importance of sea ice biology in the Southern Ocean. *Antarctic Science*, *16*(4), pp.471-486.
- Beal, L.M., De Ruijter, W.P., Biastoch, A., Zahn, R., Cronin, M., Hermes, J., Lutjeharms, J., Quartly, G., Tozuka, T., Baker-Yeboah, S. and Bornman, T., 2011. On the role of the Agulhas system in ocean circulation and climate. *Nature*, *472*(7344), p.429.
- Behrendt, A., Dierking, W., Fahrbach, E. and Witte, H., 2013. Sea ice draft in the Weddell Sea, measured by upward looking sonars. *Earth System Science Data*, *5*(1), pp.209-226.
- Belkin, I.M. and Gordon, A.L., 1996. Southern Ocean fronts from the Greenwich meridian to Tasmania. *Journal of Geophysical Research: Oceans*, *101*(C2), pp.3675-3696.
- Billany, W., Swart, S., Hermes, J. and Reason, C.J.C., 2010. Variability of the Southern Ocean fronts at the Greenwich Meridian. *Journal of Marine Systems*, *82*(4), pp.304-310.
- Bindoff, N.L. and McDougall, T.J., 2000. Decadal changes along an Indian Ocean section at 32 S and their interpretation. *Journal of Physical Oceanography*, *30*(6), pp.1207-1222.
- Bintanja, R., Van Oldenborgh, G.J., Drijfhout, S.S., Wouters, B. and Katsman, C.A., 2013. Important role for ocean warming and increased ice-shelf melt in Antarctic sea-ice expansion. *Nature Geoscience*, *6*(5), p.376.

- Bitz, C.M. and Polvani, L.M., 2012. Antarctic climate response to stratospheric ozone depletion in a fine resolution ocean climate model. *Geophysical Research Letters*, *39*(20).
- Bonjean, F. and Lagerloef, G.S., 2002. Diagnostic model and analysis of the surface currents in the tropical Pacific Ocean. *Journal of Physical Oceanography*, *32*(10), pp.2938-2954.
- Böning, C.W., Dispert, A., Visbeck, M., Rintoul, S.R. and Schwarzkopf, F.U., 2008. The response of the Antarctic Circumpolar Current to recent climate change. *Nature Geoscience*, *1*(12), p.864.
- Botnikov, V.N., 1963. Geographical position of the Antarctic Convergence Zone in the Antarctic Ocean. *Soviet Antarctic Exped. Inform. Bull.*, *41*, pp.324-327.
- Boyd, P.W. and Ellwood, M.J., 2010. The biogeochemical cycle of iron in the ocean. *Nature Geoscience*, *3*(10), p.675.
- Boyer, T.P., Levitus, S., Antonov, J.I., Locarnini, R.A. and Garcia, H.E., 2005. Linear trends in salinity for the World Ocean, 1955–1998. *Geophysical Research Letters*, *32*(1).
- Bromwich, D.H., Robasky, F.M., Cullather, R.I. and Van Woert, M.L., 1995. The atmospheric hydrologic cycle over the Southern Ocean and Antarctica from operational numerical analyses. *Monthly Weather Review*, *123*(12), pp.3518-3538.
- Buinitsky, V.K., 1973. Sea ice and icebergs of the Antarctic. *University of Leningrad, 225p*.

- Carleton, A.M., 2003. Atmospheric teleconnections involving the Southern Ocean. *Journal of Geophysical Research: Oceans*, *108*(C4).
- Carmack, E.C. and Foster, T.D., 1975, November. On the flow of water out of the Weddell Sea. In *Deep Sea Research and Oceanographic Abstracts* (Vol. 22, No. 11, pp. 711-724). Elsevier.
- CFSOA (Committee on Future Science Opportunities in Antarctica and the Southern Ocean), 2011. Future Science Opportunities in Antarctica and the Southern Ocean. National Research Council, The National Academies Press, Washington, D.C., 189 pp.
- Chaigneau, A., Morrow, R.A. and Rintoul, S.R., 2004. Seasonal and interannual evolution of the mixed layer in the Antarctic Zone south of Tasmania. *Deep Sea Research Part I: Oceanographic Research Papers*, *51*(12), pp.2047-2072.
- Chapman, C.C. and Morrow, R., 2014. Variability of Southern Ocean jets near topography. *Journal of Physical Oceanography*, *44*(2), pp.676-693.
- Chase, T. E., Seekins, B. A., Young, J. D., and Eittrim, S. L.,1987. Marine topography of offshore Antarctica, in The Antarctic Continental Margin: Geology and Geophysics of Offshore Wilkes Land, Earth Sci. Ser., vol. 5, A, edited by S. L. Eittrim, and M. A. Hampton, Circum-Pac. Counc. for Energy and Miner. Resour., Houston, Tex. pp. 147–150.
- Chelton, D.B., Schlax, M.G., Witter, D.L. and Richman, J.G., 1990. Geosat altimeter observations of the surface circulation of the Southern

Ocean. *Journal of Geophysical Research: Oceans*, *95*(C10), pp.17877-17903.

- Colton, M.T. and Chase, R.R., 1983. Interaction of the Antarctic Circumpolar Current with bottom topography: An investigation using satellite altimetry. *Journal of Geophysical Research: Oceans*, *88*(C3), pp.1825-1843.
- Constable, A.J., Melbourne-Thomas, J., Corney, S.P., Arrigo, K.R., Barbraud, C., Barnes, D.K., Bindoff, N.L., Boyd, P.W., Brandt, A., Costa, D.P. and Davidson, A.T., 2014. Climate change and Southern Ocean ecosystems I: how changes in physical habitats directly affect marine biota. *Global Change Biology*, *20*(10), pp.3004-3025.
- Couldrey, M.P., Jullion, L., Naveira Garabato, A.C., Rye, C., Herráiz-Borreguero, L., Brown, P.J., Meredith, M.P. and Speer, K.L., 2013. Remotely induced warming of Antarctic Bottom Water in the eastern Weddell gyre. *Geophysical Research Letters*, *40*(11), pp.2755-2760.
- Craneguy, P. and Park, Y.H., 1999. Contrôle topographique du courant circumpolaire antarctique dans l'océan Indien sud. *Comptes Rendus de l'Académie des Sciences-Series IIA-Earth and Planetary Science*, *328*(9), pp.583-589.
- Curry, W.B., Shackleton, N.J. and Richter, C., 1995. Leg 154. *Synthesis. Proceedings ODP, Initial Reports*, *154*, pp.421-442.

- Curry, R., Dickson, B. and Yashayaev, I., 2003. A change in the freshwater balance of the Atlantic Ocean over the past four decades. *Nature*, *426*(6968), p.826.
- Darbyshire, M., 1966, February. The surface waters near the coasts of southern Africa. In *Deep Sea Research and Oceanographic Abstracts* (Vol. 13, No. 1, pp. 57-81). Elsevier.
- Deacon, G.E., 1933. A general account of the hydrology of the South Atlantic Ocean. *Discovery Reports*, *7*, pp.171-238.
- Deacon, G.E.R., 1937. The hydrology of the Southern Ocean. *Discovery Rep.*, *15*, pp.3-122.
- Deacon, G.E.R., 1979. The Weddell Gyre. *Deep Sea Research Part A. Oceanographic Research Papers*, *26*(9), pp.981-995.
- Deacon, G.E.R., 1982. Physical and biological zonation in the Southern Ocean. *Deep Sea Research Part A. Oceanographic Research Papers*, *29*(1), pp.1-15.
- Dee, D.P., Uppala, S.M., Simmons, A.J., Berrisford, P., Poli, P., Kobayashi, S., Andrae, U., Balmaseda, M.A., Balsamo, G., Bauer, D.P. and Bechtold, P., 2011. The ERA-Interim reanalysis: Configuration and performance of the data assimilation system. *Quarterly Journal of the royal meteorological society*, *137*(656), pp.553-597.
- de Szoeke, R.A. and Levine, M.D., 1981. The advective flux of heat by mean geostrophic motions in the Southern Ocean. *Deep Sea Research Part A. Oceanographic Research Papers*, *28*(10), pp.1057-1085.

- Dickson, B., Yashayaev, I., Meincke, J., Turrell, B., Dye, S. and Holfort, J., 2002. Rapid freshening of the deep North Atlantic Ocean over the past four decades. *Nature*, *416*(6883), p.832.
- Dijkstra, H.A. and Ghil, M., 2005. Low-frequency variability of the large-scale ocean circulation: A dynamical systems approach. *Reviews of Geophysics*, *43*(3).
- Doney, S.C., Large, W.G. and Bryan, F.O., 1998. Surface ocean fluxes and water-mass transformation rates in the coupled NCAR Climate System Model. *Journal of Climate*, *11*(6), pp.1420-1441.
- Dong, S., Sprintall, J. and Gille, S.T., 2006. Location of the Antarctic polar front from AMSR-E satellite sea surface temperature measurements. *Journal of Physical Oceanography*, *36*(11), pp.2075-2089.
- Dubischar, C.D. and Bathmann, U.V., 1997. Grazing impact of copepods and salps on phytoplankton in the Atlantic sector of the Southern Ocean. *Deep Sea Research Part II: Topical Studies in Oceanography*, *44*(1-2), pp.415-433.
- Ducklow, H.W., Schofield, O., Vernet, M., Stammerjohn, S. and Erickson, M., 2012. Multiscale control of bacterial production by phytoplankton dynamics and sea ice along the western Antarctic Peninsula: a regional and decadal investigation. *Journal of Marine Systems*, *98*, pp.26-39.
- Durack, P.J. and Wijffels, S.E., 2010. Fifty-year trends in global ocean salinities and their relationship to broad-scale warming. *Journal of Climate*, *23*(16), pp.4342-4362.

- El-Sayed, S., 1984. Productivity of the Antarctic waters—a reappraisal. In *Marine phytoplankton and productivity* (pp. 19-34). Springer, Berlin, Heidelberg.
- Fahrbach, E., Rohardt, G., Scheele, N., Schröder, M., Strass, V. and Wisotzki, A., 1995. Formation and discharge of deep and bottom water in the northwestern Weddell Sea. *Journal of Marine Research*, *53*(4), pp.515-538.
- Farneti, R., Delworth, T.L., Rosati, A.J., Griffies, S.M. and Zeng, F., 2010. The role of mesoscale eddies in the rectification of the Southern Ocean response to climate change. *Journal of Physical Oceanography*, *40*(7), pp.1539-1557.
- Ferrari, R. and Nikurashin, M., 2010. Suppression of eddy diffusivity across jets in the Southern Ocean. *Journal of Physical Oceanography*, *40*(7), pp.1501-1519.
- Ferreira, D., Marshall, J., Bitz, C.M., Solomon, S. and Plumb, A., 2015. Antarctic Ocean and sea ice response to ozone depletion: A two-time-scale problem. *Journal of Climate*, *28*(3), pp.1206-1226.
- Figa-Saldaña, J., Wilson, J.J., Attema, E., Gelsthorpe, R., Drinkwater, M.R. and Stoffelen, A., 2002. The advanced scatterometer (ASCAT) on the meteorological operational (MetOp) platform: A follow on for European wind scatterometers. *Canadian Journal of Remote Sensing*, *28*(3), pp.404-412.

- Fine, R.A., 1993. Circulation of Antarctic intermediate water in the South Indian Ocean. *Deep Sea Research Part I: Oceanographic Research Papers*, *40*(10), pp.2021-2042.
- Fletcher, J. O., 1969. Ice extent on the Southern Ocean and its relation to world climate, Memo. RM-5793-NSF, 108 pp., Rand Corp., Santa Monica, Calif.,
- Foldvik, A., Gammelsrød, T., Østerhus, S., Fahrbach, E., Rohardt, G., Schröder, M., Nicholls, K.W., Padman, L. and Woodgate, R.A., 2004. Ice shelf water overflow and bottom water formation in the southern Weddell Sea. *Journal of Geophysical Research: Oceans*, *109*(C2).
- Foster, T.D. and Carmack, E.C., 1976, April. Frontal zone mixing and Antarctic Bottom Water formation in the southern Weddell Sea. In *Deep Sea Research and Oceanographic Abstracts* (Vol. 23, No. 4, pp. 301-317). Elsevier.
- Fyfe, J.C., 2006. Southern Ocean warming due to human influence. *Geophysical Research Letters*, *33*(19).
- Fyfe, J.C., Saenko, O.A., Zickfeld, K., Eby, M. and Weaver, A.J., 2007. The role of poleward-intensifying winds on Southern Ocean warming. *Journal of Climate*, *20*(21), pp.5391-5400.
- Ganachaud, A. and Wunsch, C., 2000. Improved estimates of global ocean circulation, heat transport and mixing from hydrographic data. *Nature*, *408*(6811), p.453.
- Gandhi, N., Ramesh, R., Laskar, A.H., Sheshshayee, M.S., Shetye, S., Anilkumar, N., Patil, S.M. and Mohan, R., 2012. Zonal variability in

primary production and nitrogen uptake rates in the southwestern Indian Ocean and the Southern Ocean. *Deep Sea Research Part I: Oceanographic Research Papers*, *67*, pp.32-43.

- Gao, Y., Fan, S.M. and Sarmiento, J.L., 2003. Aeolian iron input to the ocean through precipitation scavenging: A modeling perspective and its implication for natural iron fertilization in the ocean. *Journal of Geophysical Research: Atmospheres*, *108*(D7).
- G, S.T., 1994. Mean sea surface height of the Antarctic Circumpolar Current from Geosat data: Method and application. *Journal of Geophysical Research: Oceans*, *99*(C9), pp.18255-18273.
- Gille, S.T., 1999. Mass, heat, and salt transport in the southeastern Pacific: A Circumpolar Current inverse model. *Journal of Geophysical Research: Oceans*, *104*(C3), pp.5191-5209.
- Gille, S.T., 2002. Warming of the Southern Ocean since the 1950s. *Science*, *295*(5558), pp.1275-1277.
- Gille, S.T., 2008. Decadal-scale temperature trends in the Southern Hemisphere ocean. *Journal of Climate*, *21*(18), pp.4749-4765.
- Gille, S.T., 2014. Meridional displacement of the Antarctic Circumpolar Current. *Phil. Trans. R. Soc. A*, *372*(2019), p.20130273.
- Gladyshev, S., Arhan, M., Sokov, A. and Speich, S., 2008. A hydrographic section from South Africa to the southern limit of the Antarctic Circumpolar Current at the Greenwich meridian. *Deep Sea Research Part I: Oceanographic Research Papers*, *55*(10), pp.1284-1303.

- Gordon, A.L. and Taylor, H.W., 1975. Seasonal change of Antarctic sea ice cover. *Science*, *187*(4174), pp.346-347.
- Gordon, A.L., Georgi, D.T. and Taylor, H.W., 1977. Antarctic polar front zone in the western Scotia Sea—Summer 1975. *Journal of Physical Oceanography*, *7*(3), pp.309-328.
- Gordon, A.L., Molinelli, E. and Baker, T., 1978. Large-scale relative dynamic topography of the Southern Ocean. *Journal of Geophysical Research: Oceans*, *83*(C6), pp.3023-3032.
- Gordon, A.L. and Molinelli, E., 1982. Southern Ocean Atlas: thermohaline and chemical distributions. *Columbia Univ., Press, New York*, p.33.
- Gordon, A.L., 1986. Interocean exchange of thermocline water. *Journal of Geophysical Research: Oceans*, *91*(C4), pp.5037-5046.
- Gordon, A.L., 1998. Western Weddell sea thermohaline stratification. *Ocean, Ice and Atmosphere: Interactions at the Antarctic Continental Margin, Antarct. Res. Ser*, *75*, pp.215-240.
- Gouretski, V.V. and Danilov, A.I., 1993. Weddell Gyre: structure of the eastern boundary. *Deep Sea Research Part I: Oceanographic Research Papers*, *40*(3), pp.561-582.
- Hall, A. and Visbeck, M., 2002. Synchronous variability in the Southern Hemisphere atmosphere, sea ice, and ocean resulting from the annular mode. *Journal of Climate*, *15*(21), pp.3043-3057.
- Hamilton, L.J., 2006. Structure of the subtropical front in the Tasman Sea. *Deep Sea Research Part I: Oceanographic Research Papers*, *53*(12), pp.1989-2009.

- Harrison, W.G. and Cota, G.F., 1991. Primary production in polar waters: relation to nutrient availability. *Polar Research*, *10*(1), pp.87-104.
- Hartmann, D.L. and Lo, F., 1998. Wave-driven zonal flow vacillation in the Southern Hemisphere. *Journal of the Atmospheric Sciences*, *55*(8), pp.1303-1315.
- Hofmann, E.E., 1985. The large-scale horizontal structure of the Antarctic Circumpolar Current from FGGE drifters. *Journal of Geophysical Research: Oceans*, *90*(C4), pp.7087-7097.
- Hogg, A.M.C. and Blundell, J.R., 2006. Interdecadal variability of the Southern Ocean. *Journal of physical oceanography*, *36*(8), pp.1626-1645.
- Hogg, A.M.C., Meredith, M.P., Blundell, J.R. and Wilson, C., 2008. Eddy heat flux in the Southern Ocean: Response to variable wind forcing. *Journal of Climate*, *21*(4), pp.608-620.
- Holland, P.R., 2014. The seasonality of Antarctic sea ice trends. *Geophysical Research Letters*, *41*(12), pp.4230-4237.
- Holliday, N.P. and Read, J.F., 1998. Surface oceanic fronts between Africa and Antarctica. *Deep Sea Research Part I: Oceanographic Research Papers*, *45*(2-3), pp.217-238.
- Holm-Hansen, O., Kahru, M. and Hewes, C.D., 2005. Deep chlorophyll a maxima (DCMs) in pelagic Antarctic waters. II. Relation to bathymetric features and dissolved iron concentrations. *Marine Ecology Progress Series*, *297*, pp.71-81.

- Hughes, C.W., Meredith, M.P. and Heywood, K.J., 1999. Wind-driven transport fluctuations through Drake Passage: A southern mode. *Journal of Physical Oceanography*, *29*(8), pp.1971-1992.
- Hughes, C.W. and Ash, E.R., 2001. Eddy forcing of the mean flow in the Southern Ocean. *Journal of Geophysical Research: Oceans*, *106*(C2), pp.2713-2722.
- Ingleby, B. and Huddleston, M., 2007. Quality control of ocean temperature and salinity profiles—Historical and real-time data. *Journal of Marine Systems*, *65*(1), pp.158-175.
- Jacobs, S.S., Jenkins, A., Giulivi, C.F. and Dutrieux, P., 2011. Stronger ocean circulation and increased melting under Pine Island Glacier ice shelf. *Nature Geoscience*, *4*(8), p.519.
- Jacobs, S.S., Giulivi, C.F. and Mele, P.A., 2002. Freshening of the Ross Sea during the late 20th century. *Science*, *297*(5580), pp.386-389.
- Jacobs, S.S., 2004. Bottom water production and its links with the thermohaline circulation. *Antarctic Science*, *16*(4), pp.427-437.
- Jacobs, S., 2006. Observations of change in the Southern Ocean. *Philosophical Transactions of the Royal Society of London A: Mathematical, Physical and Engineering Sciences*, *364*(1844), pp.1657-1681.
- Jacobs, S.S. and Giulivi, C.F., 2010. Large multidecadal salinity trends near the Pacific–Antarctic continental margin. *Journal of Climate*, *23*(17), pp.4508-4524.

- Jacobs, S.S., Jenkins, A., Giulivi, C.F. and Dutrieux, P., 2011. Stronger ocean circulation and increased melting under Pine Island Glacier ice shelf. *Nature Geoscience*, *4*(8), p.519.
- James, C., Tomczak, M., Helmond, I. and Pender, L., 2002. Summer and winter surveys of the Subtropical Front of the southeastern Indian Ocean 1997–1998. *Journal of Marine Systems*, *37*(1-3), pp.129-149.
- Jasmine, P., Muraleedharan, K.R., Madhu, N.V., Devi, C.A., Alagarsamy, R., Achuthankutty, C.T., Jayan, Z., Sanjeevan, V.N. and Sahayak, S., 2009. Hydrographic and productivity characteristics along 45 E longitude in the southwestern Indian Ocean and Southern Ocean during Austral summer 2004. *Marine Ecology Progress Series*, *389*, pp.97-116.
- Jenkins, A., 1999. The impact of melting ice on ocean waters. *Journal of physical oceanograpLehy*, *29*(9), pp.2370-2381.
- Jia, F., Wu, L., Lan, J. and Qiu, B., 2011. Interannual modulation of eddy kinetic energy in the southeast Indian Ocean by Southern Annular Mode. *Journal of Geophysical Research: Oceans*, *116*(C2).
- Johnson, G.C., 2008. Quantifying Antarctic bottom water and North Atlantic deep water volumes. *Journal of Geophysical Research: Oceans*, *113*(C5).
- Jones, E.P., Nelson, D.M and Treguer, P., 1990. Chemical Oceanography. In: Polar Oceanography, Part B: Chemistry,Biology and Geology, Academic Press, London, pp. 407-476.
- Jullion, L., Naveira Garabato, A.C., Meredith, M.P., Holland, P.R., Courtois, P. and King, B.A., 2013. Decadal freshening of the Antarctic

Bottom Water exported from the Weddell Sea. *Journal of Climate*, *26*(20), pp.8111-8125.

- Keeling, C.D. and Bolin, B., 1967. The simultaneous use of chemical tracers in oceanic studies I. General theory of reservoir models 1, 2. *Tellus*, *19*(4), pp.566-581.
- Killworth, P.D., 1974, October. A baroclinic model of motions on Antarctic continental shelves. In *Deep Sea Research and Oceanographic Abstracts* (Vol. 21, No. 10, pp. 815-837). Elsevier.
- Kostianoy, A.G., Ginzburg, A.I., Frankignoulle, M. and Delille, B., 2004. Fronts in the Southern Indian Ocean as inferred from satellite sea surface temperature data. *Journal of Marine Systems*, *45*(1-2), pp.55-73.
- Krauss, W. and Käse, R. H., 1984. Mean circulation and eddy kinetic energy in the eastern North Atlantic. *Journal of Geophysical Research: Oceans*, (89), pp 3407–3415.
- Lee, M.M., Nurser, A.G., Coward, A.C. and De Cuevas, B.A., 2007. Eddy advective and diffusive transports of heat and salt in the Southern Ocean. *Journal of physical oceanography*, *37*(5), pp.1376-1393.
- Lefebvre, W., Goosse, H., Timmermann, R. and Fichefet, T., 2004. Influence of the Southern Annular Mode on the sea ice–ocean system. *Journal of Geophysical Research: Oceans*, *109*(C9).
- Lenn, Y.D. and Chereskin, T.K., 2009. Observations of Ekman currents in the Southern Ocean. *Journal of Physical Oceanography*, *39*(3), pp.768-779.

- Lovenduski, N.S. and Gruber, N., 2005. Impact of the Southern Annular Mode on Southern Ocean circulation and biology. *Geophysical Research Letters*, *32*(11).
- Iudicone, D., Speich, S., Madec, G. and Blanke, B., 2008. The global conveyor belt from a Southern Ocean perspective. *Journal of Physical Oceanography*, *38*(7), pp.1401-1425.
- Luis, A.J. and Sudhakar, M., 2009. Upper-ocean hydrodynamics along meridional sections in the southwest Indian sector of the Southern Ocean during austral summer 2007. *Polar Science*, *3*(1), pp.13-30.
- Lumpkin, R. and Speer, K., 2007. Global ocean meridional overturning. *Journal of Physical Oceanography*, *37*(10), pp.2550-2562.
- Lutjeharms, J.R.E. and Baker Jr, D.J., 1980. A statistical analysis of the meso-scale dynamics of the Southern Ocean. *Deep Sea Research Part A. Oceanographic Research Papers*, *27*(2), pp.145-159.
- Lutjeharms, J.E. and Valentine, H.R., 1984. Southern Ocean thermal fronts south of Africa. *Deep Sea Research Part A. Oceanographic Research Papers*, *31*(12), pp.1461-1475.
- Lutjeharms, J.R.E. and Ansorge, I.J., 2001. The Agulhas return current. *Journal of Marine Systems*, *30*(1-2), pp.115-138.
- Madec, G., 2008. NEMO ocean general circulation model reference manuel. In *Internal Report*. LODYC/IPSL Paris.
- Marshall, G.J., 2003. Trends in the Southern Annular Mode from observations and reanalyses. *Journal of Climate*, *16*(24), pp.4134-4143.

- Marshall, G.J., Stott, P.A., Turner, J., Connolley, W.M., King, J.C. and Lachlan-Cope, T.A., 2004. Causes of exceptional atmospheric circulation changes in the Southern Hemisphere. *Geophysical Research Letters*, *31*(14).
- Marshall, G.J., Orr, A., Van Lipzig, N.P. and King, J.C., 2006. The impact of a changing Southern Hemisphere Annular Mode on Antarctic Peninsula summer temperatures. *Journal of Climate*, *19*(20), pp.5388-5404.
- Marshall, J. and Speer, K., 2012. Closure of the meridional overturning circulation through Southern Ocean upwelling. *Nature Geoscience*, *5*(3), p.171.
- Martin, J.H. and Fitzwater, S.E., 1988. Iron deficiency limits phytoplankton growth in the north-east Pacific subarctic. *Nature*, *331*(6154), p.341
- Martin, J.H., Gordon, R.M. and Fitzwater, S.E., 1990. Iron in Antarctic waters. *Nature*, *345*(6271), p.156.
- Martinson, D.G., 2012. Antarctic circumpolar current's role in the Antarctic ice system: An overview. *Palaeogeography, Palaeoclimatology, Palaeoecology*, *335*, pp.71-74.
- Massom, R.A. and Stammerjohn, S.E., 2010. Antarctic sea ice change and variability–physical and ecological implications. *Polar Science*, *4*(2), pp.149-186.
- McCartney, M.S., 1977. Subantarctic Mode Water. In. *A Voyage of Discovery, Deep Sea Research*, *24*, pp.103-119.

- McGrath, D., Steffen, K., Rajaram, H., Scambos, T., Abdalati, W. and Rignot, E., 2012. Basal crevasses on the Larsen C Ice Shelf, Antarctica: Implications for meltwater ponding and hydrofracture. *Geophysical research letters*, *39*(16).
- Meehl, G. A. et al. in IPCC Climate Change 2007: The Physical Science Basis. Contribution of Working Group I to the Fourth Assessment Report of the Intergovernmental Panel on Climate Change (eds Solomon, S. et al.) (Cambridge Univ. Press, 2007).
- Meijers, A.J., Shuckburgh, E., Bruneau, N., Sallee, J.B., Bracegirdle, T.J. and Wang, Z., 2012. Representation of the Antarctic Circumpolar Current in the CMIP5 climate models and future changes under warming scenarios. *Journal of Geophysical Research: Oceans*, *117*(C12).
- Meijers, A.J.S., 2014. The Southern Ocean in the coupled model intercomparison project phase 5. *Phil. Trans. R. Soc. A*, *372*(2019), p.20130296.
- Meredith, M.P. and Hogg, A.M., 2006. Circumpolar response of Southern Ocean eddy activity to a change in the Southern Annular Mode. *Geophysical Research Letters*, *33*(16).
- Meredith, M.P., Garabato, A.C.N., Gordon, A.L. and Johnson, G.C., 2008. Evolution of the deep and bottom waters of the Scotia Sea, Southern Ocean, during 1995–2005. *Journal of Climate*, *21*(13), pp.3327-3343.
- Mikaloff Fletcher, S.E., Gruber, N., Jacobson, A.R., Doney, S.C., Dutkiewicz, S., Gerber, M., Follows, M., Joos, F., Lindsay, K., Menemenlis, D. and Mouchet, A., 2006. Inverse estimates of

anthropogenic CO2 uptake, transport, and storage by the ocean. *Global Biogeochemical Cycles*, *20*(2).

- Mitchell, B.G., Brody, E.A., Holm-Hansen, O., McClain, C. and Bishop, J., 1991. Light limitation of phytoplankton biomass and macronutrient utilization in the Southern Ocean. *Limnology and Oceanography*, *36*(8), pp.1662-1677.
- Molinelli, E.J., 1981. The Antarctic influence on Antarctic intermediate water. *J. mar. Res.*, *39*, pp.267-293.
- Moore, J.K., Abbott, M.R. and Richman, J.G., 1997. Variability in the location of the Antarctic Polar Front (90–20 W) from satellite sea surface temperature data. *Journal of Geophysical Research: Oceans*, *102*(C13), pp.27825-27833.
- Moore, J.K., Abbott, M.R. and Richman, J.G., 1999. Location and dynamics of the Antarctic Polar Front from satellite sea surface temperature data. *Journal of Geophysical Research: Oceans*, *104*(C2), pp.3059-3073.
- Morrow, R., Valladeau, G. and Sallee, J.B., 2008. Observed subsurface signature of Southern Ocean sea level rise. *Progress in Oceanography*, *77*(4), pp.351-366.
- Morrow, R., Ward, M.L., Hogg, A.M. and Pasquet, S., 2010. Eddy response to Southern Ocean climate modes. *Journal of Geophysical Research: Oceans*, *115*(C10).
- Nelson, D.M. and Smith Jr, W.0., 1991. Sverdrup revisited: Critical depths, maximum chlorophyll levels, and the control of Southern Ocean

productivity by the irradiance-mixing regime. *Limnology and Oceanography*, *36*(8), pp.1650-1661.

- Nicholls, K.W., Østerhus, S., Makinson, K., Gammelsrød, T. and Fahrbach, E., 2009. Ice-ocean processes over the continental shelf of the southern Weddell Sea, Antarctica: A review. *Reviews of Geophysics*, *47*(3).
- Nielsen, S.H., Koç, N. and Crosta, X., 2004. Holocene climate in the Atlantic sector of the Southern Ocean: controlled by insolation or oceanic circulation?. *Geology*, *32*(4), pp.317-320.
- Nowlin Jr, W.D. and Clifford, M., 1982. The kinematic and thermohaline zonation of the Antarctic Circumpolar Current at Drake Passage. *Journal of Marine Research*, *40*, pp.481-507.
- Nowlin Jr, W.D. and Klinck, J.M., 1986. The physics of the Antarctic circumpolar current. *Reviews of Geophysics*, *24*(3), pp.469-491.
- Nuncio, M., Luis, A.J. and Yuan, X., 2011. Topographic meandering of Antarctic Circumpolar Current and Antarctic Circumpolar Wave in the ice-ocean-atmosphere system. *Geophysical Research Letters*, *38*(13).
- Ohshima, K.I., Fukamachi, Y., Williams, G.D., Nihashi, S., Roquet, F., Kitade, Y., Tamura, T., Hirano, D., Herraiz-Borreguero, L., Field, I. and Hindell, M., 2013. Antarctic Bottom Water production by intense sea-ice formation in the Cape Darnley polynya. *Nature Geoscience*, *6*(3), p.235.
- Oke, P.R. and England, M.H., 2004. Oceanic response to changes in the latitude of the Southern Hemisphere subpolar westerly winds. *Journal of Climate*, *17*(5), pp.1040-1054.

- Orsi, A.H., Nowlin Jr, W.D. and Whitworth III, T., 1993. On the circulation and stratification of the Weddell Gyre. *Deep Sea Research Part I: Oceanographic Research Papers*, *40*(1), pp.169-203.
- Orsi, A.H., Whitworth III, T. and Nowlin Jr, W.D., 1995. On the meridional extent and fronts of the Antarctic Circumpolar Current. *Deep Sea Research Part I: Oceanographic Research Papers*, *42*(5), pp.641-673.
- Orsi, A.H., Johnson, G.C. and Bullister, J.L., 1999. Circulation, mixing, and production of Antarctic Bottom Water. *Progress in Oceanography*, *43*(1), pp.55-109.
- Orsi, A.H., Jacobs, S.S., Gordon, A.L. and Visbeck, M., 2001. Cooling and ventilating the abyssal ocean. *Geophysical Research Letters*, *28*(15), pp.2923-2926.
- Orsi, A.H., Smethie, W.M. and Bullister, J.L., 2002. On the total input of Antarctic waters to the deep ocean: A preliminary estimate from chlorofluorocarbon measurements. *Journal of Geophysical Research: Oceans*, *107*(C8), pp.31-1.
- Park, Y.H., Gambéroni, L. and Charriaud, E., 1991. Frontal structure and transport of the Antarctic Circumpolar Current in the south Indian Ocean sector, 40–80 E. *Marine Chemistry*, *35*(1-4), pp.45-62.
- Park, Y.H., Gamberoni, L. and Charriaud, E., 1993. Frontal structure, water masses, and circulation in the Crozet Basin. *Journal of Geophysical Research: Oceans*, *98*(C7), pp.12361-12385.

- Park, Y.H., Charriaud, E. and Fieux, M., 1998. Thermohaline structure of the Antarctic surface water/winter water in the Indian sector of the Southern Ocean. *Journal of Marine Systems*, *17*(1-4), pp.5-23.
- Park, M.G., Yang, S.R., Kang, S.H., Chung, K.H. and Shim, J.H., 1999. Phytoplankton biomass and primary production in the marginal ice zone of the northwestern Weddell Sea during austral summer. *Polar Biology*, *21*(4), pp.251-261
- Park, K.A., Kang, C.K., Kim, K.R. and Park, J.E., 2014. Role of sea ice on satellite-observed chlorophyll-a concentration variations during spring bloom in the East/Japan sea. *Deep Sea Research Part I: Oceanographic Research Papers*, *83*, pp.34-44.
- Parkinson, C.L., 2004. Southern Ocean sea ice and its wider linkages: insights revealed from models and observations. *Antarctic Science*, *16*(4), pp.387-400.
- Peterson, R.G. and Whitworth, T., 1989. The Subantarctic and Polar Fronts in relation to deep water masses through the southwestern Atlantic. *Journal of Geophysical Research: Oceans*, *94*(C8), pp.10817-10838.
- Pond, S. and Pickard, G.L., 1978. Introductory dynamic oceanography, 241 pp.
- Priddle, J., Hawes, I., Ellis-Evans, J.C. and Smith, T.J., 1986. Antarctic aquatic ecosystems as habitats for phytoplankton. *Biological Reviews*, *61*(3), pp.199-238.

- Pritchard, H., Ligtenberg, S.R.M., Fricker, H.A., Vaughan, D.G., Van den Broeke, M.R. and Padman, L., 2012. Antarctic ice-sheet loss driven by basal melting of ice shelves. *Nature*, *484*(7395), p.502.
- Purkey, S.G. and Johnson, G.C., 2010. Warming of global abyssal and deep Southern Ocean waters between the 1990s and 2000s: Contributions to global heat and sea level rise budgets. *Journal of Climate*, *23*(23), pp.6336-6351.
- Purkey, S.G. and Johnson, G.C., 2012. Global contraction of Antarctic Bottom Water between the 1980s and 2000s. *Journal of Climate*, *25*(17), pp.5830-5844.
- Rayner, N.A., Parker, D.E., Horton, E.B., Folland, C.K., Alexander, L.V., Rowell, D.P., Kent, E.C. and Kaplan, A., 2003. Global analyses of sea surface temperature, sea ice, and night marine air temperature since the late nineteenth century. *Journal of Geophysical Research: Atmospheres*, *108*(D14).
- Read, J.F. and Pollard, R.T., 1993. Structure and transport of the Antarctic circumpolar current and Agulhas return current at 40 E. *Journal of Geophysical Research: Oceans*, *98*(C7), pp.12281-12295.
- Read, J.F., Lucas, M.I., Holley, S.E. and Pollard, R.T., 2000. Phytoplankton, nutrients and hydrography in the frontal zone between the Southwest Indian Subtropical gyre and the Southern Ocean. *Deep Sea Research Part I: Oceanographic Research Papers*, *47*(12), pp.2341-2367.

- Richardson, P.L., 1983. Eddy kinetic energy in the North Atlantic from surface drifters. *Journal of Geophysical Research: Oceans*, *88*(C7), pp.4355-4367.
- Rignot, E., Bamber, J.L., Van Den Broeke, M.R., Davis, C., Li, Y., Van De Berg, W.J. and Van Meijgaard, E., 2008. Recent Antarctic ice mass loss from radar interferometry and regional climate modelling. *Nature geoscience*, *1*(2), p.106.
- Rignot, E., Jacobs, S., Mouginot, J. and Scheuchl, B., 2013. Ice-shelf melting around Antarctica. *Science*, *341*(6143), pp.266-270.
- Rind, D., Healy, R., Parkinson, C. and Martinson, D., 1995. The role of sea ice in 2× CO2 climate model sensitivity. Part I: The total influence of sea ice thickness and extent. *Journal of Climate*, *8*(3), pp.449-463.
- Rintoul, S.R., 1991. South Atlantic interbasin exchange. *Journal of Geophysical Research: Oceans*, *96*(C2), pp.2675-2692.
- Rintoul, S.R., Donguy, J.R. and Roemmich, D.H., 1998. Seasonal evolution of upper ocean thermal structure between Tasmania and Antarctica. *Oceanographic Literature Review*, *2*(45), p.225.
- Rintoul, S.R. and Bullister, J.L., 1999. A late winter hydrographic section from Tasmania to Antarctica. *Deep Sea Research Part I: Oceanographic Research Papers*, *46*(8), pp.1417-1454.
- Rintoul, S.R., Hughes, C.W. and Olbers, D., 2001. .6 The antarctic circumpolar current system. In *International Geophysics* (Vol. 77, pp. 271-XXXVI). Academic Press.

- Rintoul, S.R. and Sokolov, S., 2001. Baroclinic transport variability of the Antarctic Circumpolar Current south of Australia (WOCE repeat section SR3). *Journal of Geophysical Research: Oceans*, *106*(C2), pp.2815-2832.
- Rintoul, S.R. and England, M.H., 2002. Ekman transport dominates local air–sea fluxes in driving variability of Subantarctic Mode Water. *Journal of Physical Oceanography*, *32*(5), pp.1308-1321.
- Rintoul, S.R., 2007. Rapid freshening of Antarctic Bottom Water formed in the Indian and Pacific oceans. *Geophysical Research Letters*, *34*(6).
- Rintoul, S. R., 2011. The Southern Ocean in the Earth System, in Science Diplomacy: Antarctica, Science, and the Governance of International Spaces , edited by P. A. Berkman et al., Smithsonian Institution Scholarly Press, Washington, D. C, pp. 175–187.
- Rintoul, S.R. and Garabato, A.C.N., 2013. Dynamics of the Southern Ocean circulation. In *International Geophysics* (Vol. 103, pp. 471-492). Academic Press.
- Rio, M.H. and Hernandez, F., 2004. A mean dynamic topography computed over the world ocean from altimetry, in situ measurements, and a geoid model. *Journal of Geophysical Research: Oceans*, *109*(C12).
- Roman, R.E. and Lutjeharms, J.R.E., 2010. Antarctic intermediate water at the Agulhas Current retroflection region. *Journal of Marine Systems*, *81*(4), pp.273-285.
- Ross, R.M., Quetin, L.B., Martinson, D.G., Iannuzzi, R.A., Stammerjohn, S.E. and Smith, R.C., 2008. Palmer LTER: Patterns of distribution of five dominant zooplankton species in the epipelagic zone west of the Antarctic

Peninsula, 1993–2004. *Deep Sea Research Part II: Topical Studies in Oceanography*, *55*(18-19), pp.2086-2105.

- Saba, G.K., Fraser, W.R., Saba, V.S., Iannuzzi, R.A., Coleman, K.E., Doney, S.C., Ducklow, H.W., Martinson, D.G., Miles, T.N., Patterson-Fraser, D.L. and Stammerjohn, S.E., 2014. Winter and spring controls on the summer food web of the coastal West Antarctic Peninsula. *Nature communications*, *5*, p.4318.
- Sabine, C.L., Feely, R.A., Gruber, N., Key, R.M., Lee, K., Bullister, J.L., Wanninkhof, R., Wong, C.S.L., Wallace, D.W., Tilbrook, B. and Millero, F.J., 2004. The oceanic sink for anthropogenic CO2. *Science*, *305*(5682), pp.367-371.
- Sakshaug, E. and Slagstad, D.A.G., 1991. Light and productivity of phytoplankton in polar marine ecosystems: a physiological view. *Polar Research*, *10*(1), pp.69-86.
- Sigman, D.M. and Boyle, E.A., 2000. Glacial/interglacial variations in atmospheric carbon dioxide. *Nature*, *407*(6806), p.859.
- Sallée, J.B., Wienders, N., Speer, K. and Morrow, R., 2006. Formation of subantarctic mode water in the southeastern Indian Ocean. *Ocean Dynamics*, *56*(5-6), pp.525-542.
- Sallée, J.B., Speer, K., Morrow, R. and Lumpkin, R., 2008. An estimate of Lagrangian eddy statistics and diffusion in the mixed layer of the Southern Ocean. *Journal of Marine Research*, *66*(4), pp.441-463.

- Schmitz Jr, W.J., 1996. On the eddy field in the Agulhas Retroflection, with some global considerations. *Journal of Geophysical Research: Oceans*, *101*(C7), pp.16259-16271.
- Séférian, R., Iudicone, D., Bopp, L., Roy, T. and Madec, G., 2012. Water mass analysis of effect of climate change on air–sea CO2 fluxes: The Southern Ocean. *Journal of Climate*, *25*(11), pp.3894-3908.
- Sheen, K.L., Garabato, A.N., Brearley, J.A., Meredith, M.P., Polzin, K.L., Smeed, D.A., Forryan, A., King, B.A., Sallée, J.B., Laurent, L.S. and Thurnherr, A.M., 2014. Eddy-induced variability in Southern Ocean abyssal mixing on climatic timescales. *Nature Geoscience*, *7*(8), p.577.
- Sievers, H.A. and Nowlin, W.D., 1984. The stratification and water masses at Drake Passage. *Journal of Geophysical Research: Oceans*, *89*(C6), pp.10489-10514.
- Shepherd, A., Wingham, D. and Rignot, E., 2004. Warm ocean is eroding West Antarctic ice sheet. *Geophysical Research Letters*, *31*(23).
- Sigman, D.M. and Boyle, E.A., 2000. Glacial/interglacial variations in atmospheric carbon dioxide. *Nature*, *407*(6806), p.859.
- Silva, T.A.M., Bigg, G.R. and Nicholls, K.W., 2006. Contribution of giant icebergs to the Southern Ocean freshwater flux. *Journal of Geophysical Research: Oceans*, *111*(C3).
- Smith, W.O. and Nelson, D.M., 1985. Phytoplankton bloom produced by a receding ice edge in the Ross Sea: spatial coherence with the density field. *Science*, *227*(4683), pp.163-166.

- Smith, W.O. and Nelson, D.M., 1986. Importance of ice edge phytoplankton production in the Southern Ocean. *BioScience*, *36*(4), pp.251-257.
- Sokolov, S., King, B.A., Rintoul, S.R. and Rojas, R.L., 2004. Upper ocean temperature and the baroclinic transport stream function relationship in Drake Passage. *Journal of Geophysical Research: Oceans*, *109*(C5).
- Sokolov, S. and Rintoul, S.R., 2007. On the relationship between fronts of the Antarctic Circumpolar Current and surface chlorophyll concentrations in the Southern Ocean. *Journal of Geophysical Research: Oceans*, *112*(C7).
- Sokolov, S. and Rintoul, S.R., 2007. Multiple jets of the Antarctic Circumpolar Current south of Australia. *Journal of Physical Oceanography*, *37*(5), pp.1394-1412.
- Sokolov, S. and Rintoul, S.R., 2009. Circumpolar structure and distribution of the Antarctic Circumpolar Current fronts: 1. Mean circumpolar paths. *Journal of Geophysical Research: Oceans*, *114*(C11).
- Sparrow, M.D., Heywood, K.J., Brown, J. and Stevens, D.P., 1996. Current structure of the south Indian Ocean. *Journal of Geophysical Research: Oceans*, *101*(C3), pp.6377-6391.
- Speich, S., Blanke, B. and Madec, G., 2001. Warm and cold water routes of an OGCM thermohaline conveyor belt. *Geophysical Research Letters*, *28*(2), pp.311-314.

- Sprintall, J., 2008. Long-term trends and interannual variability of temperature in Drake Passage. *Progress in Oceanography*, *77*(4), pp.316-330.
- Stammerjohn, S.E., Martinson, D.G., Smith, R.C., Yuan, X. and Rind, D., 2008. Trends in Antarctic annual sea ice retreat and advance and their relation to El Niño–Southern Oscillation and Southern Annular Mode variability. *Journal of Geophysical Research: Oceans*, *113*(C3).
- Stammerjohn, S., Massom, R., Rind, D. and Martinson, D., 2012. Regions of rapid sea ice change: An inter-hemispheric seasonal comparison. *Geophysical Research Letters*, *39*(6).
- Steinberg, D.K., Ruck, K.E., Gleiber, M.R., Garzio, L.M., Cope, J.S., Bernard, K.S., Stammerjohn, S.E., Schofield, O.M., Quetin, L.B. and Ross, R.M., 2015. Long-term (1993–2013) changes in macrozooplankton off the Western Antarctic Peninsula. *Deep Sea Research Part I: Oceanographic Research Papers*, *101*, pp.54-70.
- Stommel, H. and Arons, A.B., 1959. On the abyssal circulation of the world ocean—I. Stationary planetary flow patterns on a sphere. *Deep Sea Research (1953)*, *6*, pp.140-154.
- Stramma, L. and Peterson, R.G., 1990. The South Atlantic Current. *Journal of Physical Oceanography*, *20*(6), pp.846-859.
- Stramma, L., 1992. The South Indian Ocean Current. *Journal of Physical Oceanography*, *22*(4), pp.421-430.
- Stramma, L., Peterson, R.G. and Tomczak, M., 1995. The south Pacific current. *Journal of Physical Oceanography*, *25*(1), pp.77-91.

- Stramma, L. and Lutjeharms, J.R., 1997. The flow field of the subtropical gyre of the South Indian Ocean. *Journal of Geophysical Research: Oceans*, *102*(C3), pp.5513-5530.
- Sverdrup, H.U., Johnson, M.W. and Fleming, R.H., 1942. *The Oceans: Their physics, chemistry, and general biology* (Vol. 7). New York: Prentice-Hall.
- Swart, S., Speich, S., Ansorge, I.J., Goni, G.J., Gladyshev, S. and Lutjeharms, J.R., 2008. Transport and variability of the Antarctic Circumpolar Current south of Africa. *Journal of Geophysical Research: Oceans*, *113*(C9).
- Swart, S. and Speich, S., 2010. An altimetry-based gravest empirical mode south of Africa: 2. Dynamic nature of the Antarctic Circumpolar Current fronts. *Journal of Geophysical Research: Oceans*, *115*(C3).
- Talley, L.D., Reid, J.L. and Robbins, P.E., 2003. Data-based meridional overturning streamfunctions for the global ocean. *Journal of Climate*, *16*(19), pp.3213-3226.
- Talley, L.D., 2008. Freshwater transport estimates and the global overturning circulation: Shallow, deep and throughflow components. *Progress in Oceanography*, *78*(4), pp.257-303.
- Talley, L.D., 2013. Closure of the global overturning circulation through the Indian, Pacific, and Southern Oceans: Schematics and transports. *Oceanography*, *26*(1), pp.80-97.

- Tamura, T., Ohshima, K.I. and Nihashi, S., 2008. Mapping of sea ice production for Antarctic coastal polynyas. *Geophysical Research Letters*, *35*(7).
- Thoma, M., Jenkins, A., Holland, D., Jacobs, S., 2008. Modelling circumpolar deep water intrusions on the Amundsen Sea continental shelf, Antarctica. Geophys. Res. Lett. 35, L18602. http://dx.doi.org/10.1029/2008GL034939.
- Thompson, D.W. and Wallace, J.M., 2000. Annular modes in the extratropical circulation. Part I: Month-to-month variability. *Journal of climate*, *13*(5), pp.1000-1016.
- Thompson, D.W. and Solomon, S., 2002. Interpretation of recent Southern Hemisphere climate change. *Science*, *296*(5569), pp.895-899.
- Thompson, D.W., Solomon, S., Kushner, P.J., England, M.H., Grise, K.M. and Karoly, D.J., 2011. Signatures of the Antarctic ozone hole in Southern Hemisphere surface climate change. *Nature Geoscience*, *4*(11), p.741.
- Thompson, A.F. and Sallée, J.B., 2012. Jets and topography: Jet transitions and the impact on transport in the Antarctic Circumpolar Current. *Journal of Physical Oceanography*, *42*(6), pp.956-972.
- Tilzer, M.M., Gieskes, W.W. and Beese, B., 1986. Light-temperature interactions in the control of photosynthesis in Antarctic phytoplankton. *Polar biology*, *5*(2), pp.105-111.
- Toggweiler, J.R., Dixon, K. and Broecker, W.S., 1991. The Peru upwelling and the ventilation of the South Pacific thermocline. *Journal of Geophysical Research: Oceans*, *96*(C11), pp.20467-20497.

- Tomczak, M. and Liefrink, S., 2005. Interannual variations of water mass volumes in the Southern Ocean. *Journal of Atmospheric & Ocean Science*, *10*(1), pp.31-42.
- Toole, J.M. and Warren, B.A., 1993. A hydrographic section across the subtropical South Indian Ocean. *Deep Sea Research Part I: Oceanographic Research Papers*, *40*(10), pp.1973-2019.
- Trathan, P.N., Brandon, M.A. and Murphy, E.J., 1997. Characterization of the Antarctic Polar Frontal Zone to the north of South Georgia in summer 1994. *Journal of Geophysical Research: Oceans*, *102*(C5), pp.10483-10497.
- Tsubouchi, T., Suga, T. and Hanawa, K., 2010. Indian Ocean Subtropical Mode Water: its water characteristics and spatial distribution. *Ocean Science*, *6*(1).
- Uppala, S.M., Kållberg, P.W., Simmons, A.J., Andrae, U., Bechtold, V.D.C., Fiorino, M., Gibson, J.K., Haseler, J., Hernandez, A., Kelly, G.A. and Li, X., 2005. The ERA-40 re-analysis. *Quarterly Journal of the royal meteorological society*, *131*(612), pp.2961-3012.
- van den Broeke, M., 2005. Strong surface melting preceded collapse of Antarctic Peninsula ice shelf. *Geophysical Research Letters*, *32*(12).
- Visbeck, M., 2009. A station-based southern annular mode index from 1884 to 2005. *Journal of Climate*, *22*(4), pp.940-950.
- Walsh, J.E., 1983. The role of sea ice in climatic variability: Theories and evidence. *Atmosphere-Ocean*, *21*(3), pp.229-242.

- Warren, B.A., LaCasce, J.H. and Robbins, P.E., 1996. On the obscurantist physics of "form drag" in theorizing about the Circumpolar Current. *Journal of physical oceanography*, *26*(10), pp.2297-2301.
- Watterson, I.G., 2000. Southern midlatitude zonal wind vacillation and its interaction with the ocean in GCM simulations. *Journal of climate*, *13*(3), pp.562-578.
- Waugh, D.W., Primeau, F., DeVries, T. and Holzer, M., 2013. Recent changes in the ventilation of the southern oceans. *science*, *339*(6119), pp.568-570.
- Waugh, D.W., 2014. Changes in the ventilation of the southern oceans. *Phil. Trans. R. Soc. A*, *372*(2019), p.20130269.
- Weaver, A.J., Saenko, O.A., Clark, P.U. and Mitrovica, J.X., 2003. Meltwater pulse 1A from Antarctica as a trigger of the Bølling-Allerød warm interval. *Science*, *299*(5613), pp.1709-1713.
- Weppernig, R., Schlosser, P., Khatiwala, S. and Fairbanks, R.G., 1996. Isotope data from Ice Station Weddell: Implications for deep water formation in the Weddell Sea. *Journal of Geophysical Research: Oceans*, *101*(C11), pp.25723-25739.
- Whitworth III, T., 1980. Zonation and geostrophic flow of the Antarctic Circumpolar Current at Drake Passage. *Deep Sea Research Part A. Oceanographic Research Papers*, *27*(7), pp.497-507.
- Whitworth III, T., 1988. The Antarctic Circumpolar Current. Oceanus, 32, 53–58. *Circulation and Water Masses of Southern Ocean*, *113*.

- Whitworth, T., A. H. Orsi,S.-J. Kim, W. D.Nowlin, and R. A. Locarnini, 1998. Water masses and mixing near the Antarctic Slope Front. *Ocean, Ice, and Atmosphere: Interactions at the Antarctic Continental Margin, Antarct. Res. Ser*, *75*, pp.1-27
- Whitworth III, T., 2002. Two modes of bottom water in the Australian-Antarctic Basin. *Geophysical Research Letters*, *29*(5).
- Wilchinsky, A.V. and Feltham, D.L., 2009. Numerical simulation of the Filchner overflow. *Journal of Geophysical Research: Oceans*, *114*(C12).
- Wilkin, J.L. and Morrow, R.A., 1994. Eddy kinetic energy and momentum flux in the Southern Ocean: Comparison of a global eddy-resolving model with altimeter, drifter, and current-meter data. *Journal of Geophysical Research: Oceans*, *99*(C4), pp.7903-7916.
- Williams, R.G. and Follows, M.J., 2003. Physical transport of nutrients and the maintenance of biological production. In *Ocean biogeochemistry* (pp. 19-51). Springer, Berlin, Heidelberg.
- Williams, G.D., Aoki, S., Jacobs, S.S., Rintoul, S.R., Tamura, T. and Bindoff, N.L., 2010. Antarctic bottom water from the Adélie and George V Land coast, East Antarctica (140–149 E). *Journal of Geophysical Research: Oceans*, *115*(C4).
- Wijffels, S.E., Willis, J., Domingues, C.M., Barker, P., White, N.J., Gronell, A., Ridgway, K. and Church, J.A., 2008. Changing expendable bathythermograph fall rates and their impact on estimates of thermosteric sea level rise. *Journal of Climate*, *21*(21), pp.5657-5672.

- Worthington, L., 1981. The water masses of the world ocean: Some results of a fine-scale census. *Evolution of Physical Oceanography*, pp.42-69.
- Wyrtki, K., 1971. *Oceanographic Atlas of the International Indian Ocean Expedition, National Science Foundation Publication, OCE*. NSF 86–00-001, Washington, DC.
- Yu, L. and Rienecker, M.M., 2000. Indian Ocean warming of 1997–1998. *Journal of Geophysical Research: Oceans*, *105*(C7), pp.16923-16939.
- Yuan, X., 2004. ENSO-related impacts on Antarctic sea ice: a synthesis of phenomenon and mechanisms. *Antarctic Science*, *16*(4), pp.415-425.
- Zenk, W. and Morozov, E., 2007. Decadal warming of the coldest Antarctic Bottom Water flow through the Vema Channel. *Geophysical Research Letters*, *34*(14), L14607, doi: 10.1029/2007GL030340.

List of Publications

As required under the University Ordinance OB-9.9-(i), the following research articles were published in peer reviewed international journals

1. **Racheal Chacko**, Nuncio Murukesh, Jenson V. George, and N. Anilkumar. (2014). Observational evidence of the southward transport of water masses in the Indian sector of the Southern Ocean. Current Science, 107(9), 1573-1581.
2. Anilkumar, N., **Racheal Chacko**, P. Sabu, Honey UK Pillai, Jenson V. George, and C. T. Achuthankutty. (2014): "Biological response to physical processes in the Indian Ocean sector of the Southern Ocean: a case study in the coastal and oceanic waters." *Environmental monitoring and assessment* 186, no. 12, 8109-8124.
3. Anilkumar, N., J. V. George, **Racheal Chacko**, Nuncio Murukesh, and P. Sabu. "Variability of fronts, fresh water input and chlorophyll in the Indian Ocean sector of the Southern Ocean." *New Zealand Journal of Marine and Freshwater Research*49, no. 1 (2015): 20-40.
4. Anilkumar, N., **Racheal Chacko**, P. Sabu, and Jenson V. George. "Freshening of Antarctic Bottom Water in the Indian ocean sector of Southern ocean." *Deep Sea Research Part II: Topical Studies in Oceanography* 118 (2015): 162-169.

Papers presented in conferences

1. **Racheal Chacko**, N. Anilkumar, Sabu P., Jenson V. George and Divya David T. Variability of the Polar Front in the Indian sector of the Southern Ocean during austral summer. Paper Presentation at the Pan Ocean Remote Sensing Conference (PORSEC)-2012, Kochi, India

2. N. Anilkumar, **Racheal Chacko**, P. Sabu, Sini Pavithran, Honey U.K. Pillai, Deepti Dessai, Jenson V. George and C. T. Achuthankutty. Environmental influence on biological production in the coastal and oceanic regions off Antarctica. Poster Presentation at the Pan Ocean Remote Sensing Conference (PORSEC)-2012, Kochi, India

3. **Racheal Chacko**, Jenson V. George, P. Sabu, N. Anilkumar. Spatio-temporal variability of the Winter Water in the Indian Sector of the Southern Ocean: Importance in mixed layer heat storage. Poster Presentation at the Word Ocean Science Congress February, 5-8 February, 2015, Kochi, India.

Observational evidence of the southward transport of water masses in the Indian sector of the Southern Ocean

Racheal Chacko*, Nuncio Murukesh, Jenson V. George and N. Anilkumar

National Centre for Antarctic and Ocean Research, Headland Sada, Vasco-da-gama, Goa 403 804, India

The southward transport of water masses in the Indian sector of the Southern Ocean (SO) is compared using the hydrographic data collected during the austral summer of 2010 and 2011. It has been found that subtropical surface water (STSW) underwent maximum southward displacement during the study period. The southward extent of STSW was at 45°S during 2011, but was restricted to 42°S during 2010. During 2011, three eddies were identified along the cruise track, whereas during 2010 eddies were absent. Satellite sea-level anomaly showed that these eddies were associated with the highly unstable Agulhas Return Current (ARC). The present study shows that STSW is transported along the peripheries of these eddies during 2011. There are indications of transport of mode water as well, but this is not resolved in the present study. Analysis of eddy kinetic energy shows a positive linear decadal trend; also, peak eddy lagged the southern annular mode by a year. This indicates that though the eddies may act locally, they are linked to the large-scale variability in the southern hemisphere.

Keywords: Eddy kinetic energy, oceanic fronts, subtropical surface water, water masses.

THE Southern Ocean (SO) is a key player in the Earth's climate for its importance in the global ocean circulation and water mass formation, inter-basin connections, and air–sea exchanges of heat, freshwater, and tracer gases[1]. The SO is characterized by a wide spectrum of variability. The high frequency variability largely arises from the wind-driven ocean variability[2–4]. Low frequency variability of inter-decadal timescales also occurs in the SO and to an extent depends on the mesoscale eddies[5], suggesting the role of intrinsic variability in the decadal variability[6]. The eddy kinetic energy (EKE; which is a measure of mesoscale activity) in topographically constrained areas in SO and within the Antarctic Circumpolar Current (ACC) is often dependent on changes in wind forcing on inter-annual to inter-decadal timescales largely associated with major climatic modes such as the Southern Annular Mode (SAM) and El Niño/Southern Oscillation (ENSO)[2,7,8]. Model studies reveal that different geographic regions within the SO respond differently. The Pacific sector is characterized by intrinsic disturbances that respond to SAM and ENSO, whereas the Atlantic sector is largely wind-driven. Satellite observations[9], buoy trajectories[10], inertial jet models[11] and hydrographic data[12–14] have revealed that high mesoscale variability in the SO is closely correlated with regions of prominent bottom relief. This variability also correlates closely with either the terminal region of a major western boundary current such as the Agulhas Current, or where the ACC interacts with prominent bottom topography such as in the Drake Passage or at the Crozet and Kerguelen Plateau[12]. Eddies are also an important feature in the SO. In SO, poleward heat flux that regulates the meridional overturning circulation is influenced by mesoscale eddies[15–17]. Recent literature shows that eddies in the Agulhas retroflection entrap subtropical properties like low oxygen and CFC, and transport to the sub Antarctic zone mostly by eddy translation[18].

The southwest Indian sector of SO is characterized by the confluence of warm Agulhas Return Current (ARC) and Subtropical Convergence[13,19]. This region is known for its enhanced primary productivity and water mass formation and high incidence of mesoscale features[20]. The present study was carried out in the southwestern Indian sector of SO during the Indian scientific expedition to the SO in the austral summer of 2010 and 2011. The study has analysed the thermohaline variations in an area characterized by mesoscale disturbances and attempted to understand the role of eddies in the southward water mass transport as well as examine the year-to-year variability in the region using available datasets and to link it with the large-scale variability.

Data and methods

This study was carried out on-board *ORV Sagar Nidhi* during the 4th and 5th Indian Expedition to SO (February 2010 and 2011). A CTD (Sea-Bird Electronics, USA; temperature precision: ±0.001°C, conductivity: ±0.0001 S/m and depth ±0.005% of the full scale) was used to collect

*For correspondence. (e-mail: racheal@ncaor.gov.in)

temperature and salinity profiles of the upper 1000 m water column at 2° intervals along 57°30′E. In addition, dense underway profiling of the upper ocean temperature and salinity was carried out with expendable conductivity–temperature–depth probes (XCTDs; Tsurumi Seiki Company Limited, Japan; type: XCTD-3; terminal depth: 1000 m; temperature/salinity accuracy: ± 0.02°C/ ± 0.03 mS cm^{-1}) at 30 nautical mile (nm) interval and supplemented full-depth CTD stations that were spaced at approximately 120 nm. Generally, three XCTDs were launched between CTD stations. Figure 1 *a* and *b* shows the station location during the cruises in February 2011 and 2010 respectively. The XCTD profiles were quality controlled by following the guidelines in the CSIRO cookbook[21].

The first mode baroclinic radius for the region can be taken as ~30 km (ref. 22). Baroclinic eddies can grow maximum to the size of $2\pi L_r$, where L_r is the Rossby deformation radius[23]. Our sampling interval is roughly 60 km. Hence smallest features that can be identified with the *in situ* measurements will have ~180 km dimension. In this case, even the largest feature, will, however, be resolved only by three data points. To supplement our *in situ* measurements we utilized satellite-derived sea-level anomaly (SLA) maps overlaid by the geostrophic velocities to show the presence of eddies along the cruise track. Geostrophic velocities were downloaded from AVISO (http://www.aviso.oceanobs.com/duacs/). Satellite altimeter SLA data were obtained from AVISO on a 1/3 Mercator grid at 7 day intervals[24]. Contour maps of dynamic height were prepared using the SLA data. From the maps, dynamic heights > 20 cm were considered as anticyclonic eddies and those < –20 cm corresponded with cyclonic eddies. The eddies observed in the study area were visually tracked in order to have an understanding of their time and location of evolution. They were tracked for a period of eight months in the time span ranging from October 2010 to May 2011. The position of the eddy cores was identified from the weekly maps and then the track followed by them was plotted. EKE was calculated by using the formula

$$\mathrm{EKE} = \frac{1}{2}(u^2 + v^2),$$

where u and v are the zonal and meridional geostrophic current anomaly components respectively. Geostrophic velocity anomalies were calculated using the SLA data as follows[25]

$$U = -\frac{g}{f}\left(\frac{\partial \mathrm{SLA}}{\partial y}\right),$$

$$V = -\frac{g}{f}\left(\frac{\partial \mathrm{SLA}}{\partial x}\right),$$

where g is the acceleration due to gravity and f is the Coriolis force.

The sea-surface temperature (SST) data for February 2010 and 2011 were obtained from the Advanced Microwave Scanning Radiometer for the Earth Observing System (AMSRE) version-5 dataset. Maps of Absolute Dynamic Topography (MADT) from CLS/Archiving, Validation and Interpretation of Satellite Oceanographic (AVISO) data was also used to identify the fronts in the study region. Ocean Surface Current Analysis–Realtime (OSCAR; http://www.oscar.noaa.gov) data were used to plot surface ocean currents[26]. The SAM monthly climate mode indices are from the NOAA Climate Prediction Center website (http://www.esrl.noaa.gov/psd/data/climateindices/list).

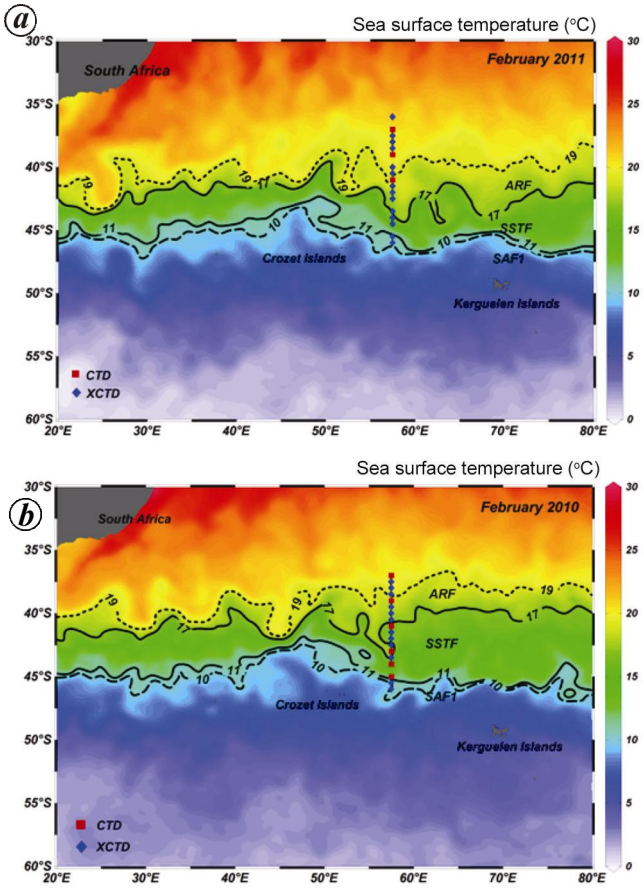

Figure 1. Cruise track overlaid by monthly sea surface temperature (SST) maps. The fronts along the cruise track have been delineated. ***a***, February 2011; ***b***, February 2010.

Results and discussion

Figure 1 *a* and *b* shows the AMSRE monthly averaged SST during February 2011 and 2010. It is clear from the figure that generally in the SO, the temperature gradually decreases southward and at the frontal locations there is a

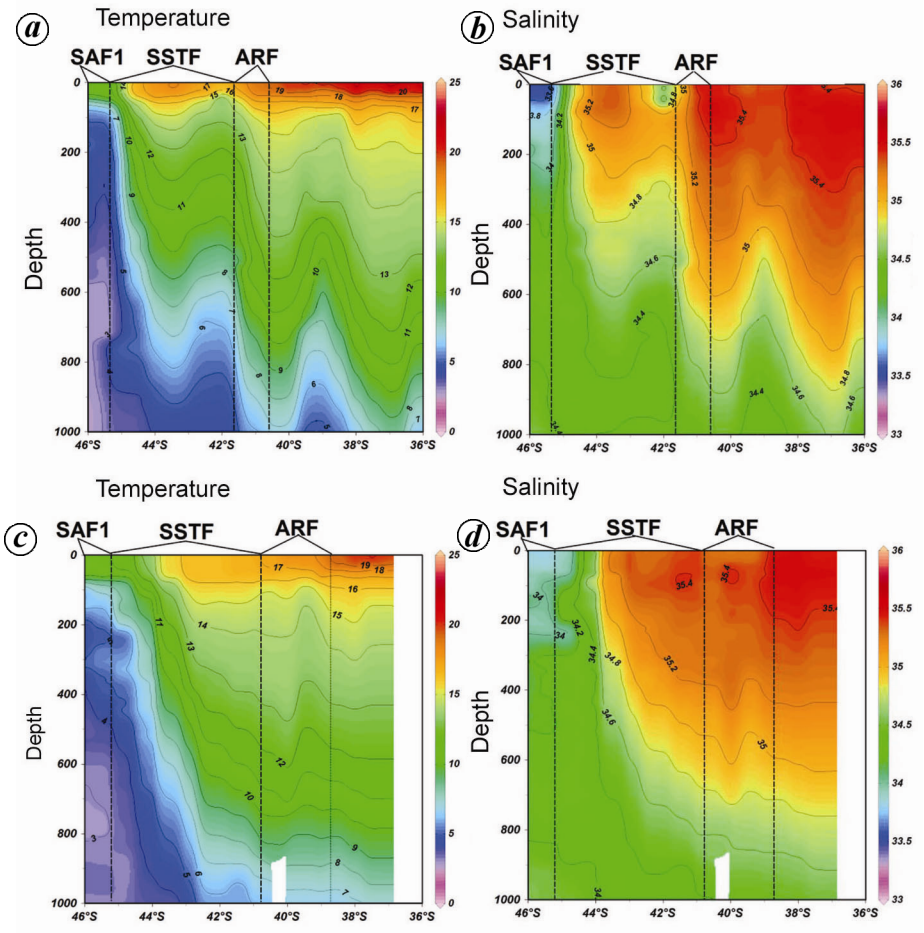

Figure 2. Vertical section of temperature and salinity in (***a***, ***b***) 2011 and (***c***, ***d***) 2010.

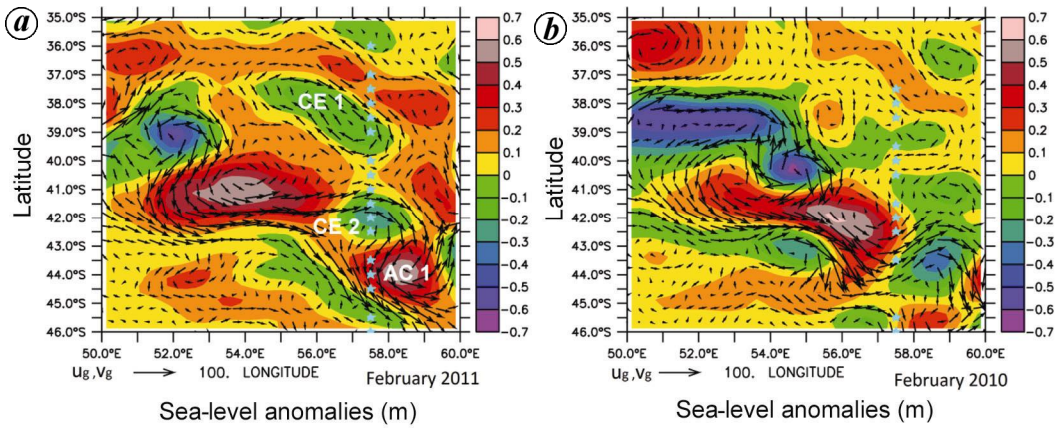

Figure 3. Sea-level anomalies overlaid by the geostrophic velocities over the study area during (***a***) 2011 and (***b***) 2010.

sudden decrease in temperature[27]. The Agulhas Return Front (ARF), Southern Subtropical Front (SSTF), and Subantarctic Front (SAF) are deemed as regions where SST decreases suddenly from 19°C to17°C, 17°C to 11°C and 11°C to 9°C respectively[28–30]. These fronts are highlighted in the Figure 1. From the satellite maps of SST it is clear that the SSTF in 2011 is a narrower front compared to that in 2010. It has been noted in earlier studies that in the western Indian sector of SO, the ARF, SSTF and SAF1 are merged as a single front[30,31]. The thermohaline section shown in Figure 2 suggests that during 2011, the section of temperature (Figure 2 *a*) and salinity (Figure 2 *b*) is characterized by troughs and ridges. However, during 2010 (Figure 2 *c* and *d*) no such features were observed, except for one at 41°S where the isotherm shoaling was noticed, but this was limited to the subsurface levels.

It can also be noted that the undulation in isolines of temperature and salinity during 2011 reached up to 1000 m. These undulations were clearly evident in the 11°C isotherm that shoaled from 600 to 700 m depth at 40.5°S to about 300 m at 42°S. During 2010, the surface temperature gradually decreased from 20°C at 36°S to about 11°C at 46°S (Figure 2 *c*). Salinity varied from 35.4 at 37°S to 33.8° at 46°S (Figure 2 *d*). This gradual variation is in contrast with the north–south variability during 2011, where low SST (17°C) is noted at 42°S and again higher SST (18°C) is noted further south at 44°S. The undulations (troughs and ridges) noted in the thermohaline sections are due to the vertical water column movements. These movements can be associated with Ekman pumping or presence of eddies across the cruise track. To understand the role of eddies along the cruise track, we will further analyse the SLA plots during February 2011 and 2010.

Figure 3 *a* and *b* shows the SLA plots overlaid by the geostrophic velocities during February 2011 and 2010 respectively. The satellite SLA for the observation period of 2011 (Figure 3 *a*) is characterized by two cyclonic (characterized by negative SLA) and one anticyclonic (characterized by positive SLA) circulation pattern centred at 39°S, 42°S and 44°S respectively, which coincides with the locations of the troughs/ridges in the temperature and salinity sections (Figure 2 *a* and *b*). However, the Ekman pumping derived from the ASCAT wind stress curl does not show any correlation with the undulation in the thermohaline section (figure not shown). Hence, it is apparent that the troughs and ridges in the thermohaline structure are the manifestations of cyclonic and anticyclonic eddies. We name these eddies as CE1, CE2 and AC1 located respectively at 39°S, 42°S and 44°S. The hydrographic transect occupied during the survey passes through the centre of CE2 and along edges of CE1 and AC1. The trajectories of the three eddies have been studied for a period of eight months from October 2010 to May 2011 (Figure 4). The cold core eddy CE1 developed in the study area on 17 November 2010. This eddy propagated in a southwesterly direction and was seen at the station location on 2 February 2011, after which it moved westwards. The second cold core eddy CE2 was located at 43°S 57°E on 6 October 2010. CE2 propagated in a northerly direction until 15 December 2010, after which it turned eastward and persisted at the station location for a period of almost 20 days and eventually moved westwards. After 2 March 2011, it was observed that CE2 turned eastward. The warm core eddy AC1 observed at station location 44°S moved in a southwesterly direction from October 2010. From the track followed by AC1 it is evident that this eddy was present near the station location for approximately 8 months. Thus except for CE1, CE2 and AC1 persisted at the station location for at least about 8 months. The track of eddies identified by the visual observations is highlighted in Figure 4. One can also notice from Figure 3 *b* that during February 2010, there were no eddies across the cruise track.

To further understand the vertical thermohaline structure of eddies noted during February 2011, we plotted the profiles of temperature, salinity and density at the eddy stations (Figure 5 *a*–*c*). One of the evident features in the profiles is the fresher and colder water column at the cyclonic eddy observed at 42°S. The profile was characterized by well-developed subsurface temperature minimum layer capped in the upper 100 m by a relatively warm and fresh surface layer. On the other hand, at the anticyclonic eddies the water column was warmer and saltier than the cyclonic eddies. The eddies appear to be density compensated below 200 m.

The water mass analysis using the temperature–salinity (*T*–*S*) plots (Figure 6 *a* and *b*) during 2011 and 2010 showed different water masses in the region. The major water masses in the upper 1000 m noted in the region are Subtropical Surface Waters (STSW), Subantarctic Surface Waters (SASW) and Subtropical Mode Waters (STMW). The STSW originates between 29°S and the Subtropical front at about 40°S (ref. 32). The Subtropical front is the boundary between the warmer and higher, saline STSW and cooler, fresher SASW. STSW is defined by temperature range 15°–24°C and salinity range 35.50–34.60 (ref. 33), and in the Crozet Basin it is characterized by relatively high temperature and salinity (> 12°C, > 35.1)[13]. SASW is defined by the characteristics temperature of

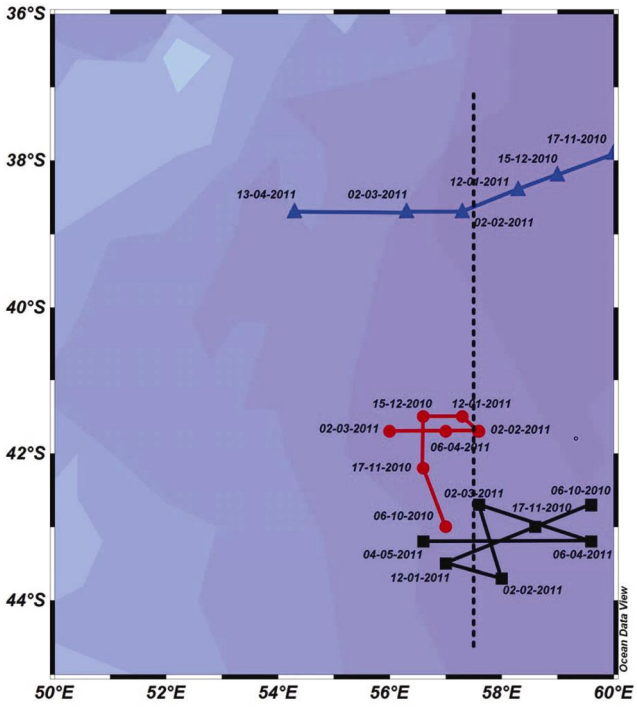

Figure 4. Eddy trajectory showing the movement of the three eddies identified in the study location, CE1 (blue triangle), CE2 (red circle) and AC1 (black square). The black dotted line shows the cruise track along which observations have been carried out.

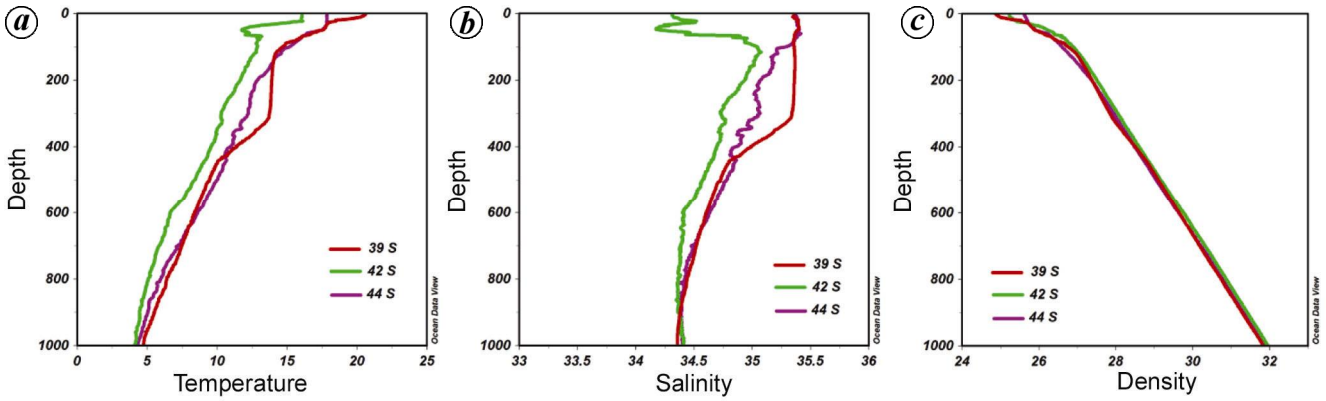

Figure 5. Profiles of (*a*) temperature, (*b*) salinity and (*c*) density at the eddy location during the 2011 expedition.

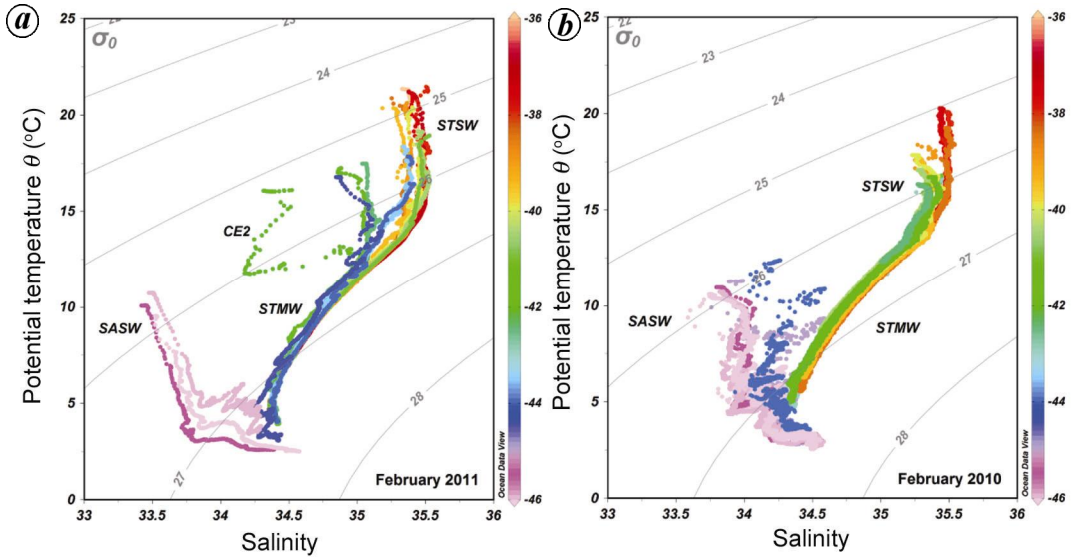

Figure 6. Water masses seen along the cruise track: (*a*) 2011; (*b*) 2010.

around 9°C and salinity < 34. STMW is usually identified in the temperature range 11°–14°C and salinity range 35–35.4. In the present study, the characteristics of STSW provided by Park *et al.*[13] have been considered because the study area is close to the Crozet Basin. *T*–*S* plots for station locations during 2011 show the presence of STSW up to 44°S (Figure 6 *a*), but the presence of this water mass was not noticed at 42°S, where a shoaling of the isolines was noticed in the thermohaline structure. The surface waters at 42°S showed neither *T*–*S* characteristic of STSW nor SASW. Studies along the southwest Indian ridge have shown that surface waters in the eddy regions often get modified either due to air–sea interactions at those latitudes or due to the injection of surface waters from different locations[34]. *T*–*S* plots for 2010 revealed characteristics of STSW up to 42°S (Figure 6 *b*). At 44°S, where signatures of STSW were noticed during 2011, temperature was in the range 2.5–12°C and salinity in the range 34–34.5. Thus, it is apparent that during 2011 the southward extent of the STSW was till 44°S, whereas during 2010 STSW was confined only to the source region. The increased southward presence of STSW during February 2011 compared to that of 2010 can be mediated by eddies in the region.

The eddies noted in the study area are associated with highly dynamic ARC flowing from the southern tip of Africa to the east up to 80°E (ref. 35, 36). This is a part of the Agulhas Current which loops and returns eastward off the coast of southern Africa. This current flows parallel or is juxtaposed to the Subtropical front[37]. Due to the presence of ARC which is dynamically unstable, STF in the SO is characterized by high mesoscale turbulence[33]. Figure 7 *a* and *b* shows the EKE distribution during February 2011 and 2010 respectively. The most evident feature in the figure is the high EKE patch and its southward meandering noted east of 50°E. Figure 7 *c* and *d* shows the OSCAR currents during 2011 and 2010 respectively. From the figure it is clear that the high EKE patch

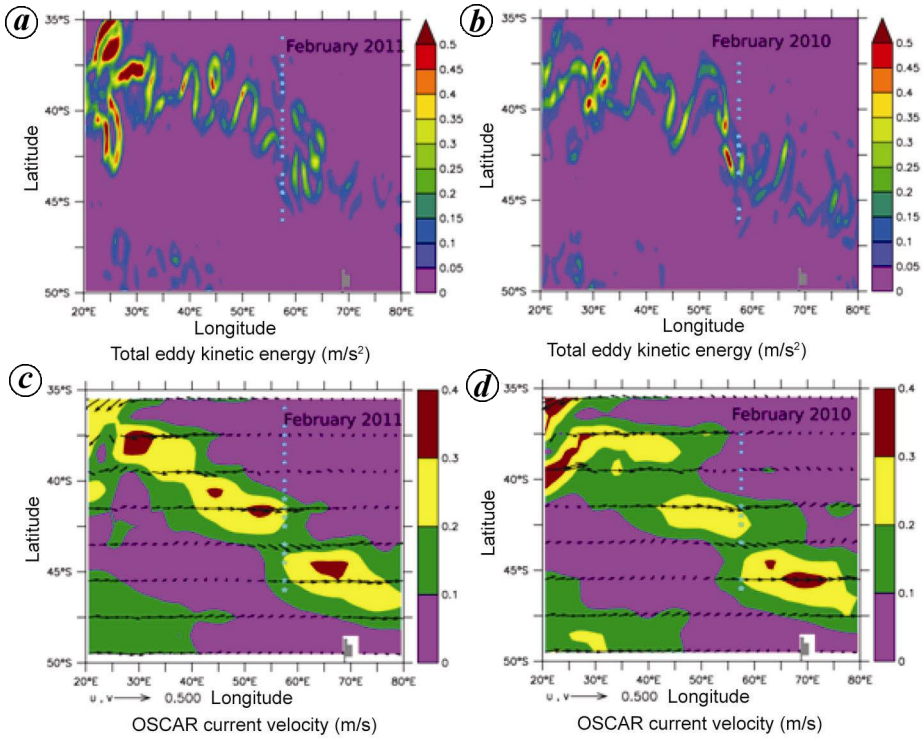

Figure 7. Eddy kinetic energy (EKE) maps over the study area during February (***a***) 2011 and (***b***) 2010. OSCAR currents over the study area during February (***c***) 2011 and (***d***) 2010.

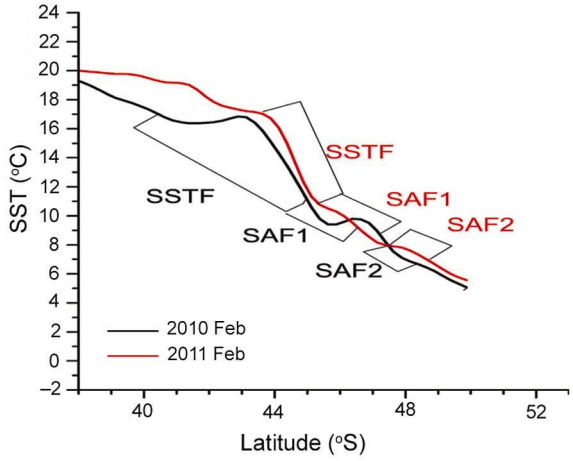

Figure 8. Maps of Absolute Dynamic Topography profiles showing the frontal extend during 2011 and 2010.

is associated with the ARC. Previous studies[29,30] suggested that according to the meandering of the ARC, the fronts shift southward and hence the presence of STSW can be noted further south. The meandering of the ARC is mainly attributed to the presence of bottom topographic features[38]. The presence of southward extension of STSW during February 2011 can be attributed to the southward meandering of the ARC. As the ARC passes from shallow topographic features in the west to deep ocean bottom eastern region to maintain the potential vorticity, the current meanders southward. However, satellite-derived frontal location based on satellite SST averaged over February 2010 and 2011 along 57.5°E clearly suggests that the SSTF location is slightly different between February 2010 and 2011 (Figure 8). These observations invite a detailed interpretation of the presence of STSW further south during 2011.

It is clear from the satellite pictures that the large-scale circulation pattern and frontal locations are different during February 2011 and 2010. It indicates that meandering of the ARC and individual eddies which are pinched off from the core of the ARC can transport STSW further southward. The presence of eddies is evident from the undulations of isotherms during the cruises. The station locations are on the eastward edge of CE1, at the centre of CE2 and at the westward edge of the anticyclonic eddy AC1. Eastward and westward edges of the cyclonic and anticyclonic eddies respectively, are characterized by southward flow that transports the warm high saline subtropical surface waters to the south. *T*–*S* plots for the station locations (Figure 6 *a*) reveal that along the peripheries of the eddies water mass characteristics are intact, whereas in the interior of the eddies the water mass characteristics are modified. This shows that peripheries of the eddies promote unaltered southward transport of the STSW (Figure 9). At the centre of the cyclonic eddy, water masses are modified as seen in the *T*–*S* plots from the stations (Figure 6 *a*). STSW could not be traced south of 45°S. Also, 45°S was characterized by sharp gradients in temperature and salinity, marking the SAF. When STSW

reached 45°S, it might have either subducted or transported eastward by the ACC. During 2010, even though the meandering of the ARC was not significantly different, the absence of eddies (Figure 3 *b*) along the hydrographic transect could have reduced the southward transport of the STSW. We do not notice this transport for deeper water masses. Evolution of eddies encountered during 2011 showed they are persistent features of the region at least for 8 months. Persistence of these eddies for about 8 months indicates a large transport of STSW towards SAF. When compared to 2010, 2011 was characterized by more eddies. This, however, could be a chance occurrence, since our survey was one time spot measurements and may not reflect the large-scale interannual variability of eddy characteristics in the region.

An estimate of the eddy-induced transport was carried out by noting the width of the maximum transport along the southward flowing limb of the AC1 and average velocity along that width. This was then multiplied with the depth of mixed layer in which the STSW can be found. The estimated amount is close to about 0.44 Sv towards the SAF. Persistence of these eddies for about 8 months indicates a large transport of STSW towards SAF during years of increased EKE. The negative trend of v component of geostrophic velocity (v_{geo}; Figure 10 *a*) obtained in the present study implies an increase in southward movement of the water masses. A coarse-resolution climate modelling study[39] has demonstrated that enhanced mesoscale eddy activity, following an increase in the wind stress, increases the poleward heat transport. Our analysis also supports these observations by the more southerly presence of STSW in 2011.

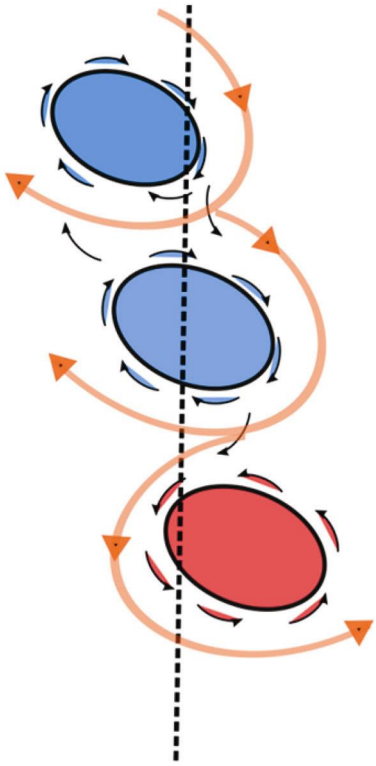

Figure 9. Schematic diagram showing the path of subtropical surface water (thick orange line) facilitated by the eddies present.

In order to gain insight into this interannual variability and to investigate whether one time measurements reflect large-scale processes, we computed the EKE averaged over a box (40–80°E, 35–45°S) in the Indian sector of the SO (Figure 10 *b*). EKE is characterized by an increasing trend with a biennial variability. It is evident from the plot that EKE was low during 2010 and reached a maximum during 2011. Thus the difference in the number of eddies we noted during 2010 and 2011 is a basin wide characteristic. Hence large-scale processes may be involved in the realization of observed variability in the thermohaline structure and water masses.

In SO, interannual variability in EKE may result from changes in SAM. In an analysis of oceanic EKE and changes in SAM[2], it was observed that EKE and SAM are characterized by a 2–3 year lag, especially for the Indian Ocean sector. In our case the lag is ~1 year, somewhat faster than expected (Figure 10 *c*). To explore the EKE–SAM relationship an eddy-resolving quasi-geostrophic model was also used[2]. The model results varied under different scenarios. For standard perturbation of a wind stress of ~0.21 Nm^{-2}, the lag in peak kinetic energy was 1.2–2 years, whereas for a strong perturbation with a wind stress of ~0.25 Nm^{-2}, the lag was found to be ~1 year. Thus the fast response we observed could be due to a strong perturbation in the wind fields. This increase in EKE was associated with the increase in the circumpolar wind stress and the lag is due to the time taken to influence the circulation in the deep ocean[2]. Thus the observed interannual variability in the thermohaline structure and the water mass is a result of large-scale variability arising from changes in annular mode.

Conclusions

Data obtained from expendable probes and CTD during the expedition to SO along 57°30′E during the austral summer 2010 and 2011 were analysed. The analysis revealed that the year-to-year variability in the hydrographic structure was due to the presence of eddies. Troughs and ridges of isotherms and isohalines were dominant in the vertical section of temperature and salinity during 2011. SSHA data clearly indicated the presence of cyclonic and anti-cyclonic eddies along the cruise track. The eddies present in the study area transported STSW southward by means of the enhanced meridional velocities along the peripheries of the eddies. Absence of eddies during 2010 restricted the southward transport of STSW to the region of its origin. Signatures of STSW south of 45°S were not clear. STSW might have either subducted or transported eastward along the SAF. Analysis

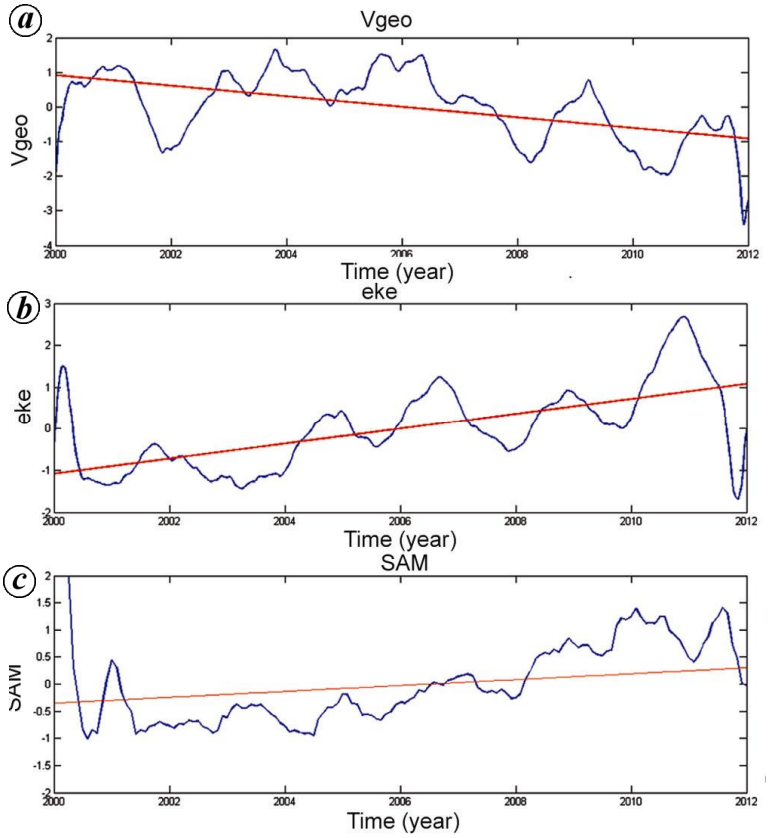

Figure 10. The variation of (***a***) *v* component of geostrophic velocity (v_{geo}); (***b***) Eddy kinetic energy; (***c***) Southern annual mode index.

of EKE shows that it peaks a year after the peak value in the SAM, suggesting the role of large-scale variability in controlling the EKE. Positive linear trend in the EKE suggests more southward transport of subtropical water masses which will have implications on the SO vertical mixing, air–sea interaction, sea-ice and water mass formation.

1. Farneti, R., Delworth, T. L., Rosati, A. J., Griffies, S. M. and Zeng, F., The role of mesoscale eddies in the rectification of the Southern Ocean response to climate change. *J. Phys. Oceanogr.*, 2010, **40**, 1539–1557.
2. Meredith, M. P. and Hogg, A. M., Circumpolar response of Southern Ocean eddy activity to a change in the Southern Annular Mode. *Geophys. Res. Lett.*, 2006, **33**, L16608.
3. Hughes, C. W., Meredith, M. P. and Heywood, K. J., Wind-driven transport fluctuations through Drake Passage: a southern mode. *J. Phys. Oceanogr.*, 1999, **29**, 1971–1992.
4. Gille, S. T., Stevens, D. P., Tokmakian, R. T. and Heywood, K. J., Antarctic Circumpolar Current response to zonally averaged winds. *J. Geophys. Res.*, 2001, **106**, 2743–2759.
5. Hogg, A. and Blundell, J. R., Interdecadal variability of the Southern Ocean. *J. Phys. Ocean.*, 2006, **36**, 1626–1645.
6. Dijkstra, H. A. and Ghil, M., Low-frequency variability of the large-scale ocean circulation: a dynamical systems approach. *Rev. Geophys.*, 2005, **43**, RG3002; doi: 10.1029/2002RG000122.
7. Sheen, K. L. *et al.*, Eddy-induced variability in Southern Ocean abyssal mixing on climatic timescales. *Nature Geosci.*, 2014, **7**, 577–582; doi: 10.1038/ngeo2200.
8. Morrow, R., Ward, M. L., Hogg, A. M. and Pasquet, S., Eddy response to Southern Ocean climate modes. *J. Geophys. Res.*, 2010, **115**, C10030.
9. Colton, M. T. and Chase, R. P., Interaction of the Antarctic Circumpolar Current with bottom topography: an investigation using satellite altimetry. *J. Geophys. Res.*, 1983, **88**, 1825–1843.
10. Hofmann, E. E., The large-scale horizontal structure of the Antarctic Circumpolar Current from FGGE drifters. *J. Geophys. Res.*, 1985, **90**, 7087–7097.
11. Craneguy, P. and Park, Y. H., Topographic control of the Antarctic Circumpolar Current in the South Indian Ocean. *C. R. Acad. Sci. Paris*, 1999, **328**, 583–589.
12. Lutjeharms, J. R. E. and Baker, D. J., A statistical analysis of the meso-scale dynamics of the Southern Ocean. *Deep-Sea Res.*, 1980, **27**, 145–159.
13. Park, Y.-H., Gamberoni, L. and Charriaud, E., Frontal structure, water masses, and circulation in the Crozet Basin. *J. Geophys. Res.*, 1993, **98**, 12361–12385.
14. Trathan, P. N., Brandon, M. A. and Murphy, E. J., Characterization of the Antarctic Polar Frontal Zone to the north of South Georgia in summer 1994. *J. Geophys. Res.*, 1997, **102**, 10483–10497.
15. Hogg, A., Meredith, M. P., Blundell, J. R. and Wilson, C., Eddy heat flux in the Southern Ocean: response to variable wind forcing. *J. Climate*, 2008, **21**, 608–620.
16. de Szoeke, R. A. and Levine, M. D., The advective flux of heat by mean geostrophic motions in the Southern Ocean. *Deep Sea Res., Part-I*, 1981, **28**, 1057–1085.
17. Lee, M. M., George Nurser, A. J., Coward, A. C. and de Cuevas, B. A., Eddy advective and diffusive transports of heat and salt in the Southern Ocean. *J. Phys. Oceanogr.*, 2007, **37**, 1376–1393.

18. Arhan, M., Speich, S., Messager, C., Dencausse, G., Fine, R. and Boye, M., Anticyclonic and cyclonic eddies of subtropical origin in the subantarctic zone south of Africa. *J. Geophys. Res*., 2011, **116**(C11004), doi: 10.1029/2011JC007140.
19. Park, Y. H., Gamberoni, L. and Charriaud, E., Frontal structure, transport and variability of the Antarctic Circumpolar Current in the South Indian Ocean sector, 401–801E. *Mar. Chem.*, 1991, **35**, 45–62.
20. Lutjeharms, J. R. E. and Valentine, H. R., Eddies at the subtropical convergence south of Africa. *J. Phys. Oceanogr*., 1988, **18**, 761–774.
21. Bailey, R., Gronell, A., Phillips, H., Tanner, E. and Meyers, G., Quality control cookbook for XBT data, Version 1.1. CSIRO Marine Laboratories Reports, 1994, p. 221.
22. Chelton, D. B., deSzoeke, R. A., Schlax, M. G., El Naggar, K., and Siwertz, N., Geographical variability of the first-baroclinic Rossby radius of deformation. *J. Phys. Oceanogr*., 1998, **28**, 433–460.
23. Kamenkovich, V. M., Koshlyakov, M. N. and Monin, A. S. (eds), *Synoptic Eddies in the Ocean*, Reidel, Dordrecht, Holland, 1986, p. 433.
24. Ducet, N., Le Traon, P. Y. and Reverdin, G., Global high resolution mapping of ocean circulation from TOPEX/POSEIDON and ERS-1/2. *J. Geophys. Res*., 2000, **105**, 19477–19498.
25. Pond, S. and Pickard, G. L., *Introductory Dynamic Oceanography*, Pergamon Press, New York, 1978.
26. Bonjean, F. and Lagerloef, G. S. E., Diagnostic model and analysis of the surface currents in the tropical Pacific Ocean. *J. Phys. Oceanogr.*, 2002, **32**, 2938–2954.
27. Deacon, G. E. R., The hydrology of the Southern Ocean. *Discov. Rep.*, 1937, 15-122.
28. Belkin, I. M. and Gordon, L., A Southern Ocean fronts from the Greenwich meridian to Tasmania. *J. Geophys. Res*., 1996, **101**, 3675–3696.
29. Holliday, N. P. and Reed, J. F., Surface oceanic fronts between Africa and Antarctica. *Deep Sea Res.*, *Part-I*, 1998, **45**, 217–238.
30. Anilkumar, N., Jenson, G. V., Chacko, R., Murukesh, N. and Sabu, P., Variability of fronts, freshwater input and chlorophyll in the Indian Ocean sector of the Southern Ocean. *N.Z. J. Mar. Freshwater Res*. (in press); doi: 10.1080/00288330.2014.924972.
31. Anilkumar, N. *et al.*, Fronts, water masses, and heat content variability in the western Indian sector of the Southern Ocean during austral summer 2004. *J. Mar. Syst*., 2006, **63**, 20–34.
32. Read, J. F. and Pollard, R. T., Structure and transport of the Antarctic Circumpolar Current and Agulhas Return Current at 401E. *J. Geophys. Res*., 1993, **98**, 12281–12295.
33. Darbyshire, M., The surface waters near the coasts of southern Africa. *Deep-Sea Res*., 1966, **13**, 57–81.
34. Ansorge, I. J. and Lutjeharms, J. R. E., Direct observations of eddy turbulence at a ridge in the Southern Ocean. *Geophys. Res. Lett*., 2005, **32**, doi: 10.1029/2005GL022588.
35. Read, J. F., Lucas, M. I., Holley, S. E. and Pollard, R. T., Phytoplankton, nutrients and hydrography in the frontal zone between the southwest Indian subtropical gyre and the Southern Ocean. *Deep Sea Res.*, *Part I*, 2000, **47**(12), 2341–2367; http://dx.doi.org/10.1016/S0967-0637(00)00021-2.
36. Beal, L. M., Ruijter, W. P., Biastoch, A. and Zahn, R., On the role of the Agulhas system in ocean circulation and climate. *Nature*, 2011, **472**, 429–436.
37. Lutjeharms, J. R. E. and Ansorge, I. J., The Agulhas Return Current. *J. Mar. Syst.*, 2001, **30**, 115–138.
38. Nuncio, M., Luis, A. J. and Yuan, X., Topographic meandering of Antarctic Circumpolar Current and Antarctic Circumpolar Wave in the ice–ocean–atmosphere system. *Geophys. Res. Lett.*, 2011, **38**, L13708; doi:10.1029/2011GL046898.
39. Fyfe, J., Saenko, O., Zickfeld, K., Eby, M. and Weaver, A., The role of poleward intensifying winds on Southern Ocean warming. *J. Climate*, 2007, **20**, 5391–5400; doi: 10.1175/2007jcli1764.1.

ACKNOWLEDGEMENTS. This work was supported by the Ministry of Earth Sciences, Government of India. We thank the Director, NCAOR, Goa for support and encouragement. We also thank the cruise participants and staff at NCAOR for help in the implementation and completion of this study. This is NCAOR contribution number 21/2014.

Received 21 January 2014; revised accepted 9 August 2014

Biological response to physical processes in the Indian Ocean sector of the Southern Ocean: a case study in the coastal and oceanic waters

N. Anilkumar, Racheal Chacko, P. Sabu, Honey U. K. Pillai, Jenson V. George & C. T. Achuthankutty

Environmental Monitoring and Assessment
An International Journal Devoted to Progress in the Use of Monitoring Data in Assessing Environmental Risks to Man and the Environment

ISSN 0167-6369
Volume 186
Number 12

Environ Monit Assess (2014)
186:8109-8124
DOI 10.1007/s10661-014-3990-4

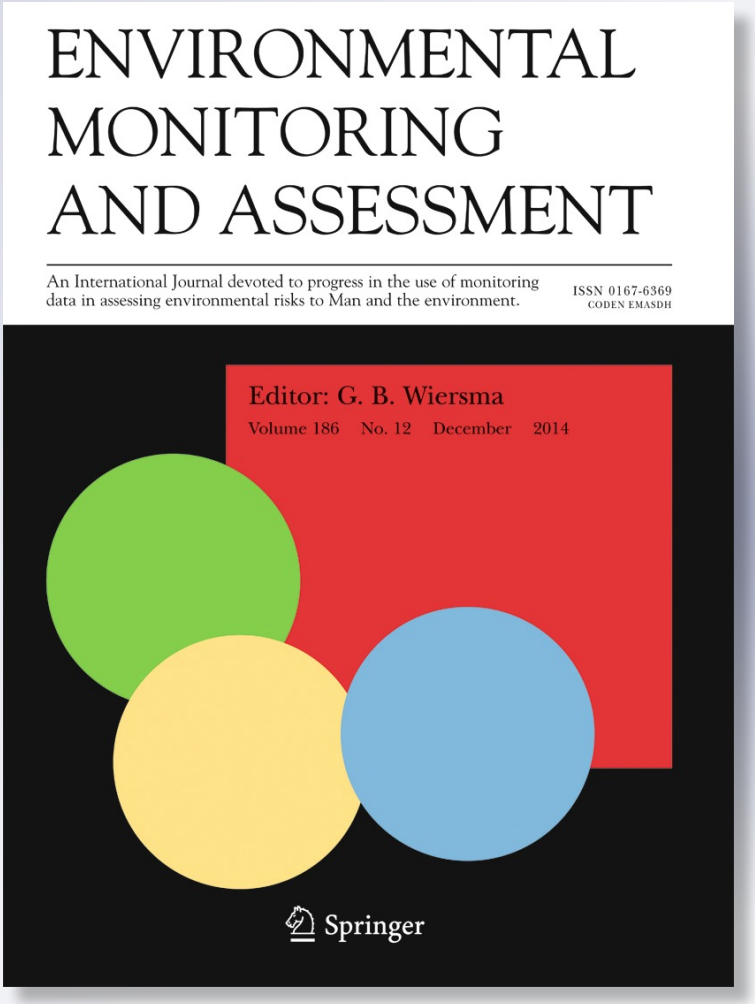

Springer

Environ Monit Assess (2014) 186:8109–8124
DOI 10.1007/s10661-014-3990-4

Biological response to physical processes in the Indian Ocean sector of the Southern Ocean: a case study in the coastal and oceanic waters

N. Anilkumar · Racheal Chacko · P. Sabu · Honey U. K. Pillai · Jenson V. George · C. T. Achuthankutty

Received: 10 November 2013 / Accepted: 31 July 2014 / Published online: 12 August 2014

Abstract The spatial variation of chlorophyll *a* (Chl *a*) and factors influencing the high Chl *a* were studied during austral summer based on the physical and biogeochemical parameters collected near the coastal waters of Antarctica in 2010 and a zonal section along 60°S in 2011. In the coastal waters, high Chl *a* (>3 mg m^{-3}) was observed near the upper layers (~15 m) between 53°30′E and 54°30′E. A comparatively higher mesozooplankton biomass (53.33 ml 100 m^{-3}) was also observed concordant with the elevated Chl *a*. Low saline water formed by melting of glacial ice and snow, as well as deep mixed-layer depth (60 m) due to strong wind (>11 ms^{-1}) could be the dominant factors for this biological response. In the open ocean, moderately high surface Chl *a* was observed (>0.6 mg m^{-3}) between 47°E and 50°E along with a Deep Chlorophyll Maximum of ~1 mg m^{-3} present at 30–40 m depth. Melt water advected from the Antarctic continent could be the prime reason for this high Chl *a*. The mesozooplankton biomass (22.76 ml 100 m^{-3}) observed in the open ocean was comparatively lower than that in the coastal waters. Physical factors such as melting, advection of melt water from Antarctic continent, water masses and wind-induced vertical mixing may be the possible reasons that led to the increase in phytoplankton biomass (Chl *a*).

N. Anilkumar · R. Chacko (✉) · P. Sabu · H. U. K. Pillai · J. V. George · C. T. Achuthankutty
National Centre for Antarctic and Ocean Research, Ministry of Earth Sciences, Headland Sada, Vasco-da-gama, Goa 403804, India
e-mail: racheal@ncaor.gov.in

Keywords Wind · Melt water · Chlorophyll *a* · Mesozooplankton · Southern Ocean

Introduction

The chlorophyll *a* (Chl *a*) concentrations in the Southern Ocean (SO) are typically quite low, despite the high concentration of major nutrients such as nitrate and phosphate in the upper water column (Moore et al. 2000; Moore and Abbott 2002), marking it as the largest high-nutrient, low-chlorophyll region (Martin 1990). Several studies have documented that these low chlorophyll concentrations are due to the limited availability of iron and silica (Martin et al. 1990; Helbling et al. 1991; de Baar et al. 1995; Van Leeuwe et al. 1997; Sedwick et al. 1997, 1999; Boyd et al. 2000, 2001; Hutchins et al. 2001). Even though the chlorophyll concentrations are generally low, phytoplankton blooms have been observed in the seasonal ice zone, in shallow coastal and shelf waters, near some fronts of the Antarctic Circumpolar Current (ACC), and are also associated with bathymetric features (Sokolov and Rintoul 2007).

Furthermore, the abundance and distribution of phytoplankton biomass in this region are significantly influenced by the mixed-layer depth (MLD) (Banse 1996) and environmental parameters such as temperature (Wright and van den Enden 2000), salinity (Fonda Umani et al. 2005; Wright et al. 2010) and light (Goffart et al. 2000). The studies carried out in the Antarctica peninsula region (between 60°S and 65°S and 45°W and 65°W) also reported the phytoplankton community

structure and it's response to physical process such as eddies, currents and vertical mixing (Mendes et al. 2012; Garcı'a-Mun˜oz et al. 2013; Sangrà et al. 2014). Fragoso and Smith (2012) have reported the influence of environmental variables on the spatial pattern and assemblage of phytoplankton in the Amundsen and Ross Seas during late summer and late spring to early summer. Previous studies in the Indian Ocean sector of SO have reported frontal variability, water masses and their influence on the phyto- and zooplankton biomass during austral summer (Anilkumar et al. 2006; Jasmine et al. 2009; Pavithran et al. 2012; Gandhi et al. 2012). The scarcity of observational data south of Polar Front (PF) has limited these studies in understanding the role of physical processes in the biological response.

The Antarctic Zone (AZ) of the SO lies between the PF and Southern Antarctic Circumpolar Current Front (SACCF), is host to a marine ecosystem that supports significant fisheries (Nicol and Foster 2000) and is an important region contributing to the global carbon cycle (Sarmiento et al. 1998; Takahashi et al. 2002). The large-scale zonal and meridional ocean circulation patterns (Whitworth et al. 1998; Bindoff et al. 2000), the annual formation and dissipation of sea ice (Gloersen et al. 1992) and the distinct seasonal surface water mass transformations (Williams et al. 2008) make the AZ a physically dynamic region. The major water masses present in this area are the Antarctic Surface Water (AASW), Shelf Water (SW), Modified Shelf Water (MSW) and Modified Circumpolar Deep Water (MCDW) (Orsi and Wiederwohl 2009). Among these, the SW is the densest water mass with a salinity maximum due to continuous freezing and ice formation (rejection of brine). The Circumpolar Deep Water (CDW) mixes with AASW and form the MCDW in the coastal waters of Antarctica. The MSW is fresher and is formed by the interaction of SW with MCDW through vertical mixing (Orsi and Wiederwohl 2009). The MCDW and the Antarctic Bottom Water (AABW) are identified as the source of Fe for surface phytoplankton production in the SO (Peloquin and Smith 2007; Gandhi et al. 2012). Thus, the water masses, with their unique characteristics, control the nutrient dynamics, which ultimately decides the phytoplankton production in this region.

In the SO, a wide range of biological data have been collected from a few large-scale surveys (Mackintosh 1973; Uno 1982; Miller and Monteiro 1988; El-Sayed 1994; Bindoff et al. 2000; Nicol et al. 2000; Strutton et al. 2000; Wright and van den Enden 2000; Hewitt et al. 2003; Brandon et al. 2004; Nicol et al. 2010). From the BROKE-West experiment, Westwood et al. (2010) have reported that the rate of primary productivity within the marginal ice zone (MIZ) were significantly higher than within the open ocean. Furthermore, they reported that the biological production (both primary and secondary) in these regions is mainly regulated by physical processes such as variability in the MLD and fronts. Thus, a conceptual understanding of the impact of physical forcing on biological factors is imperative in fully exploring the various components of the ecosystem. In the present study, we have made an attempt to understand some of the biological response due to influence of physical processes on in the coastal and open waters of the Indian Ocean sector of SO.

Materials and methods

Hydrographic and biological measurements in the Indian sector of the SO were made near the coastal waters of Antarctica at four stations, around 65.4°S latitude, between 51° and 57° 30′E longitude (1 or 2° longitude intervals), and further CTD profiling was carried out at nine stations along 57°30′E between 59°30′S and 66°30′S (1 or 2° latitude intervals) during the austral summer 2010 (13th–19th February) up to 1,000 m depth to understand the characteristics of various water masses prevailing in the study area (Fig. 1). Additionally, multidisciplinary observations were made at six stations along 60°S between 47°E and 57°30′E (2° longitude interval) during the austral summer 2011 (15th–17th February). A Seabird 911 plus CTD was used for recording temperature (accuracy ±0.001 °C) and salinity (conductivity ±0.0001 S/m) profiles up to 1,000 m depth with a bin size of 1 m. Salinity values from the CTD were calibrated against the values obtained from water samples measured using the Autosal (Guildline 8400A) onboard. The data collected using XCTD-3 s (Make: Tsurumi-Seiki Co. TSK Ltd., Yokohama, Japan. type: XCTD-3; precision ±2 % of depth, ±0.03 mS/cm for conductivity and ±0.02 °C for temperature) in the coastal region were used to understand the fine scale thermohaline variability. The MLD was computed based on the density difference criteria and was considered as the depth at which potential density increased by 0.03 from 10 m depth value (Dong et al. 2008). Oceanic water masses and fronts were identified by using the

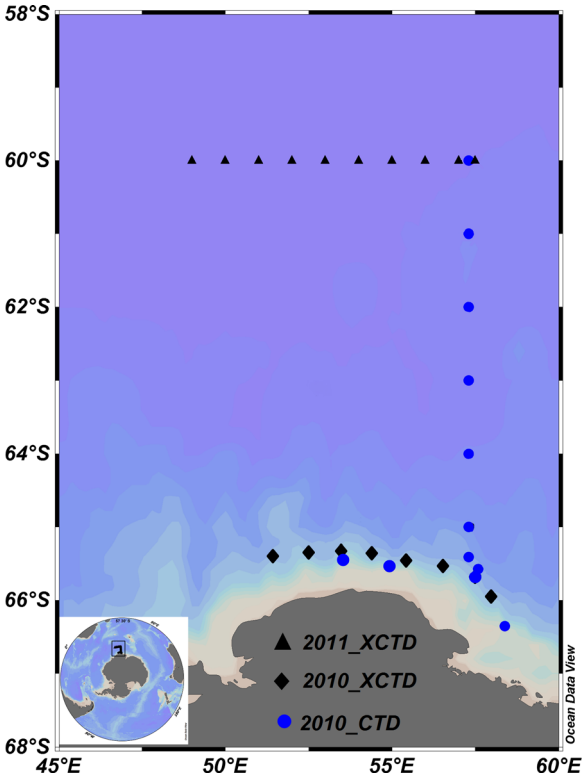

Fig. 1 The study area showing station locations in the coastal (2010) and oceanic regions (2011). *Inset* map includes the South Polar orthographic projection, and the *box* within indicates the magnified region

characteristic property indicators and the criteria adopted from other studies (Peloquin and Smith 2007; Orsi and Wiederwohl 2009; Meijers et al. 2010). The adopted property indicators for identification of water masses and fronts are given in Tables 1 and 2, respectively. Vertical profiles of photosynthetically active radiation (PAR) were collected using a biospherical QSP-2300 underwater PAR sensor attached with the CTD. Depth of the euphotic zone was defined as the penetration depth of 1 % surface irradiance based on the Beer–Lambert's law (Morel and Berthon 1989). Sea water samples were collected from standard depths (0, 10, 20, 30, 50, 75, 100 and 120 m) with General Oceanics Niskin samplers (5 l) fitted on a rosette along with the CTD. Nutrient analysis was carried out following the standard methods (Grasshoff et al. 1983). Seawater subsamples were collected in 250 ml Nalgene bottles and kept frozen at −20 °C till the nutrient analysis. Prior to analyses, the samples were thawed and brought to room temperature. In 2010, the nitrate, phosphate and silicate were analysed using a UV–vis spectrophotometer (Perkin-Elmer). In 2011, nutrients were analysed onboard using an autoanalyser (Skalar 107 Analytical Sanplus 8505 Interface v3.05). Chl *a* samples were filtered through GF/F filter (pore size 0.7 μm), extracted with 90 % acetone overnight and estimated. Chl *a* analyses were carried out following the standard procedures (Strickland and Parsons 1972). In 2010, Chl *a* analysis were made using a UV–vis spectrophotometer (Perkin-Elmer). In 2011, the Chl *a* analysis was carried out using Turner Designs AU-10 Flurometer.

Table 1 Hydrographic parameters (temperature, salinity and density) used for identification of water masses

Water mass	Temperature(°C)	Salinity	Density(kg m^{-3})
AASW	$-1.84<\theta<2$	>34	<28.3
CDW	>1.5	>34.5	$28.03<\sigma<28.27$
MCDW	<1.5	<34.7	$28.03<\sigma<28.27$
AABW	> −1.7	>34.6	>28.27

Mesozooplankton samples were collected consistently day and night from the MLD of each station by vertical hauls (speed, 1 m/s) using a Multiple Plankton Net (Hydro-Bios, mouth area 0.25 m^2, mesh size 200 μm). The volume of water filtered was measured using the formula a^2D [*a*=mouth area, *D*=depth of the water column], and biomass was estimated by dividing displacement volume of the sample with volume of water filtered and converted to 100 m^{-3}. The samples were preserved in 5 % buffered formaldehyde solution for later laboratory analysis. Zooplankton samples were separated using a Folsom sample splitter, and different taxa were sorted out from 25 % aliquots and converted to the whole sample volume. The biomass is expressed as milliliters per 100 cubic meters, and abundance of individual taxa is presented as individuals per 100 cubic meters. In addition to the in situ data, ASCAT winds (25 km×25 km) and merged sea surface height anomalies (1/3°×1/3°) from AVISO were also used in this study. Weekly composite Chl *a* data (4 km×4 km) from MODerate resolution Imaging Spectrometer (MODIS) Aqua was also analysed to identify the phytoplankton biomass in the study region. The statistical analysis was carried out using the statistical software PRIMER 6 (Plymouth Routines in Multivariate Ecological Research). For this analysis, the column data (depth wise data on temperature, salinity, nitrate, silicate, phosphate, and Chl *a*) for all stations were subject to log transformation and normalisation, followed by non-metric multi-dimensional scaling (nMDS) based on Euclidean distance. Since the

Table 2 Criteria adopted for identification of various fronts

Front	Property indicator	Reference
Antarctic Slope Front (ASF)	Southern most penetration of the 0 °C isotherm below the winter water; a strong horizontal T-S gradient at 200–400 m as the northern limit	Ainley and Jacobs 1981; Whitworth et al. 1998; Meijers et al. 2010
ACC (SB)	Southern extend of the upper CDW oxygen-minimum waters which closely correspond to the 1.5 °C isotherm	Williams et al. 2010
SACCF	θ>1.8 °C and S>34.73	Orsi et al. 1995; Meijers et al. 2010

distinction between coastal and oceanic region was clearly noted at all depths, the column data were pooled (averaged) for the entire water column up to 120 m, and data on wind speed, MLD and mesozooplankton abundance were also included in a subsequent cluster analysis based on Euclidean distance (using log-transformed and normalised station-wise data).

Results

Thermo-haline structure

Figure 2a and b shows the vertical structure of temperature and salinity along 65° 40′S (coastal waters) during austral summer, 2010. The thermal structure was vertically homogeneous in the upper 60 m, where the temperature was around 0 °C. Low saline water (~33.5) was observed in the upper 40 m, but the salinity gradually increased with increase in depth. Along the 2010 meridional section (57°30′E), maximum SST of 2 °C was observed in the AZ whereas minimum SST of around 1 °C was observed near the coastal region of the Antarctica (Fig. 2c). The upper water column along this section was also well mixed in the upper 50 m with a temperature of 1 °C. The surface salinity was <34 within the AZ, and comparatively low saline (<33.4) waters were observed near the coastal region (Fig. 2d). The vertical distribution of temperature along the 2011 zonal section (60°S) showed a well-mixed water column

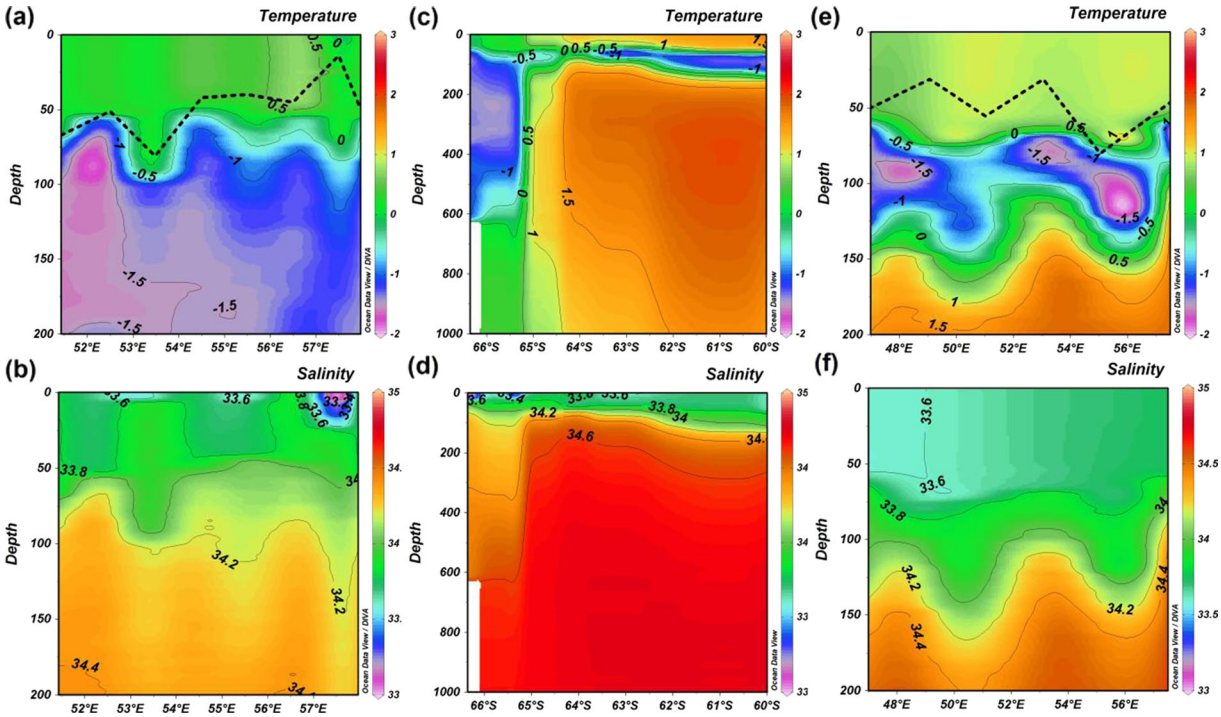

Fig. 2 The vertical structure of **a** temperature (degrees Celsius), **b** salinity near the coastal waters of Antarctica and **c** temperature (degrees Celsius), **d** salinity along 57° 30′E during 2010; **e** vertical distribution of temperature (degrees Celsius), **f** salinity along 60°S during 2011. The *black dotted line* represents the MLD of the study area

(~70 m) with a temperature of ~1.5 °C (Fig. 2e). The distribution of salinity was also quite homogeneous in the upper 70 m with low variation (33.6 to 33.8) in the entire AZ (Fig. 2f).

Water masses and fronts

During 2010 along the meridional section 57°30′E, 60°S to 66°S (near the coastal waters of Antarctica), we observed the signatures of AASW between 0 and 120 m, MCDW between 100 and 150 m (from 60°S to 65°S) and CDW between 300 and 850 m (from 60°S to 64°S). AABW was observed only at two locations (65°41′S and 65°57′S) between 580 and 760 m (Fig. 3a). Along 60°S, AASW was identified between 0 and 120 m and CDW between 500 and 1,000 m during 2011 (Fig. 3b). The characteristics of various water masses identified in the present study are given in Table 1.

The Antarctic Slope Front (ASF) is the strong subsurface horizontal gradient of temperature and salinity separating the lighter AASW from the denser MCDW, found over the continental slope, and the CDW further to the north. In the present study, the southern boundary of ASF was identified at 66°35′S and the northern limit at 64°30′S in 2010 (Fig. 2c) which separated the AASW and CDW at 200 to 400 m depth (Fig. 3a). The southern boundary of ACC (SB) is defined as the southern extent of the upper CDW oxygen-minimum waters which closely corresponds to the 1.5 °C isotherm. In the present study, the positions of the SACCF and SB were reported from the southernmost position of the subsurface 1.8 and 1.5 °C isotherms, respectively. The SB was identified between 64°S and 64°30′S and SACCF between 60°S and 61°S in 2010 (Fig. 2c and d).

Nutrients, chlorophyll and mesozooplankton biomass

Statistical analysis

To determine the biological responses to physical processes in the coastal and oceanic waters, the sampled locations were classified into sub-regions (coastal vs. oceanic), and the distinct variations observed in these

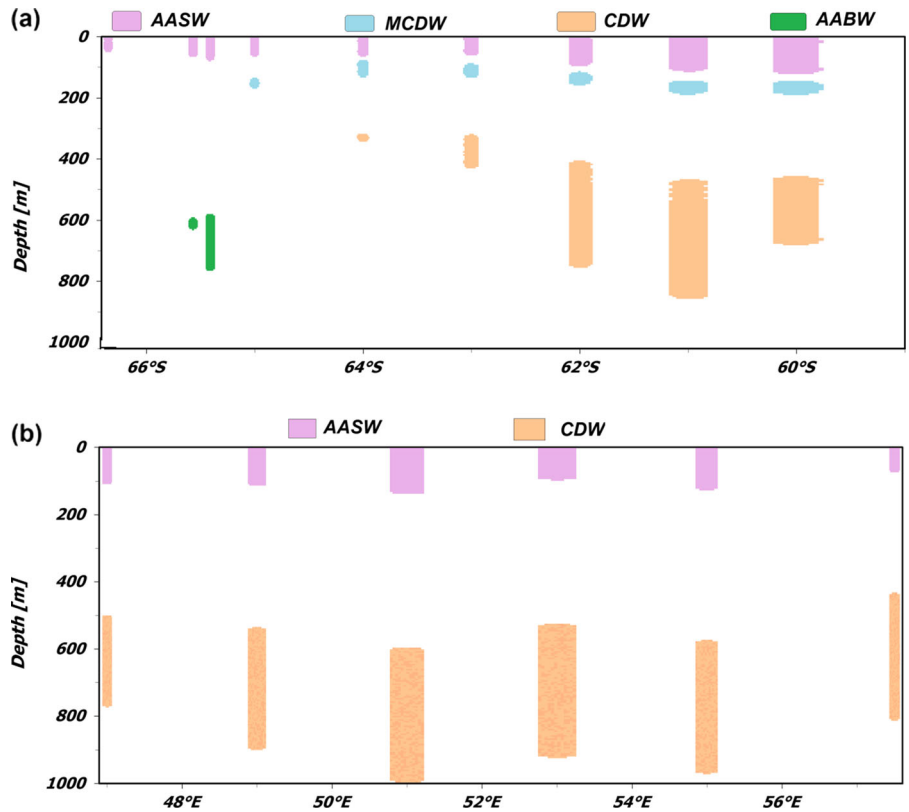

Fig. 3 Water masses identified in the study region **a** in 2010 and **b** in 2011 [Antarctic Surface Water (AASW), Modified Circumpolar Deep Water (MCDW), Circumpolar Deep Water (CDW) and Antarctic Bottom Water (AABW)]

sub regions were further tested for its statistical significance by using cluster analysis. In the nMDS plot (Fig. 4a), the coastal and oceanic stations were clearly separated into two distinct, statistically significant clusters (ANOSIM R=0.711, P=0.1 %). Since the distinction between coastal and oceanic region was clearly noted at all depths, the column data were pooled (averaged) for the entire water column up to 120 m, and data on wind speed, MLD and mesozooplankton abundance were also included in a subsequent cluster analysis based on Euclidean distance (using log-transformed and normalised station-wise data). A similar distinction was noted between coastal and oceanic stations (R=0.963, P=1.2 %), even though the distance from coast was not treated as a parameter in this analysis (Fig. 4b).

Coastal region

During the period of observation, the nitrate and silicate (NO_3 ~40 μM; SiO_3~ between 67.82 and 83.14 μM) concentration in the coastal waters was significantly higher in the upper 120 m of the water column compared with phosphate (2.17 to 3.04 μM) as shown in Fig. 5a, b and c. The surface Chl *a* was high (>3 mg m^{-3}) between 52°E and 56°30′E (Fig. 5d). The

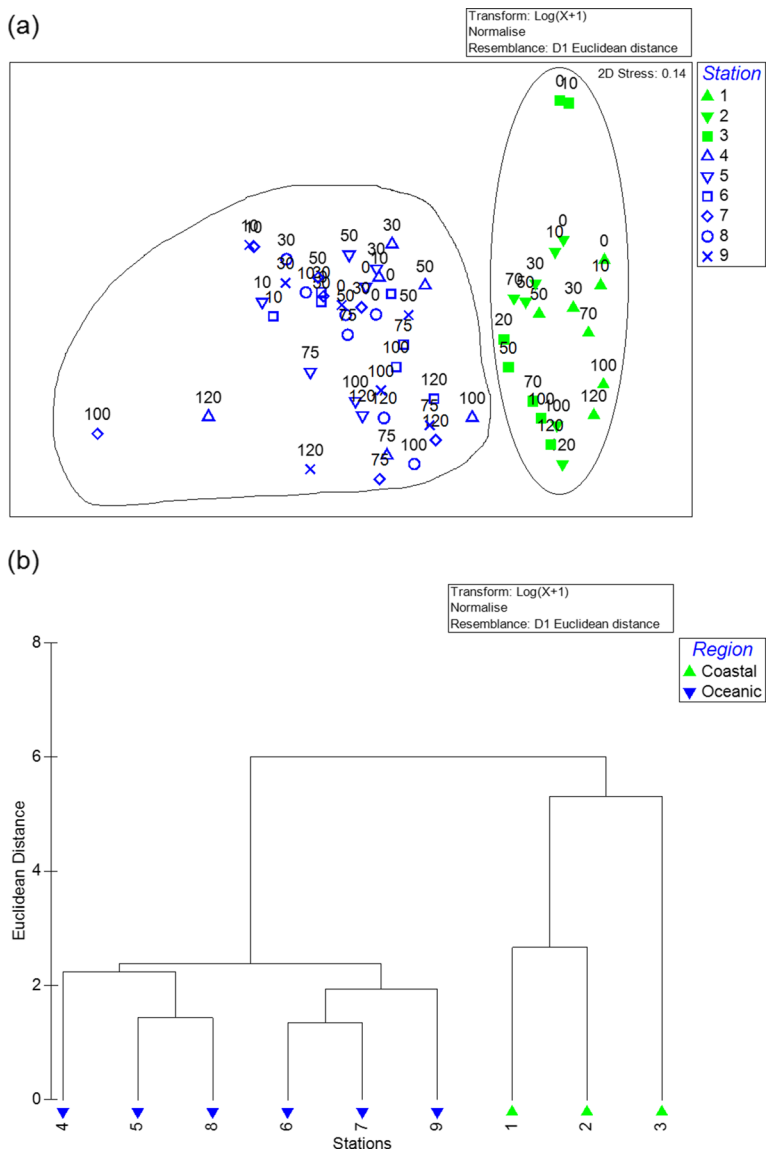

Fig. 4 Non-metric multi-dimensional scaling (nMDS) plot showing statistical significance of sub-regions based on **a** depth-wise data of temperature, salinity, nutrients (nitrate, silicate, phosphate) and chlorophyll; **b** wind speed, MLD and depth averaged data of temperature, salinity, nutrients, chlorophyll and mesozooplankton abundance

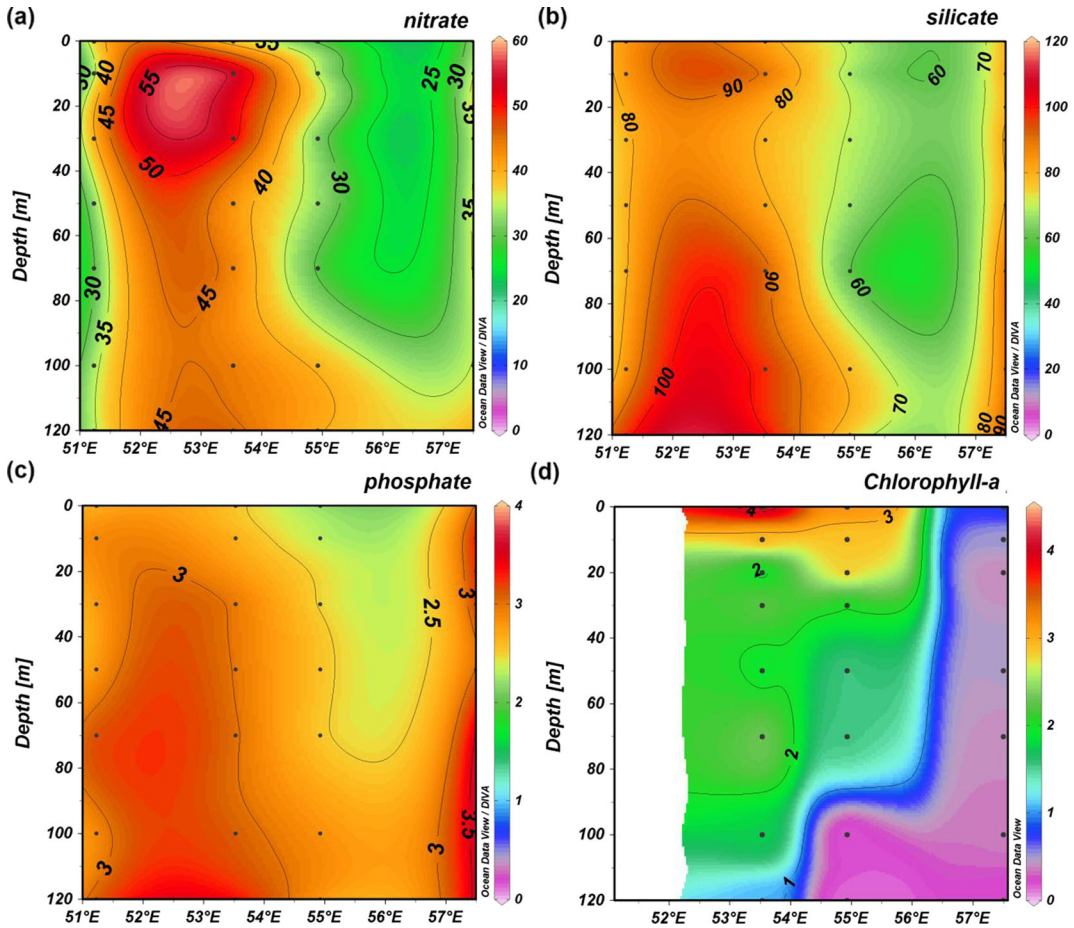

Fig. 5 The vertical structure of **a** nitrate (μM), **b** silicate (μM), **c** phosphate (μM) and **d** Chl *a* (mg m^{-3}) near the coastal region

monthly mean Chl *a* derived from the satellite imageries (MODIS Aqua) during the study period also showed an increase in Chl *a* concentration (>1.2 mg m^{-3}) in this region (Fig. 6a). The satellite Chl *a* correlated well with in situ Chl *a* (R=0.742, P=0.028, n=9). The observed euphotic depth and PAR was 50 m and 200 μEinsteins m^{-2} s^{-1}, respectively (Table 3). The average mesozooplankton biomass and numerical abundance observed in the area was 20.7±28 ml 100 m^{-3} and 17,568±5,742 ind 100 m^{-3},

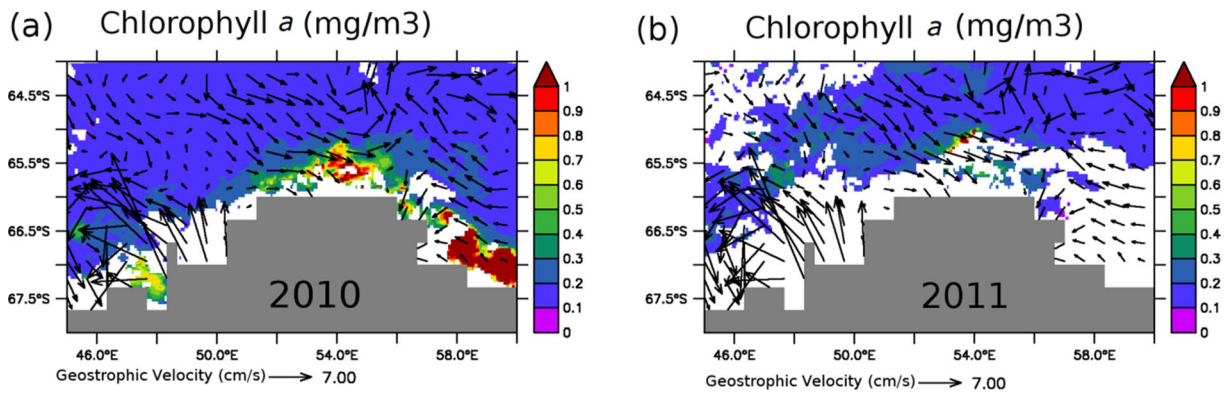

Fig. 6 Spatial distribution of satellite Chl *a* overlaid with geostrophic velocity during **a** February 2010 and **b** February 2011

Table 3 Averaged MLD, PAR, Euphotic depth, Chl *a* and mesozooplankton biomass in the coastal and oceanic regions

Region	MLD (m)	Average PAR (μ Einsteins m^{-2} s^{-1})	Euphotic depth (m)	Chl *a* (mg m^{-3})	Average mesozooplankton biomass (ml 100 m^{-3})
Coastal	50 m	200	51	1.07	20.71
Open ocean	60 m	480	58	0.34	22.76

respectively (Table 3). The in situ surface Chl *a* and mesozooplankton biomass of all the coastal stations showed a strong positive relation (R=0.99). Consistent with the high in situ phytoplankton biomass (Chl *a*) observed at the location 65°27′S 53° 32′E, the mesozooplankton standing stock was also high (53.3 ml 100 m^{-3}). A total of six mesozooplankton taxa were observed in the study area. Copepods formed the predominant taxa (~98 %), and the other minor contributors include chaetognatha (0.44 %), ostracoda (~0.18 %) and polychaeta larvae (0.02 %) (Table 4).

Oceanic region

In the oceanic region, the nitrate (>15 μM) and silicate (>20 μM) were also high in the upper 120 m water column, whereas phosphate varied between 1.5 to 2 μM (Fig. 7 a, b and c). The average Chl *a* concentration of the entire transect was 0.44 mg m^{-3}. However, west of 51°E, the Chl *a* concentration was slightly higher (0.51 mg m^{-3}) compared with east of 51°E (0.34 mg m^{-3}). The observed euphotic depth in this region was ~60 m and PAR was ~480 μEinsteins m^{-2} s^{-1}. Another feature observed was the occurrence of a Deep Chlorophyll Maximum (DCM) with a concentration of ~1.2 mg m^{-3} at 30–40 m between 47° and 48°E (Fig. 8a), and the concentration gradually decreased eastwards (Fig. 8b). The average mesozooplankton biomass observed in the area was 22.76 ml 100 m^{-3}. West of 51°E mesozooplankton biomass also exhibited higher concentration (25.86±8.82 ml 100 m^{-3}) compared with the east of 51°E (average 19.67+17.62 ml 100 m^{-3}). A total of seven mesozooplankton taxa were identified. Copepoda formed the predominant taxon (~99.9 %) as observed in the coastal region. Other minor groups include chaetognaths (0.03 %), euphausiids (~0.03 %), amphipods (~0.01 %), polychaete larvae (0.01 %), appendicularian (~0.01 %) and fish larvae (~0.01 %) (Table 4).

Table 4 Mixed-layer mesozooplankton groups and percentage contribution in the coastal and oceanic regions

SI. no	Mesozooplankton groups	% contribution in mixed layer	
		Coastal	Oceanic
1	Copepoda	98.26	99.90
2	Chaetognatha	0.44	0.03
3	Ostracoda	0.18	–
4	Polycheata larvae	0.02	0.01
5	Salps	1.06	–
6	Amphipoda	0.03	0.01
7	Euphausiids	–	0.03
8	Appedicularian	–	0.01
9	Fish larvae	–	0.01

Discussion

Physical processes and biological response

Coastal region

The Chl *a* which is a measure of phytoplankton biomass and biological productivity is dependent on the light and nutrient availability. Furthermore, phytoplankton in SO tends to be adapted to low light conditions and can operate at their maximal photosynthetic capability at low light levels (Dierssen and Smith 2000). Based on the euphotic depth (50 m) and PAR observed in the coastal region, it could be deduced that light and nutrient (NO_3 ~40 μM SiO_3~ 67 to 83 μM) levels were sufficient for surface phytoplankton growth during the time of observation.

The changing environmental characteristics of water masses around Antarctica significantly influence the phytoplankton production in the coastal region (Bianchi et al. 1992). The wind, sea ice cover and meltwater or freshwater input from glaciers, fronts and variation in currents are some of the reasons for changes in the

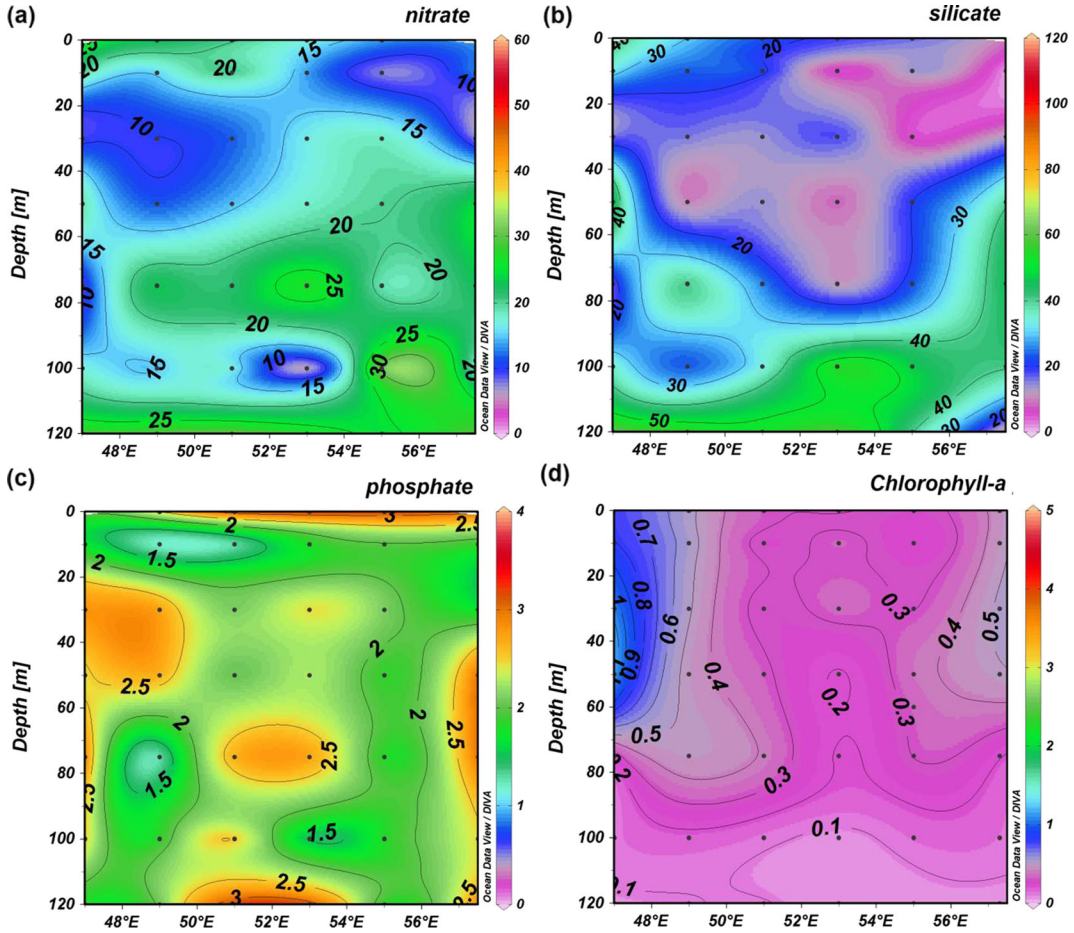

Fig. 7 Vertical distribution of **a** nitrate (μM), **b** silicate (μM), **c** phosphate (μM) and **d** Chl *a* (mg m^{-3}) along the open ocean

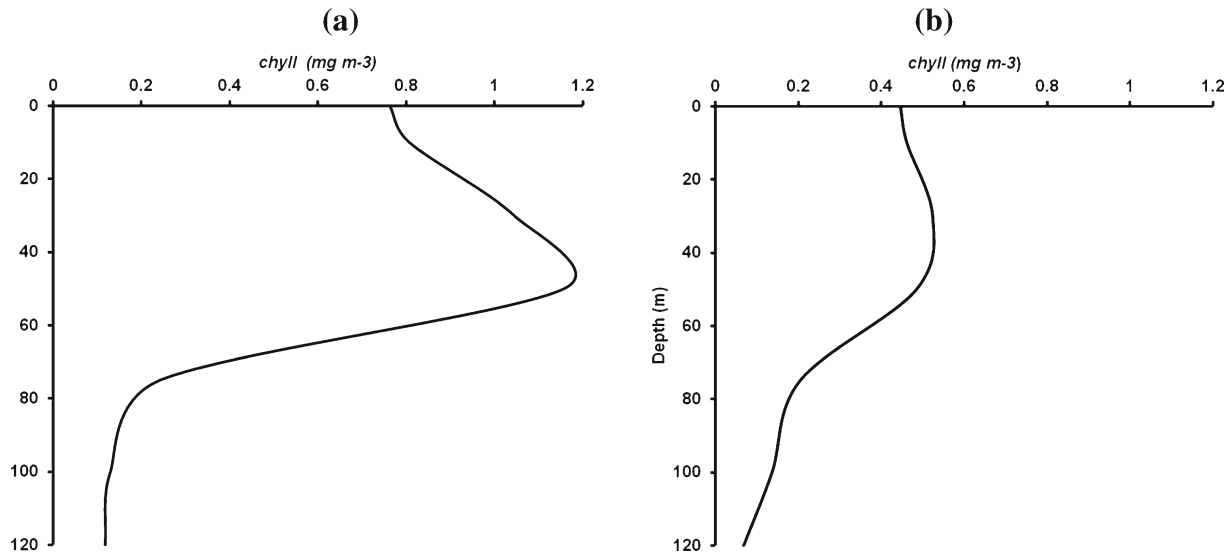

Fig. 8 Typical distribution of Chl *a* on the **a** western side (60°S 47°E) and **b** eastern side (60°S 57°30′E) of the study region

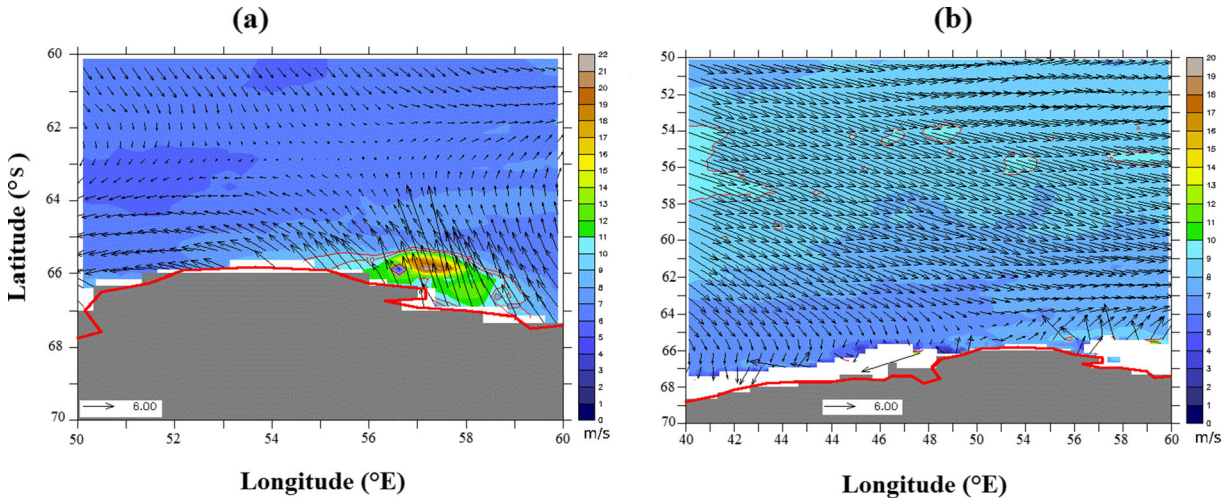

Fig. 9 Spatial distribution of wind during **a** February, 2010 and **b** February, 2011

Antarctic water characteristics (Smith and Nelson 1986; Kopczynska 1988, Boyd et al. 2007). Monthly mean wind during February was analysed to understand the role of wind. The strong southeast winds (>11 ms^{-1}) prevailing over the coastal region (Fig. 9a) might have enhanced the upward flux of micronutrients (probably Fe, not measured in this study) into the euphotic zone (~50 m) by increasing the mixed layer (60 m). Local wind stress plays an important role in driving Ekman pumping. To examine the influence of local winds on Chl *a*, daily wind stress curl and the resultant Ekman pumping velocity (W_e) in the area (52° to 54°E, 63.5° to 65.5°S) during February, 2010, were analysed (Fig. 10). It can be seen that the wind stress curl shows a larger variability between 12th and 18th February with a strong negative curl (-12×10^{-7} cm s^{-1}) on 12th February, and then again back to negative on 17th February. The figure also shows the associated positive Ekman pumping which shows the favourable condition for upwelling in the area. This low frequency variability of the wind stress has induced strong Ekman pumping, producing divergence in the upper water column, which may cause the upward movement of deep water to the surface, and the uplifting of the nitrate and silicate was also evident in the study area (Fig. 5a and b).

The intrusion of MCDW is suggested to be a source of iron for phytoplankton production (Peloquin and Smith 2007). In the present study, MCDW was observed

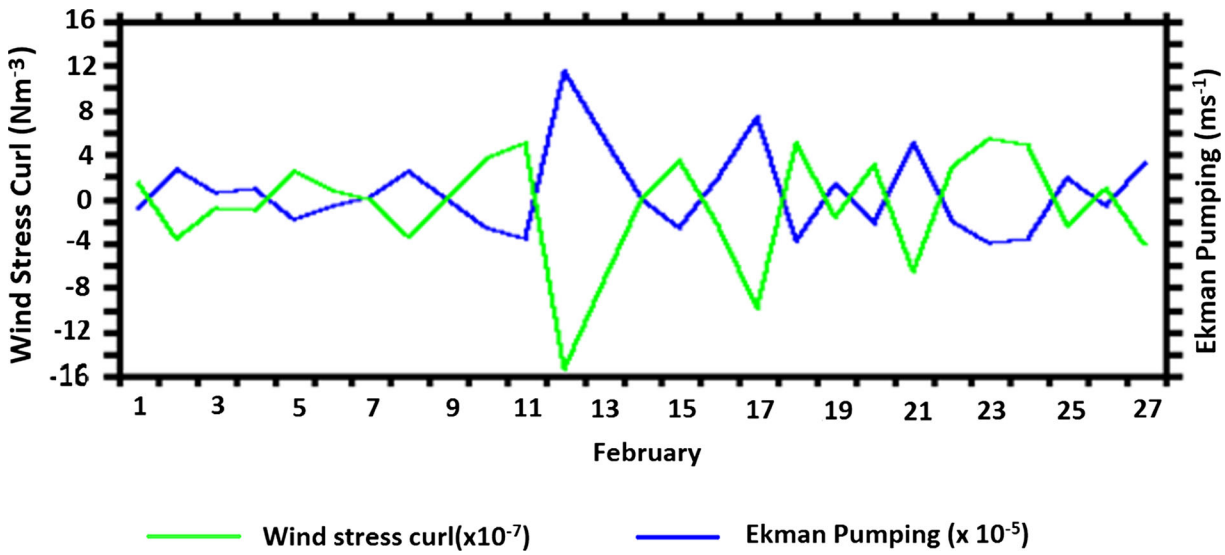

Fig. 10 Variation of wind stress curl and resultant Ekman pumping in the study area

between 100 and 150 m depth. Upwelling and subsequent mixing (~60 m) of MCDW may possibly favour the phytoplankton growth in the study region, which may fuel the herbivorous food web and eventually result in high mesozooplankton biomass. Fragoso and Smith (2012) reported the significant linear relationship between the phytoplankton bloom and MCDW present in the subsurface waters (<200 m) of the Ross Sea. Furthermore, the low saline waters observed in the coastal region may have originated from the Antarctic continent as a result of melting of glacial ice and snow which is commonly seen along the continental shelf of Antarctica during late summer to early fall (January–March). The surface salinity of the meltwater can be as low as 30.5 but averages to around 33.5 (Dierssen et al. 2002). The low saline water formed due to melting of glacial ice and snow may further fuel the phytoplankton growth in the study region. Previous studies have shown that the presence of meltwater, which is a possible source of iron (de Baar et al. 1990; Smith et al. 2007), can be linked to increase in phytoplankton blooms in the near shore waters of Antarctica (Mitchell and Holm-Hansen 1991; Moline and Prezelin 1996; Moline et al. 2000).

It was also reported that between 80°E and 150°E, the Antarctic slope current (ASC) plays an important role in the distribution of krill, cetaceans and Chl *a* (Nicol et al. 2000). Bindoff et al. (2000) showed that, in the region between 80°E and 150°E, the ASC has westward barotropic and baroclinic transport components. Along the Mawson coast between 61°E and 65°E, a westward current associated with the southern end of the ASF has been reported (Williams et al. 2008, 2010). Furthermore, they associated this current with the horizontal pressure gradient of the ASF and referred to it as ASC. In the BROKE West experiment, the ASC was observed immediately north of the shelf break as a surface-intensified westward flowing current. The ASC jet immediately north of the shelf break is significant particularly for biological features, due to its very strong, coherent structure in the velocity field. This extends from the surface to the bottom over the maximum gradient in the shelf break. The surface component of this westward velocity is stronger compared with the bottom component (Meijers et al. 2010; Heywood et al. 1999; Bindoff et al. 2000). It is proposed that the elevated Chl *a* concentrations observed in the surface layer of the marginal ice zone are retained south of the fast, narrow jet of enhanced ASC on the upper continental slope (Williams et al. 2010). Furthermore, they reported that the enhanced Chl *a* is retained to the south of ASC jet on and offshore of the Antarctic shelf break. Iceberg and sea ice transport by the ASC jet also show that it could be a mechanism for the transport of biological signatures from east to west around East Antarctica (Williams et al. 2010). The region between 50°E and 60°E is located between two distinct gyres, the Weddell Gyre in the west and Prydz Bay gyre in the east. The transport of the ASC is greatest at 80°E (westwards) and becomes steadily weaker towards the west, reaching to a minimum at 50°E, and this weakening could be due to the influence of Prydz Bay gyre (Meijers et al. 2010). The region between 50°E and 60°E is reported as a region of converging flow, since the ASC is directed north westwards by the topography along the Mawson Coast and meets the ACC and outer limb of the Weddell Gyre north of Cape Anne (Williams et al. 2010). In the present study, the observational and satellite data (Fig. 6a and b) indicated high Chl *a* between 52°E and 60°E with a maximum between 52°E and 54°E. The high Chl *a* patch was also evident in the coastal region between 52°E and 54°E in the 2011 satellite data. Hence, we presume that, due to the influence of Prydz Bay gyre, the transport of the westward-flowing ASC is getting reduced between 50°E and 60°E, and there is a possibility of Chl *a* coming from the east which may be getting accumulated between 52°E and 54°E (Fig. 6).

All the above discussed physical factors seem to enhance the phytoplankton biomass and hence the mesozooplankton biomass in the coastal waters of the study area. The high concentration of Chl *a* observed in the coastal waters may be due to the higher abundance of diatoms in the phytoplankton community which has also been reported by Estrada and Delgado (1990). The high mesozooplankton biomass and numerical abundance observed in the coastal waters of Antarctica is also in agreement with the findings of Swadling et al. (2010) in the BROKE-West experiment (30°E–80°E). They reported high mesozooplankton assemblage, ranging from 660 to more than 180,000 individuals per 1,000 m^3 across the survey region. As in the present study, the earlier studies (Hunt and Hosie 2005; Calbet et al. 2005; Swadling et al. 2010) have also reported the dominance of copepods in the coastal waters of Antarctica. As copepods are active grazers of phytoplankton, their higher abundance in the coastal region may be due to the high concentration of Chl *a*.

Oceanic region

The high PAR and the deep euphotic depth (~60 m) observed in the entire study area tend to suggest that the phytoplankton abundance of AZ was not light limited. The average concentration of Chl *a* of the entire transect was 0.44 mg m^{-3} with maximum concentration between 47°E and 50°E. The enhanced Chl *a* could be an indication of a diatom bloom, probably fuelled by the availability of high silicate concentration in the western part of the study area. Earlier studies have reported the significance of the silicate concentration on diatom growth (Assmy et al. 2013; Dugdale and Wilkerson 2001). The study carried out by Mendes et al. (2012) exhibited the domination of diatoms in the coastal region of Antarctic Peninsula. Diatoms often dominate the phytoplankton community south of the Polar frontal zone (Kopczynska et al. 2001). During summer, the Antarctic polar frontal zone is characterised by patches and bands of higher Chl *a* (Laubscher et al. 1993; Dafner and Mordasov 1994; Bathmann et al. 1997; Jasmine et al. 2009). Sokolov (2008) has reported a longer occurrence (September–April) of phytoplankton blooms in the AZ than in subtropical waters. Another interesting feature observed was the occurrence of a strong DCM in the western side of the study area. South of PF, DCM is a recurrent and widespread phenomenon in the pelagic regime of the SO (Holm-Hansen et al. 2005). The intense DCM in the western region may be due to the sinking of diatoms cells (Parslow et al. 2001).

The observed high westerly winds (>11 m/s) enhanced the vertical mixing and contributed to the deep MLD (~70 m) in the AZ (Fig. 9b). These winds generate northward Ekman transport in the AZ and the region south of PF (Fig. 11). The increase in the northward Ekman transport from south during the study period could be due to the southward shift of the westerlies. This shifting of westerlies can be a manifestation of positive SAM (SAM index 0.86) during 2011 February. Hence, we suggest that the increased northward Ekman

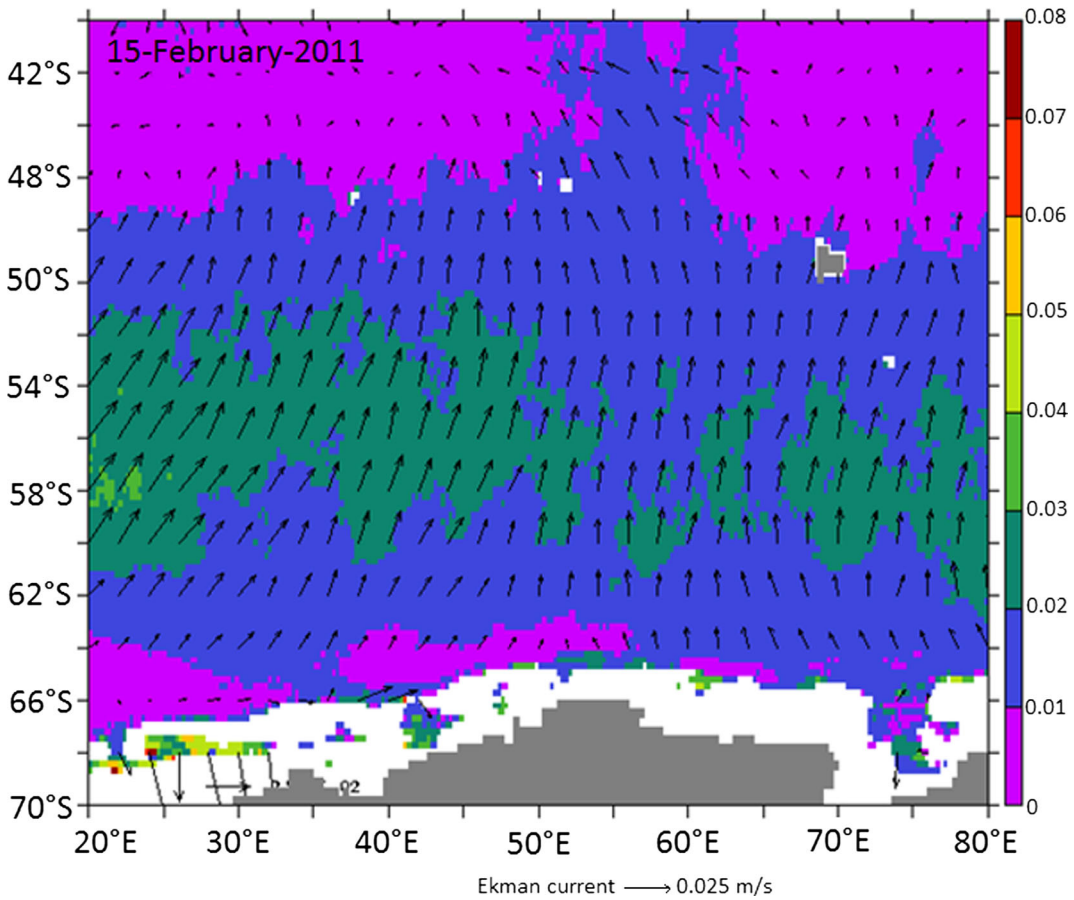

Fig. 11 Spatial distribution of Ekman currents in the study region

transport of melt water from Antarctica by melting of ice and snow could be the reason for high Chl *a* observed in the offshore region of AZ. Within the seasonal ice zone, the summer phytoplankton blooms are primarily driven by the melting of sea ice (Sokolov and Rintoul 2007). The melt water from the western side of the study area through eastward-flowing ACC may also play a role for this increase in Chl *a*. Observational and modelling studies have shown that advection disperses phytoplankton away from their main centres of production, thereby extending the regions of enhanced concentrations and distributing these populations over wider geographical ranges (Hofmann and Murphy 2004).

Even though the Chl *a* concentration was high in the study area, the observed mesozooplankton biomass was fairly low. This may be attributed to the abundance of large-sized diatoms in the area and further avoidance of feeding by mesozooplankton (Ohman and Runge 1994; Cowles and Fessenden 1995). However, similar to Chl *a*, distribution on the western side exhibited relatively higher biomass than the eastern side. Earlier studies (Goswami 1983) also reported high biomass (62.4 ml 100 m^{-3}) in the western side of the AZ (59°58′S 26°49′E); this could be related with the abundance of comparatively large-sized copepods, which were high during the spring and austral summer. The high mesozooplankton standing stock and abundance of copepods (>99 %) observed here could be attributed to the high phytoplankton (Chl *a*), and this may indicate the possibility of a conventional food web operating in this region.

Conclusion

The physical processes that influence the biological production in the coastal and oceanic region of Antarctica are discussed. The low saline waters formed by melting of glacial ice and snow could be the predominant factor for the high Chl *a* (>3 mg m^{-3}), resulting in high mesozooplankton biomass and abundance along the coastal region in 2010. During 2011, high surface Chl *a* was observed (>0.6 mg m^{-3}) between 47°E and 50°E along with a DCM of ~1.2 mg m^{-3} at ~40 m depth in the oceanic region. Melt water advected from Antarctic Continent could be the major driving force for this high Chl *a*. Some physical processes such as the strong wind induced vertical mixing of water column; upwelling and the transport of advected melt water by the ACC could also be the causative factors for the increased Chl *a*. A detailed study of waters from the Antarctic coast to the PF may provide further information on the dynamics of food web in this region.

Acknowledgements This work was supported by the Ministry of Earth Sciences, Government of India. We are thankful to Director, NCAOR, for his constant support and encouragement. We are indebted to Ms. Usha Parameshwaran and Dr. Abdul Jaleel, CMLRE, Kochi, for the statistical analysis. The authors acknowledge the contribution towards data collection and analysis carried out by Dr. Sini Pavithran, Dr. Mandar Nanajkar, Dr. Deepti Dessai and Ms. Sharon B. Noronha. Help rendered in the implementation and completion of this study by cruise participants and staff at NCAOR is acknowledged. The authors are grateful to the anonymous reviewer for the valuable suggestions. This is NCAOR contribution no 18/2014.

References

Ainley, D., & Jacobs, S. (1981). Sea-bird affinities for ocean and ice boundaries in the Antarctic. *Deep-Sea Research Part I, 1*(28), 1173–1185.

Anilkumar, N., Luis, A. J., Somayajulu, Y. K., Ramesh Babu, V., Dash, M. K., Pednekar, S. M., Babu, K. N., Sudhakar, M., & Pandey, P. C. (2006). Fronts, water masses and heat content variability in the western Indian sector of Southern Ocean during austral summer 2004. *Journal of Marine Systems, 63*, 20–34.

Assmy, P., Smetacek, V., Montresor, M., Klaas, C., Henjes, J., Strass, V. H., Arrieta, J. M., Bathmann, U., et al. (2013). Thick-shelled, grazer-protected diatoms decouple ocean carbon and silicon cycles in the iron-limited Antarctic circumpolar current. *Proceedings of the National Academy of Science*. doi:10.1073/pnas.1309345110.

Banse, K. (1996). Low seasonality of low concentrations of surface chlorophyll in the sub Antarctic water ring: underwater irradiance, iron, or grazing? *Progress in Oceanography, 37*, 241–291.

Bathmann, U. V., Scharek, R., Klaas, C., Dubischar, C. D., & Smetacek, V. (1997). Spring development of phytoplankton biomass and composition in major water masses of the Atlantic sector of the Southern Ocean. *Deep-Sea Research Part I, 44*, 51–67.

Bianchi, F., Boldrin, A., Cioce, F., Dieckmann, G., Kuosa, H., Larsson, A. M., Nothig, E. M., Sehlstedt, P. I., Socal, G., & Syvertsen, E. E. (1992). Phytoplankton distribution in relation to sea ice, hydrography and nutrients in the northwestern Weddell Sea in early spring 1988 during EPOS. *Polar Biology, 12*, 225–235.

Bindoff, N., Rosenberg, M., & Warner, M. (2000). On the circulation and water masses over the Antarctic continental slope and rise between 80°E and 150°E. *Deep Sea Research, Part II, 47*, 2299–2326.

Boyd, P. W., Watson, A. J., Law, C. S., Abraham, E. R., Trull, T., et al. (2000). A mesoscale phytoplankton bloom in the polar

Southern Ocean stimulated by iron fertilization. *Nature, 407*, 695–702.

Boyd, P. W., Jickells, T., Law, C. S., Blain, S., Boyle, E. A., Buesseler, K. O., Coale, K. H., Cullen, J. J., debar, H. J. W., Follows, M., Harvey, M., Lancelot, C., Levasseur, M., Owens, N. P. J., Pollard, R., Rivkin, R. B., Sarmiento, J., Schoemann, V., Smetacek, V., Takeda, S., Tsuda, A., Turner, S., & Watson, A. J. (2007). Mesoscale iron enrichment experiments1993–2005: Synthesis and future directions. *Nature, 315*, 612–617.

Brandon, M. A., Naganobu, M., Deme, D. A., Chernyshkov, P., Trathan, P. N., Thorpe, S. E., Kameda, T., Berezhinskiy, O. A., Hawker, E. J., & Grant, S. (2004). Physical oceanography in the Scotia Sea during the CCAMLR 2000 survey, austral summer 2000. *Deep-Sea Research Part II, 51*, 1301–1321.

Calbet, A., Alcaraz, M., Atienza, D., Broglio, E., & Vaque, D. (2005). Zooplankton biomass distribution patterns along the western Antarctic Peninsula (December 2002). *Journal of Plankton Research, 27*, 1195–1203.

Cowles, T. J., & Fessenden, L. M. (1995). Copepod grazing and fine scale distribution patterns during the marine light-mixed layers experiment. *Journal of Geophysical Research, 100*, 6677–6686.

Dafner, E. V., & Mordasov, N. V. (1994). Influence of biotic factors on the hydrochemical structure of surface water in the polar frontal zone of the Atlantic Antarctic. *Marine Chemistry, 45*, 137–148.

De Baar, H. J. W., Buma, A. G. J., Nolting, R. F., Cadée, R. F., Jacques, G., & Tréguer, P. J. (1990). On iron limitation of the Southern Ocean: Experimental observations in the Weddell and Scotia seas. *Marine Ecology Progress Series, 6*, 105–122.

De Baar, H. J. W., de Jong, J. T. M., Bakker, D. C. E., Löscher, B. M., Veth, C., Bathmann, U. V., & Smetacek, V. (1995). Importance of iron for phytoplankton blooms and carbon dioxide drawdown in the Southern Ocean. *Nature, 373*, 412–415.

Dierssen, H., & Smith, R. C. (2000). Bio-optical properties and remote sensing ocean color algorithms for Antarctic Peninsula waters. *Journal of Geophysical Research, 105*, 26301–26312.

Dierssen, H. M., Smith, R. C., & Vernet, M. (2002). Glacial meltwater dynamics in coastal waters west of the Antarctic Peninsula. *Proceedings of the National Academy of Sciences, 99*, 1790–1795.

Dong, S., Sprintall, J., Gille, S. T., & Talley, L. (2008). Southern Ocean mixed-layer depth from Argo float profiles. *Journal of Geophysical Research, 113*, C06013. doi:10.1029/2006JC004051.

Dugdale, R. C., & Wilkerson, F. P. (2001). Sources and fates of silicon in the ocean: The role of diatoms in the climate and glacial cycles. *Scientia Marina, 65*(Suppl 2), 141–152.

El-Sayed, S. (1994). Southern Ocean ecology: The BIOMASS perspective. CCAMLR science.

Estrada, M., & Delgado, M. (1990). Summer phytoplankton distributions in the Weddell Sea. *Polar Biology, 10*, 441–449.

Fonda Umani, S., Monti, M., Bergamasco, A., et al. (2005). Plankton community structure and dynamics versus physical structure from Terra Nova Bay to Ross Ice Shelf (Antarctica). *Journal of Marine Systems, 55*, 31–46.

Fragoso, G. M., & Smith, W. O., Jr. (2012). Influence of hydrography on phytoplankton distribution in the Amundsen and Ross Seas, Antarctica. *Journal of Marine Systems, 89*, 19–29.

Gandhi, N., Ramesh, R., Laskar, A. H., Sheshshayee, M. S., Shetye, S., Anilkumar, N., Patil, S. M., & Mohan, R. (2012). Zonal variability in primary production and nitrogen uptake rates in the southwestern Indian Ocean and the Southern Ocean. *Deep-Sea Research Part I, 67*, 32–43.

Garcı'a-Mun˜oz, C., Lubia'n, L. M., Carlos, M., Garcı'a, C. M., Marrero-Dı'az, A., Sangra, P., & Vernet, M. (2013). A mesoscale study of phytoplankton assemblages around the South Shetland Islands (Antarctica). *Polar Biology, 36*, 1107–1123.

Gloersen, P., Campbell, W. J., Cavalieri, D. J., Comiso, J. C., Parkinson, C. L., & Zwally, H. J. (1992). *Arctic and Antarctic sea ice, 1978–1987: Satellite passive–microwave observations and analysis*. Washington: National Aeronautics and Space Administration (NASA-SP511).

Goffart, A., Catalano, G., & Hecq, J. H. (2000). Factors controlling the distribution of diatoms and *Phaeocystis* in the Ross Sea. *Journal of Marine Systems, 27*, 161–175.

Goswami, S.C. (1983). Zooplankton of the Antarctica waters scientific report of first Indian expedition to Antarctica, technical publication 1.

Grasshoff, K. (1983). Methods of seawater analysis (eds Grasshoff, K., Ehrhardt, M. and Kremling, K.), Verlag Chemie, Weinheim, 2nd edn. p. 419.

Helbling, E. W., Villafan˜e, V., & Holm-Hansen, O. (1991). Effect of iron on productivity and size distribution of Antarctic phytoplankton. *Limnology and Oceanography, 36*, 1879–1885.

Hewitt, R. P., Demer, D. A., & Emery, J. H. (2003). An 8-year cycle in krill biomass density inferred from acoustic surveys conducted in the vicinity of the South Shetland Islands during the austral summers of 1991–1992 through 2001–2002. *Aquatic Living Resources, 16*, 205–213.

Heywood, K., Sparrow, M., Brown, J., & Dickson, R. (1999). Frontal structures and Antarctic bottom water flow through the princess Elizabeth trough, Antarctica. *Deep-Sea Research Part I, 46*(7), 1181–1200.

Hofmann, E. E., & Murphy, E. J. (2004). Advection, krill, and Antarctic marine ecosystems. *Antarctic Science, 16*, 487–499.

Holm-Hansen, O., Kahru, M., & Hewes, C. D. (2005). Deep chlorophyll *a* maxima (DCMs) in pelagic Antarctic waters. II. Relation to bathymetric features and dissolved iron concentrations. *Marine Ecology Progress Series, 297*, 71–81.

Hunt, B. P. V., & Hosie, G. W. (2005). Zonal structure of zooplankton communities in the Southern Ocean South of Australia: Results from a 2150 km continuous plankton recorder transect. *Deep Sea Research, Part I, 52*, 1241–1271.

Hutchins, D. A., Sedwick, P. N., DiTullio, G. R., Boyd, P. W., Queguiner, B., Griffiths, F. B., & Crossley, C. (2001). Control of phytoplankton growth by iron and silicic acid availability in the sub Antarctic Southern Ocean: Experimental results from the SAZ project. *Journal of Geophysical Research, Oceans, 106*, 31559–31572.

Jasmine, P., Muraleedharan, K. R., Madhu, N. V., Asha Devi, C. R., Alagarswamy, R., Achuthan Kutty, C. T., Jayan, Z., Sanjeevan, V. N., & Sahayak, S. (2009). Hydrographic and

productivity characteristics along 45oE longitude in the southwestern Indian Ocean and Southern Ocean during Austral summer 2004. *Marine Ecology Progress Series, 389*, 97–116.

Kopczynska, E. E. (1988). Spatial structure of phytoplankton in the Scotia Front west Elephant Island (BIOMASSIII, October–November1986). *Polish Polar Research, 9*, 231–242.

Kopczynska, E. E., Dehairs, F., Elskens, M., & Wright, S. (2001). Phytoplankton variability between the subtropical and polar fronts south off Australia: Thriving under regenerative and new production in late summer. *Journal of Geophysical Research, Oceans, 106*, 31597–31609.

Laubscher, R. K., Perissinotto, R., & McQuaid, C. D. (1993). Phytoplankton production and biomass at frontal zones in the Atlantic sector of the Southern Ocean. *Polar Biology, 13*, 471–481.

Mackintosh, N. (1973). Distribution of post-larval krill in the Antarctic. *Discovery Reports, 36*, 1–94.

Martin, J. H. (1990). Glacial–interglacial CO2: The iron hypothesis. *Paleoceanography, 5*, 1–13.

Martin, J. H., Fitzwater, S. E., & Gordon, R. M. (1990). Iron deficiency limits phytoplankton growth in Antarctic waters. *Global Biogeochemical Cycles, 4*, 5–12.

Meijers, A. J. S., Klocker, A., Bindoff, N. L., Williams, G. D., & Marsland, S. J. (2010). The circulation and water masses of the Antarctic shelf and continental slope between 30 and 80°E. *Deep-Sea Research Part II, 57*, 723–737.

Mendes, C. R., de Souza, M. S., Garcia, V. M. T., Leal, M. C., Brotas, V., & Garcia, C. A. E. (2012). Dynamics of phytoplankton communities during late summer around the tip of the Antarctic Peninsula. *Deep-Sea Research Part I, 65*, 1–14.

Miller, D., & Monteiro, P. (1988). *Antarctic Ocean and resources variability*. Berlin: Springer.

Mitchell, B. G., & Holm-Hansen, O. (1991). Observations and modelling of the Antarctic phytoplankton crop in relation to mixing depth. *Deep Sea Research, 38*, 981–1007.

Moline, M., & Prezelin, B. B. (1996). Long-term monitoring and analyses of physical factors regulating variability in coastal Antarctic phytoplankton biomass, productivity and taxonomic composition over sub seasonal, seasonal and interannual time scales. *Marine Ecology Progress Series, 145*, 143–160.

Moline, M. A., Claustre, H., Frazer, T. K., Grzymski, J., Schofield, O., & Vernet, M. (2000). Antarctic ecosystems: Models for wider ecological understanding, eds. Davison, E., Howard-Williams, C. & Broady, P. (New Zealand Natural Sciences, Canterbury University, Christchurch, New Zealand).

Moore, J. K., & Abbott, M. R. (2002). Surface chlorophyll concentrations in relation to the Antarctic polar front: Seasonal and spatial patterns from satellite observations. *Journal of Marine Systems, 37*, 69–86.

Moore, J. K., Abbott, M. R., Richman, J. G., & Nelson, D. (2000). The Southern Ocean at the last glacial maximum: A strong sink for atmospheric carbon dioxide. *Global Biogeochemical Cycles, 14*, 455–475.

Morel, A., & Berthon, J. (1989). Surface pigments, algal biomass profiles, and potential production of the euphotic layer: Relationships reinvestigated in view of remote-sensing applications. *Limnology and Oceanography, 34*, 1545–1562.

Nicol, S., & Foster, J. (2000). Recent trends in the fishery for Antarctic krill. *Aquatic Living Resources, 47*, 2489–2517.

Nicol, S., Pauly, T., Bindoff, N., & Strutton, P. (2000). "BROKE" a biological/oceanographic survey off the coast of east Antarctica (80–150E) carried out in January–March 1996. *Deep-Sea Research Part II, 47*, 2281–2298.

Nicol, S., Meiners, K., & Raymond, B. (2010). BROKE-West, a large ecosystem survey of the South West Indian Ocean sector of the Southern Ocean (CCAMLR Division 58.4.2). *Deep-Sea Research Part II, 57*(9–10), 693–700.

Ohman, M. D., & Runge, J. A. (1994). Sustained fecundity when phytoplankton resources are in short supply: Omnivory by *Calanus finmarchicus* in the Gulf of St. Lawrence. *Limnology and Oceanography, 39*, 21–36.

Orsi, A. H., & Wiederwohl, C. L. (2009). A recount of Ross Sea waters. *Deep Sea Research, Part II, 56*, 778–795.

Orsi, A., Whitworth, T., III, Worth, D., & Nowlin, W., Jr. (1995). On the meridional extent and fronts of the Antarctic circumpolar current. *Deep Sea Research, Part I, 42*, 641–673.

Parslow, J. S., Boyd, P. W., Rintoul, S. R., et al. (2001). A persistent subsurface chlorophyll maximum in the interpolar frontal zone south of Australia: Seasonal progression and implications for phytoplankton-light-nutrient interactions. *Journal of Geophysical Research, 106*, 31543–31557.

Pavithran, S., Anilkumar, N., Krishnan, K. P., Sharon, B. N., Jenson, V. G., Nanajkar, M., Chacko, R., Dessai, D. G. G., & Achuthankutty, C. T. (2012). Contrasting pattern in chlorophyll a distribution within the polar front of the Indian sector of Southern Ocean during austral summer 2010. *Current Science, 102*(6), 899.

Peloquin, J.A., & Smith Jr., W.O. (2007). Phytoplankton blooms in the Ross Sea, Antarctica: Interannual variability in magnitude, temporal patterns, and composition. *Journal of Geophysical Research-Oceans,* 112, doi: 10.1029/2006JC003816.

Sangrà, P., García-Muñoz, C., García, C. M., Marrero-Díaz, A., Sobrino, C., Mouriño-Carballido, B., Aguiar-González, B., Henríquez-Pastene, C., Rodríguez-Santana, A., Lubián, L. M., Hernández-Arencibia, M., Hernández-León, S., Vázquez, E., & Estrada-Allis, S. N. (2014). Coupling between upper ocean layer variability and size-fractionated phytoplankton in a non-nutrient-limited environment. *Marine Ecology Progress Series, 499*, 35–46. doi:10.3354/meps10668.

Sarmiento, J. L., Hughes, T. M. C., Stouffer, R. J., & Manabe, S. (1998). Simulated response of the ocean carbon cycle to anthropogenic climate warming. *Nature, 393*(6682), 245–249.

Sedwick, P. N., Edwards, P. R., Mackey, D. J., Griffiths, F. B., & Parslow, J. S. (1997). Iron and manganese in surface waters of the Australian sub Antarctic region. *Deep-Sea Research Part I, 44*, 1239–1253.

Sedwick, P. N., DiTullio, G. R., Hutchins, D. A., Boyd, P. W., Griffiths, F. B., Crossley, A. C., Trull, T. W., & Que'guiner, B. (1999). Limitation of algal growth by iron deficiency in the Australian Subantarctic region. *Geophysical Research Letters, 26*, 2865–2868.

Smith, W. O., Jr., & Nelson, D. M. (1986). Importance of ice edge phytoplankton production in the Southern Ocean. *Bioscience, 36*, 251–257.

Smith, W. O., Ainley, D. G., & Catteneo-Vietti, R. (2007). Trophic interactions within the Ross Sea continental shelf ecosystem. *Philosophical Transactions of the Royal Society B, 362*, 95–111.

Sokolov, S. (2008). Chlorophyll blooms in the Antarctic Zone south of Australia and New Zealand in reference to the

Antarctic circumpolar current fronts and sea ice forcing. *Journal of Geophysical Research Oceans, 113*, C03022. doi:10.1029/2007JC004329.

Sokolov, S., & Rintoul, S. R. (2007). Multiple jets of the Antarctic circumpolar current south of Australia. *Journal of Physical Oceanography, 37*, 1394–1412.

Strickland, J. D. H., & Parsons, T. R. (1972). A practical handbook of seawater analysis. *Journal of the Fisheries Research Board of Canada, 167*, 310.

Strutton, P., Griffiths, B., Waters, R., Wright, S., & Bindoff, N. L. (2000). Primary productivity off the coast of East Antarctica (80 to 150°E): January to March 1996. *Deep-Sea Research Part II, 47*, 2327–2363.

Swadling, K. M., Kowaguchi, S., & Hosie, G. W. (2010). Antarctic mesozooplankton community structure during BROKE-WEST (301E-801E), January–February 2006. *Deep Sea Research, Part II, 57*, 887–904.

Takahashi, T., Sutherland, S. C., Sweeney, C., Poisson, A., Metzl, N., Tilbrook, B., Bates, N., Wanninkhof, R., Feely, R. A., Sabine, C., Olafsson, J., & Nojiri, Y. (2002). Global sea–air CO_2 flux based on climatological surface ocean pCO_2, and seasonal biological and temperature effect. *Deep Sea Research, Part II, 49*, 1601–1622.

Uno, S. (1982). Distribution and stocking stock of chlorophyll a in the Antarctic Ocean, from December 1980 to January1981. *Memoirs of the National Institute for Polar Research (Special Issue), 23*, 20–27.

Van Leeuwe, M. A., Scharek, R., de Baar, H. J. W., de Jong, J. T. M., & Goeyens, L. (1997). Iron enrichment experiments in the Southern Ocean: Physiological responses of plankton communities. *Deep Sea Research, Part II, 44*, 189–208.

Westwood, K., Griffiths, F., Meiners, K., & Williams, G. (2010). Primary productivity off the Antarctic coast from 30° to 80°E; BROKE-West survey, 2006. *Deep Sea Research, Part II, 57*(9–10), 794–814.

Whitworth, T., III, Orsi, A., Kim, S.-J., & Nowlin, W., Jr. (1998). Water masses and mixing near the Antarctic slope front. In S. Jacobs & R. Weiss (Eds.), *Ocean, ice and atmosphere: Interactions at the Antarctic continental margin* (pp. 1–27). Washington: American Geophysical Union.

Williams, G. D., Nicol, S., Raymond, B., & Meiners, K. (2008). On the summer time mixed layer development in the marginal sea-ice zone off the Mawson coast, east Antarctica. *Deep-Sea Research Part II, 55*, 365–376.

Williams, G. D., Nicol, S., Aoki, S., Meijers, A. J. S., Bindoff, N. L., Iijima, Y., Marsland, S. J., & Klocker, A. (2010). Surface oceanography of BROKE-West, along the Antarctic margin of the south-west Indian Ocean (30 to 80°E). *Deep-Sea Research Part II, 57*, 738–757.

Wright, S. W., & van den Enden, R. L. (2000). Phytoplankton community structure and stocks in the East Antarctic marginal ice zone (BROKE survey, Jan–Mar. 1996) determined by CHEMTAX analysis of HPLC pigment signatures. *Deep Sea Research, Part II, 47*, 2363–2400.

Wright, S. W., van den Enden, R. L., Pearce, I., Davidson, A. T., & Scott, F. (2010). Phytoplankton community structure and stocks in the Southern Ocean (30–801E) determined by CHEMTAX analysis of HPLC pigment signatures. *Deep Sea Research, Part II, 57*(9–10), 758–778.

Deep-Sea Research II ∎ (∎∎∎∎) ∎∎∎–∎∎∎

Contents lists available at ScienceDirect

Deep-Sea Research II

journal homepage: www.elsevier.com/locate/dsr2

Freshening of Antarctic Bottom Water in the Indian Ocean sector of Southern Ocean

N. Anilkumar, Racheal Chacko*, P. Sabu, Jenson V. George

National Centre for Antarctic and Ocean Research, Headland Sada, Vasco-Da-Gama, Goa-403804, India

ARTICLE INFO

Keywords:
Salinity
Freshening
Antarctic Bottom Water
Southern Ocean
SAM

ABSTRACT

Recent observations reveal a rapid reduction in salinity and density of Antarctic Bottom Water (AABW) in the Indian Ocean sector of Southern Ocean. Previous studies have shown fast freshening of AABW since 1995, but an increased rate of freshening from 2006 to 2010 was exhibited in the present study by both ECMWF (ORAS4) reanalysis data as well as in-situ data. During the same period the degrees of change observed in the AABW were more predominant in the in-situ data, becoming warmer (~0.05 °C), fresher (~0.01) and lighter (~0.01 kg m^{-3}). Between 2006 and 2010 the height of fresh water added per unit area for 500 m thickness (4000–4500 m) was 2.2 cm per annum (cm a^{-1}). The AABW observed in the present study could have originated from Weddell Sea or Cape Darnley polynya. The decadal changes indicate an enhanced sea-ice formation, due to increased positive phases of Southern Annular Mode (SAM), which may have led to the increase in fresh water input, resulting in freshening of AABW.

1. Introduction

The transport of heat, carbon, and other climatically important tracers around the planet is mainly controlled by the meridional overturning circulation (Ganachaud and Wunsch, 2000). Hence overturning circulation is one of the key mechanisms that determine Earth's climate. It is driven by the global network of deep western boundary currents, which exports the cold, dense water formed in the high-latitude North Atlantic Ocean and the Southern Ocean (SO) and is supplied as the deep branch of overturning circulation (Stommel and Arons, 1961). Orsi et al. (2002) have reported that the Southern Ocean limb of the overturning ventilates the deep ocean at about the same rate as the North Atlantic and is dynamically coupled to the Atlantic overturning (Weaver et al., 2003) and this is also potentially sensitive to future climate change (Meehl et al.,2007). During the past four decades a significant decrease in salinity of the North Atlantic Deep Water has been observed (Dickson et al., 2002). In the abyssal layer, around 30–40% of the global ocean mass is accounted by the cold, dense Antarctic Bottom Water (AABW) (Johnson, 2008). For global overturning circulation, AABW production is a key contributor (Johnson, 2008; Marshall, and Speer, 2012) and is also an important sink for heat and CO_2 (Sigman and Boyle, 2000). The AABW is generally produced at a few specific high-latitude regions of the Southern Ocean (Couldrey et al.,2013). The largest source of AABW is the Weddell Sea which supplies 60% of the total volume (Orsi et al.,2002). The remaining is supplied by the Ross Sea and the Mertz Polynya region of the Ade´lie Land coast near 145°E (Orsi et al., 2002; Rintoul, 1998). A recent study by Ohshima et al. (2013) also reported Cape Darnley polynya (CDP) region (65°–69°E) as a significant source of AABW.

The air–sea–ice interactions near the Antarctic margins play a key role in the formation of AABW and are sensitive to climatic forcing (Orsi et al., 1999). In many regions AABW has warmed significantly, most strongly in the Atlantic (e.g., Meredith et al., 2008; Zenk and Morozov, 2007). In the North Atlantic, this warming has slowed down the meridional overturning of Antarctic-derived waters (Johnson et al., 2008) and is significantly influencing the global heat budget and calculations of sea level rise (Purkey and Johnson, 2010). Further, Whitworth (2002) reported a shift from salty mode to fresh mode of bottom water in the Australian Antarctic basin. Also, in the region between 140°E and 150°E and southwards of 65°S, Jacobs (2004, 2006) has reported that the bottom water properties vary strongly with season and location, reflecting the narrow bottom currents and rough bathymetry over the continental rise and slope (Chase et al., 1987). From repeated hydrographic sections Rintoul (2007) has reported that the freshening of AABW has been increased from 1995 to 2005. Even though the observations are limited in the present study, an attempt has been made to compare the rate of freshening of AABW in the Indian Ocean sector of Southern Ocean (IOSSO) with the previously published results.

* Corresponding author. Tel.: +918322525636; fax: +918322525512.
E-mail address: racheal@ncaor.gov.in (R. Chacko).

http://dx.doi.org/10.1016/j.dsr2.2015.03.009
0967-0645/

2. Data and methods

To have an understanding of the freshening trend in AABW in the IOSSO three model data products over a period of 10 years were analysed. They are University of Reading (Reading, UK) UR025.4 reanalysis (Valdivieso and Haines, 2011), ECMWF ORAS4.0 (Balmaseda et al., 2013) reanalysis and SODA (Zheng and Giese, 2009) reanalysis. Among these the ECMWF (ORAS4,) reanalysis data showed a decrease in the AABW salinity and hence this data set was used. The ORAS4 uses the NEMO V 3.0, in the ORCA1 configuration (approximately $1\times1^\circ$ with equatorial refinement) and gives data from 42 levels in the vertical, 18 of which are in the first 200 m (http://apdrc.soest.hawaii.edu/). Reanalysis provides a physical picture of the global climate over a period during which observational data are available. This makes it possible to minimize the information gaps in spatial and temporal coverage in data sparse regions especially the SO. Temperature and salinity data collected during the expedition to the IOSSO in the austral summer of 2010 along 57°30′E was also used to substantiate the freshening of AABW observed in the model data results. A portable CTD (Make: SBE 19 plus SEACAT profiler with accuracy: temperature ±0.001 °C, conductivity ±0.0001 S/m and depth $\pm0.005\%$ of full scale) was used for water column profiling. Two full depth stations >4500 m located south of 60°S (62°S and 64°S) were chosen to study the changes associated with AABW (Fig. 1). These locations lie in an area which is relatively poorly sampled as compared to other areas around Antarctica. The sampling region has the outer eastern limb of the Weddell gyre on the west, the Prydz Bay gyre on the east and the Antarctic Coastal Current to the south. Also, in this region, the Antarctic Circumpolar Current (ACC) and its southern fronts, i.e. the southern ACC front (SACCF) and Southern Boundary (SB), are forced southward by the Kerguelen Plateau. This makes the IOSSO an interesting region to study the freshening in AABW. The hydrographic data at 61°48′S 57°30′E from the WOCE S041 line 2006 was also used to compare the changes observed in AABW. In the present study, signatures of AABW was identified with following characteristics, $-0.3<\theta<0$, $28.26<\gamma_n<28.36$. The positions of Weddell gyre (near to Weddell Sea in the west), Prydz Bay gyre (near to Cape Darnley in the east) and Antarctic coastal currents are also shown in Fig. 1.

Based on the in-situ data an approximate estimate was made to understand the annual fresh water input per unit area in the study region by using the equation for conservation of salt $[\rho_1 S_1 H=\rho_2 S_2(H+F)]$, where ρ is density of seawater, S is the average salinity in a layer of thickness H, F is the height of freshwater added or removed per unit area, and the subscripts refer to observations at two time periods. In addition to the above data sets, long term changes in the sea surface temperature (SST), air temperature, wind and sea ice concentration were studied using ICOADS data sets ($1\times1^\circ$) and Hadley Centre sea ice data set version 1 (HadISST1) ($1\times1^\circ$). The Southern Annular Mode (SAM) and Multivariate Enso Index (MEI) (http://www.esrl.noaa.gov/psd/data/climateindices/list) were used to understand the long term variability of SAM and ENSO.

3. Results and discussion

3.1. Freshening of AABW in model and in-situ data

Analysis of the ORAS4 (Fig. 2) showed that from 1995 to 2009, the potential temperature changed from -0.573 to -0.589 °C while the salinity varied from 34.658 to 34.657. Potential temperature, overall

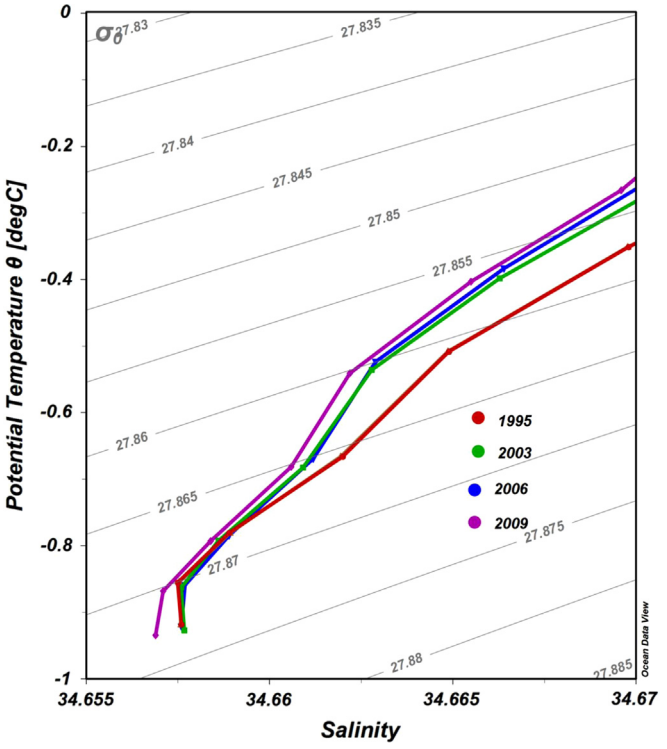

Fig. 2. θ–S plot showing the freshening of AABW from 1995 to 2009 using model data (ECMWF (ORAS4)).

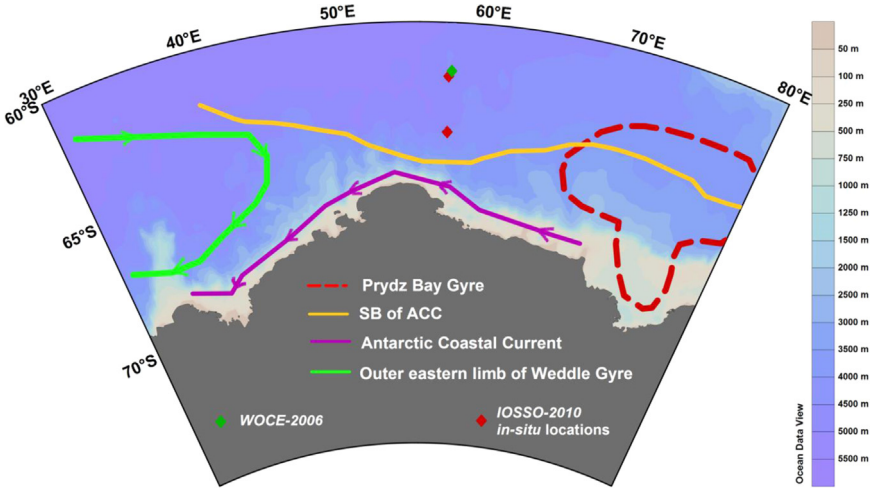

Fig. 1. Schematic representation of the general circulation (Williams et al., 2010) of the study area. Red and green dots represent Southern Ocean Expedition 2010 and WOCE 2006 location, respectively. (For interpretation of the references to color in this figure legend, the reader is referred to the web version of this article.)

Please cite this article as: Anilkumar, N., et al., Freshening of Antarctic Bottom Water in the Indian Ocean sector of Southern Ocean. Deep-Sea Res. II (2015), http://dx.doi.org/10.1016/j.dsr2.2015.03.009

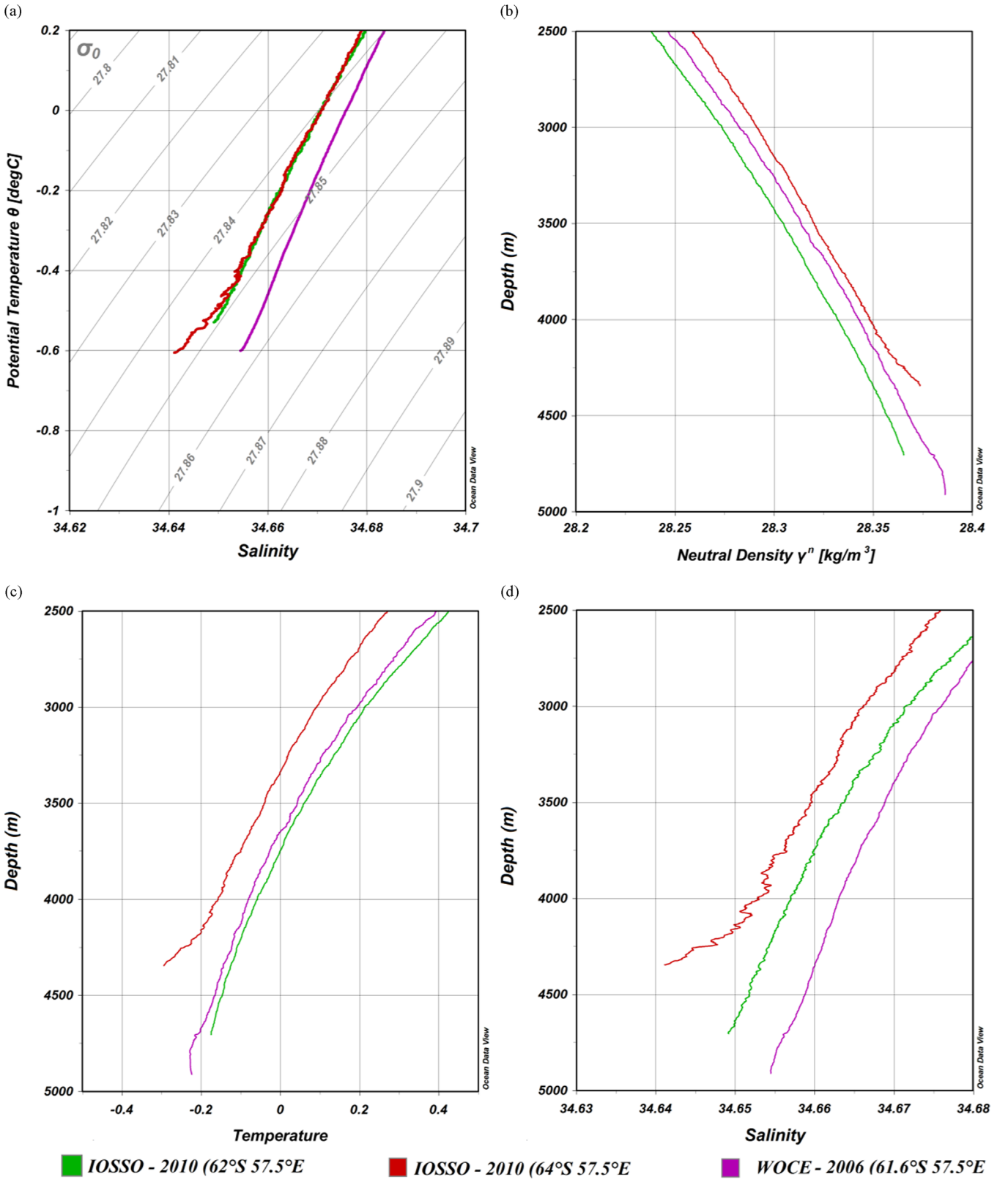

Fig. 3. Comparison between IOSSO Expedition 2010 (IOSSO-10) and WOCE 2006 (a) θ-S plot showing the presence of AABW (b) vertical structure of neutral density (c) vertical structure of temperature (d) vertical structure of salinity.

showed an increasing (warming) trend and salinity showed a decreasing trend (freshening). As compared to 1995, the temperature increased by 0.003 °C in 2006 but from 2006 to 2009 the change in temperature was by 0.017 °C. Similarly decrease in salinity was negligible from 1995 to 2006 but from 2006 to 2009, salinity decreased by 0.001. In-situ data from a point location (62°S 57°30′E) were taken and the *T–S* distribution has been plotted to observe the variability in AABW for two years 2006 and 2010. AABW was identified at depths > 3026 m at 62°S 57° 30′E and > 2748 m at 64°S57° 30′E (Fig. 3). AABW exhibited a freshening of ~0.01 below

Please cite this article as: Anilkumar, N., et al., Freshening of Antarctic Bottom Water in the Indian Ocean sector of Southern Ocean. Deep-Sea Res. II (2015), http://dx.doi.org/10.1016/j.dsr2.2015.03.009

Table 1
Characteristics of AABW.

Region		Temperature [°C]	Salinity	Neutral density [kg/m^3]
Weddell Sea (Jullion et al., 2013)	Lighter AABW	$-0.7 < \theta < 0$	$34.665 < S < 34.67$	$28.26 < \gamma^n < 28.31$
	Denser AABW	$\theta < -0.07$	$S < 34.64$	$\gamma^n > 28.31$
Cape Darnley (Couldrey et al., 2013)		$-0.7 < \theta < -0.6$	$S < 34.64$	$\gamma^n > 28.27$

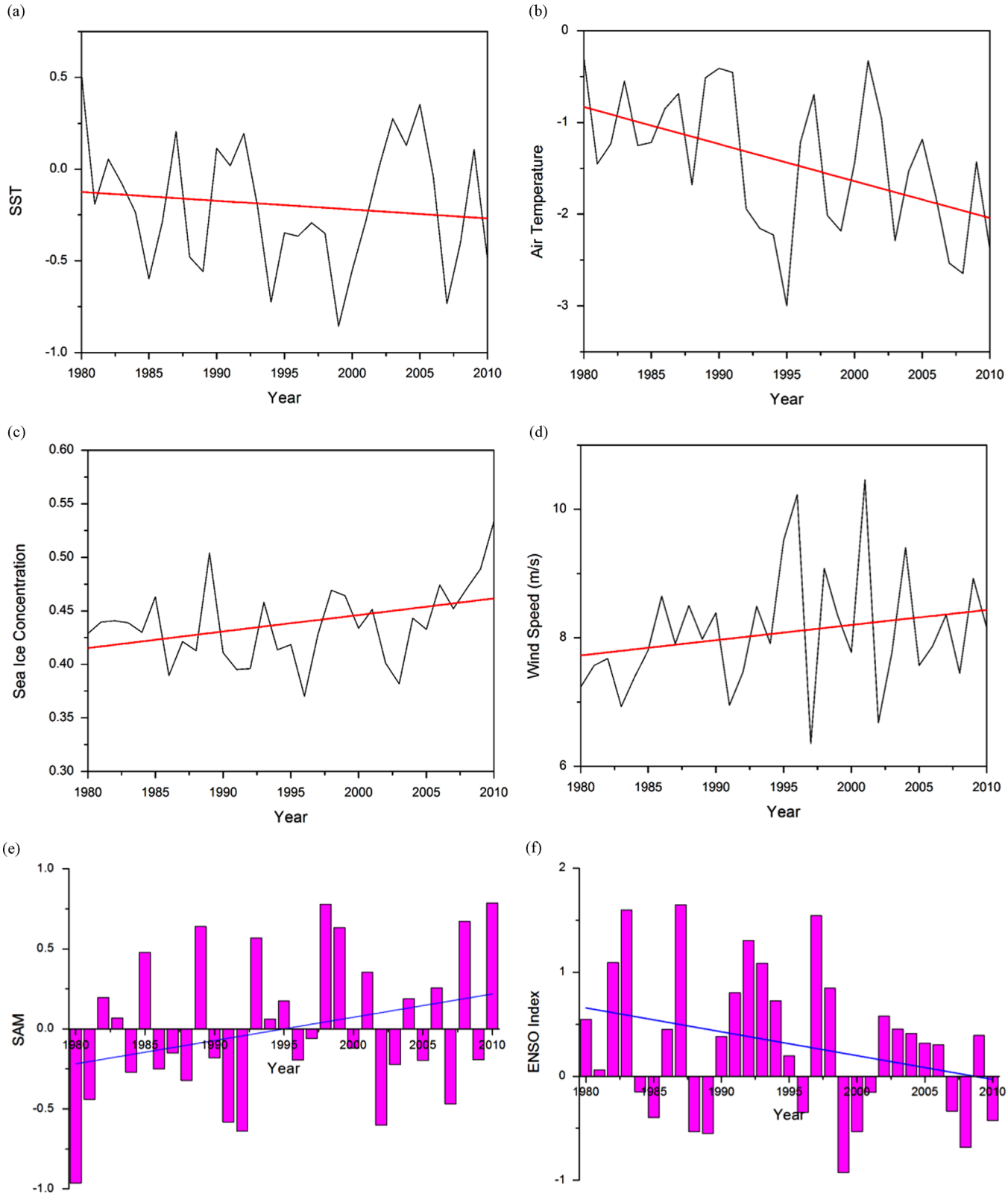

Fig. 4. Long term annual mean of (a) SST (b) Air temperature (c) sea ice concentration (d) wind speed (e) Sam index and (f) ENSO index.

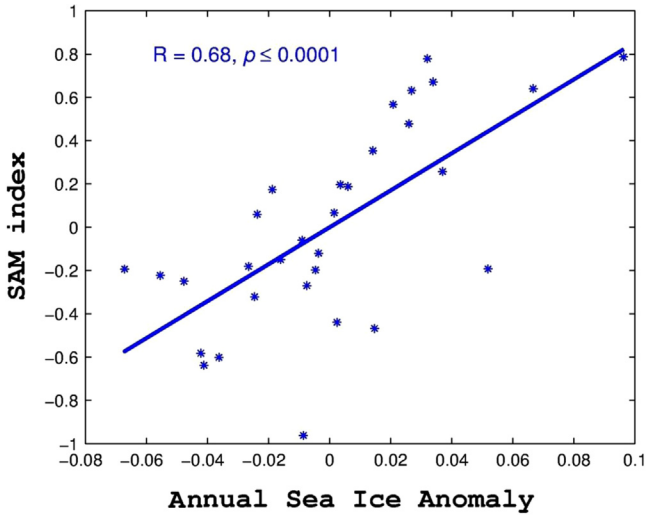

Fig. 5. Correlation between SAM index and annual sea ice anomaly.

3500 m at 62°S in 2010 compared to that in 2006 and the AABW became lighter by 0.01 kg m^{-3} from 2006 to 2010 (Fig. 3a and b). The temperature profiles showed warming of ~0.04 °C below 4500 m depth during the same period (Fig. 3c).

During 2010 observation, the near bottom salinity at 62°S and 64°S along 57°30′E were ~34.647 and ~34.636 (Fig. 3d). AABW was observed to be nearly isohaline with salinity between ~34.675 and ~34.670 during 1990 which was warmer than that observed in 1971, and further in 2005, it was warmer, fresher and less dense than that observed in the mid-1990s (Rintoul, 2007). These studies indicate that the decadal decrease of salinity was negligible from 1970s to 1990s, however from 1990s to 2005, it decreased by ~0.01. In the present investigation, a higher degree of decrease in salinity (~0.01) from 2006 to 2010 was exhibited by the in-situ data collected from the IOSSO (Fig. 3d). As mentioned earlier, the previous studies using in-situ data have reported that the rate of freshening between 1995 and 2005 (~0.01) was greater than that observed between 1970 and 1995 (~0.005). In the present investigation, the observations made during the period between 2006 and 2010 exhibited that the AABW became warmer (~0.05 °C), fresher (~0.01) and lighter (~0.01 kg m^{-3}) with a higher rate of freshening compared to the earlier observations. In the present study both the model and in-situ data portrayed the freshening of AABW however the model data underestimated the degree of freshening compared to in-situ data.

Jacobs et al. (2002) and Shepherd et al. (2004a, 2004b) reported the freshening of Ross Sea shelf waters of 46 Gt a^{-1} because of inflow of melt from glaciers to the east. In the Australian Antarctic Basin (80°E to 140°E), freshening observed between 1995 and 2005 was 13 ± 5 Gt a^{-1} (Rintoul, 2007). In the present study, the height of fresh water added per unit area computed at 62°S for 500 m thickness (4000–4500 m) between 2006 and 2010 was 2.2 cm a^{-1}. This value reflects the influence of additional freshwater supply from external sources that may be one of the probable reasons for the freshening of AABW observed in the study region. The characteristics of AABW observed in the present study are comparable with the AABW reported from the Weddell Sea and Cape Darnley (Table 1). Hence the signatures of AABW observed in the present investigation could be attributed to the AABW originated from Cape Darnley or Weddell Sea.

3.2. Source and probable causes of AABW freshening

Cape Darnley polynya (CDP): The CDP, between 65°E and 69°E located northwest of the Amery Ice Shelf, has the second highest ice production around Antarctica after the Ross Sea Polynya (Tamura et al., 2008) and more melt water can be expected from this region. Rintoul (2007) has attributed the freshening of dense water formed in both hemispheres to the high latitude freshwater balance and the rapid transmission of these changes in surface climate into the deep ocean. The most likely cause of the freshening is an increase in the influence of melt water from continental ice (Jacobs, 2006). To understand the influence of surface climatic indices into the deep ocean, long term SST, wind, air temperature, SAM and ENSO from1980 to 2010 were analyzed in the region between 60°–67°S and 40–80°E.

The yearly average of SST and air temperature exhibited a decreasing trend from 1980 to 2010 (Fig. 4a & b) whereas the sea ice concentration and wind (Fig. 4c & d) portrayed an increasing trend for the same period. In previous studies (Marshall et al., 2004; Thompson and Solomon, 2002) they have reported that the westerly winds at high southern latitudes are strengthened with poleward shift over the past thirty years due to the positive trend in the SAM. This causes a southward shift and strengthening of the Antarctic Circumpolar Current (ACC), stronger northward Ekman transport and upwelling of relatively warm deep water (Hall and Visbeck, 2002). Jullion et al. (2013), Martinson (2012) reported that that across a wide sector of the Southern Ocean there has been a marked freshening of the shelf and bottom waters is attributed to accelerated glacial melt in response to a southward shift and further greater flux of warm waters from the ACC onto the shelves of West Antarctica.

In the present study, the SAM index and the sea ice concentration over the last 30 years exhibited a positive trend (Fig. 4c & e). For the Indian Ocean sector, south of 55°S positive correlations have been found between the SAM index and surface salinity (Lefebvre et al., 2004) and sea ice extent (Rayner et al., 2003). A strong positive correlation was portrayed between annual sea ice concentration anomaly and SAM index (Fig. 5). Studies have also shown that ENSO variability can be related to sea-ice extent in the Southern Indian Ocean, as well as the speed and variability of the ACC (Carleton, 2003). Stammerjohn et al. (2008) have reported the positive relation between the La Nina and sea ice concentration around Antarctica. Long term MEI index showed an increasing occurrence of strong La Nina events on a global scale since 1995 (Fig. 4f),which may be another possible reason for the increase in sea-ice concentration around Antarctica. Accelerated basal melting of Antarctic ice shelves is likely to have contributed significantly to sea-ice expansion (Bintanja et al., 2013) and the further melting of this sea ice may cause the freshening of AABW.

Widespread warming of AABW since 1980 across much of the global ocean abyss has been reported by Purkey and Johnson (2010, 2012). In the earlier studies (Jacobs et al., 2002; Rintoul, 2007; Jacobs and Giulivi, 2010) it has been reported that in the Ross Sea and off Adélie Land the AABW formed had freshened by ~0.01 between the late 1960s and 1990s, but between the mid-1990s and the mid-2000s the freshening was ~0.03 (Aoki et al., 2005; Rintoul, 2007). The degree of freshening indicated by the in-situ data in IOSSO during this study was higher (~0.01 in four years) compared to the freshening observed from 1990 to 2005 (~0.01 in 15 years) by Rintoul (2007). This increase in the rate of freshening has not been reported in the IOSSO so far. Mass loss of ice sheet in Antarctica by enhanced basal melting linked to shelf water freshening could be the reason for the freshening of AABW (Jacobs et al., 2002; Jacobs and Giulivi, 2010; Pritchard et al., 2012). Indeed, the nearby CDP was reported as a significant source of new bottom water, contributing of Atlantic sector AABW production, although the role of the Amery Ice Shelf could not be dismissed (Ohshima et al., 2013). The eastward flow pattern exhibited in this study for 1000 m depth (Fig. 6a) and 4000 m depth (Fig. 6b) indicate the influence of AABW of CDP origin to the IOSSO region.

Please cite this article as: Anilkumar, N., et al., Freshening of Antarctic Bottom Water in the Indian Ocean sector of Southern Ocean. Deep-Sea Res. II (2015), http://dx.doi.org/10.1016/j.dsr2.2015.03.009

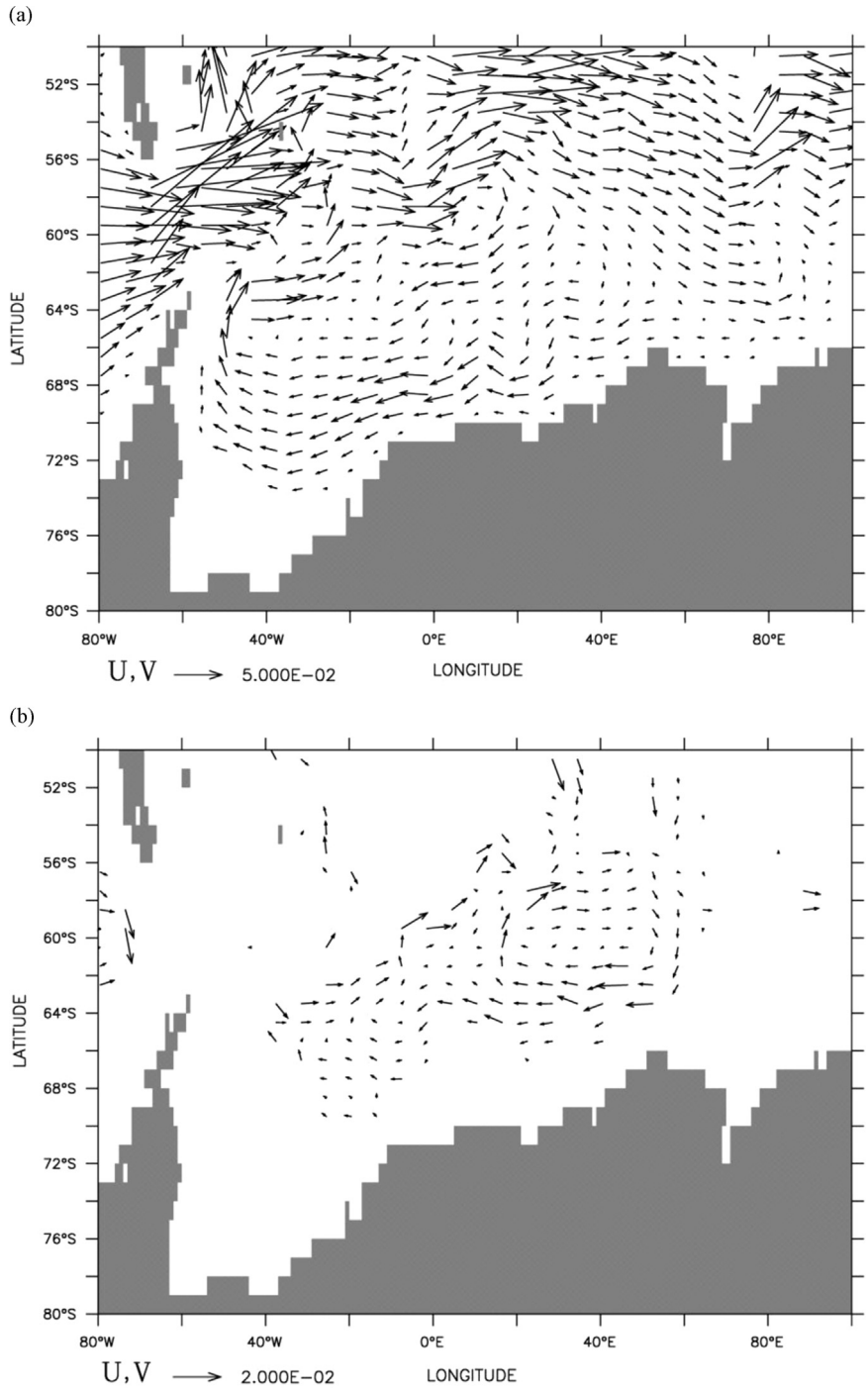

Fig. 6. Current pattern (a) 1000m depth and (b) 4000m depth.

Weddell Sea (WS): The WS is a deep embayment of the Antarctic coastline that forms the southernmost tip of the Atlantic Ocean. Centering at about 73°S, 45°W, the WS is bounded on the west by the Antarctic Peninsula of West Antarctica, on the east by Coats Land of East Antarctica, and on the extreme south by frontal barriers of the Filchner and Ronne ice shelves. The WS is one of the few places in the World Ocean where deep and bottom water masses participating in the global thermohaline circulation are formed. Weddell Gyre (WG), the large-scale horizontal circulation in the WS, is one of the most conspicuous circulation features of the Antarctic Zone of the Southern Ocean. To the south and to the west, the WG is bounded by the Antarctic continent and the Antarctic Peninsula. The ridge system north of 55°S, which consists of the South Scotia, North Weddell and Southwest Indian Ridge, forms the approximate northern boundary. WG extends as far as about 30°E into the Enderby Basin (Deacon, 1937; Gouretski and Danilov, 1993), where the water mass transition between the WG and the ACC bends southwards and approaches the Antarctic continent as close as a few hundred kilometers (Orsi et al., 1993).

Previous studies have reported that the seawater density modification through air–sea-ice interactions near the Antarctic margins plays a role in the formation of AABW (Orsi et al., 1999). Interactions between ocean, atmosphere and cryosphere in the margins of Antarctica, often determine the characteristics of AABW, are very sensitive to the climatic changes occurring in the region (Foster and Carmack, 1976; Gill, 1973; Orsi et al., 1999; Jacobs, 2004; Nicholls et al.,

Please cite this article as: Anilkumar, N., et al., Freshening of Antarctic Bottom Water in the Indian Ocean sector of Southern Ocean. Deep-Sea Res. II (2015), http://dx.doi.org/10.1016/j.dsr2.2015.03.009

2009). West of 30°W, Warm Deep Water (WDW) interacts with the dense shelf waters off the Filchner–Ronne Ice Shelf (Whitworth et al., 1998) that are made saline by brine rejection during sea ice formation results in AABW formation (Killworth, 1974; Carmack and Foster, 1975; Foldvik et al., 2004; Wilchinsky and Feltham, 2009; Jullion et al., 2013). Although the Filchner–Ronne Ice Shelf have been traditionally regarded as the principal source region of AABW in the WS, significant AABW production has been reported off the eastern Antarctic Peninsula, particularly near the Larsen Ice Shelf (Fahrbach et al., 2011; Weppernig et al., 1996; Gordon, 1998). Accelerated melting of the ice shelves of West Antarctica may be the origin of freshening trend in the Indo-Pacific sector of the Southern Ocean (Shepherd et al., 2004a, 2004b; Rintoul, 2007; Jacobs et al., 2002; Jacobs and Giulivi, 2010), where the warm water brought by ACC flood the coastal areas of the continent (Thoma et al., 2008; Jacobs et al., 2011). Jullion et al. (2013) suggested that the increased glacial loss from the Larsen ice shelves is likely to be a significant player in the freshening of AABW exported from the WS. Previous studies (Jullian et al., 2013; Thomson and Solomon, 2002; van den Broeke, 2005; Marshall et al., 2006) indicated that the summer time intensification of westerly winds over SO leads to advection of warm maritime air to eastern side of Antarctica peninsula and further increase in air temperature during summer resulting the glacier melting.

The current pattern at 4000 m depth levels from the model data showed a cyclonic circulation pattern between 40°W and 60°E indicates the influence of WS waters in the study area. The flow of water from the west (WS region) by the eastwards flowing currents (Fig. 6b) also could be one of the causative factors affecting the freshening of AABW observed in the study region.

Hence the signatures of the AABW observed in the present study could be of WS and CDP origin. To substantiate these results more long term observations are required to be carried out in the IOSSO region in future.

4. Conclusion

Studies of southern hemisphere climate variability have been severely hampered by the lack of sustained observations. The monotonic freshening of AABW reported in earlier studies and the fact that a consistent signal observed in the decline of salinity in the present and previous studies support the argument that the changes described here reflect a sustained freshening of the bottom water. Earlier studies reported that the rate of freshening between 1995 and 2005 (~0.01) is greater than that observed between 1970 and 1995 (~0.005). The results obtained from the in-situ data corroborate with the model data, exhibited an increased rate of freshening in the period 2006–2010. Swifter freshening in the same direction from 2006 to 2010 has been portrayed in the present study and in the same period the AABW became warmer (~0.05 °C) and lighter (~0.01 kg m^{-3}). The height of fresh water added per unit area computed was 2.2 cm a^{-1}. The increased fresh water input may be attributed to melting of ice shelves as well as changes observed in sea-ice formation, sea surface temperature and climatic indices. Earlier reports suggested that the causes for the freshening of dense water could be the freshwater balance and rapidly transmitting signature of changes in surface climate into the deep ocean. The AABW observed in the present investigations shall be attributed to both the WS and CDP origin. The hydrographic data used here is inadequate to distinguish between a trend and high frequency variability in the freshening of AABW. However an understanding of the global overturning circulation and its response to changes in forcing require an observing system that provides sustained measurements of the main pathways of the overturning circulation in both hemispheres.

Acknowledgement

The authors are thankful to Ministry of Earth Sciences, Government of India for all support provided to implement this programme. They are thankful to Director, NCAOR for his constant support and encouragement. The suggestions given by Dr. C. T. Achuthankutty are acknowledged. Help rendered in the implementation and completion of this study by all SO group members of NCAOR and all cruise participants is acknowledged. This is NCAOR contribution no **07/ 2015**

References

Aoki, S., Rintoul, S.R., Ushio, S., Watanabe, S., Bindoff, N.L., 2005. Freshening of the Adélie Land Bottom Water near 140°E. Geophys. Res. Lett. 32, L23601. http://dx.doi.org/10.1029/2005GL024246.

Balmaseda, M.A., Mogensen, K., Weaver, A.T., 2013. Evaluation of the ECMWF ocean reanalysis system ORAS4. Q. J. R. Meteorolog. Soc. 139, 1132–1161. http://dx.doi.org/10.1002/qj.2063.

Bintanja, R., van Oldenborgh, G.J., Drijfhout, S.S., Wouters, B., Katsman, C.A., 2013. Important role for ocean warming and increased ice-shelf melt in Antarctic sea-ice expansion. Nat. Geosci. 6, 376–379. http://dx.doi.org/10.1018/NGEO1767.

Carleton, A.M., 2003. Atmospheric teleconnections involving the Southern Ocean. J. Geophys. Res. 108, 8080. http://dx.doi.org/10.1029/2000JC000379, C4.

Carmack, E., Foster, T., 1975. Flow of water out of the Weddell Sea. Deep Sea Res. 22, 711–724.

Chase, T.E., Seekins, B.A.,Young, J.D., Eittrim,S.L., 1987. Marine topography of offshore Antarctica. In: The Antarctic Continental Margin: Geology and Geophysics of Offshore Wilkes Land, Earth Sci. Ser., (Eds.), S. L. Eittrim and M. A. Hampton, CircumPac. Counc. for Energy and Miner. Resour., Houston, TX, vol. 5A, pp. 147–150.

Couldrey, M.P., Jullion, L., Naveira Garabato, A.C., Rye, C., Herráiz-Borreguero, L., Brown, P.J., Meredith, M.P., Speer, K.L., 2013. Remotely induced warming of Antarctic Bottom Water in the eastern Weddell gyre. Geophys. Res. Lett. 40, 2755–2760. http://dx.doi.org/10.1002/grl.50526.

Deacon, G.E.R., 1937. The Hydrology of the Southern Ocean. Discovery Report 15, 1–24.

Dickson, B., Yashayaev, I., Meincke, J., Turrell, B., Dye, S., Holfort, J., 2002. Rapid freshening of the deep North Atlantic Ocean over the past four decades. Nature 416, 832–837.

Fahrbach, E., Hoppema, M., Rohardt, G., Boebel, O., Klatt, O., Wisotzki, A., 2011. Warming of deep and abyssal water masses along the Greenwich meridian on decadal time scales: the Weddell Gyre as a heat buffer. Deep Sea Res. II 58, 2509–2523. http://dx.doi.org/10.1016/j.dsr2.2011.06.007.

Foldvik, A, et al., 2004. Ice shelf water overflow and bottom water formation in the southern Weddell Sea. J. Geophys. Res. 109, C02015. http://dx.doi.org/10.1029/2003JC002008.

Foster, T.D., Carmack, E.C., 1976. Frontal zone mixing and Antarctic bottom water formation in the southern Weddell Sea. Deep-Sea Res. 23, 301–317.

Ganachaud, A., Wunsch, C., 2000. Improved estimates of global ocean circulation, heat transport and mixing from hydrographic data. Nature 408, 453–457.

Gill, A.E., 1973. Circulation and bottom water formation in the Weddell Sea. Deep-Sea Res. 20, 111–140.

Gordon, A.L., 1998. Western Weddell Sea thermohaline stratification. In: Jacobs, S.S., Weiss, R. (Eds.), Ocean, Ice and Atmosphere: Interactions at the Antarctic Continental Margin, vol. 75. Antarctic Research Series, AGU, Washington, DC, pp. 215–240.

Gouretski, V., Danilov, A.I., 1993. Weddell Gyre: structure of the eastern boundary. Deep-Sea Res. 40, 561–582.

Hall, A., Visbeck, M., 2002. Synchronous variability in the Southern Hemisphere atmosphere, sea ice, and ocean resulting from the annular mode. J. Clim. 15, 3043–3057.

Jacobs, S.S., Guilivi, C.F., Merle, P., 2002. Freshening of the Ross Sea during the late 20th century. Science 297, 386–389.

Jacobs, S.S., 2004. Bottom water production and its links with the thermohaline circulation. Antarct. Sci. 16 (4), 427–437.

Jacobs, S.S., 2006. Observations of change in the Southern Ocean. Philos. Trans. R. Soc., Ser. A 364, 1657–1681. http://dx.doi.org/10.1098/rsta.2006.1794.

Jacobs, S.S., Giulivi, C.F., 2010. Large multidecadal salinity trends near the Pacific-Antarctic continental margin. J. Clim. 23, 4508–4524. http://dx.doi.org/10.1175/2010JCLI3284.1.

Jacobs, S.S., Jenkins, A., Giulivi, C.F., Dutrieux, P., 2011. Stronger ocean circulation and increased melting under Pine Island Glacier ice shelf. Nat. Geosci. 4, 519–523. http://dx.doi.org/10.1038/ngeo1188.

Johnson, G.C., Purkey, S.G., Toole, J.M., 2008. Reduced Antarctic meridional overturning circulation reaches the North Atlantic Ocean. Geophys. Res. Lett. 35, L22601. http://dx.doi.org/10.1029/2008GL035619.

Johnson, G.C., 2008. Quantifying Antarctic Bottom Water and North Atlantic Deep Water volumes. J. Geophys. Res. 113, C05027. http://dx.doi.org/10.1029/2007JC004477.

Please cite this article as: Anilkumar, N., et al., Freshening of Antarctic Bottom Water in the Indian Ocean sector of Southern Ocean. Deep-Sea Res. II (2015), http://dx.doi.org/10.1016/j.dsr2.2015.03.009

Jullion, L., Garabato Naveira, A.C., Meredith, M.P., Holland, P.A., Courtois, P., King, B. A., 2013. Decadal freshening of waters exported from the Weddell Sea. J. Clim. 26, 8111–8125. http://dx.doi.org/10.1175/JCLI-D-12-00765.1.

Killworth, P., 1974. Baroclinic model of motions on Antarctic continental shelves. Deep Sea Res. 21, 815–837.

Lefebvre, W., Goosse, H., Timmermann, R., Fichefet, T., 2004. Influence of the Southern Annular mode on the sea ice-ocean system. J. Geophys. Res. 109, C09005. http://dx.doi.org/10.1029/2004JC002403.

Marshall, G.J., Stott, P.A., Turner, J., Connelly, W.M., King, J.C., Lachlan-Cope, T.A., 2004. Causes of exceptional atmospheric circulation changes in the Southern Hemisphere. Geophys. Res. Lett. 31, L14205. http://dx.doi.org/10.1029/2004GL019952.

Marshall, G.J., Orr, A., Van Lipzig, N.P.M., King, J.C., 2006. The impact of a changing Southern hemisphere annular mode on Antarctic Peninsula summer temperatures. J. Clim. 19, 5388–5404.

Marshall, J., Speer, K., 2012. Closure of the meridional overturning circulation through Southern Ocean upwelling. Nat. Geosci. , http://dx.doi.org/10.1038/ngeo1391.

Meehl, G.A., et al., 2007. In: Solomon, S., et al. (Eds.), In: IPCC Climate Change 2007: The Physical Science Basis. Contribution of Working Group I to the Fourth Assessment Report of the Intergovernmental Panel on Climate Change. Cambridge Univ. Press.

Meredith, M.P., et al., 2008. Evolution of the deep and bottom waters of the Scotia Sea, Southern Ocean, 1995–2005. J. Clim. 21, 3327–3343. http://dx.doi.org/10.1175/2007JCLI2238.1.

Martinson, D.G., 2012. Antarctic circumpolar current's role in the Antarctic ice system: an overview. Palaeogeogr. Palaeoclimatol. Palaeoecol. 335, 71–74.

Nicholls, K.W., Osterhus, S., Makinson, K., Gammelsrod, T., Fahrbach, E., 2009. Ice-ocean processes over the continental shelf of the southern Weddell Sea, Antarctica: a review. Rev. of Geophys. 47, RG3003.

Ohshima, K.I., et al., 2013. Antarctic Bottom Water production by intense sea-ice formation in the Cape Darnley Polynya. Nat. Geosci. 6, 235–240. http://dx.doi.org/10.1038/ngeo1738.

Orsi, A.H., Johnson, G.C., Bullister, J.L., 1999. Circulation, mixing, and production of Antarctic Bottom Water. Prog. Oceanogr. 43 (1), 55–109.

Orsi, A.H., Nowlin Jr., W.D., Whitworth III, T., 1993. On the circulation and stratification of the Weddell Gyre. Deep Sea Res., Part I 40, 169–203.

Orsi, A.J., Smethie Jr., W.M., Bullister, J.L., 2002. On the total input of Antarctic waters to the deep ocean: a preliminary estimate from chlorofluorocarbon measurements. J. Geophys. Res. 107, 3122. http://dx.doi.org/10.1029/2001JC000976.

Pritchard, H.D., Ligtenberg, S.R.M., Fricker, H.A., Vaughan, D.G., van den Broeke, M.R., Padman, L., 2012. Antarctic ice-sheet loss driven by basal melting of ice shelves. Nature 484, 502–505. http://dx.doi.org/10.1038/nature10968.

Purkey, S.G., Johnson, G.C., 2010. Antarctic Bottom Water warming between the 1990s and the 2000s: contributions to global heat and sea level rise budgets. J. Clim. , http://dx.doi.org/10.1175/2010JCLI3682.1.

Purkey, S.G., Johnson, G.C., 2012. Global contraction of Antarctic Bottom Water between the 1980s and 2000s. J. Clim. 25, 5830–5844. http://dx.doi.org/10.1175/JCLI-D-11-00612.1.

Rayner, N.A., Parker, D.E., Horton, E.B., Folland, C.K., Alexander, L.V., Rowell, D.P., Kent, E.C., Kaplan, A., 2003. Global analyses of sea surface temperature, sea ice, and night marine air temperature since the late nineteenth century. J. Geophys. Res. 108, 4407. http://dx.doi.org/10.1029/2002JD002670, D14.

Rintoul, S.R., 1998. On the origin and influence of Ade´lie Land Bottom Water, in Ocean, Ice, and Atmosphere: interactions at the Antarctic Continental Margin. In: Jacobs, S.S., Weiss, R.F. (Eds.), Antarct. Res. Ser, vol. 75. AGU, Washington, DC, pp. 151–171.

Rintoul, S.R., 2007. Rapid freshening of Antarctic Bottom Water formed in the Indian and Pacific oceans. Geophys. Res. Lett. 34, L06606. http://dx.doi.org/10.1029/2006GL028550.

Shepherd, A., Wingham, D., Rignot, E., 2004a. Warm ocean is eroding West Antarctic ice sheet. Geophys. Res. Lett. 31, L23402. http://dx.doi.org/10.1029/2004GL021106.

Sigman, D.M., Boyle, E.A., 2000. Glacial/interglacial variations in atmospheric carbon dioxide. Nature 407, 859–869.

Stammerjohn, S.E., Martinson, D.G., Smith, R.C., Yuan, X., Rind, D., 2008. Trends in Antarctic annual sea ice retreat and advance and their relation to ElNin~o–Southern Oscillation and Southern Annular Mode variability. J. Geophys. Res, 113, C03S90. http://dx.doi.org/10.1029/2007JC004269.

Stommel, H., Arons, A.B., 1961. On the abyssal circulation of the world ocean-I. Stationary planetary flow patterns on a sphere. Deep Sea Res. 6, 140–154.

Shepherd, A., Wingham, D., Rignot, E., 2004b. Warm ocean is eroding West Antarctic Ice Sheet. Geophys. Res. Lett. 31, L23402. http://dx.doi.org/10.1029/2004GL021106.

Tamura, T., Ohshima, K.I., Nihashi, S., 2008. Mapping of sea-ice production for Antarctic coastal polynyas. Geophys. Res. Lett. 35, L07606.

Thoma, M., Jenkins, A., Holland, D., Jacobs, S., 2008. Modelling circumpolar deep water intrusions on the Amundsen Sea continental shelf, Antarctica. Geophys. Res. Lett. 35, L18602. http://dx.doi.org/10.1029/2008GL034939.

Thomson, D.W., Solomon, S., 2002. Interpretation of recent Southern Hemisphere climate change. Science 296, 895–899.

Thompson, D.W.J., Solomon, S., 2002. Interpretation of recent Southern Hemisphere climate change. Science 296, 895–899. http://dx.doi.org/10.1126/science.1069270.

Valdivieso M., Haines, K., 2011. Scientific Validation Report (ScVR) for v1 Reprocessed Analysis and Reanalysis. GMES Marine Core Services Technical Report WP04-GLO-U-Reading_v1, 28 pp, March 2011.

van den Broeke, M., 2005. Strong surface melting preceded collapse of Antarctic Peninsula ice shelf. Geophys. Res. Lett. 32, L12815. http://dx.doi.org/10.1029/2005GL023247.

Weaver, A.J., Saenko, O.A., Clark, P.U., Mitrovica, J.X., 2003. Meltwater pulse 1A from Antarctica as a trigger of the Bølling–Allerød warm interval. Science , http://dx.doi.org/10.1126/science.1081002.

Weppernig, R., Schlosser, P., Khatiwala, S., Fairbanks, R.G., 1996. Isotope data from ice station Weddell: implications for deep water formation in the Weddell Sea. J. Geophys. Res. 101, http://dx.doi.org/10.1029/96JC01895.

Whitworth III, T., 2002. Two modes of bottom water in the Australian–Antarctic Basin. Geophys. Res. Lett. 29 (5), 1073. http://dx.doi.org/10.1029/2001GL014282.

Whitworth III, T., Orsi, A.H., Kim, S.-J., Nowlin Jr., W.D., Locarnini, R.A., 1998. Water masses and mixing near the Antarctic slope front. In: Jacobs, S.S., Weiss, R.F. (Eds.), Ocean, Ice, and Atmosphere: Interactions at the Antarctic Continental Margin, vol. 75. Antarctic Research Series, pp. 1–27.

Wilchinsky, A.V., Feltham, D.L., 2009. Numerical simulation of the Filchner overflow. J. Geophys. Res. 114, C12012. http://dx.doi.org/10.1029/2008JC005013.

Williams, G.D., Aoki, S., Jacobs, S.S., Rintoul, S.R., Tamura, T., Bindoff, N.L., 2010. Antarctic Bottom Water from the Adelie and George V Land coast, East Antarctica (140–149°E). J. Geophys. Res. 115, C04027. http://dx.doi.org/10.1029/2009JC005812.

Zheng, Y., Giese, B.S., 2009. Ocean heat structure in simple ocean data assimilation: structure and mechanism. J. Geophys. Res. 114, http://dx.doi.org/10.1029/2008JC005190.

Zenk, W., Morozov, E., 2007. Decadal warming of the coldest Antarctic Bottom Water flow through the Vema Channel. Geophys. Res. Lett. 34, L14607. http://dx.doi.org/10.1029/2007GL030340.

Please cite this article as: Anilkumar, N., et al., Freshening of Antarctic Bottom Water in the Indian Ocean sector of Southern Ocean. Deep-Sea Res. II (2015), http://dx.doi.org/10.1016/j.dsr2.2015.03.009

New Zealand Journal of Marine and Freshwater Research, 2014
http://dx.doi.org/10.1080/00288330.2014.924972

Taylor & Francis
Taylor & Francis Group

RESEARCH ARTICLE

Variability of fronts, fresh water input and chlorophyll in the Indian Ocean sector of the Southern Ocean

N Anilkumar*, JV George, R Chacko, N Nuncio and P Sabu

National Centre for Antarctic and Ocean Research, Vasco Da Gama, India

(*Received 3 April 2013; accepted 30 April 2014*)

The aim of this study was to understand the variability in the fronts and water masses, and the effect of melt water on the concentration of chlorophyll (Chl *a*) in the Indian Ocean sector of the Southern Ocean using hydrographic data collected during the austral summer (February 2010 and 2011). The Southern Subtropical Front (SSTF) and Northern Sub Antarctic Front (SAF1) were found to be further south at 57°30′E than at 47–48°E. This southward shift of the fronts was consistent with the southward meandering (c. 2°) of the Antarctic Circumpolar Current (ACC) core from the western section to the eastern section, which could have been caused by the bottom topography. The intrusion of water masses also differed between the western and eastern transects of the study region as a result of the meandering of the ACC core. Fresh water layer thickness relative to the winter water in 2011 was more compared to that during 2010. This could have been due to the larger amount of sea ice that was present in the winter of 2010, which subsequently melted, resulting in the advection of melt water from the south and west of the study region. In situ observations and satellite data detected a high Chl *a* concentration (c. 0.38 mg m^{-3}) south of the Northern Polar Front (PF1) in 2011, which was caused by this melt water.

Keywords: Argo floats; geostrophic currents; Indian sector of Southern Ocean; oceanic fronts; water masses

Introduction

The Indian Ocean sector of the Southern Ocean (SO) has a complicated quasi-zonal frontal system that has remarkable regional differences determined by peculiarities of the bottom topography (Kostianoy et al. 2004) and variability of the Agulhas Return Current (ARC) (Belkin & Gordon 1996). The intensity of these fronts (as measured by the meridional property gradients) varies, and the individual branches often merge and diverge in response to interactions with the bathymetry (Sokolov & Rintoul 2007a, 2009a). Together, these frontal systems form the eastward-flowing Antarctic Circumpolar Current (ACC), the inter-basin connectivity of which allows water masses, heat and climatic anomalies to propagate between the ocean basins (Rintoul et al. 2001). The ACC is characterised by a high degree of eddy activity, largely as a result of the dynamic instability of the frontal systems (Stammer 1998; Hughes 2005). Further, it is composed of many jets and high-speed filaments (Sokolov & Rintoul 2007a; Lenn et al. 2011), which are often marked by ocean fronts where the thermohaline properties change rapidly with latitude. The ACC plays a major role in the climate system (Gordon 1986; Rintoul 1991; Speich et al. 2001), making it imperative that we have a detailed understanding of the fronts flowing across it.

The Agulhas Return Front (ARF), which is associated with the Agulhas retroflection, merges with the Subtropical Front (STF) in some parts of

*Corresponding author. Email: anil@ncaor.gov.in

the Indian Ocean (Lutjeharms & Ansorge 2001). The STF marks the boundary between subtropical and subantarctic waters (Deacon 1937; Hamilton 2006), and lies between 35°S and 45°S. Further south, the major ACC fronts are the Subantarctic Front (SAF), Polar Front (PF), Southern ACC Front (SACCF) and southern boundary of the ACC (SB). Since the ACC is a deep-reaching barotropic current, the fronts across it also extend through the water column (Belkin & Gordon 1996; Meijers et al. 2010). Earlier studies have investigated the concurrence of frontal positions across the ACC using maps of absolute dynamic topography (MADT) and in situ hydrographic data (Sokolov & Rintoul 2007a; Swart et al. 2008; Sokolov & Rintoul, 2009a, b; Swart & Speich 2010). Jasmine et al. (2009) found that the fronts and zones in the ACC exhibit wide differences in hydrographic as well as biological characteristics. Previous studies have also highlighted the significance of the Crozet Plateau, where the fronts join to form one of the strongest oceanic frontal systems in the world (Orsi et al. 1995; Belkin & Gordon 1996; Sparrow et al. 1996; Holliday & Read 1998; Kostianoy et al. 2004).

Another important feature of the SO during the austral summer is the presence of winter water (WW), which is the remnant of the mixed layer of the previous winter capped by seasonal warming and freshening (Deacon 1937). The SO is characterised by a temperature minimum subsurface layer in the upper 300 m (Park et al. 1998). During the ice-free period, the ocean surface is exposed to winds, which enhances mixing, resulting in this temperature minimum layer becoming mixed with the surface and subsurface layers, thereby altering the heat budget of the region (Yuan et al. 2004). Since the WW has a close relationship with the heat budget, ice melt and freshening in the SO is believed to be a major source of micronutrients (Boyd & Ellwood 2010), and may regulate the chlorophyll (Chl *a*) blooms in the region. The study of WW also has climatic relevance.

In this study, we investigate the inter-annual variability in the fronts, the north–south intrusion of water masses from the subtropics to the coastal waters of Antarctica and the role of melt water in enhancing the Chl *a* concentration in the Indian Ocean sector of the SO. The frontal positions are compared using MADT, satellite SST and in situ hydrographic data, and the influence of the ACC on frontal variability has been delineated. Further, the sources of fresh water input into the study area and its influence on variations in Chl *a* concentrations across the ACC, as well as in the coastal waters of Antarctica, are discussed.

Data and methods

This study used hydrographic measurements taken from the Indian Ocean sector of the SO during the austral summers (February) of 2010 and 2011. In both years, expeditions were made onboard the Oceanographic Research Vessel *Sagar Nidhi* (ORV-SN), which launched from Mauritius. During 2010, observations were made from 40°S 57° 30′E to the coastal waters of Antarctica (65°27′S 53°28′E), and were then continued along a track between 65°27′S and 40°S, and between 53°28′E and 48°E (hereafter referred to as Track-1; see Fig. 1A). During 2011, observations were made from 40°S to 60°S along the meridional section 57°30′E, and from 60°S to 40°S along the meridional section 47°E.

During both expeditions, a CTD (Sea-Bird Electronics, USA; temperature: ± 0.001 °C; conductivity: ± 0.0001 S m^{-1}; and depth: ± 0.005% of the full scale) and XCTDs (Tsurumi-Seiki Co. TSK Ltd, Yokohama, Japan; type: XCTD-3; temperature: ± 0.02 °C; conductivity: ± 0.03 mS cm^{-1}; and depth: ± 2%) were deployed to collect the temperature and salinity profiles. XCTD probes were launched at c. 30 nautical mile intervals between the CTD stations. The station locations for CTD and XCTD operations during 2010 and 2011 are shown in Fig. 1A and B, respectively. The XCTD profiles were quality controlled by following the guidelines in the CSIRO Cookbook (1993). The salinity data from the CTD were calibrated against water samples analysed using a high-precision salinometer (Guildline AUTOSAL).

Oceanic fronts were identified using the characteristic property indicators following the criteria listed by Belkin & Gordon (1996), Sparrow et al. (1996), Holliday & Read (1998), Kostianoy et al.

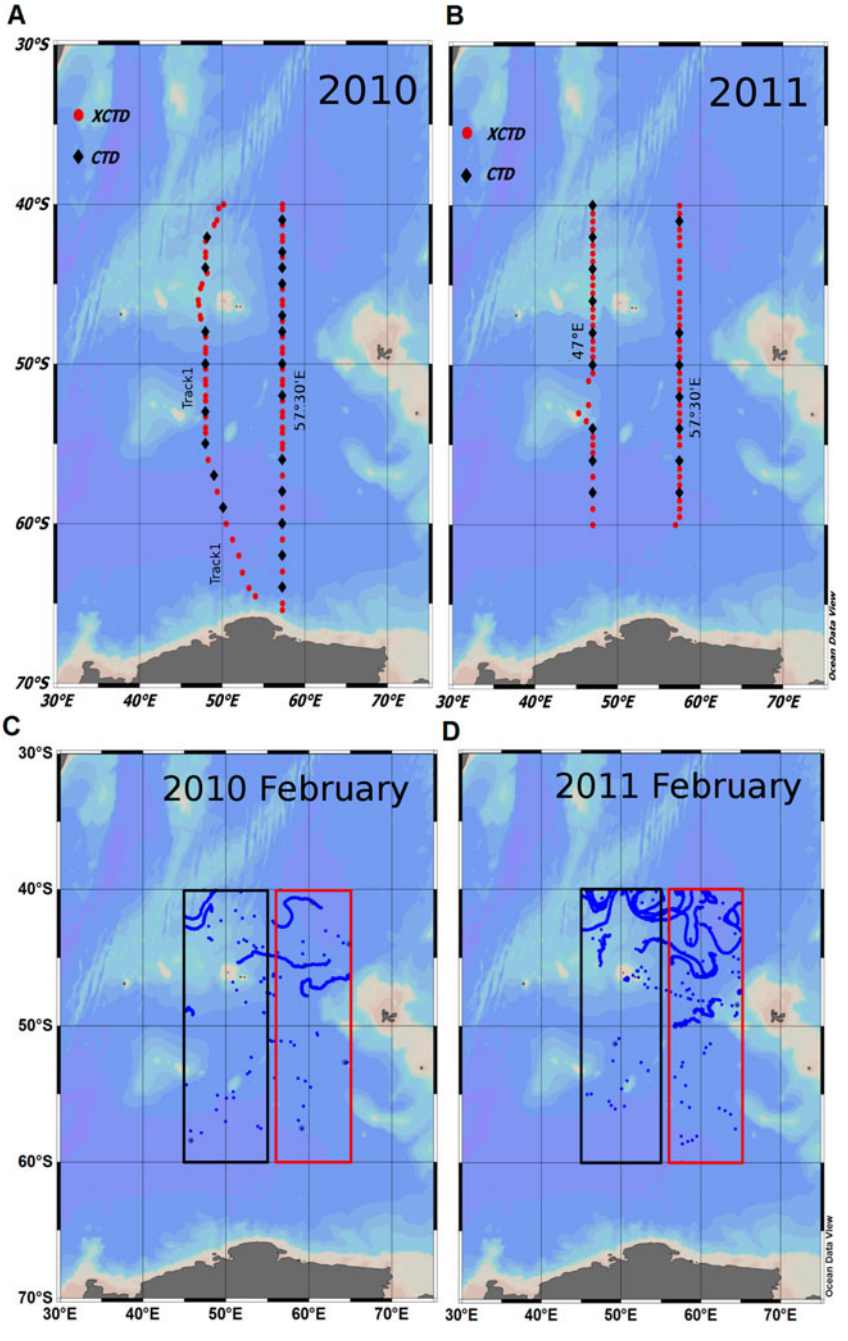

Figure 1 CTD/XCTD locations in **A**, February 2010 and **B**, February 2011; and Argo locations in **C**, February 2010 and **D**, February 2011.

(2004), and Billany et al. (2010). The properties that were used to identify fronts in the study area are provided in Table 1. In addition, MADT from CLS/AVISO and monthly SSTs from the Group for High Resolution Sea Surface Temperature (GHRSST) on 1/4° grids (http://podaac.jpl.nasa.gov/dataset/NCDC-L4LRblend-GLOB-AVHRR_AMSR_OI) were also used to identify the fronts in the study region. The thickness of the fresh water input in the surface layer relative to the WW in the study region was estimated using the formula of Park et al. (1998):

$$h = \frac{D_C(S_W - S^{\text{bar}})}{S_W}, S^{\text{bar}} = \frac{1}{D_C}\left[\int_{-D_C}^{0} Sdz\right], \quad (1)$$

where h is the thickness of the fresh water input per unit surface area, D_c is the WW depth, S_w is the WW salinity, and S^{bar} is the depth-averaged salinity between the surface and WW depth. Surface ocean currents were plotted using Ocean Surface Current Analysis–Realtime data (OSCAR, http://www.oscar.noaa.gov) (Bonjean & Lagerloef 2002). Monthly ASCAT wind stress, Ekman current, MODIS Aqua photosynthetically available radiation (PAR) and AMSR-E ice coverage data from ERDDAP were used in the present study. The Argo data during February 2010 and February 2011 from the Coriolis Data Center (http://www.coriolis.eu.org/cdc) were also used. The locations of the Argo floats that were used during February 2010 and 2011 are shown in Fig. 1C and D, respectively. The western box is over the southwest Indian ridge centred at 50°E and the eastern box is over a flat-bottomed deep region centred at 60°E.

Results and discussion

Frontal system variability

The temperature and salinity structures derived from the CTD/XCTD data collected during 2010 along Track-1 are shown in Fig. 2A and B. No signature of the northern branch of the Subtropical Front (NSTF) was noticed along this track, which is not surprising given that the NSTF is always

Table 1 Properties used for the identification of various fronts in the study area.

Front	Temperature	Salinity
Northern Subtropical Front (NSTF)	21–22 °C at surface	surface salinity c. 35.5
Agulhas Return Front (AF)	19–17 °C at surface; 10 °C isotherm from 300 to 800 m	35.54–35.39 at surface; 35.57–34.90 at 200 m
Southern Subtropical Front (SSTF)	17–11 °C at surface; 12–10 °C at 100 m	35.35–34.05 at surface; 35–34.6 at 100 m; 34.92–34.42 at 200 m
Subantarctic Front (SAF1)	11–9 °C at surface; 8–5 °C at 200 m (along 45°E) 11–10 °C at surface; 8–5 °C at 200 m (along 57°30′E)	34.0–33.85 at surface; 34.40–34.11 at 200 m
Subantarctic Front (SAF2)	7–6 °C at surface 4 °C isotherm at 200 m depth (along 45°E) 9–8 °C at surface 4 °C isotherm at 200 m depth (along 57°30′E)	surface salinity c. 33.85 south of SAF
Polar Front (PF1)	5–4 °C at surface northern limit of the 2 °C isotherm below 200 m	33.8–33.9 at surface
Polar Front (PF2)	3–2 °C at surface	33.8–33.9 surface
Southern Antarctic Circumpolar Current Front (SACCF)	Temperature maximum $T_{\max} > 1.8$ °C	Salinity maximum $S_{\max} > 34{:}73$
Southern Boundary of ACC (SB)	1.5 °C isotherm	

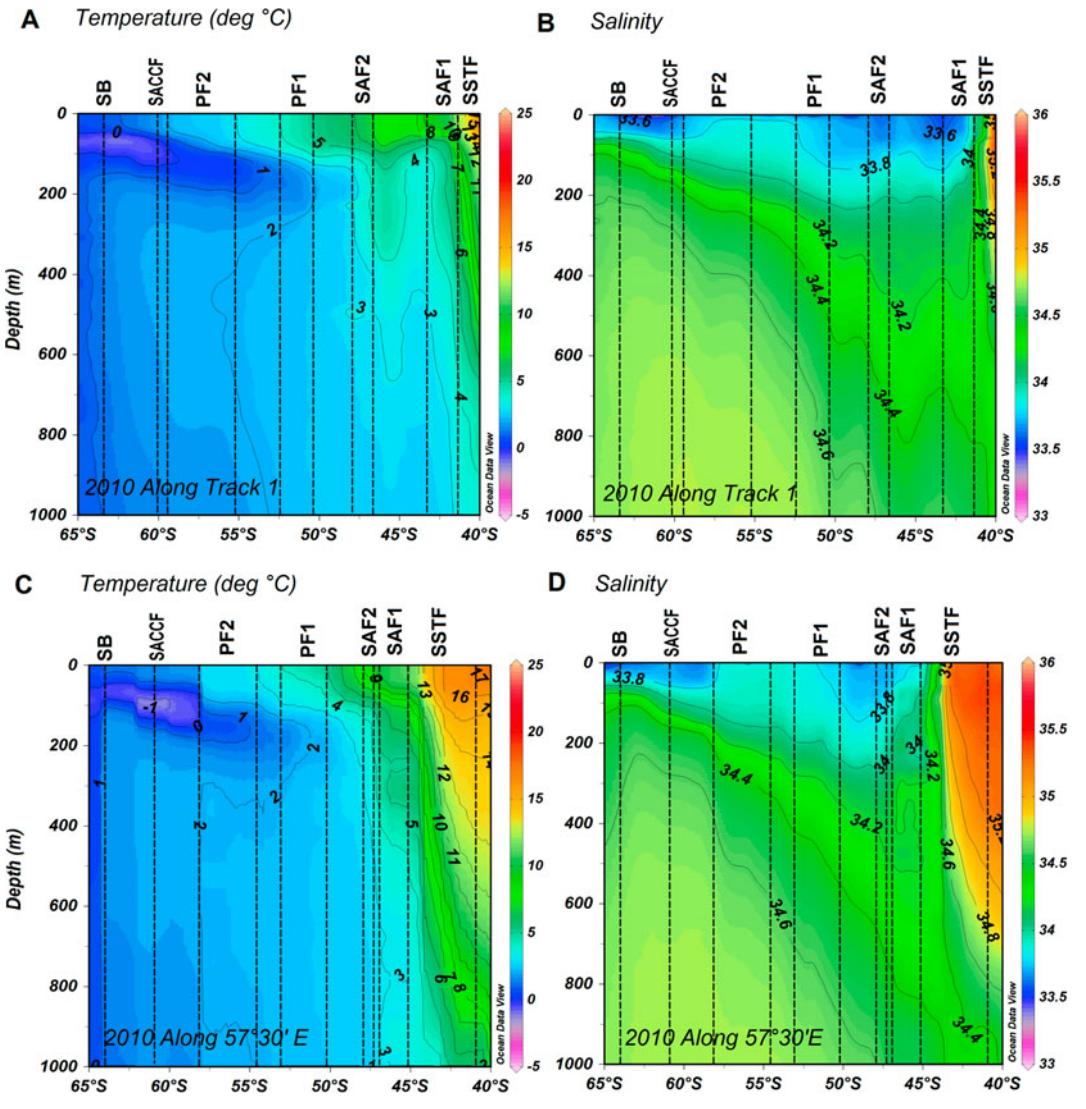

Figure 2 Vertical structure of **A**, temperature (°C) and **B**, salinity along the track between 65°41′S 57°30′E and 55° S 48°E, and further northwards along 48°E (Track-1); and **C**, temperature (°C) and **D**, salinity along 57°30′E in 2010.

located north of 40°S (Belkin & Gordon 1996), whereas our observations were from south of 40°S. Along this section, the Southern Subtropical Front (SSTF) and Northern Subantarctic Front (SAF1) were observed between 40°S and 41°30′S, and between 41°30′S and 44°S, respectively, with a drop in temperature from 16 to 9 °C (Fig. 2A) and a decrease in salinity from 35.54 to 34.11 (Fig. 2B). The Southern Subantarctic Front (SAF2), Northern Polar Front (PF1) and Southern Polar Front (PF2) were identified between 46°30′S and 48°S, 50°S and 52°30′S, and 54°30′S and 59°30′S, respectively (Table 2). The SACCF and SB can be identified from the most southerly position of the subsurface 1.8 °C and 1.5 °C isotherms, respectively. However, in the present study, the SACCF was demarcated between 60°S and 61°S, and the SB was between 64°30′S and 64°S.

Table 2 Comparison of frontal locations between the present and previous studies.

Fronts	Present location along Track-1 and 47°E	Previously reported locations west of 48°E
Northern Subtropical Front (NSTF)	Not encountered	31°S–38°S (Belkin & Gordon 1996)
Agulhas Return Front (AF)	40°S–41°18′S	38°S–41.5°S (Holliday & Read 1998)
Southern Subtropical Front (SSTF)	40°S–41°30′S	Observed as a merged front along with ARF and SAF at about 43°S, 45°E (Read et al. 2000) 40°S and 42°S along 55°E, (Holliday & Read 1998)
Subantarctic Front (SAF1)	41°30′S–44°S	44°S–45°S (Kostianoy et al. 2004)
Subantarctic Front (SAF2)	46°30′S–48°S	48.5°S–49°S (Kostianoy et al. 2004)
Polar Front (PF1)	50°S–52°30′S	50°S–52°S (Holliday & Read 1998)
Polar Front (PF2)	54°30′S–59°30′S	55°S–57°S (Holliday & Read 1998)
Southern Antarctic Circumpolar Current Front (SACCF)	60°S–61°S	c. 60°S–63°S (Meijers et al. 2010)
Southern Boundary of ACC (SB)	64°S–64°30′S	c. 64°S–65°S (Meijers et al. 2010)

The temperature and salinity sections along 57°30′E during 2010 are presented in Fig. 2C and D. Along this transect, the SSTF was identified between 41°S and 45°S; SAF1 between 45°S and 47°S; SAF2 between 47°S and 48°S; PF1 between 50°S and 52°30′S; and PF2 as a wide front between 55°S and 59°30′S. The SACCF and SB were identified at the same latitudes as observed along Track-1. Holliday & Read (1998) reported the occurrence of the STF between 40°S and 42°S along 55°E; and during 2004, the merged Agulhas Front (AF) and the SSTF were identified between 43°30′S and 45°S, SAF1 was between 45°30′S and 46°30′S, and SAF2 was south of 47°S along 57°30′E (see Figs 5 and 6 in Anilkumar et al. 2006).

During 2011, the AF+SSTF+SAF1 front was observed (Fig. 3A and B) between 41°S and 44°30′S along 47°E. However, along 57°30′E, this complex front was identified as a wide frontal system between 40°30′S and 46°30′S (Fig. 3C and D). East of 54°E, Belkin & Gordon (1996) identified this merged frontal system as the Crozet Front. Park et al. (1993) Sparrow et al. (1996) and Kostianoy et al. (2004) reported more spatial variation in this merged frontal system than was seen in the present study. The SAF2 was identified between 47°30′S and 48°30′S along 47°E, whereas its position was observed to be relatively more northward along 57°30′E, lying between 46°30′S and 47°30′S. The PF1 was identified between 50°30′S and 52°S, lying almost in the same position along 47°E and 57°30′E; while the PF2 was seen as a relatively wider front along 57°30′E (between 53°30′S and 56°30′S) than along 47°E (between 52°30′S and 54°S). Moore et al. (1997, 1999) used satellite SST maps to study the dynamics of the PF, and showed its position as lying between 49°30′S and 52°S; however, this was not compatible with the positions of the PF1 and PF2 that were identified in this study. During 2011, the AF was identified as a separate front along 47°E and 57°30′E, confirming the earlier findings of Belkin & Gordon (1996). Kostianoy et al. (2004) opined that the AF's cyclonic meander can increase the distance between the AF and the STF/SAF by up to 3° latitude.

In the present study, a southward shift of > 2° latitude from west (Track-1 and 47°E) to east (57°30′E) was observed in the positions of the SSTF and SAF1 (Figs 2A–D and 3A–D). Gladyshev et al. (2008) reported that the locations of the SAF, PF and SACCF are controlled by the neighbouring ridges. The position of the SAF in the present study differed from that found in previous studies (Park et al. 1993; Belkin & Gordon 1996; Sparrow et al. 1996). In earlier reports, it was observed to be surrounding the Crozet Plateau

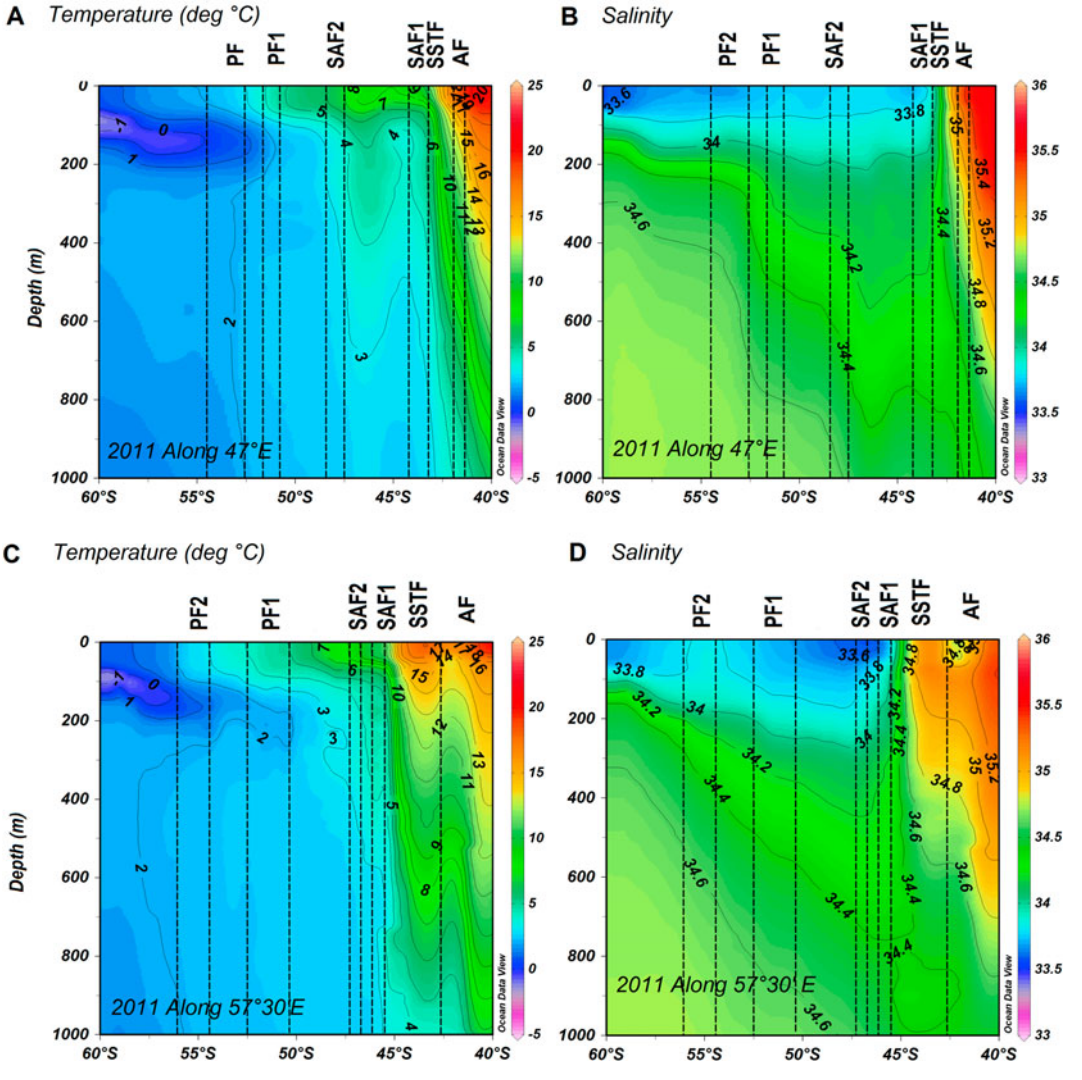

Figure 3 Vertical structure of **A**, temperature (°C) and **B**, salinity along 47°E; and **C**, temperature (°C) and **D**, salinity along 57°30′E in 2011.

(Moore et al. 1999); and Holliday & Read (1998) reported a width of c. 1.5° latitude along 45°E, while Lutjeharms & Valentine (1984) reported a width of c. 2.5° latitude. By contrast, the SAF was distinguished as two separate fronts (SAF1 and SAF2) along all the tracks in the present study, and so its width was not comparable with previous findings. These results attest to the significant inter-annual variability in the frontal systems of the SO. A comparison of the frontal locations observed in the present and previous studies is provided in Table 2.

Following the method of Swart & Speich. (2010), the mean MADT calculated from 1992 to 2010 was used to compute the meridional gradients per 100 km of mean MADT. These gradients were then used to identify the core locations of various fronts along 48°E and 57°30′E (Fig. 4A and B). Swart & Speich (2010) suggested that isolines of MADT coincide with constant water mass

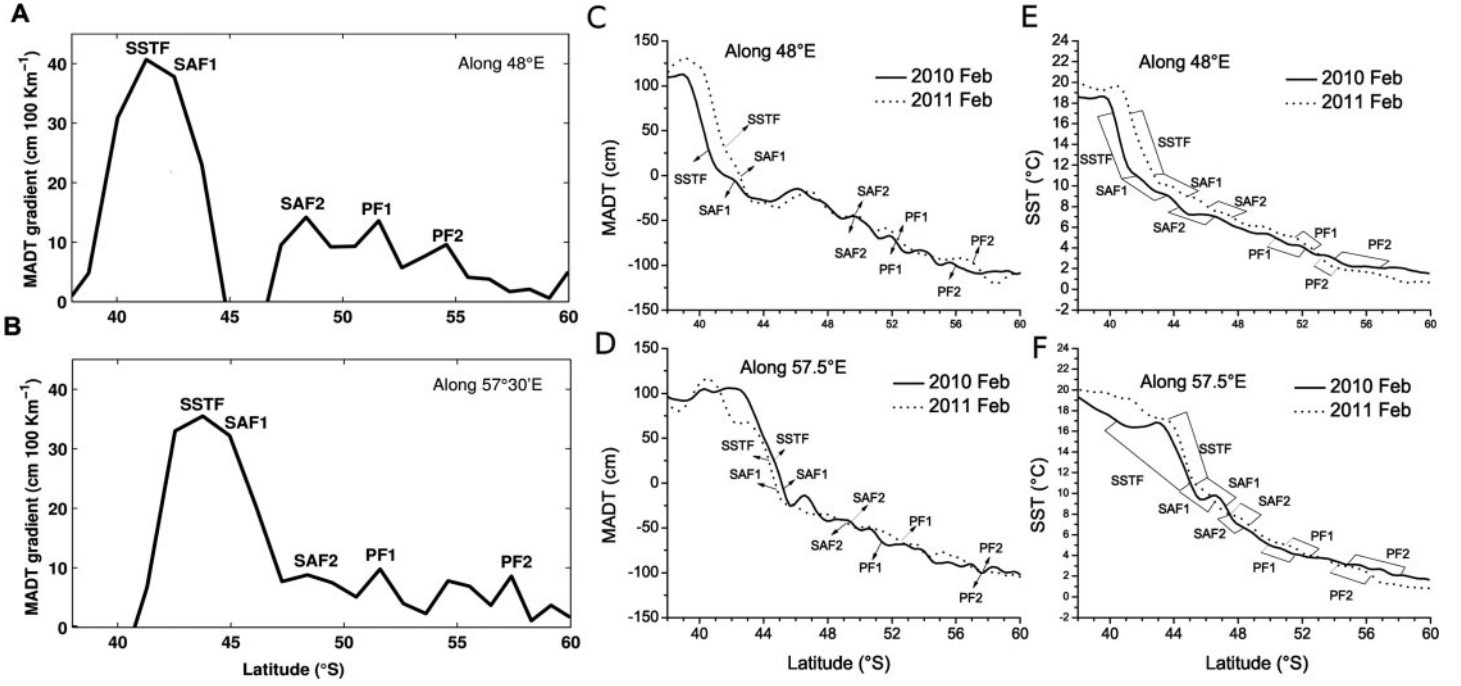

Figure 4 Mean MADT gradient (cm 100 km^{-1}) (computed from weekly MADT data from 1992 to 2010) along **A**, 48°30′E and **B**, 57°30′E; core frontal locations determined using MADT along **C**, 48°E and **D**, 57°30′E; and frontal location and its width using satellite SST (GHRSST) along **E**, 48°E and **F**, 57°30′E.

properties and thus the fronts. Along 48°E, the MADT gradient exhibited the SSTF at 41°S, the SAF1 at 42°30′S and the SAF2 at 48°30′S. The PF1 was observed to be located at 51°30′S and the PF2 at 54°30′S. Along 57°30′E, the SSTF, SAF1 and SAF2 were identified at 43°30′S, 45°S and 48°30′S, respectively. Further, the PF1 and PF2 were observed at 51°30′S and 57°30′S, respectively. Table 3 shows the mean characteristic MADT for each frontal position located in the study region. The frontal locations from the MADT gradient showed a southward meandering of the SSTF and SAF1 by > 2° latitude. In the present study, the locations of the gradient maxima and the associated lines of MADT were almost identical to the frontal positions identified using the hydrographic data. The characteristic MADT for each front in Table 3 was used to analyse frontal variability during February 2010 and February 2011 (Fig. 4C and D); and based on the SST characteristics of fronts given in Table 1, the satellite-derived SST plots were also used to depict the frontal locations during these 2 years (Fig. 4E and F). The core locations of fronts derived from both the MADT and the satellite SST were consistent with those of the hydrographic data.

Therefore, from the present study it can be deduced that the meandering of fronts in the ACC was only exhibited by the SSTF and SAF1. The other fronts had almost identical positions along the western and eastern transects of the study region. In the following sections, we discuss the sources for the input of fresh water in the study region and further delineate the strength of currents in the study area where meandering fronts were observed in the ACC.

Water masses and winter water properties

Water masses

The characteristics of the water masses in the study area are given in Table 4. Signatures of the Subtropical Surface Water (STSW) were identified up to 41°S along Track-1 in 2010 and up to 42°S along 47°E in 2011 (Fig. 5A and C). The southward intrusion of this water mass was observed up to 44°S in 2010 and 45°S in 2011 along 57°30′E (Fig. 5B and D). The signatures of the Subtropical Mode Water (STMW) that were observed in the present investigation (Fig. 5) were similar to those reported previously by McCartney (1977) and Park et al. (1991), whereas Tsubouchi et al. (2010) observed its signatures in the regions 28°E–45°E and 60°E–80°E. The STMW can be identified in the depth range of 400 to 700 m, with a potential density anomaly range of 26.5 to 26.8 kg m^{-3}, where the potential density pycnostad develops (Park et al. 1993). It has been reported that the STMW is formed in the Crozet Basin (see Fig. 4 of Belkin & Gordon 1996). Along Track-1 and 47°E, we identified the southward extent of the STMW up to 41°S and 42°S, respectively (Fig. 5A and C), concurring with the findings of Park et al. (1993) and Belkin & Gordon (1996). Along 57°30′E, the STMW was identified up to 44°S and 45°S in 2010 and 2011, respectively, with

Table 3 Mean frontal locations as determined using mean MADT at (a) 48°E and (b) 57°30′E.

	Along 48°E		Along 57°30′E	
Fronts	Mean location (°S)	Mean MADT (cm)	Mean location (°S)	Mean MADT (cm)
Southern Subtropical Front (SSTF)	41.30	29.4	43.76	25.20
Subantarctic Front (SAF1)	42.54	–8.40	44.95	–7
Subantarctic Front (SAF2)	48.38	–42.80	48.38	–43.80
Polar Front (PF1)	51.59	–74.90	51.59	–66.2
Polar Front (PF2)	54.59	–97.80	57.39	–99.50

Table 4 Water mass characteristics.

Water mass	Characteristics			Depth (m)
	Temperature (°C)	Salinity (psu)	Density (kg m^{-3})	
Subtropical Surface Water (STSW)	> 12	> 35.1		0–200
Subantarctic Surface Water (SASW)	9	< 34		0–200
Antarctic Surface Water (AASW)	< 5	< 34		0–200
Sub Tropical Mode Water (STMW)	11 to 14	35 to 35.4	26.5 to 26.8	400–700
Antarctic Intermediate Water (AAIW)	c. 4.4	c. 34.42	c. 27.24	700–1200
Circumpolar Deep Water (CDW)	c. 2	c. 34.77	c. 27.8	2000–3800
Antarctic Bottom Water (ABW)	c. 0.165 to 0.62	c. 34.67 to 34.652	c. 27.85 to 27.85	> 3000

the southward intrusion of more than 4° latitude (Fig. 5B and D) compared with Track-1 and 47°E.

The Antarctic Intermediate Water (AAIW) was identified up to 43°S (Fig. 5A and C) along Track-1 and 47°E. The AAIW from the southwest Indian Ocean sector of the SO is the dominant AAIW type east of the Agulhas Current retroflection (Roman & Lutjeharms 2010). The AAIW identified in the Crozet Basin mainly originates from the region near the Kerguelen Plateau (Molinelli 1981; Fine 1993;

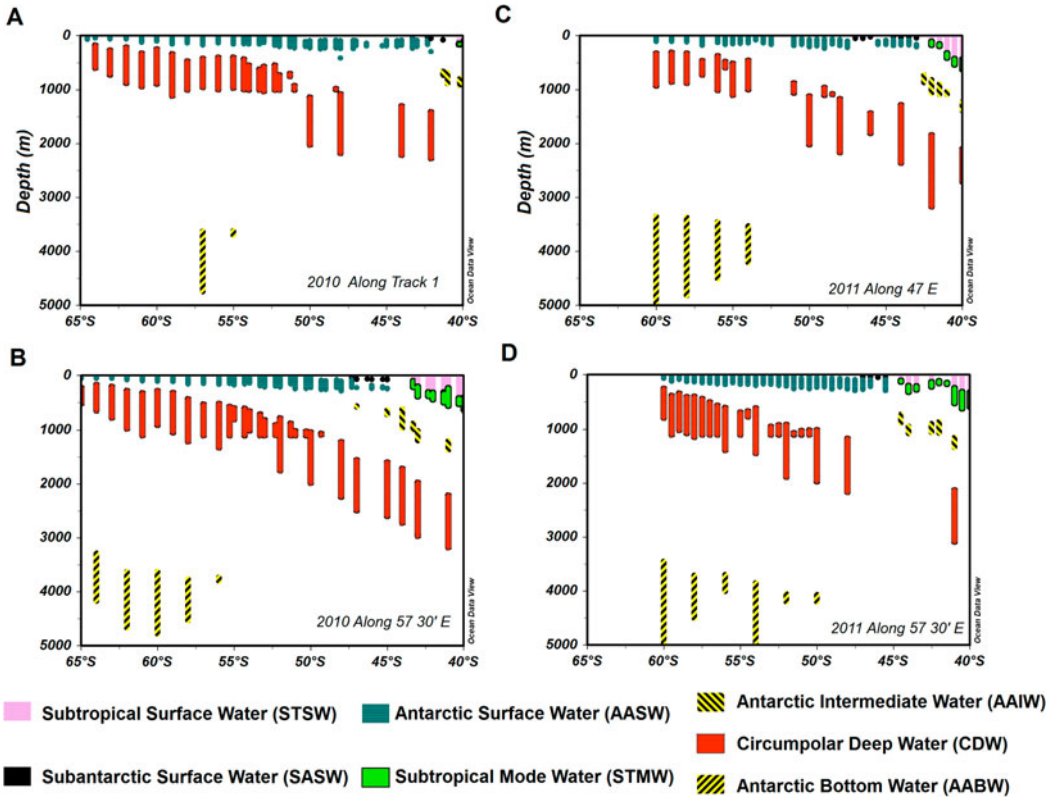

Figure 5 Water masses along **A**, Track-1 and **B**, 57°30′E in 2010; and **C**, 47°E and **D**, 57°30′E in 2011.

Toole & Warren 1993). The depth of this water mass has been reported to be between c. 1000 and c. 1300 m (Park et al. 1993; Bindoff & McDougall 1999). In the present study, the features of the AAIW were observed between 1000 and 1500 m. The southward extent of the AAIW was observed up to 45°S in 2010 and 2011 along 57°30′E (Fig. 5B and D), which is more than 2° latitude southwards of that observed along Track-1 and 47°E.

Signatures of the Subantarctic Surface Water (SASW) were observed between 42° and 43°S along Track-1, and between 43°S and 47°S along 47°E (Fig. 5A and C); however, this water mass was identified between 45°S and 47°S along 57°30′E (Fig. 5B and D). The Antarctic Surface Water (AASW) was identified up to 42°S along Track-1 in 2010 (Fig. 5A) and up to 43°S along 47°E in 2011 (Fig. 5C); however, the signatures of this water mass were observed only up to 45°S along 57°30′E in 2010 and 2011 (Fig. 5B and D). This means that the northward intrusion of the SASW and AASW was more pronounced in the western transects (Track-1 and 47°E). Along these transects, the Circumpolar Deep Water (CDW) was identified up to 42°S (Fig. 5A and C), while it was observed up to 58°S–60°S along 57°30′E. However, the CDW was observed deeper than 2000 m north of 45°S, and its northward intrusion was seen beyond 42°S during 2010 and 2011 (Fig. 5B and C). According to Toole & Warren (1993), the CDW occupies a depth range of 2000–3800 m north of 45°S and rises sharply to shallower depths south of this latitude. A northward intrusion of Antarctic Bottom Water (AABW) was observed up to 55°S and 56°S along Track-1 and 57°30′E, respectively, in 2010 (Fig. 5A and B). In 2011, the intrusion of AABW was seen up to 54°S and 50°S along 47°E and 57°30′E, respectively (Fig. 5C and D). Observations from Argo data (Fig. 6) were consistent with the in situ CTD results, showing a more northward intrusion of SASW and AASW in the western region (45°E–55°E). By contrast, the STSW, STMW and AAIW showed a further southward intrusion in the eastern region (57°E–65°E).

Anilkumar et al. (2006) previously identified water masses along 45°E; however, this was based on CTD data from only one transect, and so the north–south movement of water masses in the western and eastern regions could not be compared. Here, we compared the spreading of water masses along Track-1, 47°E and 57°30′E during 2010 and 2011, and found disparity in their intrusion along the western and eastern transects of the study region. It is likely that the intrusions of water masses in the upper layers are controlled by the meandering of the ACC flow.

Winter water properties

The temperature minimum layer (c. 1.4 °C lower than the surface temperature) was located 50–200 m south of 50°S in the study region in both 2010 and 2011 (Figs 2 and 3). This temperature minimum layer corresponds with the AASW and is capped above the CDW (Yuan et al. 2004), and can be attributed to the WW. Below this layer, the temperature gradually increased by c. 2 °C up to 350 m and then exhibited isothermal characteristics further down. Following Park et al. (1998), the WW depth ($\boldsymbol{D_c}$) is defined as the WW core depth at which the absolute minimum subsurface temperature is observed. During 2010 and 2011, the WW was observed up to the PF1 from the south, and the temperature and core depth of WW increased from south to north in both meridional sections. The shallowest WW depth was noted in the Antarctic divergence region (c. 63°S to 60°S). In general, cooler WW was observed in 2011 than 2010 along Track-1/47°E (Fig. 7A and B), and the fresh water thickness (as calculated following Park et al. 1998) showed higher values during 2011 than 2010 along the western section (Track-1/48°E) (Fig. 7C and D).

This layer of low temperature is the result of surface freshening during the austral summer, mainly due to ice melting and subsequent warming of the surface layer (Park et al. 1998), but also from precipitation and the advection of melt water. Bromwich et al. (1995) reported a low level of precipitation (30 cm yr^{-1}) at 50°S, based on the analysis of zonal averaged net precipitation derived from the European Centre for Medium-Range Weather Forecasts, and in the present study, the fresh water input received south of 50°S along

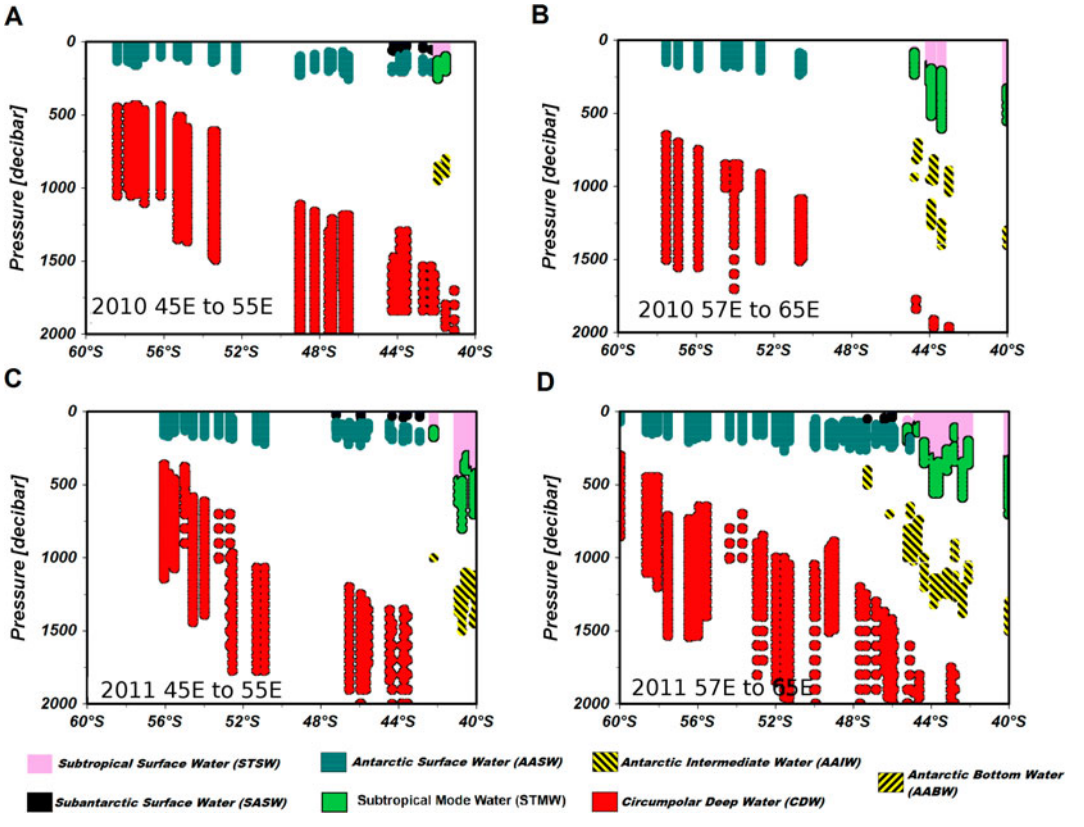

Figure 6 Water masses from Argo data in two regions: **A**, from 45°E to 55°E (eastern region) and **B**, from 56°E to 65°E (western region) in 2010; and **C**, from 45°E to 55°E and **D**, from 56°E to 65°E in 2011.

both transects has not been attributed to net precipitation. Rather, the source of fresh water could be locally produced melt water and/or advection from the in situ melting of sea ice originating from the south and west. The extent of sea ice along 48° E and 57°30′E during 2009 and 2010 is shown in Fig. 8A and B, from which it can be seen that the maximum sea ice limit was up to c. 59°S during the winter of 2009 and up to c. 57°S during the winter of 2010 along both sections. The peak extent of the sea ice was observed in September, after which it started to melt through to March. This larger and more northward extent of sea ice during winter 2010 could explain the greater thickness of the fresh water layer and cooler WW temperature observed during the summer of 2011.

The Ekman currents overlaid on the averaged wind stress suggest the northward Ekman transport of melt water from south (Fig. 8C and D). It can also be seen that the high stress patch (c. 0.3 Pa) of westerlies that was centred at 50°S during February 2010 shifted further south to 56°S during February 2011, which may have caused the increase in the northward Ekman transport from the south (c. 60°S) during February 2011. The shifting of the westerlies could be a manifestation of the positive Southern Annular Mode (SAM) during February 2011 (SAM index = 0.86) and the negative SAM during February 2010 (SAM index = −2.12) (Marshall 2003), and so the increased northward Ekman transport of melt water from the south could also explain the comparative increase in fresh water

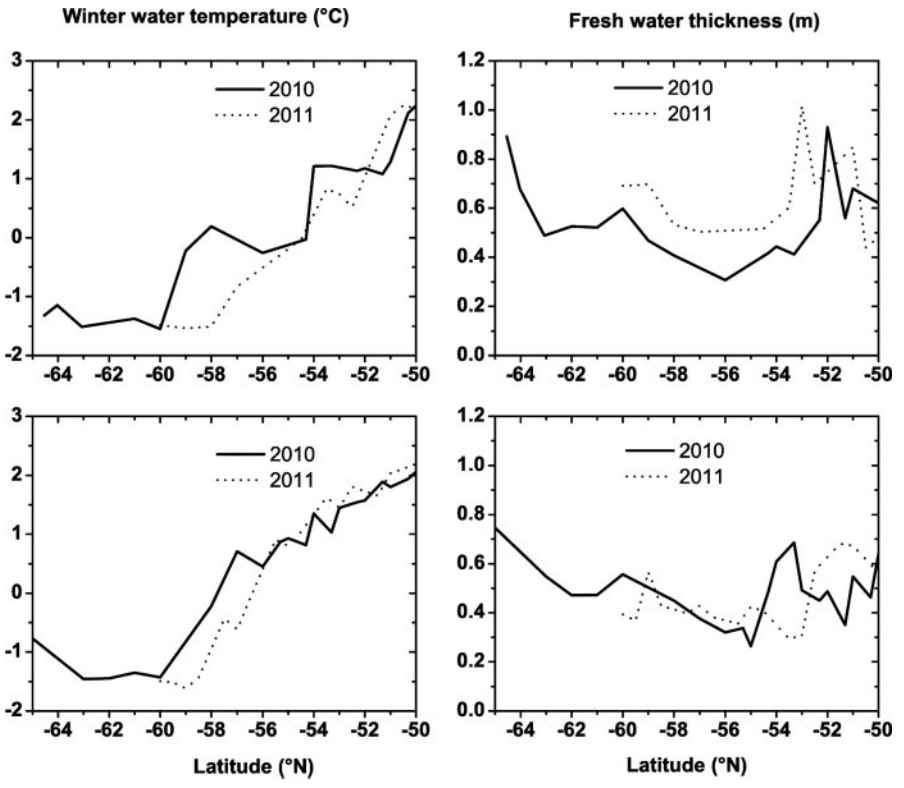

Figure 7 Winter water temperature (°C) **A**, along Track-1 in 2010 and along 47°E in 2011, and **B**, along 57°30′E in 2010 and 2011; and fresh water thickness (m) **C**, along Track-1 in 2010 and along 47°E in 2011, and **D**, along 57°30′E in 2010 and 2011.

thickness during February 2011. In general, however, the Ekman currents in the SO are weak compared with the background geostrophic currents (Lenn & Chereskin 2009).

Recent studies suggest an increased rate of melting in the Bellingshausen–Amundsen Sea, west of the Antarctic Peninsula (Pritchard et al. 2012; Rignot et al. 2013), and this low-saline melt water enters the Indian Ocean sector, possibly via the ACC. Hence, the melt water that is transported from west of the Antarctic Peninsula may contribute to the low salinity waters that are observed in the Indian Ocean sector of the SO. The total current during February 2010 and 2011, as derived from the OSCAR (Fig. 9A and B), also suggested a net eastward flow in the SO. It is also expected that melting in the Weddell Sea would contribute to the observed thickness of the fresh water layer. The Weddell Gyre is a cyclonic circulation regime centred at c. 30°W, which has a major role in transferring heat and salt from the ACC to the Antarctic continental shelves (Orsi et al. 1993), and which eventually helps with the sea ice melting in the region. However, the northward flow in the Weddell Sea was found to be weak during summer 2010 (Fig. 8C).

Finally, it should be noted that there was greater variability in the thickness of the fresh water layer and WW temperature between February 2010 and February 2011 along Track-1 and 47°E than along 57.5°E (Fig. 7). However, more observations are required to explain this variability. In the following section, we have delineated the strength of currents in the study area in regions where meandering of the ACC was observed.

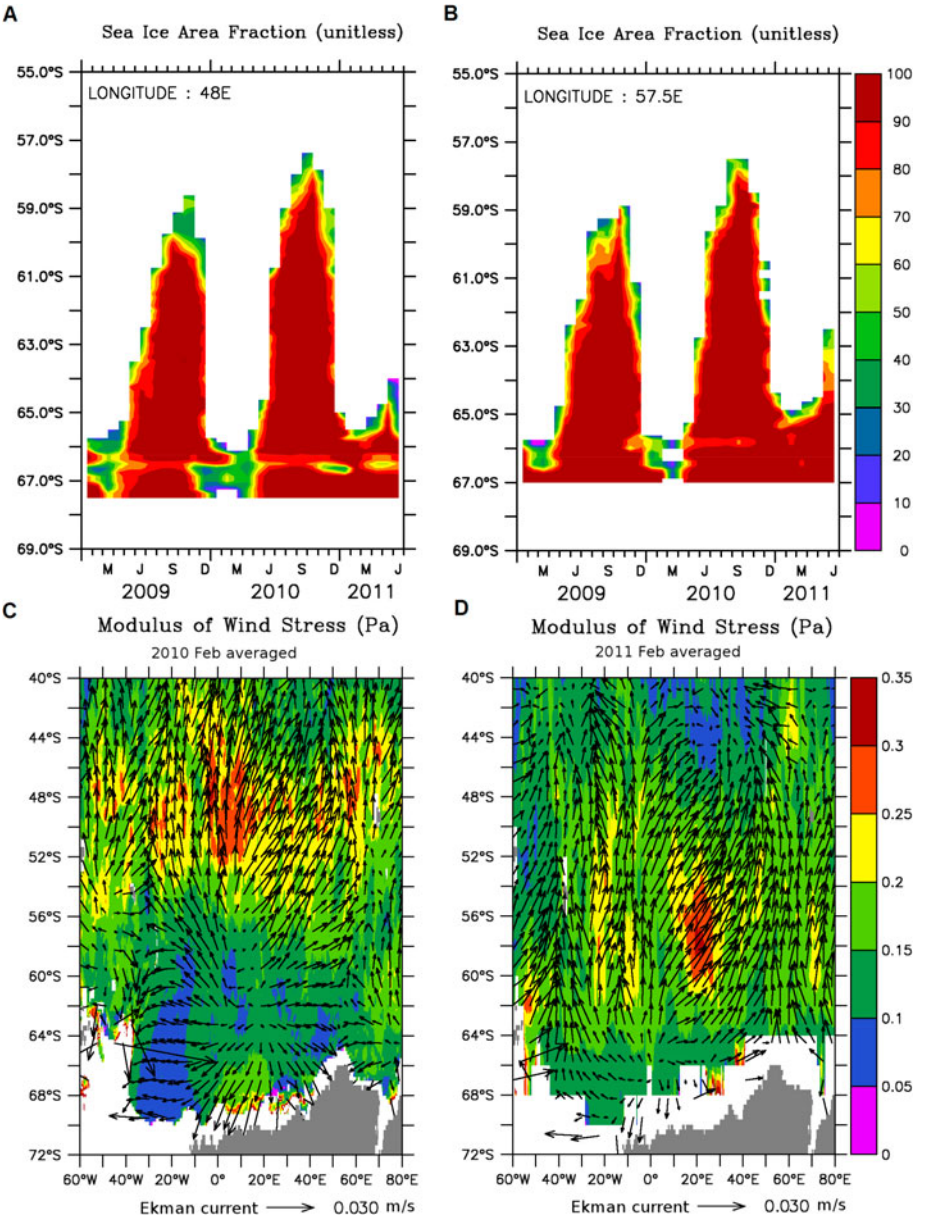

Figure 8 Sea ice fraction derived from AMSRE along **A**, 48°E and **B**, 57°30′E; and wind stress (Pa) overlaid by Ekman currents (m s^{-1}) derived from ASCAT during **C**, February 2010 and **D**, February 2011.

ACC variability in the study region

In the study region, the ACC flows from west to east and depicts a complex current pattern, with strong zonal currents in the merged frontal region. Geostrophic currents across the cruise tracks were computed for 2010 and 2011 (Fig. 10). Along 57° 30′E, the current velocity was stronger (> 30 cm s^{-1}) in the SSTF+SAF1 region (ACC core) during 2010 (Fig. 10B). Two patches of high geostrophic currents were observed, with velocities of c. 30 cm s^{-1}

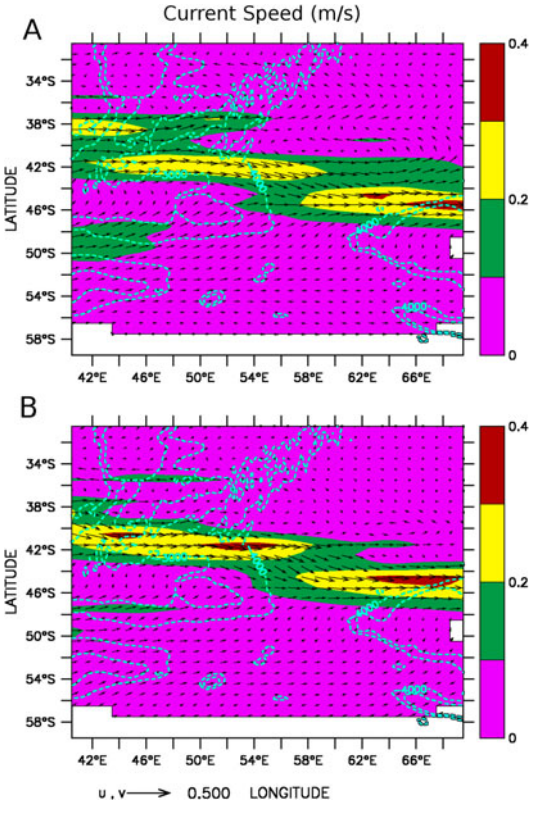

Figure 9 OSCAR monthly averaged currents (m s^{-1}) in **A**, 2010 and **B**, 2011. The 3000 m and 4000 m deep isobaths are overlaid as dashed lines.

and c. 15 cm s^{-1}, which were separated by an opposite current of 5 cm s^{-1} (Fig. 10C) (unless specified otherwise, the directions of geostrophic currents were positive eastward). This pattern could have been caused by an eddy that has been identified in this region (Chacko et al. in press). In the SSTF +SAF1 region, a stronger geostrophic current (c. 30 cm s^{-1}) was observed along 47°E and 57°30′E in 2011 than along Track-1 (< 5 cm s^{-1}) and 57°30′E (< 25 cm s^{-1}) in 2010 (Fig. 10). These results demonstrate the inter-annual variability in the ACC.

A southward shift of the ACC core was also observed in the geostrophic currents between the 47° E/Track-1 and 57°30′E transects during both 2010 and 2011. The OSCAR monthly averaged currents overlaid by the 3000 m and 4000 m deep isobaths are shown in Fig. 9. From this, it can be seen that the ACC core was observed between 42°S and 44°S in the western region (westwards of 56°E), and between 44°S and 47°S in the eastern region (eastwards of 56° E). It can also be seen that, along the core of the ACC (c. 42°S to c. 47°S), the meandering was associated with the bottom topography. When the ACC passes from a shallow (< 4000 m, Crozet plateau and Southwest Indian ridge) to a deep (> 4000 m) region, the ACC meanders southwards to conserve its potential vorticity. Previous studies by Kostianoy et al. (2004), Anilkumar et al. (2007) and Nuncio et al. (2011) have also shown that the meandering of the ACC was governed by the bottom topography. Analysis of the wind stress curl (data not shown) and the Ekman currents (Fig. 8) suggests that the meandering of the ACC in the study region may not be driven by wind. It can also be noted from Fig. 10 that the meandering of the ACC is not a surface feature, but rather extends to deeper depths. The fronts in this region also meander, and mark the northward extension of the SASW and AASW in the west (45°E to 55°E) and the southward intrusion of the STSW, STMW and AAIW in the east (57°E to 65°E).

In the Indian Ocean sector of the SO, the PF was found to be bifurcated into two components, PF1 and PF2, which is compatible with the previous observations of Holliday & Read (1998). Further, the SB was observed up to 64°30′S along both Track-1 and 57°30′E in 2010. Previous studies have reported that the maximum southward movement of the SB was apparent in the Indian Ocean sector of the SO (Orsi et al. 1995, 1999; Meijers et al. 2010; Couldrey et al. 2013), rather than the Atlantic or Pacific sectors. The region between 50°E and 60°E is located between two distinct gyres—the Weddell Gyre in the west and Prydz Bay Gyre in the east. The transport of the Antarctic Slope Current (ASC) is greatest at 80°E (westwards), and becomes steadily weaker towards the west, reaching a minimum at 50°E. This weakening could be a result of the Prydz Bay Gyre (Meijers et al. 2010). The present study area (between 45°E and 60°E) lies between the two gyres, where the transport of the ASC is weaker and the ACC extends more southwards, resulting in the peculiar behaviour of the ACC in the Indian Ocean sector of the SO.

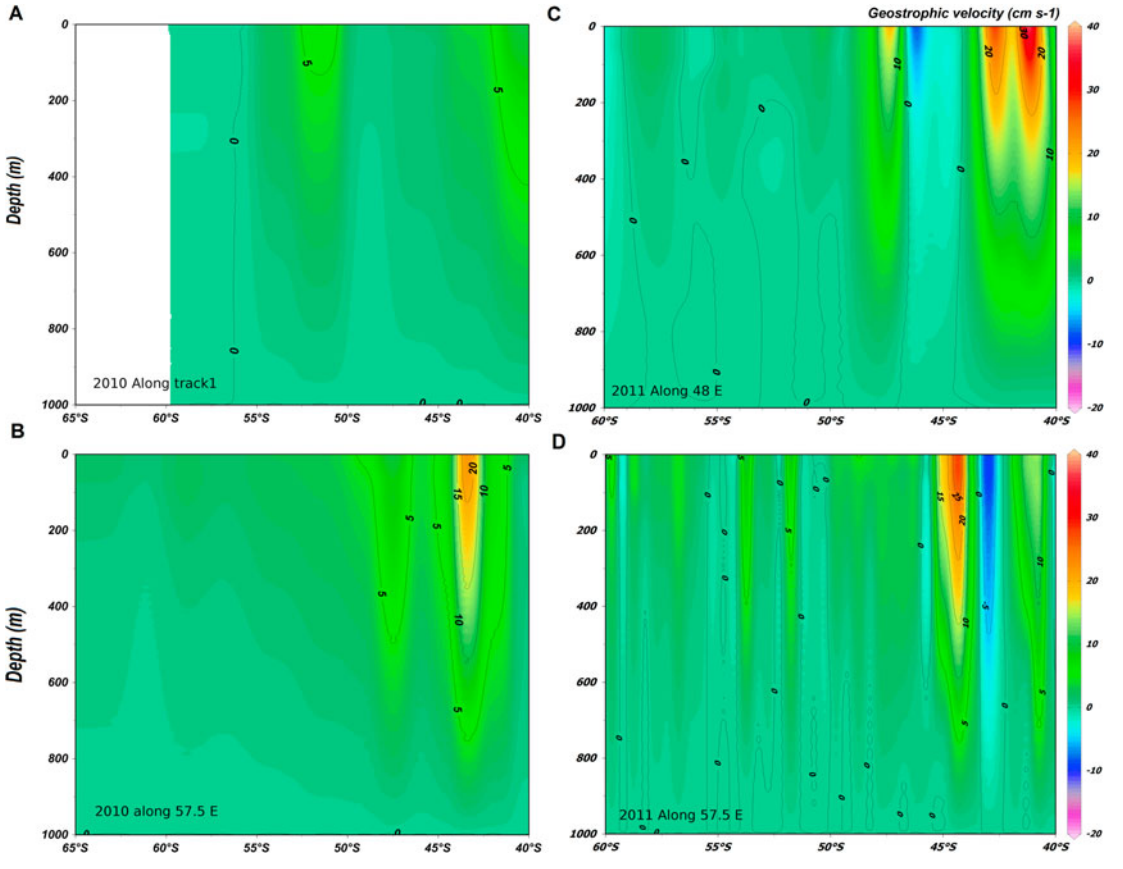

Figure 10 Geostrophic currents (cm s^{-1}) along **A**, Track-1 and **B**, 57°30′E in 2010; and **C**, 47°E and **D**, 57°30′E in 2011.

Chlorophyll variability

Table 5 shows the in situ concentrations of Chl *a* that were measured along 57°30′E during February 2010 and 2011, and Fig. 11 provides the monthly averaged satellite data for the same months. Several previous studies (Jasmine et al. 2009; Gandhi et al. 2012) have reported that the SSTF is one of the most productive regions in the SO. In the present study, the SSTF was characterised by high surface concentrations of Chl *a* (> 0.24 mg m^{-3}) along both

Table 5 Variation in surface concentrations of Chl *a* along 57.30°E.

Area	Chl *a* (mg m^{-3}) during 2010 (along 57°30′E)	Chl *a* (mg m^{-3}) during 2011 (along 57°30′E)
Subtropical region	0.53 (43°S)	0.24 (44°S)
Polar frontal region (PF1)	0.36 (52°S)	0.38 (52°S)
Polar frontal region (PF2)	c. 0.1	0.38 (56°S)
Coastal region	4.1	–

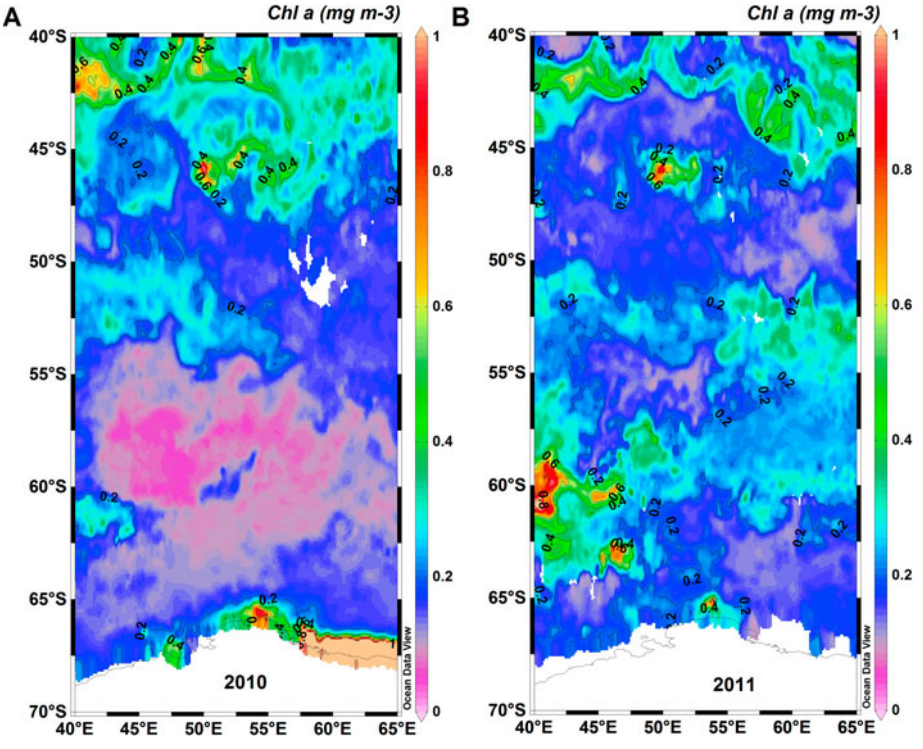

Figure 11 Monthly Chl *a* (mg m^{-3}) images over the study area during **A**, 2010 and **B**, 2011.

transects during 2010 and 2011. However, a higher concentration of Chl *a* was observed during 2010 (0.5 mg m^{-3}) than 2011 (0.24 mg m^{-3}). This could be due to variability in the PAR, which was slightly lower during February 2011 (45 Einstein m^{-2} day^{-1}) than in 2010 (55 Einstein m^{-2} day^{-1}) (data not shown).

In the PF1 region, there was a moderately high concentration of Chl *a* (> 0.36 mg m^{-3}) during both years. However, south of PF1, the concentration of Chl *a* was lower in 2010 (0.1 mg m^{-3}) than in 2011 (0.38 mg m^{-3}) (Table 5 and Fig. 11). One of the major constraints for Chl *a* production in the SO is the low availability of micronutrients, particularly iron (Holm-Hansen et al. 2005).

In general, the PF2 region between 40°E and 60°E, which is deeper than 2000 m, is less productive (Sokolov & Rintoul 2007b). It has previously been reported that, in oceans that have deep bottom topography, there is a greatly reduced supply of iron from the bottom to the surface via upwelling associated with deep currents of the ACC (Sokolov & Rintoul 2007b; Holm-Hansen et al. 2005). A higher concentration of Chl *a* was observed in PF2 in 2011 than in 2010, which can be attributed to the larger amount and more northward extent of the sea ice (Fig. 8A and B) during winter 2010 compared with winter 2009. Melting sea ice is known to be one of the major sources of iron because sea ice accumulates aeolian deposits (Gao et al. 2003), which are subsequently released during ice melt. Thus, it is possible that the supply of micronutrients resulting from the melting of sea ice may increase the concentration of Chl *a* (Boyd & Ellwood 2010). Melt water can also enhance stratification, resulting in a shallow mixed layer, which leads to increased light availability for phytoplankton growth (Park et al. 2014). The greater thickness of the fresh water layer that was observed in the hydrographic section during

February 2011 (especially in the western region along c. 47°E) also supports the observed high concentration of Chl *a*.

A high in situ concentration of Chl *a* was observed in the coastal waters of Antarctica during 2010 (c. 4 mg m^{-3}) (Table 5). The monthly averaged satellite data also showed high concentrations of Chl *a* (c. 0.8 mg m^{-3}) in the coastal region during 2010 and 2011 (Fig. 11). The elevated levels of micronutrients in the coastal waters as a result of glacial melting may stimulate the significant phytoplankton blooms in the SO (Smith & Nelson 1985; Park et al. 1999). Previous studies have reported that the SO is a high nutrient–low chlorophyll (HN-LC) region due to light limitation because of the deep mixing (Mitchell et al. 1991; Nelson & Smith 1991), grazing pressure (Dubischar & Bathmann 1997), non-availability of trace metals (Martin et al. 1990) and limited photosynthetic rate as a result of low water temperatures (Tilzer et al. 1986; Sakshaug & Slagstad 1991). However, the high concentrations of Chl *a* observed south of PF1 during 2011 in the present investigation can be attributed to the local melting of sea ice and advected melt water from the south and west.

Conclusion

This study investigated inter-annual variability in the fronts and water masses, and variation in the concentration of Chl *a* across various frontal systems in the Indian Ocean sector of the SO. The SSTF and SAF1 were characterised by a southward shift of 2° latitude along 57°30′E compared with their position along 47°E/Track-1, which was consistent with the southward meandering of the ACC core from west to east. This meandering was likely to have been caused by topographic steering of the ACC between the western and eastern transects. While passing through the shallow topographic features (Crozet plateau and Southwest Indian ridge) to the deep region (> 4000 m), the ACC meanders southwards to conserve its potential vorticity. The northward extension of the SASW and AASW in the west (45°E to 55°E), and the southward intrusion of the STSW, STMW and AAIW in the east (57°E to 65°E), are probably linked to the meandering of the ACC. A large amount of sea ice was present in the study region during winter 2010 compared with winter 2009, and our findings suggest that the greater thickness of the fresh water layer in 2011 compared with 2010 was the result of the melting of the previous winter's sea ice, and advection of the melt water from the south and west of the study region. One of the major consequences of this advection was the greater concentration of Chl *a* (c. 0.38 mg m^{-3}) south of PF1 during 2011 compared with 2010. More detailed in situ hydrographic observations in the future may provide a comprehensive understanding of the biophysical coupling that occurs in the SO.

Acknowledgements

The authors sincerely thank Secretary Ministry of Earth Sciences, Government of India, for implementing the two expeditions. The constant encouragement and support extended by the Director, National Centre for Antarctic and Ocean Research (NCAOR), Goa, for the execution of the expeditions is gratefully acknowledged. Help rendered by the cruise participants and the NCAOR staff for the implementation and successful completion of this study is acknowledged. We are grateful to Dr C.T. Achuthankutty, Visiting Scientist, NCAOR, for his critical comments and suggestions for improving the quality and presentation of the manuscript. We thank Dr Sini Pavithran for Chl *a* analysis. We are also grateful to the anonymous reviewers for their critical comments and suggestions. This is NCAOR contribution number 09/2014.

References

Anilkumar N, Alvarinho JL, Somayajulu YK, Ramesh Babu V, Dash MK, Pednekar SM et al. 2006. Fronts, water masses and heat content variability in the Western Indian sector of the Southern Ocean during austral summer 2004. Journal of Marine Systems 63: 20–34.

Anilkumar N, Pednekar SM, Sudhakar M 2007 Influence of ridges on hydrographic parameters in the Southwest Indian Ocean. Marine Geophysical Researches 28: 191–199.

Belkin IM, Gordon AL 1996. Southern Ocean fronts from the Greenwich Meridian to Tasmania. Journal of Geophysical Research 101: 3675–3696.

Billany W, Swart S, Hermes J, Reason CJC 2010. Variability of Southern Ocean fronts at the Greenwich Meridian. Journal of Marine Systems 82: 304–310.

Bindoff NL, McDougall 1999. Decadal changes along an Indian Ocean section at 32°S and their interpretation. Journal of Physical Oceanography 30: 1207–1222.

Bonjean F, Lagerloef GSE 2002. Diagnostic model and analysis of the surface currents in the Tropical Pacific Ocean. Journal of Physical Oceanography 32: 2938–2954.

Boyd, PW, Ellwood MJ 2010. The biogeochemical cycle of iron in the ocean. Nature Geoscience 3: 675–682.

Bromwich DH, Robasky FM, Culather RI, Van Woert ML 1995. The atmospheric hydrologic cycle over the Southern Ocean and Antarctica from operational numerical analyses. Monthly Weather Review 123: 3518–3538.

Chacko R, Nuncio M, George JV, Anilkumar N in press. Observational evidence of the southward transport of watermasses in the Indian sector of Southern Ocean. Current Science.

CSIRO Cookbook for Quality Control of Expendable Bathythermograph (XBT) Data. (1993). Hobart, Tasmania, CSIRO. 74 p.

Couldrey MP, Jullion L, Naveira Garabato AC, Rye C, Herráiz-Borreguero L, Brown PJ et al. 2013. Remotely induced warming of Antarctic Bottom Water in the eastern Weddell gyre. Geophysical Research Letters 40: 2755–2760.

Deacon GER 1937. The hydrology of the Southern Ocean. Discovery Reports 15: 3–122.

Dubischar CD, Bathmann, UV 1997. Grazing impact of copepods and salps on phytoplankton in the Atlantic sector of the southern ocean. Deep-Sea Research II 44: 415–433.

Fine RA 1993. Circulation of Antarctic intermediate water in the South Indian Ocean. Deep Sea Research Part I: Oceanographic Research Papers 40: 2021–2042.

Gandhi N, Ramesh R, Laskar AH, Sheshshayee MS, Suhas Shetye, Anilkumar N et al. 2012. Zonal variability in primary production and nitrogen uptake rates in the southwestern Indian Ocean and the Southern Ocean. Deep Sea Research Part I: Oceanographic Research Papers 67: 32–43.

Gao Y, Fan SM, Sarmiento JL 2003. Aeolian iron input to the ocean through precipitation scavenging: A modeling perspective and its implication for natural iron fertilization in the ocean. Journal of Geophysical Research 108: 4221.

Gladyshev S, Arhan M, Sokov A, Speich S 2008. A hydrographic section from South Africa to the southern limit of the Antarctic Circumpolar Current at the Greenwich meridian. Deep Sea Research Part I: Oceanographic Research Papers 55: 1284–1303.

Gordon AL 1986. Interocean exchange of thermocline water. Journal of Geophysical Research 91: 5037–5046.

Hamilton LJ 2006. Structure of the subtropical front in the Tasman Sea. Deep-Sea Research I 53: 1989–2009.

Holliday NP, Read JF 1998. Surface oceanic fronts between Africa and Antarctica. Deep-Sea Research I 45: 217–238.

Holm-Hansen O, Kahru M, Christopher DH 2005. Deep chlorophyll a maxima (DCMs) in pelagic Antarctic waters. II. Relation to bathymetric features and dissolved iron concentrations. Marine Ecology Progress Series 297: 71–81.

Hughes CW 2005. Nonlinear vorticity balance of the Antarctic Circumpolar Current. Journal of Geophysical Research 110: C11008.

Jasmine P, Muraleedharan KR, Madhu NV, Ashadevi, CR, Alagarsamy R, Achuthankutty CT et al. 2009. Hydrographic and productivity characteristics along 45°E longitude in the southwestern Indian Ocean and Southern Ocean during austral summer 2004. Marine Ecological Progress Series 389: 97–116.

Kostianoy AG, Ginzburg AI, Frankignoulle M, Delille B 2004. Fronts in the Southern Indian Ocean as inferred from satellite sea surface temperature data. Journal of Marine Systems 45: 55–73.

Lenn YD, Chereskin TK, Sprintall J, McClean JL 2011. Near-surface eddy heat and momentum fluxes in the Antarctic Circumpolar Current in Drake Passage. Journal of Physical Oceanography 41: 1385–1407.

Lenn YD, Chereskin TK 2009. Observations of Ekman currents in the Southern Ocean. Journal of Physical Oceanography 39: 768–779.

Lutjeharms JRE, Ansorge IJ 2001. The Agulhas return current. Journal of Marine Systems 30: 115–138.

Lutjeharms JRE, Valentine HR 1984. Southern ocean thermal fronts south of Africa. Deep Sea Research Part A. Oceanographic Research Papers 31: 1461–1475.

Marshall GJ 2003. Trends in the Southern Annular Mode from observations and reanalyses. Journal of Climate 16: 4134–4143.

Martin JH, Gordon RM, Fitzwater SE 1990. Iron in Antarctic waters. Nature 345: 156–158.

McCartney MS 1977. Sub Antarctic mode water. In: Angel, MV ed. A voyage of discovery. New York, Pergamon. Pp. 103–119.

Meijers, AJS, Klocker A, Bindoff NL, Williams GD, Marsland SJ 2010. The circulation and water masses of the Antarctic shelf and continental slope between 30 and 80° E. Deep Sea Research Part II: Topical Studies in Oceanography 57: 723–737.

Mitchell BG, Brody EA, Holm-Hansen O, McClain C, Bishop J 1991. Light limitation of phytoplankton biomass and macronutrient utilization in the Southern Ocean. Limnology and Oceanography 36: 1662–1677.

Molinelli EJ 1981. The Antarctic influence on Antarctic Intermediate Water. Journal of Marine Research 39: 267–293.

Moore JK, Abbott MR, Richman JG 1997. Variability in the location of the Antarctic Polar Front (90–20W) from satellite sea surface temperature data. Journal of Geophysical Research 102: 27825–27833.

Moore JK, Abbott MR, Richman JG 1999. Location and dynamics of the Antarctic Polar Front from satellite sea surface temperature data. Journal of Geophysical Research 104: 3059–3073.

Nelson DM, Smith WO Jr. 1991. Sverdrup revisited: critical depths, maximum chlorophyll levels, and the control of southern ocean productivity by the irradiance-mixing regime. Limnology and Oceanography 36: 1650–1661.

Nuncio M, Alvarinho JL, Yuan X 2011. Topographic meandering of Antarctic Circumpolar Current and Antarctic Circumpolar Wave in the ice-ocean-atmosphere system. Geophysical Research Letters 38, 13: n/a.

Orsi AH, Nowlin WD Jr, Whitworth T 1993. On the circulation and stratification of the Weddell Gyre. Deep Sea Research Part I: Oceanographic Research Papers 1 40: 169–203.

Orsi AH, Johnson GC, Bullister JL 1999. Circulation, mixing, and production of Antarctic Bottom Water. Progress in Oceanography 43: 55–109.

Orsi AH, Whitworth T III, Nowlin WD Jr. 1995. On the meridional extent and fronts of the Antarctic Circumpolar Current. Deep Sea Research Part I: Oceanographic Research Papers 42: 641–673.

Park YH, Charriaud E, Fieux M 1998. Thermohaline structure of Antarctic surface water/winter water in the Indian sector of the Southern Ocean. Journal of Marine Systems 17: 5–23.

Park YH, Gamberoni L, Charriaud E 1991. Frontal structure and transport of the Antarctic Circumpolar Current in the South Indian Ocean sector, 40°–80°E. Marine Chemistry 35: 45–62.

Park YH, Gamberoni L, Charriaud E 1993. Frontal structure, water masses and circulation in the Crozet Basin. Journal of Geophysical Research 98: 12361–12385.

Park K, Kang C-K, Kim K-R, Park J-E 2014. Role of sea ice on satellite-observed chlorophyll *a* concentration variations during spring bloom in the East/Japan sea. Deep Sea Research Part I 83: 34–44.

Park MG, Yang SR, Kang SH, Chung KH, Shim JH 1999. Phytoplankton biomass and primary production in the marginal ice zone of the northwestern Weddell Sea during austral summer. Polar Biology 21: 251–261.

Pritchard HD, Ligtenberg SRM, Fricker HA, Vaughan DG, Van den Broeke MR, Padman, L 2012. Antarctic ice-sheet loss driven by basal melting of ice shelves. Nature 484: 502–505.

Read JF, Lucas MI, Holley SE, Pollard RT 2000. Phytoplankton, nutrients and hydrography in the frontal zone between the Southwest Indian Subtropical gyre and the Southern Ocean. Deep Sea Research I 47: 2341–2368.

Rignot E, Jacobs S, Mouginot J, Scheuchl B 2013. Ice shelf melting around Antarctica. Science 341: 266–270.

Rintoul SR 1991. South Atlantic interbasin exchange. Journal of Geophysical Research 96: 2675–2692.

Rintoul SR, Hughes C, Olbers D 2001. The Antarctic Circumpolar System, in Ocean Circulation and climate. International Geophysical Services 77: 271–302.

Roman RE, Lutjeharms JRE 2010. Antarctic Intermediate Water at the Agulhas Current retroflection region. Journal of Marine Systems 81: 273–285.

Sakshaug E, Slagstad D 1991. Light and productivity of phytoplankton in polar marine ecosystems – a physiological review. Polar Research 10: 69–85.

Smith WO Jr., Nelson DM 1985. Phytoplankton bloom produced by a receding ice edge in the Ross Sea: spatial coherence with the density field. Science 227: 163–166.

Sokolov S, Rintoul SR 2007a. Multiple jets of the Antarctic Circumpolar Current south of Australia. Journal of Physical Oceanography 37: 1394–1412.

Sokolov S, Rintoul SR 2007b. On the relationship between fronts of the Antarctic Circumpolar Current and surface chlorophyll concentrations in the Southern Ocean. Journal of Geophysical Research 112: C07030.

Sokolov S, Rintoul SR 2009a. Circumpolar structure and distribution of the Antarctic Circumpolar Current fronts: 1.Mean circumpolar paths. Journal of Geophysical Research 114: C11018.

Sokolov S, Rintoul SR 2009b. Circumpolar structure and distribution of the Antarctic Circumpolar Current fronts: 2. Variability and relationship to sea surface height. Journal of Geophysical Research 114: C11019.

Sparrow MD, Heywood KJ, Brown J, Stevens DP 1996. Current structure of the South Indian Ocean. Journal of Geophysical Research 101: 6377–6391.

Speich S, Blanke B, Madec G 2001 Warm and cold water routes of an OGCM thermohaline Conveyor Belt. Geophysical Research Letters 28: 311–314.

Stammer D 1998. On eddy characteristics, eddy transports, and mean flow properties. Journal of Physical Oceanography 28: 727–739.

Swart S, Speich S 2010. An altimetry-based gravest empirical mode south of Africa: 2. Dynamic nature of the Antarctic Circumpolar Current fronts. Journal of Geophysical Research 115: C03003.

Swart S, Speich S, Ansorge IJ, Goni GJ, Gladyshev S, Lutjeharms JRE 2008. Transport and variability of the Antarctic Circumpolar Current south of Africa. Journal of Geophysical Research 113: C09014.

Tilzer MM, Elbrachter M, Gieskes WW, Beese B 1986. Light-temperature interactions in the control of photosynthesis in Antarctic phytoplankton. Polar Biology 5: 105–111.

Toole JM, Warren BA 1993. A hydrographic section across the subtropical South Indian Ocean. Deep Sea Research Part I: Oceanographic Research Papers 40: 1973–2019.

Tsubouchi T, Suga T, Hanawa K 2010. Indian Ocean Subtropical Mode Water: its water characteristics and spatial distribution. Ocean Science 6: 41–50.

Yuan X, Martinson DG, Dong Z 2004. Upper ocean thermohaline structure and its temporal variability in the southeast Indian Ocean. Deep Sea Research Part I: Oceanographic Research Papers 51: 333–347.